ANALYTICA CHIMICA ACTA

International monthly devoted to all branches of analytical chemistry
Revue mensuelle internationale consacrée à tous les domaines de la chimie analytique
Internationale Monatsschrift für alle Gebiete der analytischen Chemie

ELSEVIER PUBLISHING COMPANY
AMSTERDAM

Anal. Chim. Acta, Vol. 51, No. 2, 141–348, August 1970
Published monthly

GENERAL INFORMATION

Languages

Papers will be published in English, French or German.

Submission of papers

Papers should be sent to: Prof. PHILIP W. WEST, Coates Chemical Laboratories, College of Chemistry and Physics, Louisiana State University, Baton Rouge 3, La. 70803 (U.S.A.)
or to
Dr. A. M. G. MACDONALD, Department of Chemistry, The University, P.O. Box 363, Birmingham 15 (Great Britain)

Manuscripts

Authors should submit two copies in double-spaced type with adequate margins on pages of uniform size. Acknowledgements, summary and references should be placed at the end of the paper.

Tables should be typed on separate pages and numbered in Roman numerals in the order in which they are mentioned in the text. All Tables should have descriptive titles. The use of chemical formulae and conventional abbreviations is encouraged in Tables and Figures but chemical formulae should not be used in the text unless they are necessary for clarity. Units of weight, volume, etc., when used with numerals should be abbreviated and unpunctuated (*e.g.*, 2%, 2 ml, 2 g, 2 μl, 2 μg, 2 ng, 2 cm, 200 mμ).

Figures should be drawn in Indian ink on drawing or tracing paper with all lettering in **thin** pencil. Standard symbols should be used in line drawings; the following are available to the printers:

▼ ▽ ■ □ ● ◎ ▪ ◘ ◈ ▣ ▪ + ×

Photographs should be submitted as clear black and white glossy prints. Figures and photographs should be of the same size as the typed pages. Legends for figures should be **typed on a separate page**. Figures should be numbered in Arabic numerals in the order in which they are mentioned in the text.

References should be given at the end of the paper and should be numbered in the order of their appearance in the text (**not** arranged alphabetically). Abbreviations of journal titles should conform to those adopted by the *Chemical Abstracts List of Periodicals*, 1961 Edition and supplements. The recommended form for references to journal papers and books is as follows:

1. J. J. LINGANE AND A. M. HARTLEY, *Anal. Chim. Acta*, 11 (1954) 475.
2. F. FEIGL, *Spot Tests in Organic Analysis*, 7th Ed., Elsevier, Amsterdam, 1966, p. 516.

For multi-author references, **all** authors must be named, and initials given, in the reference list, although the use of, for example, SMITH *et al.*, is desirable in the text.

Summaries are published in English, French and German; authors must always provide a summary in the language of the paper, and are encouraged to supply translations where convenient. No summaries are needed for Short Communications.

Reprints

Fifty reprints will be supplied of charge. Additional reprints (minimum 100) can be ordered at quoted prices. They must be ordered on order forms which are sent together with the proofs.

Publication

Analytica Chimica Acta has three issues to the volume, and four vols. will appear in 1970. Subscription prices: $ 17.50 or Dfl. 63.— per volume: $ 70.00 or Dfl. 252.— for 1970, plus postage. Additional cost for copies by airmail available on request. For subscribers in the U.S.A. and Canada, 2nd class postage paid at New York, N.Y. For advertising rates apply to the publishers.

Subscriptions

Subscriptions should be sent to:

ELSEVIER PUBLISHING COMPANY, P.O. Box 211, Amsterdam, The Netherlands

VERLAG
CHEMIE

Soeben erscheint:

Günter Ege

Zahlentafeln zur Massenspektrometrie und Elementaranalyse

Ermittlung von CHNO(S)-Summenformeln

Tables for Mass Spectrometry and Elementary Analysis
Determination of CHNO(S) Molecular Formulae
Tableaux pour la spectrométrie de masse et l'analyse élémentaire
Détermination des formules moléculaires des CHNO(S)

Die Ermittlung der Summenformel einer organischen Verbindung ist häufig der erste Schritt auf dem Weg zu ihrer Konstitutionsaufklärung. Liegt neben der CH-Analyse ein massenspektrometrisch ermitteltes Molgewicht vor, so benötigt man eine Tabelle, in der die Summenformeln nach Massenzahlen und CH-Prozentwerten angeordnet sind.

Die vorliegenden Zahlentafeln ermöglichen das schnelle und sichere Auffinden der Summenformeln von CHNO(S)-Verbindungen mit Hilfe der ganzzahligen Massenzahl und der Elementarzusammensetzung. Die Summenformel kann häufig auch dann noch ermittelt werden, wenn die Analysenwerte geringfügig außerhalb der konventionellen Fehlergrenze von ±0,3 % liegen. Die Zahlentafeln sind auf die Elemente Kohlenstoff, Wasserstoff, Stickstoff und Sauerstoff beschränkt. Schwefel kann berücksichtigt werden, wenn man jeweils zwei Atome Sauerstoff durch ein Atom Schwefel ersetzt.

Die Tabellen enthalten analytische Daten für Summenformeln bis zu 40 Kohlenstoffatomen, 6 Stickstoffatomen und 12 Sauerstoffatomen. Damit sich die Tabellen auch für die hochauflösende Massenspektrometrie verwenden lassen, werden die exakten Massen auf 5 Dezimalstellen angegeben. Außer der Summenformel sind der Prozentanteil der (M+1)-Spitze bezogen auf die Molekülionenspitze, das Molekulargewicht und die Unsättigungszahl aufgeführt. Die Berechnungen wurden auf der Datenverarbeitungsanlage Siemens 2002 mit den Atomgewichten von 1967 durchgeführt.

Alle Begleittexte sind dreisprachig deutsch, englisch und französisch abgefaßt. Die Zahlentafeln können überall dort verwendet werden, wo es um die Aufstellung einer CHNO(S)-Summenformel geht.

1970. XXVI, 352 Seiten mit 356 Tabellen. Kunststoffeinband DM 88,—.
Verlangen sie unseren Sonderprospekt!

VERLAG CHEMIE · GMBH · WEINHEIM/BERGSTR.

A new North-Holland publication in:

Biochemistry, Molecular Biology, Microbial Genetics, Microbiology, Virology.

RNA-Polymerase and Transcription

Proceedings of the First Lepetit Colloquium, Florence, November 1969

Edited by L. G. SILVESTRI, Milan

1970. 348 pages. Hfl. 43.– (100 s.) ISBN 7204 4056 4

The sessions were chaired by *Drs. J. Hurwitz, E. P. Geiduschek, W. Zillig, S. Spiegelman, A. Tissières* and *N. D. Zinder*. The general discussion and summing-up at the end of the conference was under the chairmanship of *Dr. J. D. Watson*.

The first Lepetit Colloquium provided an opportunity for outstanding workers in the field to assemble for the first time to discuss their work. Lively and far-reaching discussions between the participants were based on the submitted papers which are published in this volume.

Contents:
The Structure and Binding of RNA-Polymerase: Binding of nucleoside triphosphate by highly purified RNA-polymerase of *Escherichia coli*. Studies with the RNA-polymerase.
The Interaction with Rifamycins: Temperature-dependent rifampicin-resistant mutations of DNA-dependent RNA-polymerase of *E. coli*. A mutation which affects the resistance of *E. coli* to rifampicin. Effects of nucleoside triphosphate concentration and structure on the transcription of T 4 DNA by *E. coli* RNA-polymerase. The inhibition of the RNA-polymerase reaction by rifampicin. Interaction of rifampicin with RNA-polymerase. Temperature-sensitive RNA-polymerase mutants of *Escherichia coli*.
The Influence of Protein Factors: Initiation and regulation of transcription by RNA-polymerase. The influence of protein factors and DNA-structure upon transcription specificity. The RNA-polymerase sigma factor: A specificity determinant. The regulation of RNA metabolism in *E. coli* infected with phage T7. On the different subunits of DNA-dependent RNA-polymerase from *E. coli* and their role in the complex function of the enzyme. Changes in structure and function of RNA-polymerase from *E. coli* after T4 infection. Studies on the RNA synthesis and RNA-polymerase in normal and phage infected *E. coli* cells. T4 anti-messenger. Synthesis and degradation of mRNA distal to nonsense codons in the *trp* operon of *E. coli*. A termination factor for RNA synthesis. Transcriptional controls in bacteriophage lambda. Termination of T4 RNA transcription in vitro. RNase V: a messenger RNase associated with *E. coli* ribosomes.
Mammalian, Plant and Viral Polymerase: Some characteristics of mammalian RNA-polymerase and factors influencing its activity. The fidelity of transcription of the ribosomal RNA genes from a toad by bacterial RNA-polymerase. The effect of rifampicin on mammalian viruses and cells. The antiviral effect of rifampicin. Formation of a stable complex in the polyoma DNA-RNA polymerase system. Effect of rifampicin on transcription in chloroplasts of *Euglena*.
List of those attending the Collquium. Subject index.

AMSTERDAM P.O. BOX 3489 **NORTH HOLLAND** PUBLISHING CO. NETHERLANDS

Sole distributors for the U.S.A. and Canada: American Elsevier Publishing Company, Inc., 52 Vanderbilt Avenue, New York, N.Y. 10017

437 G

SUMMARIES OF PAPERS PUBLISHED IN ANALYTICA CHIMICA ACTA

Vol. 51, No. 2, August 1970

HIGH-SOLID SAMPLES IN ATOMIC-ABSORPTION FLAME SPECTROPHOTOMETRY

Determination of low analyte concentrations in samples with high concentrations of concomitants is discussed. Highly saline samples often cause problems when examined with burners designed for high-sensitivity operation, unless they are very greatly diluted. Use of new burners designed to handle solutions with high-solid contents is described and illustrated with some practical examples. These burners, which operate with cold spray chambers, offer improvements of sensitivity compared with other cold-operation burners, as well as low clogging disturbances and low memory effects. They also can be used with strongly acidic solutions and with a wide variety of flames.

A. Hell and J. Ramírez-Muñoz,
Anal. Chim. Acta, 51 (1970) 141–149

THE DETERMINATION OF COPPER IN IRON AND STEEL BY 14-MeV NEUTRON ACTIVATION ANALYSIS

A fast (10 min) non-destructive determination of copper in steel and cast iron by 14-MeV neutron activation analysis is described. The 0.511-MeV annihilation radiation of ^{62}Cu ($T_{\frac{1}{2}}=9.8$ min), induced by the reaction ^{63}Cu(n,2n)^{62}Cu, is counted by two opposing NaI(Tl) detectors operating in coincidence. An oxygen flux monitor is used to normalise the irradiations. For high phosphorus contents, two measurements are made and the 9-min activity contribution is calculated. As the iron content of the samples is known, the use of pure iron samples allows correction for ^{53}Fe activity from the reaction ^{54}Fe(n,2n)^{53}Fe ($T_{\frac{1}{2}}=8.9$ min). When the phosphorus and silicon activities are low, the procedure of counting and computing can be greatly simplified. Nuclear interferences of most common alloying and impurity elements were investigated. The precision is 2–3% for steels containing above 1% Cu, and *ca.* 10% for 0.1% Cu.

R. Van Grieken, A. Speecke and J. Hoste,
Anal. Chim. Acta, 51 (1970) 151–162

THE MASS SPECTRA OF ORGANIC MOLECULES

by J. H. Beynon, R. A. Saunders and A. E. Williams, Research Department,
Imperial Chemical Industries Ltd., Manchester, Great Britain

7 x 10″, ix + 510 pages, 20 tables, 181 illus., 547 lit. refs., 1968, Dfl. 97.50

Contents: 1. The principles and methods of mass spectrometry. 2. Types of ions in the mass spectra of organic compounds. 3. The mass spectra of hydrocarbons. 4. The mass spectra of oxygenated compounds. 5. The mass spectra of nitrogen compounds. 6. The mass spectra of sulphur compounds. 7. The mass spectra of halogenated compounds. 8. The mass spectra of boron compounds. 9. The mass spectra of phosphorus compounds. 10. The mass spectra of silicon compounds. 11. Examples of structure determination from mass spectra. Appendix 1. Peaks commonly encountered in the mass spectra of organic compounds. Appendix 2. The masses and abundances of nuclides commonly encountered in the mass spectra of organic compounds. References. Indexes.

MASS SPECTROMETRIC ANALYSIS OF SOLIDS

edited by A. J. Ahearn, Member of Technical Staff, Bell Telephone Laboratories, Inc.,
Murray Hill, New Jersey, U.S.A.

5½ x 8½″, viii + 175 pages, 13 tables, 46 illus., 242 lit. refs., 1966, Dfl. 30.00

Contents: 1. Introductory survey. 2. The production of ions from solids. 3. Photographic emulsions as ion detectors in quantitative mass spectrography. 4. Analysis of special samples. 5. Mass spectrographic microprobe analysis. Indexes.

ATOMIC-ABSORPTION SPECTROSCOPY

and Analysis by Atomic-Absorption Flame Photometry

by J. Ramírez-Muñoz, Principal Applications Chemist at Beckman Instruments Inc. and Scientific Research Collaborator of the C.S.I.C., Spain

6 x 9″, xii + 493 pages, 23 tables, 156 illus., 950 lit. refs., 1968, Dfl. 80.00

Contents: *Part I: Fundamentals.* 1. Origins of the method and nomenclature. 2. General principles and characteristics. 3. Absorption and emission. 4. The literature of atomic-absorption spectroscopy. 5. Theory. *Part II: Instrumental Systems.* 6. Instrumental systems. 7. Emission systems. 8. Absorption system. 9. Selection system. 10. Photometric system. 11. Instruments. *Part III: Range and Limitations of Atomic Absorption Methods.* 12. Determinable elements. Choice of lines. 13. Sensitivity. 14. Limitations in atomic absorption. *Part IV: Experimental Methods.* 15. Experimental process. 16. Standard solutions. 17. Preparation of the sample. 18. Experimental measurements and calibration. *Part V: Applications.* 19. Applications. Appendix. Bibliography.

Still available:

MASS SPECTROMETRY AND ITS APPLICATIONS TO ORGANIC CHEMISTRY

by J. H. Beynon

7 x 10″, xii + 640 pages, 11 tables, 185 illus., 2213 lit. refs., 1960, reprinted 1964 and 1967, Dfl. 85.00

TABLE OF META-STABLE TRANSITIONS FOR USE IN MASS SPECTROMETRY

by J. H. Beynon, R. A. Saunders and A. E. Williams

10 x 7″, xix + 392 pages, 1965, Dfl. 50.00

MASS AND ABUNDANCE TABLES FOR USE IN MASS SPECTROMETRY

by J. H. Beynon and A. E. Williams

10 x 7″, xxi + 570 pages, 1963, Dfl. 60.00

Elsevier
Publishing
Company

Amsterdam London New York

408 E

RADIOCHEMICAL NEUTRON ACTIVATION ANALYSIS OF INDIUM, CADMIUM, YTTRIUM AND THE 14 RARE EARTH ELEMENTS IN ROCKS

Indium, cadmium, yttrium and the 14 rare earth elements were simultaneously separated in the U.S. Geological Survey standard rocks, BCR-1 (basalt), G-2 (granite), and DTS-1 (dunite), and determined by γ-spectrometry with a 3×3 in NaI(Tl) well crystal and associated electronics. This method enabled the accurate determination of all the rare earths within a short time compared with instrumental methods. Indium and cadmium were separated in about 1.5 h and 4 h, respectively. Results for indium, cadmium and the rare earths are in excellent agreement with literature values. Indium and cadmium show decreasing concentrations in the sequence BCR-1/G-2/DTS-1. Relative to the rare earth distribution pattern in chondritic meteorites, the rare earth patterns observed in BCR-1 and G-2 are similar to other basalts and granites; however, the rare earth pattern in DTS-1 is V-shaped with a minimum at terbium and is similar to rare earth patterns observed in olivine minerals.

P. Rey, H. Wakita and R. A. Schmitt,
Anal. Chim. Acta, 51 (1970) 163–178

MULTI-ELEMENT ATOMIC FLUORESCENCE SPECTROSCOPY

PART I. STIMULATION OF ATOMIC FLUORESCENCE OF MIXTURES OF BISMUTH, MERCURY, SELENIUM AND TELLURIUM; CADMIUM AND ZINC; GALLIUM AND INDIUM BY MEANS OF MULTI-ELEMENT MICROWAVE-EXCITED ELECTRODELESS DISCHARGE TUBES

The construction and use of multi-element electrodeless discharge tubes for excitation of the atomic fluorescence of bismuth, mercury, selenium and tellurium; cadmium and zinc; and gallium and indium, are described. The tubes are operated at *ca.* 50–60 W and 2450 MHz in a three-quarter wave resonant cavity and the fluorescence is generated in a premixed air–propane flame. The performance and fluorescence detection limits obtained with the multi-element tubes are of the same order as those obtained with the individual single-element tubes. There is no spectral interference from the presence of 100-fold excesses of the co-elements in the analyte solution.

The atomic fluorescence detection limit for indium is three times better than the corresponding detection limit for flame photometry at its most sensitive wavelength of 451.1 nm, on the same apparatus at similar instrumental settings.

G. B. Marshall and T. S. West,
Anal. Chim. Acta, 51 (1970) 179–190

INORGANIC ELECTRONIC SPECTROSCOPY

by A. B. P. LEVER, Associate Professor of Chemistry,
York University, Toronto, Canada

The first monograph in the series PHYSICAL INORGANIC CHEMISTRY, edited by M. F. LAPPERT

Electronic spectroscopy has become, in recent years, a commonplace tool in inorganic research and development although few books dealing with the topic have appeared. Those books dealing with spectroscopy in general devote but a few pages to a discussion of the electronic spectra of inorganic compounds.

The aim of this book is (a) to provide the reader with a basic understanding of the methods and procedures involved in a study of the electronic spectra of inorganic compounds, (b) to discuss the information which may be derived from such study, with particular emphasis on stereochemistry and chemical bonding, and (c) to provide a reference text.

A beginning is made at a level which can be understood by an average student with a first degree, the first third of the book dealing with atomic theory, symmetry and group theory. In progressing further with the material presented, the reader can proceed from the construction of qualitative energy level diagrams and the assignment of transitions observed in the spectra of cubic molecules, to quantitative diagrams and the spectra of non-cubic molecules.

Having mastered this material the reader is shown how to derive useful information concerning stereochemistry and chemical bonding and even, qualitatively, such properties as effective nuclear charge and mean *d*-orbital radii. The spectra of the more common transition metal ions in their many oxidation states and stereochemistries are discussed in Chapter 9, which is a mine of information for the practising inorganic spectroscopist.

The book is unique in being the only reference work available which will bring the new graduate up to the level where he can read and usefully digest the original research papers in inorganic spectroscopy. Much of the material has not appeared in book form before and some of it has not appeared in print at all.

Contents: Preface. 1. Atomic structure. 2. Molecular symmetry. 3. Group theory. 4. Crystal field diagrams. 5. Term diagrams. 6. Selection rules, band intensities and dichroism. 7. Some theoretical aspects of electronic spectra. 8. Charge transfer spectra. 9. Crystal field spectra. Appendices. Indexes.

xii + 420 pages, 78 tables, 130 illus., 465 lit. refs., 1968, Dfl. 90.00, £11 10.0.

**Elsevier
Publishing
Company** Amsterdam London New York

262 E

PHOTOCHEMICAL COMPLEXATION TITRATIONS WITH FLUORIMETRIC END-POINTS

A fluorimetric end-point method has been developed for the photochemical decomposition of cobalt(III) oxalate to produce cobalt(II) ion as titrant. The method is used in titrating the fluorescent complexes formed between 8-hydroxyquinoline-5-sulfonic acid and Mg(II), Cd(II) and Zn(II) by displacement of the metal ion by cobalt(II), which forms a non-fluorescent complex. A back-titration of an excess of cadmium(II) complex is used for the determination of copper(II) which also forms a non-fluorescent complex with the ligand. A single ultraviolet source is used for photolysis and fluorescence excitation. The method is made possible by favorable UV absorption spectra of the various complexes involved.

J. L. Beck, J. M. Fitzgerald and J. A. Bishop,
Anal. Chim. Acta, 51 (1970) 191–198

ON THE USE OF THE PROTOLYTIC EFFECT OF COMPLEXATION REACTIONS FOR THE INDICATION OF END-POINTS IN COMPLEXIMETRIC TITRATIONS

Almost every complexation reaction gives rise to a protolytic effect, whose influence is usually decreased by adding a buffer. The use of the protolytic effect for locating the end-points of compleximetric titrations is discussed. Expressions are given for the linear titration graphs which can be obtained by photometric or potentiometric methods under different conditions. Examples of each case are described. The advantages of the method are its general applicability and high sensitivity.

H. Poppe, G. den Boef and F. Freese,
Anal. Chim. Acta, 51 (1970) 199–207

COPPER(I) SULFIDE CERAMIC MEMBRANES AS SELECTIVE ELECTRODES FOR COPPER(II)

A new type of copper(II)-selective electrode has been developed, based on copper(I) sulfide ceramic membranes prepared by an annealing process. The response time was very short even at low concentrations and the potentials were steady and reproducible. The Nernst equation was obeyed in the concentration range of 10^{-1}–10^{-6} M copper(II) and the analytical range was 10^{-1}–10^{-8} M. Among the common ions, silver, ammonium, iron(III) and iodide interfered.

H. Hirata, K. Higashiyama and K. Date,
Anal. Chim. Acta, 51 (1970) 209–212

TREATISE ON ELECTROCHEMISTRY

Second, completely revised edition

by G. Kortüm

Professor of Physical Chemistry, University of Tübingen, Germany

7 × 10″, xxii + 637 pages, 71 tables, 151 illust., 882 lit.refs., 1965, Dfl. 85.00, £ 10

Contents: 1. Definitions and fundamental laws. 2. Fundamental principles of thermodynamics. 3. The solvation of ions. 4. Weak and strong electrolytes. 5. Theory of ionic interaction. 6. Association and incomplete dissociation of strong electrolytes. 7. The results and applications of conductance measurements. 8. Electromotive forces. 9. Practical applications of potentiometric measurements. 10. Acids and bases. 11. Potential differences at phase boundaries. 12. Electrical polarization and the kinetics of electrode processes. 13. Applications of electrochemical processes. Appendix. Subject index.

OXIDATION AND COMBUSTION REVIEWS

edited by C. F. H. Tipper,

Department of Inorganic, Physical and Industrial Chemistry, University of Liverpool, Great Britain

Volume 1

6 × 9″, viii + 344 pages, 29 tables, 45 illus., 815 lit.refs., 1965, Dfl. 40.00, 110s.

Contents: 1. Application of the theory of branched chain reactions in low temperature combustion. 2. Oxidation reactions induced by ionising radiation. 3. Gas phase photo-oxidation. 4 Oxidation reactions involving nitrogen dioxide. 5. Oxidative degradation high polymers. 6. The heterogeneous selective oxidation of hydrocarbons. Author and subject indexes.

Volume 2

6 × 9″, viii + 301 pages, 19 tables, 64 illus., 311 lit.refs., 1967, Dfl. 60.00, 150s.

Contents: 1. Thermal explosion theory. 2. Some fundamentals of combustion instability 3. The use of adiabatic compression and mass spectrometry in the study of combustion. 4. Trapped radicals and combustion. Author and subject indexes.

Volume 3 and subsequent volumes are published as a review journal under the same title

ATMOSPHERIC OXIDATION AND ANTIOXIDANTS

by G. Scott,

Head of Works Research and Development Department, Dyestuffs Division, Imperial Chemical Industries Ltd., Grangemouth, Stirlingshire, Great Britain

7 × 10″, x + 528 pages, 172 tables, 174 illus., 1206 lit.refs., 1965, Dfl. 72.50, £ 8.10.0

Contents: 1. The historical development of antioxidants. 2. Peroxides. 3. Autoxidation. 4. Antioxidants: radical chain-breaking mechanisms. 5. Antioxidants: Preventive mechanisms. 6. Measurement of oxidative deterioration. 7. Oxidative deterioration of saturated oils and polymers. 8. Oxidation of olefinic oils, fats and polymers. 9. Degradation of vulcanised rubber. 10. Mechano-oxidation of polymers. Index.

Elsevier
Publishing
Company **Amsterdam London New York**

357E

THE BEHAVIOUR OF ION-SELECTIVE SILICONE-RUBBER MEMBRANE ELECTRODES IN SOME NON-AQUEOUS SOLVENTS

The applicability of silicone-rubber ion-selective electrodes was studied in mixtures of distilled water with methanol, ethanol, propanol, or isopropanol. The limit of applicability of the electrodes lies at a 90 % alcohol concentration in aqueous methanol or ethanol solutions, and at 40 % alcohol concentration in aqueous *n*-propanol or isopropanol solutions. The solubility products of the silver halide salts and the selectivity constants of an iodide-selective electrode for other halide ions were measured in aqueous alcohol solutions. The equation previously derived for potentials in aqueous media involving selectivity constants is also valid in non-aqueous media.

N. A. KAZARJAN AND E. PUNGOR,
Anal. Chim. Acta, 51 (1970) 213–220

DETERMINATION OF CYANIDES WITH ION-SELECTIVE MEMBRANE ELECTRODES

The direct and indirect determination of cyanides can be carried out with a silver iodide-based ion-selective electrode. The electrode measures only cyanide ions and does not respond to hydrocyanic acid. A detailed study of metal–cyanide complexes shows that the cadmium and zinc cyanide complexes can participate in the exchange reaction on the membrane surface, but that metal cyanide complexes of higher stability than silver dicyanide have no effect on the electrode. The cyanide-sensitive electrodes can be employed for continuously recording the cyanide content of effluents.

K. TÓTH AND E. PUNGOR,
Anal. Chim. Acta, 51 (1970) 221–230

PREPARATION AND SOME ANALYTICAL APPLICATIONS OF A NEW SULFIDE-SELECTIVE HETEROGENEOUS MEMBRANE ELECTRODE

A new sulfide-selective heterogeneous membrane electrode has been developed by thermomoulding a mixture of silver sulfide and a thermoplastic polymer such as polythene. The membrane is attached to a rigid polythene tubing by suitable treatment without any adhesive. The electrodes show a rapid and stable response and follow the Nernst equation for both silver and sulfide ions. Some applications of these electrodes are discussed.

M. MASCINI AND A. LIBERTI,
Anal. Chim. Acta, 51 (1970) 231–237

ANALYTICAL APPLICATIONS OF THE SILVER–IMIDAZOLE COMPLEX ELECTRODE

(in French)

A quantitative study of the equilibria in the complex formation between silver(I) and imidazole at 25° in 0.5 *M* potassium nitrate has made it possible to determine this ligand very rapidly. Moreover, the stability constants of the complexes of a second metal which is in competition with silver(I) under the same conditions can be established. The principle has been applied to the determination of the stability constants of the cadmium(II)–imidazole system.

G. BERTHON AND C. LUCA,
Anal. Chim. Acta, 51 (1970) 239–248

ADHESION AND ADHESIVES

2nd, completely revised, edition

edited by R. Houwink and G. Salomon

Volume 1

Adhesives

7 × 10", xvi + 548 pages, 72 tables, 150 illus., 1965, £ 8.0.0, Dfl. 67.50

The introductory chapter of this first volume is a concise guide to the scientific background of all adhesive processes. Surface science and bulk properties of solids, as related to adhesive bonding, are discussed and illustrated by recent examples from the technology of metals, glass, rubber and plastics. An annotated bibliography is provided for the reader who wants access to more highly specialized works. The further nine chapters, making up the volume, cover the basic materials used in adhesion technology. Greatest attention is paid to synthetic adhesives, especially the classical thermohardening and the new epoxy resins. Fields previously examined in the first edition have been extended, and a brief contribution added on the adhesion of glass and on glass-to-metal bonding.

CONTENTS:

1. Adhesion. 2. Animal glue and related protein adhesives. 3. Vegetable adhesives. 4. Synthetic organic adhesives. 5. Bituminous binders and coatings. 6. Rubbers. 7. Glass, enamels and ceramics. 8. Inorganic adhesives and cements. Part A: Soluble silicates. 9. Inorganic adhesives and cements. Part B: Miscellaneous inorganic materials. 10. Metallic adhesives. Appendix: Historical table. Subject index.

Volume 2

Applications

7 × 10", xiv + 590 pages, 21 tables, 300 illus., 1967, £ 8.0.0, Dfl. 67.50

In this second volume the main trends in industrial application are outlined by sixteen specialists. Assessment of surface geometry, choice of surface treatment, and selection of the most economical bonding process — the correct decision in each case is the basis for any successful engineering process. The introductory chapter deals with this general background; it links the two volumes and extends the annotated bibliography to 1966. Two compact "adhesives charts" facilitate the choice of a candidate adhesive and of processing methods. The work also contains a Subject Index to Volume 2 and an Author Index to both volumes.

CONTENTS:

Introduction. 11. Surface texture. 12. Surface treatment of adherends. 13. Adhesive bonding processes. 14. Wood, reconstituted wood and glued laminated structures. 15. Adhesive-bonded metal structures. 16. Bonded composite structures. 17. Pressure-sensitive adhesive tapes. 18. Rubber-textile structures. 19. The tack of printing inks. 20. Adhesion in paint technology. 21. Miscellaneous applications. 22. Testing of adhesives. 23. Mechanical testing of bonded joints. Appendix: Adhesives charts. Subject index. Author index to Volumes 1 and 2.

Elsevier
Publishing
Company

Amsterdam London New York

194E

METAL–PYRIDINE-2-ALDEHYDE-2′-PYRIDYLHYDRAZONE COMPLEXES AS VISUAL ACID–BASE INDICATORS

PART I. INDICATOR CONSTANTS, COLOUR CHANGES AND TITRATIONS

The PAPHY complexes of certain metals are suggested as acid–base indicators. The colour change intervals of aqueous solutions of the complexes of Cu(II), Fe(II), Ni(II), Zn(II), and Cd(II) have been studied. Apparent indicator constants have been determined. The performance of the indicators in titrations of weak and strong acid and bases is excellent

A. J. Cameron and N. A. Gibson,
Anal. Chim. Acta, 51 (1970) 249–256

METAL–PYRIDINE-2-ALDEHYDE-2′-PYRIDYLHYDRAZONE COMPLEXES AS VISUAL ACID–BASE INDICATORS

PART II. EXTRACTIVE END-POINT TITRATIONS AND pH OF EXTRACTION

The PAPHY complexes of copper(II), iron(II) and nickel(II) are shown to be very good indicators for extractive end-point in acid–base titrations. The pH ranges for extraction of the complexes have been established, and their relevance to the extractive end-points is discussed.

A. J. Cameron and N. A. Gibson,
Anal. Chim. Acta, 51 (1970) 257–263

STABILITY CONSTANTS OF METAL COMPLEXES OF BITHIONOL, FENTICLOR AND HEXACHLOROPHENE

The stability constants of several metal complexes of bithionol, fenticlor and hexachlorophene in $3+1$ (v/v) ethanol–water at ionic strength 1 have been determined. Values of log K_1 for complexes of bithionol and fenticlor follow the Irving–Williams' order, but the values of log K_2 for nickel are greater than those for copper.

A. G. Fogg, A. Gray and D. Thorburn Burns,
Anal. Chim. Acta, 51 (1970) 265–270

AN EXTRACTION–SPECTROPHOTOMETRIC METHOD FOR THE DETERMINATION OF ZINC WITH 1-[(5-CHLORO-2-PYRIDYL)AZO]-2-NAPHTHOL

Zinc(II) reacts with 1-[(5-chloro-2-pyridyl)azo]-2-naphthol (5-Cl-β-PAN) in aqueous solution; the complex can be extracted with various organic solvents at pH 8–11.0 to give a red solution with an absorbance peak at 564–570 nm. The colour in ether is stable and the system conforms to Beer's law; the optimal range for measurement in 1.00-cm cells is 0.05–0.5 p.p.m. zinc in the ether layer. Common anions and cations do not interfere. Large amounts of some cations can be masked by potassium cyanide, the zinc cyanide complex being demasked by formaldehyde. The proposed method is one of the most sensitive and selective procedures for the determination of zinc. The molar absorptivity in the ether extract is $8.4 \cdot 10^4$ l mole^{-1} cm^{-1} at 564 nm.

S. Shibata, M. Furukawa and S. Sasaki,
Anal. Chim. Acta, 51 (1970) 271–276

Elsevier Titles in Chemistry

INORGANIC CHEMISTRY

A Guide to Advanced Study

Third, completely revised edition

by **R. B. Heslop** and **P. L. Robinson**

6×9″, viii+774 pages, 155 tables, 400 illus., 227 lit. ref., 1967, Dfl. 32.50, 65s.

Contents: Modern inorganic chemistry. The atomic nucleus: genesis of the elements. Radiochemistry. Electronic structures of atoms. The periodic table. Valency; nature and classification of chemical bonding. Structure and shape of molecules. Bonding and structure in compounds of non-transition elements. Bonding in transition-metal complexes. The solid state. Oxidation-reduction: redox reactions. Acids and bases. Hydrogen. The hydrides. The noble gases. The alkali metals. Beryllium, magnesium and the alkaline earth metals. Boron and aluminium. Gallium, indium and thallium. Carbon and silicon. Organometallic compounds. Germanium, tin and lead. Nitrogen and phosphorus. Arsenic, antimony and bismuth. Oxygen, sulphur, selenium, tellurium and polonium. The oxides. Peroxides and peroxo-compounds. The halogens. The halides and pseudohalides. The transition metals. Complex or co-ordination compounds and ions. Substitution reactions of metal complexes. The lanthanides, scandium and yttrium The actinides. Titanium, zirconium and hafnium. Vanadium, niobium and tantalum. Chromium, molybdenum and tungsten. Manganese, technetium and rhenium. Iron, cobalt and nickel. The platinum metals. Copper, silver and gold. Zinc, cadmium and mercury. Index.

INTRODUCTION TO THE ATOMIC NUCLEUS

Volume 3 in a collection of monographs on "*Topics in Inorganic and General Chemistry*" edited by P. L. Robinson

by **J. G. Cuninghame**

5½×8½, xi+220 pages, 3 tables, 58 illus., 170 lit. refs., 1964, Dfl. 15.00, 35s.

Contents: Historical introduction. General definitions and properties. Nuclear forces. Stable nuclides. Radioactivity. Nuclear models. Nuclear reactions. Fission. Alpha-decay. Beta-decay. Gamma-emission. Interaction of particles and rays with matter. Index.

INTRODUCTION TO NUCLEAR CHEMISTRY

by **D. J. Carswell**

5½×8½″, ix+279 pages, 23 tables, 69 illus., 1967, Dfl. 32.50, 70s.

Contents: The development of nuclear chemistry. Fundamental particles and nuclear structure. Nuclear reactions and radioactivity. Properties of nuclear radiations. The detection and measurement of nuclear radiation. Nuclear instrumentation. Radiation chemistry. Isotope measurement and separation methods. Charged particle accelerators, neutron sources, production and properties of the actinide elements. Uses of isotopes. Experimental nuclear chemistry. Index.

RADIOCHEMICAL SURVEY OF THE ELEMENTS

Principal Characteristics and Applications of the Elements and their Isotopes

by **M. Haïssinsky** and **J.-P. Adloff**

6×9″, ix+177 pages, 1965, Dfl. 32.50, 75s.

Contents: Introduction. The elements in alphabetical order. Element 102. Element 104.

THE STRUCTURE OF INORGANIC RADICALS

An Application of Electron Spin Resonance to the Study of Molecular Structure

by **P. W. Atkins** and **M. C. R. Symons**

6×9″, x+280 pages, 57 tables, 74 illus., 357 lit. refs., 1967, Dfl. 60.00, £7.0.0.

Contents: Introduction. An introduction to electron spin resonance. Formation and trapping of radicals. Trapped and solvated electrons. Atoms and monatomic ions. Diatomic radicals. Triatomic radicals. Tetra-atomic radicals. Penta-atomic radicals. Summary and conclusions.

Appendices: The language of group theory. The spin hamiltonian. Calculation of *g*-values. Determination of spin-density distribution and bond angles. Analysis of electron spin resonance spectra. Index.

Elsevier
Publishing
Company

Amsterdam London New York

DETERMINATION OF THE MINIMUM SOLUBILITY OF THE NEW CHROMOGENIC REAGENT PALLADIAZO BY A SPECTROPHOTOMETRIC METHOD BASED ON ISOSBESTIC POINTS

The instability characteristics of various 1,8-dihydroxynaphthalene-3,6-disulphonic-2,7-bis[azophenyl-*p*-arsonic] acid (palladiazo) solutions in different perchloric acid media have been studied in detail. Isosbestic points corresponding to stepwise protonation equilibria were utilized in a spectrophotometric method for determining the minimum solubility of palladiazo. The minimal solubility ($4.63 \cdot 10^{-6}$ M; 3.6 mg l^{-1}) was found at an acidity value $H_0 = -1.55$ (*ca.* 3.5 M perchloric acid). The semicolloidal nature of the reagent was established. The most probable nature and structure of the precipitated palladiazo species are discussed. The experimental conditions for minimal solubility are valuable for purification of the reagent.

J. A. Pérez-Bustamante and F. Burriel-Martí,
Anal. Chim. Acta, 51 (1970) 277–285

THE DETERMINATION OF INDIUM IN SEA WATER

A chelating ion-exchange technique is used for the concentration of indium from sea water. After purification by chloro-anion exchange, the separated indium is determined by neutron activation analysis. The concentration of indium in Atlantic Ocean water was found to be *ca.* 0.1 ng l^{-1}. The method has a sensitivity of 0.006 ng l^{-1}.

A. D. Matthews and J. P. Riley,
Anal. Chim. Acta, 51 (1970) 287–294

A STUDY OF SUGAWARA'S METHOD FOR THE DETERMINATION OF IODINE IN SEA WATER

Several sources of error have been found in Sugawara's method for the determination of iodine in sea water. These are minimized in the modified procedure which has been developed. Iodide is coprecipitated quantitatively with silver chloride by silver ions slowly liberated into the water by the dissolution of silver citrate. The iodide present in the precipitate is oxidized to iodate by means of bromine under the influence of ultrasonic agitation. After destruction of hypobromite, iodine is determined either by photometric titration, or by spectrophotometry. Iodate is not coprecipitated by silver chloride, but can be determined after reduction with hydrazine sulphate. The titrimetric and spectrophotometric methods give recoveries of iodide- and iodate-iodine of 99.0±0.4% and 98.5±0.6% respectively, and have coefficients of variation of ±0.4% and ±0.8%.

A. D. Matthews and J. P. Riley,
Anal. Chim. Acta, 51 (1970) 295–301

SPOT TESTS IN ORGANIC ANALYSIS

Seventh English Edition, completely revised and enlarged

by FRITZ FEIGL in collaboration with VINZENZ ANGER

6 x 9", xxiii + 772 pages, 19 tables, over 2000 lit.refs., 1966, Dfl. 85.00, £10.0.0.

This 7th edition has involved complete revision and reorganisation of the subject in order to present a still clearer picture of the multitudinous applications open to organic spot test analysis. The amount of new work which is appearing has certainly necessitated expansion, but the author has kept this to a minimum by omitting the chapter on spot test techniques (which are covered in the companion volume *Spot Tests in Inorganic Analysis*) and by limiting the number of tables and structural formulae.
Comparison with the 6th edition reveals the following differences:

	Number in	
	6th Edn.	7th Edn.
Preliminary tests	32	45
Functional group tests	70	109
Individual compound tests	133	148
Detection of particular structures and types of compounds	0	74
Differentiation of isomers etc.	0	54
Applications in the testing of materials etc.	111	131

In total the book now gives in 561 sections information on more than 900 tests compared with 600 tests in 346 sections in the preceding edition.

An important feature is the inclusion of a large number of recently developed tests and comments which have not hitherto been published in any form.

It is the author's hope that this work will help to correct the widespread impression that physical instrumentation is always superior to chemical methods for solving analytical problems. Each of the chapters presents instances of problems for which no solutions by physical means have yet been developed, or for which the rapid spot tests are equal or superior to the expensive instrumental procedure.

CONTENTS: 1. Development, present state and prospects of organic spot test analysis. 2. Preliminary (exploratory) tests. 3. Detection of characteristic functional groups in organic compounds. 4. Detection of structures and certain types of organic compounds. 5. Identification of individual organic compounds. 6. Application of spot tests in the differentiation of isomers and homologous compounds. Determination of constitutions. 7. Application of spot reactions in the testing of materials, examinations of purity, characterization of pharmaceutical products, etc... Appendix: Individual compounds and products examined. Author index. Subject index.

OM REVIEWS OF THE NEW EDITION

... As we have come to expect, Professor FEIGL has once more provided an outstanding service to the chemical community ...

Analytica Chimica Acta

... C'est pourquoi le livre du professeur FEIGL est extrêmement précieux pour le chimiste comme le montre la succession des éditions ...

Bulletin de la Société Chimique de France

... This volume, together with its companion on "Spot Tests in Inorganic Analysis" (5th ed., 1958), is a useful and authoritative source of information not only to analytical chemists but also to organic chemists, pharmaceutical chemists, and biochemists. Advanced students and research workers in analytical chemistry will find these two volumes stimulating and helpful ...

Analytical Chemistry

... As each successive edition of this book appeared, it was greeted with ever increasing praise. It is difficult, therefore, to find adequate superlatives to describe this new, completely revised edition ...
... The astonishing range of applications of the tests makes this book essential for every chemist concerned with organic compounds ...

Chemistry in Britain

Elsevier
Publishing
Company AMSTERDAM LONDON NEW YORK

147E

A RAPID METHOD FOR RESIDUE ANALYSIS BY COLUMN LIQUID CHROMATOGRAPHY WITH POLAROGRAPHIC DETECTION

APPLICATION TO THE DETERMINATION OF PARATHION AND METHYLPARATHION ON CROPS

A rapid, sensitive, selective and simple method for the determination of residues of methylparathion and parathion on crops is described. Extraction is carried out with ethanol. The extract is diluted with an aqueous acetate buffer solution and immediately analysed by means of column liquid chromatography with polarographic detection. For lettuce the recovery is about 90%. The limit of analysis is about 0.03 p.p.m. Quantitative measurements of residue traces on crops can be carried out with a precision of better than 10%.

J. G. KOEN AND J. F. K. HUBER,
Anal. Chim. Acta, 51 (1970) 303–307

CHARACTERISATION OF AMIDINES AS PICRATES THROUGH THIN-LAYER CHROMATOGRAPHY

Picrates of a series of amidines, including some 2- and 4-amino-substituted N-heterocycles, have been prepared. All were titratable with perchloric acid in glacial acetic acid. All the amidines investigated formed only monopicrates except guanidinoacetic acid which formed both a monopicrate and a semipicrate. Thin-layer chromatography on silica gel showed that aliphatic amidines and most 2-amino-substituted N-heterocycles could be characterised through their R_{Pi} values (with reference to picric acid) with ethyl acetate as the mobile phase. With 4-amino-substituted N-heterocycles and with three 2-amino-substituted pyridazines investigated, the mobile phase caused partial dissociation, thus invalidating the use of TLC for these substances. Perchlorates of the amino-substituted pyridazines were isolated. One of the diaminopyridazines formed a stable diperchlorate, another diaminopyridazine gave an unstable diperchlorate. The monoamino-substituted pyridazines formed only monoperchlorates.

S. VEIBEL,
Anal. Chim. Acta, 51 (1970) 309–315

ANALYSIS OF BINARY MIXTURES OF HEXAALKYLDITIN COMPOUNDS BY A DIFFERENTIAL RATE METHOD

Differential analysis of mixtures of alkylditin compounds, based on their different rates of reaction toward silver ions, is discussed. Binary mixtures of hexamethyl-, hexaethyl- and hexabutylditin can readily be determined.

P. ZAIA, V. PERUZZO AND G. PLAZZOGNA,
Anal. Chim. Acta, 51 (1970) 317–321

THE CHEMICAL COMPOSITION OF ACID-OXIDIZED, WET-ASHED RESIDUES

The chemical composition of inorganic residues after typical acid oxidation treatment has been investigated. X-Ray diffraction and infrared data are included for particular chemicals and biological materials which have been wet-ashed.

R. E. MANSELL, R. P. TESSNER AND E. J. HUNEMORDER,
Anal. Chim. Acta, 51 (1970) 323–328

Announcing a NEW Journal

thermochimica acta

Editor-in-Chief:

W. W. Wendlandt (Houston, Texas, U.S.A.)

THERMOCHIMICA ACTA is concerned with the broader aspects of thermochemistry and its applications to chemical problems. It will publish original research contributions in the field of thermochemistry and chemical thermodynamics.

Specific areas involved are static calorimetry of all types, dynamic calorimetry of all types, including differential scanning calorimetry, specific heat calorimetry and other types of calorimetric measurements, high temperature chemical thermodynamic studies, the thermochemistry of high temperature reactions and thermoanalytical studies of all kinds.

The main field of science to be covered will be the chemical research areas of inorganic, organic, physical and analytical chemistry. However thermochemical studies in other areas such as biochemistry, geochemistry, metallurgy, soil science, geology and ceramic science may also be included.

THERMOCHIMICA ACTA will be published in yearly volumes of six bimonthly issues. The subscription price per volume will be approximately Dfl. 81.00 plus Dfl. 5.40 postage or, equivalent (US$22.50 plus US$1.50 or £9.8.0 plus 13s. as of August 15, 1969). The first issue is scheduled for publication in early 1970.

A notice to Authors and a free specimen copy are available from the publisher at the address below. Subscription orders may be placed with your usual supplier or direct with Elsevier Publishing Company, P.O. Box 211, Amsterdam, The Netherlands.

Elsevier

P.O. Box 211
AMSTERDAM - The Netherlands

436 E

SEQUENTIAL SPECTROPOLARIMETRIC ANALYSIS OF MIXTURES OF BARIUM–CALCIUM, CADMIUM–COPPER AND CADMIUM–ZINC

A direct sequential spectropolarimetric titration method based on the stereospecific ligand D-(−)-1,2-propylenediamine tetraacetic acid was developed for the following three mixtures: barium–calcium, cadmium–copper, and cadmium–zinc. In a single titration, without changing the pH or other environmental conditions, mixtures that cannot be sequentially titrated visually in aqueous solution, can be successfully titrated. Because the optically active titrant and the stereospecifically formed complexes have molecular rotations significantly different from each other, they serve as self-indicators for the two titration end-points. Both the precision and accuracy of the sequential spectropolarimetric titrations are excellent and the range of the average deviations was 0.0 to 0.37%.

R. J. Palma, Sr., P. E. Reinbold and K. H. Pearson,
Anal. Chim. Acta, 51 (1970) 329–335

A SIMPLE CHEAP CONTINUOUS FLUX MONITOR FOR 14-MeV NEUTRONS

(Short Communication)

P. J. Mathew and K. P. Pohl,
Anal. Chim. Acta, 51 (1970) 336–338

SEMI-CONTINUOUS AMPEROMETRIC TECHNIQUE FOR ION-EXCHANGE KINETICS

(Short Communication)

J. Kendler and C. Heitner-Wirguin,
Anal. Chim. Acta, 51 (1970) 338–341

DETERMINATION OF NANOGRAM AMOUNTS OF CHROMIUM BY THE COPPER-SPARK METHOD

(Short Communication)

C. D. Manning and K. Beyermann,
Anal. Chim. Acta, 51 (1970) 342–343

THE USE OF AN ALTERNATING ELECTROMAGNETIC FIELD TO MODULATE LIGHT IN AN ELECTRODELESS TUBE FOR THE DETERMINATION OF NEON AND ARGON IN HELIUM BY ATOMIC ABSORPTION

(Short Communication)

J. A. Goleb,
Anal. Chim. Acta, 51 (1970) 343–347

OXIDATION AND COMBUSTION REVIEWS

edited by **C. F. H. TIPPER,** *Senior Lecturer in the Department of Inorganic, Physical and Industrial Chemistry, University of Liverpool, England*

Volume 1

APPLICATION OF THE THEORY OF BRANCHED CHAIN REACTIONS IN LOW-TEMPERATURE COMBUSTION. **R. Ben–Aim and M. Lucquin**
OXIDATION REACTIONS INDUCED BY IONISING RADIATION. **G. Hughes**
GAS PHASE PHOTO-OXIDATION. **G. R. McMillan and J. G. Calvert**
OXIDATION REACTIONS INVOLVING NITROGEN DIOXIDE. **J. H. Thomas**
OXIDATIVE DEGRADATION OF HIGH POLYMERS. **W. L. Hawkins**
THE HETEROGENEOUS SELECTIVE OXIDATION OF HYDROCARBONS. **R. J. Sampson and D. Shooter**

6 x 9", vii + 344 pages, 29 tables, 45 illus., 815 lit. refs., 1966 hardbound only, US$15,00 plus $0.50 postage

Volume 2

THERMAL EXPLOSION THEORY. **P. Gray and P. R. Lee**
SOME FUNDAMENTALS OF COMBUSTION INSTABILITY. **R. F. Salant and Tau–Yi Toong**
THE USE OF ADIABATIC COMPRESSION AND MASS SPECTROMETRY IN THE STUDY OF COMBUSTION. **A. Martinengo and K. H. Homann**
TRAPPED RADICALS AND COMBUSTION. **A. Thomas**

6 x 9", vii + 301 pages, 19 tables, 64 illus., 311 lit. refs., 1967, hardbound only, US$15.00 plus $0.50 postage

Volume 3

THE MECHANISM OF COMBUSTION OF DROPLETS AND SPRAYS OF LIQUID FUELS. **A. Williams**
THE LOW TEMPERATURE GAS-PHASE OXIDATION OF LOWER ALIPHATIC ALDEHYDES. **J. F. Griffiths and G. Skirrow**
IONIZATION IN COMBUSTION PROCESSES. **W. J. Miller**
AMMONIUM PERCHLORATE AS AN OXIDIZER. **A. R. Hall and G. S. Pearson**

1968, two issues, US$12.50 plus US$0.50 postage

Volume 4

PERCHLORATE OXIDIZERS. **G. S. Pearson**
FORMATION AND BEHAVIOUR OF CHEMI-IONS IN FLAMES. **J. Peeters, C. Vinckier and A. van Tiggelen**
THE USE OF ISOTOPES IN THE STUDY OF OXIDATION AND COMBUSTION PROCESSES. **D. Gál**
GAS PHASE REACTIONS OF THE HYDROXYL RADICAL. **D. D. Drysdale and A. C. Lloyd**

1969, two issues, US$12.50 plus US$0.50 postage

For 1970. One volume, two issues. Subscription price: US$12.50 plus $0.50 postage per volume

A free specimen copy will be sent on request
Orders should be sent to: Dept. OXCOM

Elsevier

P.O. Box 211
Amsterdam – The Netherlands
107Ea

Analytica Chimica Acta
Elsevier Publishing Company, Amsterdam
Printed in The Netherlands

HIGH-SOLID SAMPLES IN ATOMIC-ABSORPTION FLAME SPECTROPHOTOMETRY*

AUGUST HELL AND JUAN RAMÍREZ-MUÑOZ
Beckman Instruments, Inc., Fullerton, Calif. 92634 (U.S.A.)

(Received April 11th, 1970)

Since atomic-absorption spectroscopy was introduced as a new instrumental analytical method, most workers in this field have been interested in obtaining the highest possible sensitivity in terms of signal size. This was reasonable since atomic-absorption spectroscopy showed great possibilities for highly sensitive determinations, and most effort was directed towards new developments which permitted quantitative data to be obtained at very low concentration ranges for a number of analytes.In 1965, a heated-chamber laminar-flow burner was introduced by HELL[1]. This burner was utilized initially with air–acetylene, air–propane, air–hydrogen and argon-entrained air–hydrogen flames; its use with nitrous oxide–acetylene flames enlarged the possibilities of determination at low concentration levels for a considerable number of elements[2,3]. At the same time, the need of instrumentation of high stability which would allow high signal-to-noise ratios was seriously considered.

The demand for high sensitivity remains and has even increased for a variety of analytical problems. Accordingly, burners that yield high sensitivity, such as the heated-chamber laminar-flow burner, should be considered as a first choice. But the extension of atomic-absorption spectroscopy to so many analytical areas has necessitated consideration of other aspects, *e.g.* the handling of samples of extreme acidity or high salt content, and the routine use of non-aqueous solutions (organic solvent extracts).

Solutions containing high concentrations of salts may produce deposits (and consequent memory effects), and strongly acidic solutions may dissolve deposits from previously sprayed solutions (memory, contaminations). Accordingly, a new laminar-flow burner, distinguished in this paper with the name of Autolam burner, which is suitable for cold operation, has been designed[4].

This paper contains a brief description of some of the features of this new burner and of some of the experimental work developed with it. The burner was carefully studied in order to improve sensitivity in comparison with existing cold-operation burners, and, at the same time, to improve its resistance to corrosion and the ease of routine cleaning operations, after prolonged use with high-solid samples.

---

* This paper was presented at the Pittsburgh Conference on Analytical Chemistry and Applied Spectroscopy, Cleveland, Ohio, March, 1970.

EXPERIMENTAL

Instruments

Determinations were performed with Beckman Model 440 and Model 448 Atomic Absorption Spectrophotometers; a general description of these instruments has been published elsewhere[5]. Although the Model 440 instrument can provide experimental data as direct readings on a digital readout (the other, Model 448, has a direct reading scale), most of the experiments have been done with the help of 10-in and 5-in potentiometer recorders.

Autolam burner

This is a new burner with a simplified design as shown in Fig. 1. Two versions have been prepared: one is completely open and without chimney, and the other is covered with a metal housing and provided with a chimney. The latter model can also be used with a round-table sampler suitable for 20 samples, which allows automatic sample feeding.

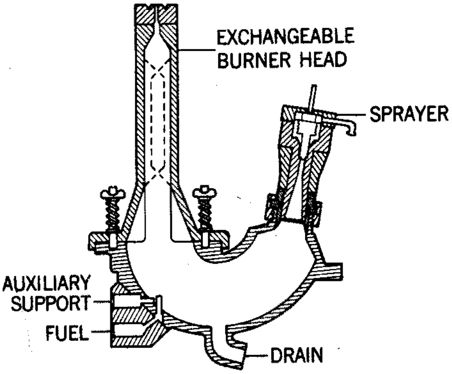

Fig. 1. Schematic view of the burner.

The sprayer is made of Penton and stainless steel in all areas which are exposed to the liquid sample or its mist. The sprayer is located in a small spray injector also made of Penton. The spray chamber which follows the spraying section is protected with a coating resistant to acids and most common solvents used in atomic absorption. Over this chamber is located the stainless steel burner head, which is maintained in position with two spring-loaded screws. The springs can release any overpressure which may build up inside the burner. The spray injector also can easily be released in such a circumstance. Two heads have been prepared: one has two slots for air–acetylene flames, and the other for nitrous oxide–acetylene flames has a single narrow slot. The Autolam burner can also be used with air–hydrogen, argon–entrained air–hydrogen and nitrous oxide–Mapp gas flames[6].

The burner has manual control valves for auxiliary support gas, and for varying the fuel flow. It also has a safety valve (covered model) to cut off the fuel flow in case of a drop in the pressure of the support gas.

The suction rate (aspiration rate) can be changed with a set of capillaries of different internal diameter.

The head of the burner can be rotated. A stop and a circular scale easily permit the operator to reproduce rotation angles. The alignment of the burner is done by means of a frontal leveling mechanism.

For cleaning, the head can be taken off by taking out the nuts of the two spring-loaded screws; the spray injector is pulled out; the lower chamber is maintained in position only by two positioning springs.

Two sets of lips have been used in the nitrous oxide–acetylene head: a 5-cm slot and a 7-cm slot. The long slot has been successfully tested in determinations with organic solvent systems.

The design of this burner was developed very carefully with consideration of different aspects as summarized in the following paragraphs.

The whole body and head of the burner were made of stainless steels as an added personal protection for the operator in case of any accidental flashback caused by incorrect use of gases or heads. The two spring-loaded screws which maintain the burner head in position and the easy release of the complete sprayer section should also be considered as relief mechanisms for the protection of the operator in case of a flashback. The head moves up, releasing the pressure, and the complete sprayer section section snaps out, remaining inside the area, tied by the tubing attached to the support gas inlet. On the other hand, these features also help in the cleaning operation of the burner, as the head and the sprayer section can be taken off leaving the rest of the burner completely accessible for flushing with water, without the need of taking the burner out of the instrument.

Every portion of the burner is designed so that any liquid settling on the walls, as a result of partial deposition of the spray, will flow freely to the lowest part where the drain is attached. By changing the direction of the mist flow by about 180°, with respect to the burner head, heavy droplets fall out, and the mist reaching the flame becomes more uniform.

The long burner head accomplished another function. While the mixture of sample fog and gas rises in the head, a pre-evaporation of the mist takes place which in its turn avoids any clogging in the slots, or in the walls of the burner head lips. At the same time, it helps to obtain a fast evaporation of the remaining fine droplets of the sample solution mist when reaching the flame.

The fuel gas is injected in the exit of the spray chamber to reduce the amount of explosive gas mixture contained in the interior of the burner.

At the exit of the spray chamber there is a Teflon diaphragm that also acts as a seal. This diaphragm has an opening of relatively small diameter in order to generate turbulence that helps to obtain good mixing of support gas and fuel, just before the point at which the gaseous combustion mixture enters into the burner head.

Perhaps one of the most important features in the design of the burner is the aspiration system, which includes a sprayer with a Penton tip and a funnel-like spray injector. The combined action of the sprayer and the spray injector is such that the suction action is not only produced by the sprayer but also by the injector funnel itself. This means in practice that the system is less sensitive against pressure fluctuation of the support gas or a slight variation of the critical sprayer orifice.

In regard to nebulization, this system acts like a sample counter-flow; strong turbulence at the sprayer tip causes a small amount of the sample solution to rotate at high frequencies at both shoulders of the sprayer. In this process the liquid is finely divided by the center jet stream and carried in the form of a very homogeneous fog out of the straight portion of the funnel. This circular oscillation of the liquid at the sprayer tip has also an extremely effective cleaning action; this eliminates any memory effects if samples of extremely different concentrations are aspirated successively. Furthermore, it prevents the formation of any deposits at the sprayer tip, which might cause clogging with highly viscous solutions, or even suspensions. The sprayer tip is made of Penton (precision molded within 0.0005 in) to give uniform spraying performance. The low heat conductivity of the sprayer tip also prevents strong cooling of the tip, owing to the consumption of heat in the mechanical action of disintegrating the liquid into fine drops. A strong cooling of the sample, otherwise, might result in a partial solid phase separation.

All these features contribute to the good performance and high reliability of the burner in highly concentrated and/or viscous sample solutions.

Solutions

Most of the tests described below were done with aqueous solutions, unless other systems are specified.

Data reduction techniques

In some cases, computer techniques were used as described elsewhere[7-9].

RESULTS AND DISCUSSION

Different aspects of the analytical behavior of this burner were studied. Some results are presented and briefly discussed in the following sections.

Sensitivity values

The response of the burner in terms of *percentual sensitivity* and *fluctuational*

TABLE I

AUTOLAM BURNER: PERCENTUAL CONCENTRATION LIMITS

(Experimental conditions: air–acetylene flame, air–acetylene burner head, no rotation, single pass, model 440 Atomic Absorption Spectrophotometer)

Analyte	*Wavelength (nm)*	*p.p.m. of analyte to produce a signal of 1% absorption*
Cadmium	228.8	0.022
Calcium	422.7	0.11
Chromium	357.9	0.095
Cobalt	240.7	0.5
Copper	324.8	0.048
Indium	304.0	0.62
Iron	248.3	0.069
Lead	283.3	0.31
Magnesium	285.2	0.0051
Manganese	279.5	0.031
Nickel	232.0	0.38
Silver	328.1	0.056
Sodium	589.0	0.0067
Zinc	213.9	0.010

sensitivity[10] was studied for a series of analytes. Values are expressed in concentration limits in p.p.m. In Table I percentual concentration limits (p.p.m. of analyte necessary to produce a signal of 1% ABSN) are compiled for several elements frequently determined by atomic absorption with air–acetylene flames. The figures shown indicate that determinations can be performed at really low concentration levels.

Fluctuational sensitivity, also expressed in terms of the corresponding fluctuational concentration limits, is represented in Table II for elements determinable with air–acetylene and nitrous oxide–acetylene flames.

TABLE II

AUTOLAM BURNER: FLUCTUATIONAL CONCENTRATION LIMITS

(Experimental conditions: AAF = air–acetylene flame with air–acetylene burner head; NOAF = nitrous oxide–acetylene flame with nitrous oxide–acetylene burner head; no rotation; single pass; model 440 Atomic Absorption Spectrophotometer; no scale expansion (1 ×); 10-sec time constant)

Analyte	*Wavelength (nm)*	*Flame*	*p.p.m. of analyte to produce a signal equal to the peak-to-peak noise (0% ABSN level)*
Aluminum	309.2	NOAF	0.15
Bismuth	223.1	NOAF	0.17
Boron	249.7	NOAF	0.22
Cadmium	228.8	AAF	0.0012
Calcium	422.7	AAF	0.0044
Chromium	357.9	AAF	0.0040
Cobalt	240.7	AAF	0.026
Copper	324.8	AAF	0.0025
Erbium	400.8	NOAF	0.10
Europium	459.4	NOAF	0.90
Gadolinium	368.4	NOAF	4.0
Germanium	265.2	NOAF	0.27
Indium	304.0	AAF	0.048
Iron	248.3	AAF	0.0060
Iron	248.3	NOAF	0.017
Lead	283.3	AAF	0.015
Magnesium	285.2	AAF	0.00040
Manganese	279.5	AAF	0.0018
Molybdenum	313.3	NOAF	0.010
Neodymium	463.4	NOAF	8.0
Nickel	232.0	AAF	0.025
Niobium	334.9	NOAF	14.0
Praseodymium	495.1	NOAF	0.90
Silicon	251.6	NOAF	0.79
Silver	328.1	AAF	0.0022
Sodium	589.0	AAF	0.00060
Tantalum	271.5	NOAF	6.3
Tin	286.3	NOAF	1.0
Tungsten	255.1	NOAF	3.4
Vanadium	318.4	NOAF	0.044
Yttrium	410.2	NOAF	0.90
Zinc	213.9	AAF	0.00064

Since many workers are interested in the limits of detection of new instrumentation, special attention was devoted to the obtaining of fluctuational concentration limits. All values presented in Tables I and II were obtained with simple aqueous solutions under optimal conditions of the instrumental system at the parameters stated in the Tables. In samples of complicated composition, smaller sensitivity should be expected (both percentual and fluctuational), as a consequence of matrix effects.

When it is necessary to work at high concentration levels of analyte, it is possible to take advantage of the rotation of the head. This capability permits the analyst to decrease the sensitivity in the analytical operation and to enlarge the dynamic concentration range towards the high concentration end.

Acidic solutions

Two cases are mentioned here: the determination of silver and the determination of copper, both in 50% nitric acid solutions. In spite of the high concentration of mineral acid, no serious damage was observed after prolonged use of the burner in routine determination of these elements. Low concentrations of silver were determined by using standards prepared also with 50% nitric acid. In the case of copper it was necessary to switch from low to high concentration and *vice versa*. Rotation of the burner head was used to cover two concentration ranges: up to 50 p.p.m. and up to 800 p.p.m. Cu. The nitrous oxide–acetylene head (single slot) was also used. This head made it possible to switch from high concentration levels to low concentration levels without any danger of contamination and memory effects.

Suspensions

An extreme case of handling of high-solid samples was the analysis of suspensions of insoluble materials in aqueous solutions with some suspending agent (gelatine, starch, agar–agar, glycerine mixed with isopropanol). Several elements have been determined with the suspension technique in soils, meteorites and cosmetics. The analysis of suspensions has been reported previously[11].

Copper–cadmium systems

This system has been studied in order to establish the necessary basis for the determination of impurities of copper in high-purity cadmium metal and cadmium salts. Copper was tested at the 5-p.p.m. Cu level for interference ratios from 7840:1 to 20:1 ([Cd]/[Cu]). Limiting interference ratios[12] were studied in sensitivity diagrams[12] at cadmium concentrations close to 40,000 p.p.m. At this high cadmium concentration, only slight depressions of the copper signal were observed. These depressions were so small that for practical purposes the copper can be determined with copper standards without any compensation for high cadmium concentrations. This is an advantage in the case of routine analysis of samples containing widely variable amounts of cadmium. No cloggings or deposits were observed during the studies performed with the copper–cadmium system[11].

Iron and copper determination in beer

Owing to the low concentrations permissible for these analytes in finished products in the beer industry, degassed undiluted samples were directly aspirated into the burner. Samples were diluted with an equal volume of water only when examined by addition method. Slight clogging was observed at the sprayer section when undiluted samples were aspirated if no flushing was used between samples. The higher final numerical values observed for copper and iron by the addition method, in comparison with determinations made with aqueous standards, demonstrate a decrease of analyte signals because of matrix interference effects. For accurate analyses, determinations by the addition method are recommended.

Biological samples

A long-term research project is in progress on the application of the Autolam burner to the analysis of a variety of biological samples. In some cases the solids contents of the original samples constituted no problem, since the sample was diluted in dilution ratios such as 1:100, 1:200, 1:500, or even smaller. These high dilutions were used mainly for magnesium, sodium, and potassium determinations (in order to bring the analyte down to the most appropriate concentration range), and minimized any effects of the high solids content of the original samples.

In other cases, only small dilution was necessary, *e.g.* in the determination of zinc in human blood serum (where 1:10 and 1:50 dilution ratios were used)[13], and the determination of zinc in cow milk (1:25 dilution ratio). Milk was also directly aspirated into the burner; no clogging or deposits were observed after 3 min of constant aspiration of indiluted milk.

Most severe cases were the determination of calcium in human urine and human blood, where 1000 p.p.m. of lanthanum was added to samples. In the examination of blood serum, samples were only diluted in the dilution ratio 1:25. Even in these extreme cases the only necessary precaution was to flush the burner from time to time with distilled water.

In the biological samples program, the determination of lead in human blood was also included. For this determination it was necessary to extract the lead with ammonium pyrrolidine dithiocarbamate (APDC) and methyl isobutyl ketone (MIBK). The Autolam burner can also easily handle MIBK systems. It was found that better flame conditions and better stability can be obtained for organic solvent systems if the nitrous oxide–acetylene head is used, even if the burner is supplied with compressed air and acetylene. This is in agreement with previous results obtained in the determination of tellurium in MIBK systems, where the same type of head was used (MIBK solutions and mixtures of MIBK and 25% of absolute methanol). Both the 5-cm and 7-cm single slots were used in lead determinations.

Accuracy and precision

Special attention was devoted to accuracy and precision tests with this new burner. Accuracy was found to be similar to that achieved with the heated-chamber laminar-flow burner. Precision remained suitable even in cases in which samples of complicated composition were examined. Actually the burner is not excessively subject to accidental variation that may result in lack of repeatability in recorded signals. The use of moderate scale expansion and moderate noise suppression have helped to improve precision values. Relative standard deviations calculated from repeated readings of the same solution were found to be between 1 and 3%. Relative standard deviations smaller than 1% were found when solutions of simple composition were examined.

Conclusions

The new burner described makes it possible to obtain some of the best sensitivity levels so far reported with a cold-spray chamber and a premix burner. The protective coating of the burner provides good protection in the handling of mineral and organic highly-acidic solutions and non-aqueous systems (organic solvents). The burner has shown virtually no clogging and/or deposit formation. In cases of accumulation of solid materials in the internal parts of the burner, the different sections of the burner can easily be taken apart and cleaned in a few minutes. The burner can be used with a variety of flames; the change of the burner head for different flames, is also an easy and rapid operation.

The authors appreciate very much the help received from Mr. M. E. ROTH in the experimental work described.

SUMMARY

Determination of low analyte concentrations in samples with high concentrations of concomitants is discussed. Highly saline samples often cause problems when examined with burners designed for high-sensitivity operation, unless they are very greatly diluted. Use of new burners designed to handle solutions with high-solid contents is described and illustrated with some practical examples. These burners, which operate with cold spray chambers, offer improvements of sensitivity compared with other cold-operation burners, as well as low clogging disturbances and low memory effects. They also can be used with strongly acidic solutions and with a wide variety of flames.

RÉSUMÉ

Une étude est effectuée sur l'utilisation de nouveaux brûleurs, en spectrophotométrie par absorption atomique, pour échantillons très concentrés. Ces brûleurs opérant avec chambre de vaporisation froide offrent une amélioration de sensibilité par rapport à d'autres dispositifs. Ils peuvent également être utilisés pour des solutions très fortement acides et avec une grande variété de flammes.

ZUSAMMENFASSUNG

Die Bestimmung kleiner Konzentrationen in Proben mit hohen Konzentrationen an Begleitstoffen wird diskutiert. Proben hoher Salzkonzentration führen häufig zu Schwierigkeiten, wenn sie mit Brennern untersucht werden, die für hochempfindliche Arbeitsweise vorgesehen sind, sofern die Lösungen nicht stark verdünnt werden. Die Anwendung von neuen, für hochkonzentrierte Lösungen entworfenen Brennern wird an Hand einiger praktischer Beispiele beschrieben. Diese Brenner, die mit kalten Zerstäuberkammern arbeiten, haben eine bessere Empfindlichkeit gegenüber anderen vergleichbaren Brennern sowie geringe Verstopfungsstörungen und kleine Memory-Effekte. Sie können auch für stark saure Lösungen und für eine Vielfalt von Flammen verwendet werden.

REFERENCES

1 A. Hell, paper presented at the *5th Australian Conference on Spectroscopy, Perth, West Australia, May 1965.*
2 J. Ramírez-Muñoz, *Flame Notes. Beckman*, 1 (1966) 38.
3 J. Ramírez-Muñoz and M. E. Roth, *Flame Notes. Beckman*, 2 (1967) 18.
4 A. Hell, unpublished work.
5 J. Ramírez-Muñoz, *American Laboratory*, August 1969, p. 25.
6 A. Hell and S. G. Ricchio, *Flame Notes. Beckman*, 4 (1969) 37, 41.
7 J. Ramírez-Muñoz, J. L. Malakoff and C. P. Aime, *Anal. Chim. Acta*, 36 (1966) 328.
8 J. L. Malakoff, J. Ramírez-Muñoz and C. P. Aime, *Anal. Chim. Acta*, 43 (1968) 37.
9 J. L. Malakoff, J. Ramírez-Muñoz and W. C. Scott, *Anal. Chim. Acta*, 42 (1968) 515.
10 J. Ramírez-Muñoz, *Talanta*, 13 (1966) 87; *Atomic-Absorption Spectroscopy*, Elsevier Publishing Co., Amsterdam, 1968.
11 J. Ramírez-Muñoz, M. E. Roth and W. F. Ulrich, paper presented in the *Pittsburgh Conference for Analytical Chemistry and Applied Spectroscopy, Cleveland, Ohio, March 2–7, 1969.*
12 J. Ramírez-Muñoz, *Talanta*, 16 (1969) 1037.
13 M. E. Roth and J. Ramírez-Muñoz, *Flame Notes. Beckman*, 4 (1969) 25.

Analytica Chimica Acta
Elsevier Publishing Company, Amsterdam
Printed in The Netherlands

THE DETERMINATION OF COPPER IN IRON AND STEEL BY 14-MeV NEUTRON ACTIVATION ANALYSIS

R. VAN GRIEKEN*, A. SPEECKE AND J. HOSTE
Institute of Nuclear Sciences, Ghent University, Ghent (Belgium)

(Received February 28th, 1970)

Activation analysis with thermal neutrons has been frequently applied to the determination of copper in various materials, as appears for instance from the survey of LUTZ *et al.*[1]. However, the use of 14-MeV neutrons, produced by a neutron generator from the reaction $^{3}H(d,n)^{4}He$, has only been investigated for the determination of copper in minerals, alloys and oil[2-5].

In this paper, a fast and non-destructive 14-MeV neutron activation method is described for the determination of copper in various kinds of steel and cast iron which could be easily applied in industry.

Nuclear data

Irradiation of copper and iron with 14-MeV neutrons gives rise to a large number of possible reactions. Only those of practical importance in this work are given in Table I.

The NaI(Tl) spectra of pure copper and iron, irradiated for 5 sec at a beam intensity of 300 μA (*i.e.* an average neutron flux of *ca.* $8 \cdot 10^{8}$ n cm^{-2} sec^{-1} at the sample) are represented in Fig. 1, curve A and Fig. 2, curve A. It appears that a sensitive copper determination can be expected from the measurement of the annihilation radiation of ^{62}Cu. The 0.511-MeV peak is, however, quite unspecific, as all β^{+} emitters yield a peak of this energy. Moreover, the Compton effect of high-energy γ-radiation due to activation products of iron and steel alloying elements is also very important in the 0.5-MeV energy region *e.g.* ^{28}Al ($T_{\frac{1}{2}}=2.24$ min) from $^{28}Si(n,p)^{28}Al$ and $^{31}P(n,\alpha)^{28}Al$; ^{29}Al ($T_{\frac{1}{2}}=6.6$ min) from $^{29}Si(n,p)^{29}Al$; ^{56}Mn(2.58 h) from $^{56}Fe(n,p)^{56}Mn$; and ^{52}V ($T_{\frac{1}{2}}=3.7$ min) from $^{52}Cr(n,p)^{52}V$ and $^{55}Mn(n,\alpha)^{52}V$. In order to reduce the importance of this interference, preference was given to coincidence measurements of the two annihilation quanta. As both quanta are emitted simultaneously at an angle of 180°, two NaI(Tl) detectors were mounted, co-axially, at opposite sides of the measuring station, and connected to a coincidence circuit. Apart from γ-radiation scattered between the two crystals and a very small number of random coincidences, the measured coincident activity results from the annihilation γ-radiation of all β^{+}-emitters. Internal or external pair production can, of course, also interfere.

The effect of normal *versus* coincidence counting on irradiated copper, iron, silicon, phosphorus and chromium can be evaluated by comparing curves A and B in Figs. 1–5. These spectra were obtained from a 5-sec irradiation at a beam intensity

---

* Aspirant of the N.F.W.O.

TABLE I

NUCLEAR REACTIONS

Element	*Reaction*	*Isotopic abundance (%)*	*Cross-section (mb)*[6,7]	*Half-life*	*Energy (MeV) and abundance (%)*[8]
Cu	^{63}Cu(n,2n)^{62}Cu	69.1	500	9.8 min	β^+ (97) 1.17 (0.5); 0.88 (0.3); 1.13 (0.1)
	^{63}Cu(n,α)^{60m}Co	69.1	30	10.5 min	IT 0.06/1.33 (0.2)
	^{65}Cu(n,α)^{62g}Co	30.9	8	1.6 min	
	^{62}Co			13.9 min	1.17 (100); 1.47 (11); 1.74 (11); 2.03 (4)
Fe	^{54}Fe(n,2n)^{53}Fe	5.82	12	8.9 min	β^+ (98) 0.38 (39)
	^{56}Fe(n,p)^{56}Mn	91.7	115	2.58 h	0.85 (99); 1.81 (29.3); 2.11 (15.5); 2.52 (1.1); 2.66 (0.7); 2.95 (0.5); 3.37 (0.2)
	^{57}Fe(n,p)^{57}Mn	2.2	60	1.7 min	Several low energy γ-rays
P	^{31}P(n,2n)^{30}P	100	10	2.6 min	β^+ (100); 2.23 (0.5)
	^{31}P(n,α)^{28}Al	100	130	2.24 min	1.78 (100)
Si	^{28}Si(n,p)^{28}Al	92.2	250	2.24 min	1.78 (100)
	^{29}Si(n,p)^{29}Al	4.7	100	6.6 min	1.28 (94); 2.43 (6)

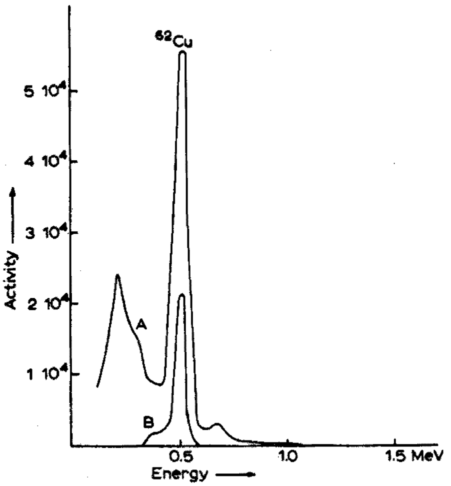

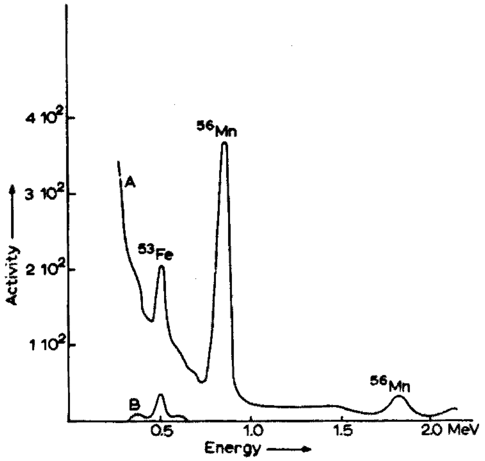

Fig. 1. NaI(Tl) spectra of irradiated copper.

Fig. 2. NaI(Tl) spectra of irradiated iron.

of 300 μA, counted 1 min after the irradiation for 3 min. All activities were normalised to the same neutron output and sample weight. It can be seen that for copper, the 0.5-MeV area activity is reduced by a factor of 4 by the coincidence counting mode; for phosphorus, iron, silicon and chromium, the activity is lowered by a factor of 10 to 70.

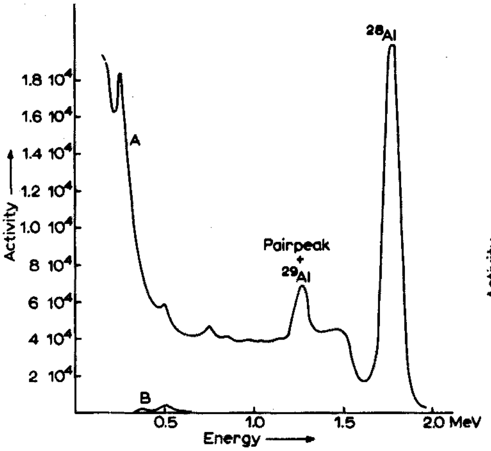

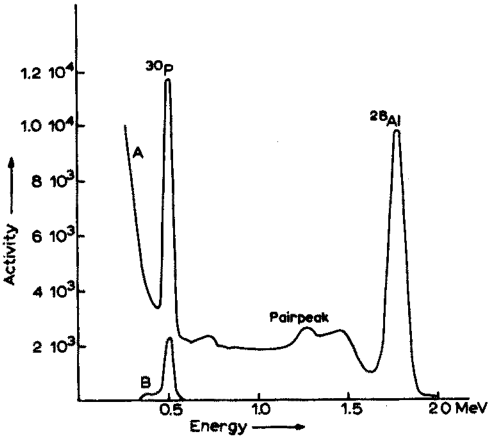

Fig. 3. NaI(Tl) spectra of irradiated silicon.

Fig. 4. NaI(Tl) spectra of irradiated phosphorus.

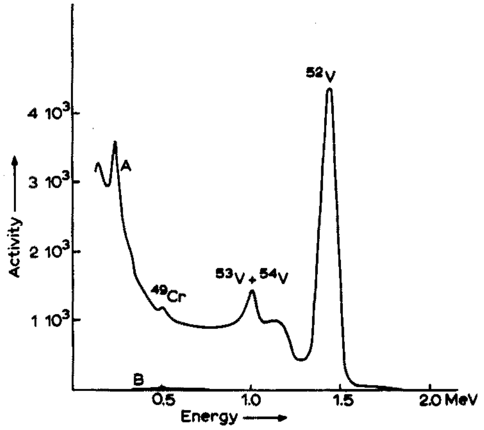

Fig. 5. NaI(Tl) spectra of irradiated chromium.

Flux monitoring

The samples and flux monitors were irradiated in the dual pneumatic transport system described previously[9] and the oxygen flux monitor[10] was also applied as monitor for the copper determinations, which is justified for 5-sec irradiations. As in the determinations of oxygen[9] and silicon[11], this flux monitor was irradiated behind the sample and the induced ^{16}N activity was counted for 30 sec, with an automatic start 2 sec after the end of the irradiation. It was assumed that the ratio of the specific activities measured on sample and flux monitor was constant. However, a standard deviation of *ca.* 1.5% was observed, owing to instrumentation errors (reproducibility of geometry at irradiation and detection places, neutron flux distribution variations, shifts in electronic devices, etc.). The eventual precision of the results is thus determined by this instrumental error and by counting statistics.

EXPERIMENTAL

Instruments

The 14-MeV neutron generator was a Sames Type J machine (150 kV, 1.5 mA and 4 Ci tritium target of 28 mm diameter). Neutron production was controlled by means of a water-cooled tantalum target, pneumatically movable out and into the deuteron beam. A double rectangular transfer system, pneumatically operated, allowed two samples to be irradiated simultaneously behind each other. The accelerator, transfer system and irradiation facilities have already been described[9].

The arrangement of the counting equipment is shown in Fig. 6. The detecting arrangement consisted of three 3 × 3" NaI(Tl) crystals with a resolution of *ca.* 8%.

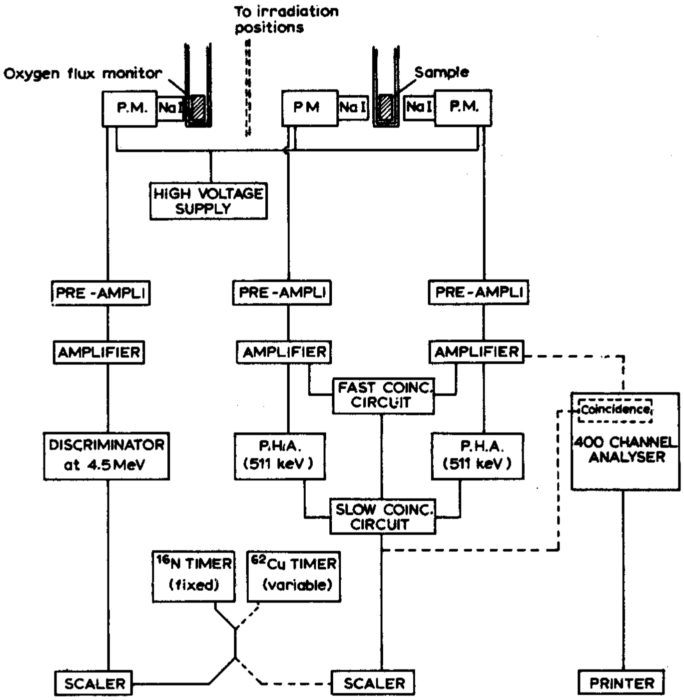

Fig. 6. Counting arrangement.

After amplification and energy selection, pulses from the two detectors viewing the sample were fed to a fast–slow coincidence circuit with a resolving time of 20 nsec. A control unit could be switched to a timing unit to start counting 2 sec after irradiation during 30 sec, or to another timing unit with two variable waiting and counting times.

A 400-channel analyser with multiscaler program unit was included as a supplementary facility.

To avoid temperature drift in the electronic equipment, the counting room was kept constant at 23 ± 0.5°.

Samples were cylindrical (diameter 26 mm, thickness 9 mm), and weighed about 35 g.

Standards

In order to avoid errors from different neutron removal cross-sections and γ-absorption, and to obtain the same geometry in samples and standards, cast iron samples (with 1–2% of copper) were used as standards. Their copper content had been determined by electrolysis, according to the A.S.T.M. procedure[12].

The contribution due to ^{53}Fe, a β^+-emitter with a half-life of 8.9 min, was evaluated by means of a series of carbon steels. Their low copper content ($\pm 0.003\%$ Cu) had been determined by X-ray fluorescence.

Calculation

One can assume that the measured coincident 0.511-MeV activity is built up from several components, originating merely from copper, iron, phosphorus and silicon. Indeed, all other normal constituents of cast iron and steel appear to yield only negligible coincidence activities under the conditions used, apart from chromium and molybdenum in the case of high-alloy steels. The registered counts are produced by different processes: β^+ annihilation radiation (^{62}Cu, ^{53}Fe, ^{30}P), internal pair production, γ-radiation scattered between the two detectors and a very small number of random coincidences.

The measured activity A, t min after the end of the irradiation, normalized to a certain flux, can be written as:

$$A = A_{\mathrm{Cu}} + A_{\mathrm{Fe}} + A_{\mathrm{P}} + A_{\mathrm{Al}} \tag{1}$$

where A_{Cu} = activity of the sum of all the copper activation products, ^{62}Cu, etc. (*cf.* Table I),

A_{Fe} = activity of the sum of all the iron activation products, *i.e.* ^{53}Fe, ^{56}Mn, etc.,

A_{P} = activity of the phosphorus activation from the reaction $^{31}P(n,2n)^{30}P$,

A_{Al} = activity of the activation of silicon and phosphorus from the reactions $^{28}Si(n,p)^{28}Al$ and $^{31}P(n,\alpha)^{28}Al$.

At the second measurement, $t+\Delta t$ min after the end of the irradiation, one can write for the total activity B, normalized to the same flux

$$\begin{aligned} B &= B_{\mathrm{Cu}} + B_{\mathrm{Fe}} + B_{\mathrm{P}} + B_{\mathrm{Al}} \\ &= A_{\mathrm{Cu}}\cdot\exp(-\lambda_{\mathrm{Cu}}\Delta t) + A_{\mathrm{Fe}}\cdot\exp(-\lambda_{\mathrm{Fe}}\Delta t) + A_{\mathrm{P}}\cdot\exp(-\lambda_{\mathrm{P}}\Delta t) + A_{\mathrm{Al}}\cdot \\ &\qquad \exp(-\lambda_{\mathrm{Al}}\Delta t) \end{aligned} \tag{2}$$

In eqn. (2) $\exp(-\lambda_{\mathrm{Cu}}\Delta t)$ and $\exp(-\lambda_{\mathrm{Fe}}\Delta t)$ represent empirical ratios of the measured activity at $t+\Delta t$ and t min after the end of the irradiation for pure copper and iron, respectively, and should not be identified with true disintegration constants. On the other hand, λ_{P} and λ_{Al} are the true disintegration constants of ^{30}P and ^{28}Al.

Equation (2) can be transformed into:

$$B = q\cdot(A_{\mathrm{Cu}} + A_{\mathrm{Fe}}) + A_{\mathrm{P}}\cdot\exp(-\lambda_{\mathrm{P}}\Delta t) + A_{\mathrm{Al}}\cdot\exp(-\lambda_{\mathrm{Al}}\Delta t) \tag{3}$$

if

$$\begin{aligned} q &= \frac{A_{\mathrm{Cu}}\cdot\exp(-\lambda_{\mathrm{Cu}}\Delta t) + A_{\mathrm{Fe}}\cdot\exp(-\lambda_{\mathrm{Fe}}\Delta t)}{A_{\mathrm{Cu}} + A_{\mathrm{Fe}}} \\ &= \frac{k_1\cdot{}^1/_{100}\cdot\%\ \mathrm{Cu}\cdot W\cdot\exp(-\lambda_{\mathrm{Cu}}\Delta t) + k_2\cdot{}^1/_{100}\cdot\%\ \mathrm{Fe}\cdot W\cdot\exp(-\lambda_{\mathrm{Fe}}\Delta t)}{k_1\cdot{}^1/_{100}\cdot\%\ \mathrm{Cu}\cdot W + k_2\cdot{}^1/_{100}\cdot\%\ \mathrm{Fe}\cdot W} \\ &= \frac{\%\ \mathrm{Cu}\cdot\exp(-\lambda_{\mathrm{Cu}}\Delta t) + k\cdot\exp(-\lambda_{\mathrm{Fe}}\Delta t)}{\%\ \mathrm{Cu} + k} \end{aligned} \tag{4}$$

where W = sample weight;
% Cu, % Fe = copper and iron content;
k_1, k_2 = specific copper and iron coincidence activities, depending on irradiating and waiting times, cross-sections, isotopic abundances, detection efficiencies, etc.;
$k = k_2/k_1 \cdot \%$ Fe, *i.e.* the copper content yielding the same activity as the iron present in the sample, namely *ca.* 0.35% for 95% of iron.
Combining eqns. (1) and (3) and eliminating A_P yields

$$\begin{aligned} Z &= A_{Fe} + A_{Cu} \qquad (5) \\ &= \{q - \exp(-\lambda_P \Delta t)\}^{-1}[B - \exp(-\lambda_P \Delta t)\cdot A + \{\exp(-\lambda_P \Delta t) - \exp(-\lambda_{Al}\Delta t)\}\cdot A_{Al}] \end{aligned}$$

Once Z, the sum of the activity produced by copper and iron, is known, one can calculate the net copper contribution, in the following way.

A copper-free iron standard allows the determination of k_2, the value of A_{Fe} for 1 g of iron. $A_{Cu} = 0$, thus

$$Z_{Fe_{st}} = k_2 \cdot {}^1/_{100} \cdot \%\,Fe_{Fe_{st}} \cdot W_{Fe_{st}} \rightarrow k_2 = \frac{Z_{Fe_{st}}}{{}^1/_{100} \cdot \%\,Fe_{Fe_{st}} \cdot W_{Fe\;st}} \qquad (6)$$

where $W_{Fe_{st}}$ = weight of the iron standard
$\%Fe_{Fe_{st}}$ = iron content of the iron standard.

From a copper standard, one can calculate k_1, the value of A_{Cu} for 1 g of copper:

$$\begin{aligned} Z_{Cu_{st}} &= k_2 \cdot {}^1/_{100} \cdot \%\,Fe_{Cu_{st}} \cdot W_{Cu_{st}} + k_1 \cdot {}^1/_{100} \cdot \%\,Cu_{Cu_{st}} \cdot W_{Cu_{st}} \\ \rightarrow k_1 &= (Z_{Cu_{st}} - k_2 \cdot {}^1/_{100} \cdot \%\,Fe_{Cu_{st}} \cdot W_{Cu_{st}})/({}^1/_{100} \cdot \%\,Cu_{Cu_{st}} \cdot W_{Cu_{st}}) \\ &= \{(Z_{Cu_{st}}/W_{Cu_{st}}) - k_2 \cdot {}^1/_{100} \cdot \%\,Fe_{Cu_{st}}\}/({}^1/_{100} \cdot \%Cu_{Cu_{st}}) \qquad (7) \end{aligned}$$

where $W_{Cu_{st}}$ = weight of the copper standard, *i.e.* a cast iron sample with known copper content $\%Cu_{Cu_{st}}$ and iron content $\%Fe_{Cu_{st}}$.

Eventually for an unknown sample X, with weight W_X and iron content $\%Fe_X$, one can calculate the copper content $\%Cu_X$ from

$$\begin{aligned} \%Cu_X &= (Z_X - k_2 \cdot {}^1/_{100} \cdot \%Fe_X \cdot W_X)/(k_1 \cdot {}^1/_{100} \cdot W_X) \\ &= \{(Z_X/W_X) - k_2 \cdot {}^1/_{100} \cdot \%Fe_X\}/({}^1/_{100} \cdot k_1) \qquad (8) \end{aligned}$$

In eqn. (5), A_{Al}, the coincident activity originating from ^{28}Al, is proportional to the ^{28}Al activity measured for the silicon determination[11] with energy discrimination at 1.6 MeV. The coefficient k_2 being known as described above, k_1 is computed by reiteration from "copper standard" results. Introducing k_1 and k_2 in the "sample results" allows the calculation of Z_X and finally $\%Cu_X$ by the same procedure.

As a matter of fact, formula (5) can be considerably simplified. It appeared that the influence of the term

$$\{\exp(-\lambda_P \Delta t) - \exp(-\lambda_{Al}\Delta t)\}\cdot A_{Al}$$

is negligible. Indeed, for 1% Si or 1.8%P, it corresponds to only +0.001% Cu.

It was found that the value of $k = (k_2/k_1) \cdot \%$ Fe in eqn. (4) can be taken as a constant, for a series of similar samples, as k_2/k_1 remains almost constant when the same measuring conditions are used. The value of k is not very critical; indeed, when

1% Cu standards are used, even if k differs 10% from the real $((k_2/k_1)\cdot\%\ \mathrm{Fe})$ value, a relative error of only 0.7% for very small sample copper contents, of 0% for a 1% Cu sample, and of –0.17% for 3% Cu samples is calculated. Even if k is erroneous by 20%, the error introduced never reaches 20% of the experimental standard deviation for a measurement.

Moreover, $\exp(-\lambda_{\mathrm{Cu}}\Delta t)$ and $\exp(-\lambda_{\mathrm{Fe}}\Delta t)$ are quite similar; for the former the value is 0.66, in agreement with the theoretical value for ^{62}Cu, whereas the latter gives 0.71, *i.e.* higher than for the decay of ^{53}Fe, owing to ^{56}Mn counts. Thus, q (in eqn. (5)) can be assumed to be a constant. Thus eqn. (5) eventually becomes

$$Z = A_{\mathrm{Fe}} + A_{\mathrm{Cu}} \sim B - \exp(-\lambda_{\mathrm{P}}\Delta t)\cdot A \tag{9}$$

and therefore, % Cu$_X$, can be calculated easily via eqns. (9), (6), (7) and (8) without reiterations.

It was calculated that the assumption of q being constant does not introduce a noticeable difference in the final result. The very simple eqn. (9) can thus be used for all practical purposes.

The iron content of the sample should be known to calculate % Cu$_X$ by eqn. (8). However, the iron content may be erroneous by 3–4% before an error of 0.01% Cu is induced.

It should be stated here that solving eqns. (1) and (3) for the 2.6-min component (A_{P}), allows a determination of phosphorus. This possibility will be investigated in a subsequent paper[13].

In the case when the phosphorus and silicon contributions are negligible, because of a very low content or decay, the total coincident 0.511-MeV activity can be considered as being built up merely from copper and iron contributions (A_{Cu} and A_{Fe}):

$$A = A_{\mathrm{Cu}} + A_{\mathrm{Fe}} \tag{1b}$$

The copper content %Cu$_X$ of an unknown sample can, in this case, be found by simply replacing Z_X in eqn. (8) by A_X, the total measured activity. Thus:

$$\%\mathrm{Cu}_X = \{(A_X/W_X) - k_2\cdot{}^1/_{100}\cdot\%\mathrm{Fe}_X\}/({}^1/_{100}\cdot k_1) \tag{8b}$$

$$k_2 = \frac{A_{\mathrm{Fe_{st}}}}{{}^1/_{100}\cdot\%\ \mathrm{Fe}_{\mathrm{Fe_{st}}}\cdot W_{\mathrm{Fe_{st}}}} \tag{6b}$$

and

$$k_1 = \{(A_{\mathrm{Cu_{st}}}/W_{\mathrm{Cu_{st}}}) - k_2\cdot{}^1/_{100}\cdot\%\ \mathrm{Fe}_{\mathrm{Cu_{st}}}\}/({}^1/_{100}\cdot\%\ \mathrm{Cu}_{\mathrm{Cu_{st}}}) \tag{7b}$$

Clearly k_1 and k_2 can be found respectively by means of iron and copper standards (see above).

The assumption that the total activity is built up only from copper and iron contributions, greatly simplifies the copper determination. One measurement can suffice, and the calculation of Z by eqn. (5) or eqn. (9) is not required. Obviously, serious restrictions must be imposed on the phosphorus and silicon content, *e.g.* after a 7-min decay, 0.2% phosphorus and 1.2% silicon introduce a +0.01% copper error.

Analysis cycles

The analysis cycle for each sample and copper and iron standard was essentially as follows:

1. Pneumatic transfer of sample and oxygen flux monitor to the irradiation positions, within 1 sec.

2. Simultaneous irradiation of sample and oxygen flux monitor behind each other during 5 sec at a beam intensity of 300 μA by pneumatic removal of the tantalum screen from the deuteron beam (new target condition).

3. Pneumatic transfer of sample and flux monitor to the counting positions.

4. After a 2-sec delay, automatic start of the counting during 30 sec of the ^{16}N activity of the flux monitor.

Count rate: *ca.* 12000 counts per 30 sec for a 412-mg oxygen standard.

5. Measurement of the coincident 0.511-MeV activity of the sample, automatically started by a second timing unit, 1 min after the end of the irradiation, during 3 min.

Count rate: *ca.* 70000 counts ^{62}Cu per 3 min for 1 g of copper.

6. Second measurement of the coincident 0.511-MeV activity during 3 min, 7 min after the end of the irradiation.

7. From the experimental data, an adequate computer program makes it possible to calculate the specific activities of the standards and the copper content of the samples, together with the standard deviation caused by counting statistics.

In the case of low silicon and phosphorus contents, when calculation is done via eqn. (8b), the analysis cycle can be simplified as follows.

1. Transfer of sample and flux monitor to the irradiation places, irradiation during 5 sec, and transfer back to the counting stations.

2. 2 sec after the end of the irradiation, automatic start of a 30-sec measurement of the ^{16}N activity induced in the oxygen flux monitor.

3. 7 min after the end of the irradiation, automatic start of a 3 -min measurement of the coincident 0.511-MeV activity induced in the sample.

4. The data are again analysed by an adequate computer program as described above.

RESULTS

Samples with different compositions and metallurgical properties were analyzed. The results for both calculation methods are listed in Table II, together with the experimental error (standard deviation on a single determination).

Interferences

The interferences of the most common alloying elements or impurities on the determination of copper were measured. Suitable compounds of the elements were irradiated in an iron box with the same dimensions as the samples. Afterwards, counting and calculation were performed exactly as described above. It was found that 1% Mo introduced an apparent copper content of +0.05% Cu; 1% Cr: +0.0015% Cu; 1% Zr and 100 p.p.m. N: +0.002% Cu; and 1% Sn: +0.001% Cu. All other examined alloying elements and impurities gave completely negligible activities, namely C, Ni, Mn, V, Al, Co, W, Pb, Ti, Mg, Nb.

Interferences were also checked when eqn. (8b) was applied, *i.e.* the simplified method. It was found that after a 7-min waiting period, apart from the already stated phosphorus and silicon interferences, 1% Mo caused an apparent copper content of

TABLE II

RESULTS

Samples	*Given Cu content (X-ray fluorescence)*	*No. of analyses*	*% Cu and error*	
			from eqn. (8)	*from eqn. (8b)*
Copper alloyed cast irons[a]				
VA	0.96	3	1.01 ± 0.04	1.02 ± 0.04
VB	0.99	3	1.06 ± 0.03	1.08 ± 0.03
VC	1.00	3	0.98 ± 0.06	1.00 ± 0.05
VD	1.00	3	0.99 ± 0.04	1.01 ± 0.04
VE	1.10	4	1.10 ± 0.02	1.13 ± 0.02
VF	2.00	3	2.01 ± 0.04	2.03 ± 0.04
VG	2.00	3	1.98 ± 0.03	2.00 ± 0.03
VH	2.06	4	2.10 ± 0.03	2.12 ± 0.03
VI	3.00	3	2.97 ± 0.09	2.96 ± 0.09
VJ	3.00	3	2.97 ± 0.09	2.98 ± 0.08
VK	0.45[e]	3	0.02 ± 0.01	0.03 ± 0.01
VL	0.45[e]	5	1.81 ± 0.09	1.84 ± 0.09
Carbon steels[b]				
IA	0.20	3	0.20 ± 0.02	0.19 ± 0.02
IB	0.06	3	0.05 ± 0.01	0.05 ± 0.01
IC	0.09	3	0.10 ± 0.01	0.08 ± 0.02
ID	0.04	3	0.05 ± 0.015	0.05 ± 0.015
IE	0.05	3	0.05 ± 0.015	0.05 ± 0.01
IF	0.05	3	0.04 ± 0.01	0.05 ± 0.01
IG	0.045	3	0.03 ± 0.01	0.05 ± 0.01
IH	0.07	3	0.06 ± 0.01	0.09 ± 0.01
II	0.07	3	0.08 ± 0.01	0.11 ± 0.02
IJ	0.08	3	0.07 ± 0.015	0.12 ± 0.01
IK	0.11	3	0.13 ± 0.01	0.12 ± 0.01
IL	0.05	3	0.04 ± 0.005	0.04 ± 0.005
IM	0.03	3	0.04 ± 0.02	0.04 ± 0.01
IN	0.04	3	0.03 ± 0.01	0.07 ± 0.01
IO	0.02	5	0.03 ± 0.01	0.05 ± 0.01
Low and medium phosphorus cast irons[c]				
DA...DE	Mean: 0.06[e]	20	Mean: 0.02±0.015	Mean: 0.01±0.01
DF	0.19	5	0.18±0.005	0.22±0.005
DG	0.18	3	0.18±0.02	0.23±0.03
DH	0.18	3	0.17±0.01	0.22±0.005
DI	0.18	3	0.16±0.02	0.22±0.01
DJ	0.18	2	0.20±0.02	0.26±0.025
DK	0.18	2	0.17±0.02	0.24±0.02
High phosphorus cast irons[d]				
DL...DO	Mean: 0.07	16	Mean: 0.07±0.02	Mean: 0.17±0.02
PA...PJ	Not determined	42	Mean: 0.01±0.015	Mean: 0.10±0.01

Known limits of alloy and impurity contents (in %):

[a] P: 0.10 to 0.15, Si: 1.2 to 2.2, Mo: up to 0.32, Cr: up to 1.8, C: 2.8 to 3.6, Mn: 0.4 to 0.7, S: 0.06 to 0.10, Sn: up to 0.06.

[b] P: 0.01 to 0.10, Si: 0.1 to 4.8, Cr: 0.02 to 0.18, C: 0.03 to 0.38, Mn: 0.08 to 0.69, S: 0.01 to 0.10, Ni: 0.03 to 0.65, Al: up to 0.10.

[c] DA...DE: P: 0.08 to 0.10, Si: 1.2 to 3.3.
DF...DK: P: 0.43 to 0.52, Si: 2.6 to 5.3.

[d] DL...DO: P: 1.23 to 1.40, Si: 2.6 to 4.7.
PA...PJ: P: 1.40 to 1.64, Si: 1.9 to 2.5, Cr: 0.032 to 0.036.
C: 3.5 to 3.9, Mn: 0.34 to 0.45, S: 0.02 to 0.03.

[e] See DISCUSSION.

+0.06% Cu; 1% Cr: +0.002% Cu; 1% Zr: +0.003% Cu; 1% Sn and 100 p.p.m. N: +0.002% Cu. All other tested elements yielded negligible activities.

Multichannel mode of counting

To visualise the energy distribution of the output of the fast–slow coincidence circuit, a 400-channel analyser was also incorporated in the counting system as shown in Fig. 6. Output pulses of the coincidence circuit were used as a gate for the multichannel coincidence system and pulses from one of the detectors as signals. From the registered spectra, results were calculated from data obtained according to COVELL's peak surface evaluation method[14]. The average results fitted completely to the scaler results, shown in Table II. Interferences were approximately the same. It appeared, however, that the theoretical as well as the experimental standard deviation was some 20% better than in the scaler mode of counting. Moreover, the iron content could be erroneous by 7% before a 0.01% error for copper was introduced.

A simple multichannel counting mode was also tested by using directly the output pulses of one of the pulse-height analysers as a gate pulse, the other amplifier output being led to the signal input of the multichannel coincidence circuit (resolving time 0.3 μsec). Results were in no respect significantly different.

When eqn. (8b) was applied, results were also computed by peak area evaluation[14] of the multichannel spectra. It appeared again that the results fitted completely the scaler results of Table II. For low copper contents, standard deviations were some 20% smaller than with the scaler methods, whereas in the 1–3% copper region, they were of the same magnitude. Again, the knowledge of the sample iron content was twice less critical.

DISCUSSION

Accuracy

For samples VK, VL, DA ...DE completely unexpected results were found by 14-MeV neutron activation analysis. Independent thermal neutron activation analyses were carried out to check the copper content of these samples. Metal chips were irradiated with thermal neutrons in the reactor Thetis for 2 h at a flux of 10^{11} n sec^{-1} cm^{-2}. After cooling for 2 days samples were dissolved and copper was separated by extraction with 0.02 *M* cuproïne solution in isoamyl alcohol[15], and by electrodeposition. The ^{64}Cu activity was counted. Results confirmed completely the 14-MeV activation analysis, *i.e.* averages of 0.022% Cu, 1.81% Cu and 0.023% Cu were found for samples VK, VL, DA...DE, respectively. For all other samples, application of eqn. (8) gave results in agreement with X-ray fluorescence analyses except in the presence of important molybdenum (VA, VB, VH) and/or chromium concentrations as appeared from high-alloy steels containing from 12 to 26% chromium. The simplified eqn. (8b) gave similar results except in cases of high phosphorus (DF...DK, DL...DO, PA...PJ) or high silicon (IH, II, IJ, IN: $\geq$3% Si) contents.

Precision

As mentioned earlier, the computer program calculated the theoretical standard deviation expected for a single determination. These standard deviations are in excellent agreement with the experimental ones. Thus, the experimental error can be entirely attributed to the statistical nature of the experimental measurements, taking into account a 1.5% standard deviation due to the instrumental error. The total standard deviation is *ca.* 2.5% relative for 3% Cu, 3% for 1% Cu, 9% for 0.2% Cu and 30% for 0.05% Cu.

It also appeared from the data that the results calculated from eqn. (8) and eqn. (8b) are of essentially equivalent precision.

Grateful acknowledgement is made to Mr. J. KIERZEC (Institute of Nuclear Research, Warsaw, Poland) for many helpful discussions, and for his important practical assistance; to Miss M. HANIN (Institut de Recherches de la Sidérurgie Française, St. Germain-en-Laye, France), Messrs. G. KISFALUDI (Centre de Recherches de Pont à Mousson, France), R. BERGER (Usines Emile Henricot, Court St. Etienne, Belgium) and to Prof. Dr. J. VIDTS (Institute of Metallurgy, University of Ghent, Belgium), who provided analysed samples.

Messrs. G. WINDELS and M. LEFIEF partially built, and maintained the electronic equipment, Mr. G. BEKE kept the mechanical parts in good condition.

We are pleased to acknowledge financial support of the "Nationaal Fonds voor Wetenschappelijk Onderzoek" and of Euratom (Contract No. 102-66-IRA/B).

SUMMARY

A fast (10 min) non-destructive determination of copper in steel and cast iron by 14-MeV neutron activation analysis is described. The 0.511-MeV annihilation radiation of ^{62}Cu ($T_{\frac{1}{2}}=9.8$ min), induced by the reaction ^{63}Cu(n,2n)^{62}Cu, is counted by two opposing NaI(Tl) detectors operating in coincidence. An oxygen flux monitor is used to normalise the irradiations. For high phosphorus contents, two measurements are made and the 9-min activity contribution is calculated. As the iron content of the samples is known, the use of pure iron samples allows correction for ^{53}Fe activity from the reaction ^{54}Fe(n,2n)^{53}Fe ($T_{\frac{1}{2}}=8.9$ min). When the phosphorus and silicon activities are low, the procedure of counting and computing can be greatly simplified. Nuclear interferences of most common alloying and impurity elements were investigated. The precision is 2–3% for steels containing above 1% Cu, and *ca.* 10% for 0.1% Cu.

RÉSUMÉ

On décrit un dosage non destructif d'une durée de 10 min, du cuivre dans les aciers et les fontes par activation au moyen de neutrons de 14 MeV. L'activité d'annihilation de 0.511 MeV du ^{62}Cu, induite par la réaction ^{63}Cu(n,2n)^{62}Cu, est comptée par deux détecteurs NaI(Tl) opérant en coïncidence. On emploie un étalon d'oxygène pour normaliser le flux. Pour une haute teneur en phosphore et silicium, on mesure deux fois et on calcule l'activité du composant ayant une demie-vie de 9 minutes. Si l'activité dûe au phosphore et au silicium est négligeable on peut simplifier la méthode de comptage et de calcul. La teneur en fer des échantillons étant de toute façon connue d'une manière approximative, on corrige pour l'activité de ^{53}Fe, induite par ^{54}Fe(n, 2n)^{53}Fe, au moyen d'étalons de fer pur. La plupart des interférences nucléaires possibles furent également examinées. La précision de la méthode est de 2–3% pour les aciers contenant plus de 1% de cuivre, et 10% pour 0.1% de cuivre.

ZUSAMMENFASSUNG

Es wird eine zerstörungsfreie Bestimmung von Kupfer in Stahl und Gieszeisen durch Aktivierung mit 14-MeV Neutronen beschrieben. Die durch die Reaktion $^{63}Cu(n,2n)^{62}Cu$ induzierte Annihilationsstrahlung des ^{62}Cu ($T_{\frac{1}{2}} = 9.8$ min) wird gezählt mit zwei NaI(Tl) Detektoren, in Koinzidenz-Schaltung. Ein Sauerstoff-Fluss-Monitor wird zur Normalisierung angewendet. Bei Anwesenheit groszer Mengen Phosphors wird zweimal gemessen, und wird die Fraktion der Aktivität mit Halbwertzeit von 9 Minuten berechnet. Wenn die Störung durch Phosphor und Silicium wesentlich klein ist kann man die Messung und Berechnung stark vereinfachen. Weil die Proben approximativ bekannte Mengen Eisen enthalten, kann man rein Eisen Proben anwenden um für die ^{53}Fe Aktivität zu korrigieren, welche durch die Reaktion $^{54}Fe(n,2n)^{53}Fe$ in der Eisenmatrix erzogen wird. Störungen durch alle normale Legierung- und Unreinheit-Elementen werden geprüft. Das Verfahren besitzt eine Reproduzierbarkeit von 2 bis 3% für Stähle und Gieszeisen die mehr als 1% Kupfer enthalten, und von 10% für Gehälte von 0.1% Kupfer.

REFERENCES

1 G. J. Lutz, R. J. Boreni, R. S. Maddock and W. W. Meinke, *Activation Analysis. A Bibliography*, NBS Technical Note 467, Sept. 1968, National Bureau of Standards, Washington D.C.
2 L. Górski, W. Kusch and J. Woitkowska, *Talanta*, 11 (1964) 1135.
3 H. P. Dibbs, *The Application of Neutron Activation Analysis to the Determination of Copper in Minerals*, Research Report R205, Dept. of Energy, Mines and Resources, Mines Branch, Ottawa, April 1969.
4 T. B. Pierce, J. W. Edwards and D. Mapper, *Application of a Sealed-tube Neutron Generator to the Determination of Copper and Silicon in Aluminium Alloys*, AERE-R-5616, 1967, Analytical Science Division, Atomic Energy Research Establishment, Harwell, Berkshire, England.
5 D. Gibbons, W. J. Mc Gabe and G. Olive, *Radiochemical Methods of Analysis*, Vol. I, I.A.E.A., Vienna, 1965.
6 A. Chatterjee, *Nucleonics*, 22(8) (1964) 108; 23(8) (1965) 112.
7 H. Neuert and N. Pollehn, *Tables of Cross Sections of Nuclear Reactions in the 14–15 MeV Energy Range*, Report Euratom, EUR 122e, 1963.
8 G. M. Lederer, J. M. Hollander and I. Perlmann, *Tables of Isotopes*, 6th Edn., John Wiley, New York, 1967.
9 J. Hoste, D. De Soete and A. Speecke, *The Determination of Oxygen in Metals by 14 MeV Neutron Activation Analysis*, Report Euratom EUR 3565e, 1967.
10 R. Gijbels, A. Speecke and J. Hoste, *Anal. Chim. Acta*, 43 (1968) 183.
11 R. van Grieken, R. Gijbels, A. Speecke and J. Hoste, *Anal. Chim. Acta*, 43 (1968) 199.
12 A. S. T. M., *Methods for Chemical Analysis of Metals*, Am. Soc. for Testing Materials, Philadelphia, 1956, p. 96.
13 R. Van Grieken, A. Speecke and J. Hoste, to be published.
14 D. F. Covell, *Anal. Chem.*, 31 (1959) 1785.
15 J. Hoste, *Anal. Chim. Acta*, 4 (1950) 23.

Analytica Chimica Acta
Elsevier Publishing Company, Amsterdam
Printed in The Netherlands

RADIOCHEMICAL NEUTRON ACTIVATION ANALYSIS OF INDIUM, CADMIUM, YTTRIUM AND THE 14 RARE EARTH ELEMENTS IN ROCKS

P. REY, H. WAKITA AND R. A. SCHMITT
Department of Chemistry and the Radiation Center, Oregon State University, Corvallis, Oreg. 97331 (U.S.A.)

(Received February 16th, 1970)

The main purposes of the work described in this paper were to develop a method for the simultaneous determination of indium, cadmium and the 14 rare earth elements plus yttrium, to obtain analytical results for three USGS standard rocks for their comparison with published values, and, finally, to obtain abundance values for the rare earths in a standard ultramafic rock, DTS-1, that is severely depleted in these elements. Achievement of the last aim was considered to be an excellent test of the method.

It became evident that cadmium, indium and some of the rare earths could not be determined accurately by instrumental neutron activation analysis and that radiochemical neutron activation analysis was essential.

Instrumental methods for the determination of some of the rare earths involving simple chemistry and the use of Ge(Li) detectors, spark source mass spectrometry, and X-ray fluorescence have been published recently. In some cases[1] the accuracy achieved was very good, but only 9 out of 14 rare earth elements were determined, because of isobaric interference and insufficient resolution. In others[2–6] the precision and accuracy were not considered adequate for the present purpose. Recently two destructive methods have been published; in one[7] the rare earths as a whole are separated from other radionuclides in order to increase the signal-to-background ratio. In this method a planar Ge(Li) detector was used. Generally, planar detectors yield better resolution than larger volume coaxial detectors at the expense of reduced counting efficiency. Ten rare earths were determined[7] for standard rocks G-1 and W-1. In the other method[8], which achieves accuracy similar to that obtained in this work, rare earths are separated by ion exchange into light and heavy groups. A 45-cm^3 coaxial Ge(Li) detector plus a 4096-channel analyzer is used for spectral measurements. MORRISON *et al.*[9] have succeeded in determining 12 of the 14 rare earth elements with considerable accuracy by means of chemical group separations after neutron activation and then measuring the radionuclides with a high resolution Ge(Li) detector in anticoincidence with a surrounding NaI(Tl) annulus in order to suppress the Compton background. Finally, HIGUCHI *et al.*[10] have determined 10 of the 14 rare earths in USGS standard rocks by group separation technique[7]. Their results agree well with the present results for G-2 and BCR-1, though there are significant discrepancies for some of the rare earths determined in DTS-1. However, these[7–10] and previously described methods require waiting periods up to a month or longer before the longer-lived rare earth radionuclides are counted, in order to eliminate interferences and reduce the Compton continuum generated by the shorter-lived isotopes. Also group separation methods have possible errors on determination of chemical yields of all rare earths, because of possible fractionation of the rare earths during chemical separation. This is a distinct disadvantage in a procedure that requires analysis of all the rare earths within a few days of total time and also the attainment of up to a few percent accuracy for selected rare earths. From the above information it is evident that highly precise and accurate methods involving the determination of all the rare earths in the p.p.m. range must be based on radiochemical neutron activation analysis; for rare earth abundances in the p.p.b. range, this method is mandatory, especially if all 14 rare earths are to be determined.

It has proved possible to separate all the elements of interest sequentially. Later, potassium, rubidium and cesium were incorporated into the separation scheme. The method described in this paper makes use of wet and ion-exchange post-irradiation chemistry. The rare earth portion of this procedure is considered an improvement over other radiochemical procedures developed to determine the rare earths[11,12], for two reasons: one, the chemical yield may be obtained more accurately by reactivation methods than by weighing of rare earth oxalate precipitates; secondly, even though the overall chemical yields of individual rare earths may be very low, even to 5%, because of mistakes incurred during the radiochemical manipulations, chemical yields obtained by reactivation are still within ±5% accuracy. Indium is separated in about 1.5 h following a procedure developed here. Two samples may be run in parallel by a team of two radiochemists and two technicians in about 20 h. Completion of analyses may require as little as four days, where reactivation for chemical yield determination is required.

The procedure was tested by analyzing three USGS standards: BCR-1, G-2, and DTS-1 in duplicate. From their silica content, G-2, BCR-1, and DTS-1 are examples of acid (granite), basic (basalt), and ultrabasic (dunite) rocks; these rocks provide different materials widely varying in major, minor and trace elemental contents. DTS-1 was adopted to test the sensitivity of the method, since it is the most depleted in rare earths and indium of all the USGS standards, and is very low in cadmium.

EXPERIMENTAL

Apparatus

For the separation of indium and cadmium no special devices were needed. In the case of rare earth separation an automatic ion-exchange fraction collector and a high-precision pH meter were used. The ion-exchange assembly consisted of two columns (10 mm i.d. and 730 mm high), a 1-l pressure equalizing funnel for a pH 4.05 solution of α-hydroxyisobutyric acid, a 1-l Wulff bottle for a pH 3.10 solution of the same acid, and two linear fractionators with tubes, racks, and Gilson photosensitive drop counter. The system operates under a very small nitrogen overpressure in order to achieve the required elution rate. The pH 4.05 solution drips into the pH 3.10 solution, gradually increasing the pH. The resultant solution feeds the top(s) of the resin bed(s). Mutual separation of the rare earths is achieved by the complexing action of the organic acid at continuously decreasing hydrogen ion concentration.

The pH measurements of both organic-acid solutions must be accurate within ±0.01 pH units in order to reduce substantially the time interval between the start of elution and the appearance of the first peak (Lu), and also to obtain the best peak separation for Lu, Yb, and Tm. To this end, a high-precision Sargent-Welch pH meter (model DR) was used.

Carriers and standards

Cadmium carrier was prepared from Fisher certified-reagent nitrate; indium and the rare earths, from spectroscopically pure oxides (Johnson Matthey & Company). The rare earth oxides were dissolved in nitric acid and diluted in 0.1 *N* acid to give a concentration of 1 mg of element per ml of solution. Indium oxide was dissolved in aqua regia; chlorine was eliminated through several evaporations to dryness with nitric acid, since it interferes for reactivation purposes, and the residual salt was diluted to 5 mg In^{3+} ml^{-1} with 0.1 *N* nitric acid. Cadmium nitrate was dissolved in 0.1 *N* nitric acid to a concentration of 5 mg Cd^{2+} ml^{-1}.

Standardization was carried out as follows. Indium was determined as the 8-hydroxyquinolinate (oxine), since its volatility prevents its transformation into oxide without losses. Cadmium was precipitated as cadmium ammonium phosphate monohydrate. The high-purity rare earth standards were converted to their respective oxides by direct evaporation of their solutions, followed by calcination at 850°. Standards to be used as comparators were made by dilution of carriers with 0.1 *N* nitric acid. The standard solutions of indium, cadmium and the rare earths were 0.4, 1.0 and between 1 and 500 μg ml^{-1}, respectively. All determinations were made in duplicate and the results agreed within 0.5%.

Note. In initial attempts to reproduce the method of HASKIN *et al.*[12] for separation of rare earths, resolution of the Lu, Yb, Tm and Er and also the Gd and Eu elution peaks was not entirely successful, perhaps because of the large amounts of carriers used. Originally 7 mg of each rare earth carrier were used, which, at 75% calculated yield, left about 5 mg per element at the start of elution. For a 10 mm × 650 mm column bed the combined amount of rare earth carriers tended to saturate the column for the above-mentioned groups. By using 2 mg of most rare earth carriers, resolution in rare earth elution was considerably improved. With this modification the chemical yields for rare earths were determined by reactivation, instead of by gravimetry, except for terbium and praseodymium, whose initial amounts of carriers were retained at 7 mg. Additionally, these rare earths are β-emitters and it is convenient to determine their chemical yields gravimetrically.

Activation

Samples (0.5–1 g) and standards were activated with thermal neutrons for 1 h at 250 kW ($7 \cdot 10^{11}$ n cm^{-2} sec^{-1}). In the simultaneous analyses of the 14 rare earths, yttrium, cadmium and indium, the specimen is activated for 4–6 h at 500 kW at least two days before the last 1-h activation in order to enhance the activities of long-lived radionuclides and to allow for a reduced level of 15-h ^{24}Na during the radiochemical procedure. The sample is allowed to decay for *ca.* 30 min after the activation before the chemical process is started.

Separation of indium

To a 50-ml nickel crucible add by pipet 20 mg In^{3+}, 20 mg Cd^{2+}, *ca.* 35 mg of combined rare earth carriers (Note 1) and *ca.* 0.1 μCi of $^{88}Y^{3+}$ tracer. Evaporate to dryness on a hot plate. Cover the bottom of the crucible with *ca.* 4 g of sodium peroxide, add the finely ground sample, and cover with another 4 g of peroxide. Melt carefully on a Meker flame until complete fusion is achieved. Heat and swirl the crucible for 2–3 min more, and cool carefully in a water bath. Place the crucible sideways in a 400-ml beaker, pour in 100 ml of water and cover immediately with a watch glass. Add 40–50 ml of concentrated hydrochloric acid and cover again, swirling gently to facilitate the acid attack. Rinse and remove the crucible. The total volume of the solution should be around 150 ml.

Add 4–5 g of ammonium chloride (Note 2) and add concentrated ammonia solution with continuous stirring until all the nickel has been complexed (deep blue color). Then adjust the pH to 9–10. Centrifuge in 50-ml C-tubes, decant the supernate, wash the precipitate with 50 ml of diluted ammonia, breaking up the precipitate with a stirring rod, centrifuge again, add the washings to the supernate, and save the liquid for the determination of cadmium.

Dissolve the precipitate with a minimum of hydrochloric acid while keeping the tube partially immersed in cool water. Transfer the solution to a 150-ml beaker. Adjust the pH as close to 2 as possible with ammonia solution without permanent formation of a hydrated iron(III) oxide precipitate; the final pH should not be less than 1 and the total volume should be about 20 ml. Add zinc dust in 100-mg batches, stirring between additions and looking for total or partial decoloration of solution. If a jelly white precipitate appears (basic zinc products) and bubbling subsides, add 6 *M* hydrochloric acid dropwise to bring the pH back to 2. Add 200 mg more of zinc and stir. Filter gently, applying moderate suction, with Whatman #41 paper, a 51-mm Coors Buchner, and a 120-ml filtering flask. Wash the precipitate with 10 ml of 0.5 *M* hydrochloric acid and save the filtrate for the determination of rare earths.

Transfer the filter paper with the precipitate to a 150-ml beaker and rinse the funnel with concentrated hydrobromic acid. Add the acid to the precipitate and heat gently until complete dissolution is obtained. Cool the beaker and filter as described above. Wash the filter with 10 ml of 4.5–5 *M* hydrobromic acid. Transfer the solution to a 120-ml separatory funnel, and extract indium with 10 ml of hydrobromic acid–saturated diisopropyl ether. Transfer the aqueous phase to a second separatory funnel. Add 20 ml of the hydrobromic acid–ether mixture to the aqueous phase in a second funnel, shake, discard the aqueous phase and combine the organic liquids in the first funnel. Add 10 ml of 4.5–5 *M* hydrobromic acid to the first funnel, shake, and reject the aqueous phase. Add 10 ml of 7 *M* hydrochloric acid, shake, and transfer the aqueous phase to a 150-ml beaker. Repeat the back-extraction and combine the aqueous layers. Reject the organic layer. Boil the solution gently on a hot plate for 10–15 min to make sure that all the isopropyl ether has been eliminated (Note 3) and cool. Precipitate indium hydroxide with ammonia solution, centrifuge, and dissolve the precipitate with nitric acid. Transfer the resultant solution to a 2-dram polyvial with a dropper, make the volume equal to that of the indium comparator, and heat-seal the vial. Count and follow the decay with a 3 × 3 in NaI(Tl) well crystal coupled to a multichannel analyzer, at the photopeaks of the 0.417, 1.09, and 1.293-MeV γ-rays. Transfer the activated indium standard quantitatively to a new polyvial, heat-seal the vial and count in the same way. After complete decay, activate the indium sample with 20 mg of indium(III) comparator for 10 min at 10 W (*ca.* $3 \cdot 10^7$ n cm^{-2} sec^{-1}), and count again to determine the chemical yield. Separation of indium is accomplished in about 1.5 h, with a purity of practically 100% and a yield between 60 and 70%. Direct separation of indium, without isolating the alkali fraction, can be performed in about 1 h.

Notes. 1. About 2 mg each of La, Ce, Nd, Sm, Eu, Gd, Tb, Ho, Er, Yb, and Lu and 7 mg each of Pr, Dy and Tm are added. For determination of alkali elements, 2 mg each of K, Rb and Cs carriers plus *ca.* 0.01 μCi ^{137}Cs are also added.

2. For the additional determination of the alkali elements, ammonium chloride is not added and the procedure is modified by a few steps. The following modifications[13] are necessary after the crucible has been removed from the solution. Add 6 *M* sodium hydroxide to precipitate the hydroxides of cadmium, indium and the rare earths at a pH of 13–14. Centrifuge and save the supernate for the determination of alkali metals. Dissolve the precipitate with hydrochloric acid, dilute to 100 ml in a beaker, and proceed as outlined, with addition of ammonium chloride.

For the determination of alkali metals, acidify the supernate with hydrochloric acid, add 5 mg of iron(III) and dilute sodium hydroxide to precipitate iron(III) hydroxide, centrifuge and discard the precipitate. Neutralize the supernate with dilute hydrochloric acid, acidify with 1–2 ml of acetic acid (methyl red indicator) and add about 0.5 g of ethylenediaminetetraacetic acid (EDTA) to complex divalent and other cations. Add 5 ml of 2% (w/v) sodium tetraphenylboron solution to precipitate potassium, rubidium and cesium; more sodium tetraphenylboron is required for proportionately larger alkali concentrations. Centrifuge and discard the supernate. Wash the precipitate with 20 ml of water, centrifuge and decant. Gently dissolve the precipitate with about 20 ml of 1 *M* nitric acid on a steam bath. Filter the solution through coarse paper in order to retain any oily material if necessary. Neutralize the clear solution with about 6 *M* sodium hydroxide, add 2 ml of acetic acid and 0.5 g of EDTA, and repeat the tetraphenylboron precipitation. Centrifuge and discard the supernate. Wash the precipitate with 20 ml of water, centrifuge and decant. Dissolve the precipitate in acetone and transfer to a glass vial that fits in the well of a 3×3 in NaI(Tl) detector. Count 12.4-h ^{42}K, and after it has decayed, count 18.7-d ^{86}Rb and 2.1-y ^{134}Cs with a Ge(Li) detector. The alkali chemical yields are ascertained by the measurement of the ^{137}Cs tracer. A ^{137}Cs comparator consists of about 0.01 μCi ^{137}Cs that is diluted to the same volume as was the final alkali solution.

3. Diisopropyl ether must be completely eliminated from the acid solution in order to avoid combination of indium with the ether, which will interfere with its subsequent precipitation as hydroxide.

Separation of cadmium

The supernate from the above centrifugation after adjustment to pH 9–10 contains practically all the cadmium plus other ammonium-complexed ions; the volume of the solution should be 250–300 ml.

Add hydrochloric acid to give pH 1–2 and then add 1.5 g of ammonium dihydrogen citrate with stirring; the resultant pH should be 2. Heat to 70–80° and bubble hydrogen sulfide through the solution. If a yellow precipitate of cadmium sulfide is not formed within 30 sec, keep adding small amounts of citrate and dilute until precipitation occurs; the pH should be 2.5 (Note 1). Warm the solution to coagulate cadmium sulfide and centrifuge in 40-ml C-tubes. Wash the precipitate in each tube with 3–4 ml of 0.01 *M* hydrochloric acid, centrifuge and discard all the washings.

Add a few drops of hydrochloric acid to each tube, heat to boiling or until cadmium sulfide dissolves (less than 1 min), and combine all solutions quantitatively in one tube (5 ml). Dilute to 30 ml to make a 2 *M* acid solution and add *ca.* 10 mg of copper(II) as chloride. Bubble hydrogen sulfide through the cold solution, centrifuge, wash the precipitate with 3–4 ml of 2 *M* hydrochloric acid, add the washings to the solution in a 100-ml beaker and reject the precipitate.

Repeat the treatment with citrate, using *ca.* 0.5 g of citrate, and hydrogen sulfide, making sure that the final pH is 2.5. Centrifuge and wash as described above.

Dissolve cadmium sulfide with a minimum of hydrochloric acid, and boil to remove hydrogen sulfide. Add some hydrochloric acid, if necessary, to avoid complete evaporation of the acid solution; the final volume is *ca.* 0.5 ml. Dilute to *ca.* 2 ml and transfer the solution to a 25-ml ion-exchange column cup. Wash the C-tube two or three times with 2–3 ml of 3 *M* hydrochloric acid and join these liquids to the original in the cup. Pass the solution through a Dowex 1-X10 bed (100–200 mesh in a column of 9 mm i.d. and 100 mm high) at a rate of 1 ml min^{-1}. Wash with 20 ml of 3 *M* hydrochloric acid to remove any remaining nickel, and then with 40 ml of 0.1 *M* hydrochloric acid to eliminate zinc and the main indium activity. Reject all liquids. Elute cadmium with 3 *M* ammonia solution and collect in a 40-ml C-tube; the final volume should be 30 ml.

Add 5 mg of iron(III) scavenger followed by hydrochloric acid to dissolve the precipitate (pH *ca.* 2). Add 0.5 ml of 6 *M* ammonium acetate and boil until basic iron(III) acetate is precipitated. Note the time for the last cadmium–indium separation and the ^{115}In growth to equilibrium (*ca.* 30 h). Centrifuge, transfer the liquid to another C-tube and reject the precipitate. Pass hydrogen sulfide to precipitate cadmium sulfide, warm to about 80°, centrifuge and reject the supernate. Dissolve the precipitate in a minimum amount of hydrochloric acid, heat to remove hydrogen sulfide and repeat cadmium sulfide precipitation in presence of ammonium dihydrogen citrate at pH 2.5. Centrifuge and reject supernate. Dissolve cadmium sulfide with hydrochloric acid and heat to insure complete removal of hydrogen sulfide.

Dilute to 3 ml and add ammonia solution to pH *ca.* 2. Add 1.5 ml of 1.5 *M* ammonium monohydrogenphosphate dropwise with stirring and stir the hot solution for about 10 min until the precipitate becomes crystalline. Filter through a 1-in diameter chimney funnel using a tared glass fiber disc (Whatman GF/A). Wash the precipitate with deionized water, alcohol and ether. Vacuum-dry as described by SCHMITT *et al.*[14], and weigh as cadmium ammonium phosphate monohydrate. Mount the sample covered with mylar plastic film (1.7 mg cm^{-2}) on a stainless steel backing with frame. Count in a low background (say *ca.* 2 counts min^{-1}) GM flow counter, using a 95.05% helium–0.95% isobutane mixture as quenching gas, and follow the decay. Calculate the weight of cadmium in the sample, using the *approximate* formula $CdNH_4PO_4 \cdot H_2O$ and add this amount of cadmium(II) carrier solution to the cadmium comparator in a test tube. Dilute to about 5 ml and proceed as described in this paragraph (Note 2).

Notes. 1. If a darkening due to incipient precipitation of nickel sulfide is noticed, add immediately 1–2 drops of hydrochloric acid to restore the pH to 2–2.5. If enough citrate is present to buffer the solution, the pH will not go above 2.5 and nickel sulfide will not precipitate (pH 3.4), though other elements of the acid sulfide group, which do not form complexes with the citrate, may precipitate.

2. The final step is done to equalize both sample and comparator thicknesses, in order to eliminate possible errors from different β-scattering and self-absorption factors.

Cadmium is separated in this way in about 4 h with over 99% purity and a yield between 60 and 70%.

Separation of rare earths

The volume of the rare earth–yttrium fraction left in the middle of the separation scheme for indium is *ca.* 50 ml.

Precipitate the rare earth–yttrium hydroxides by adding concentrated ammonia solution to give pH 9–10. Centrifuge, decant and wash the precipitate. Dissolve in a minimum of concentrated hydrochloric acid, dilute to *ca.* 50 ml and adjust to pH 13–14 with 8 M sodium hydroxide to solubilize aluminium. Centrifuge, decant, and wash the precipitate twice with water. Again dissolve the precipitate with hydrochloric acid, transfer the solution to a 40-ml polycarbonate C-tube, and dilute to *ca.* 15 ml. Precipitate the rare earth–yttrium fluorides with 1 ml of saturated ammonium hydrogen fluoride solution and 1 ml of hydrofluoric acid. Centrifuge, discard the supernate, wash with 10 ml of water, centrifuge again and discard the supernate. Add 1–2 ml of saturated boric acid solution, heat, and add 1 ml of concentrated nitric acid with stirring to dissolve the precipitate. Precipitate the hydroxides with ammonia solution, centrifuge, discard the supernate, wash with 10 ml of water, centrifuge again, and discard the supernate. Dissolve the hydroxides with a minimum of hydrochloric acid and repeat the precipitation of the fluorides and the hydroxides three times in order to eliminate silica, scandium and iron through complex formation.

Dissolve the hydroxides with a minimum of hydrochloric acid and dilute to 10–15 ml; the pH should be between 1.5 and 2. Add 1 ml of neutral, 1/4 heavy, graded, wet Dowex AG50W-X12, 200–400 mesh, prepared as indicated by HASKIN *et al.*[12]. Stir for a minute, centrifuge, discard the supernate, wash twice with 5–10 ml of distilled water, centrifuge again, and discard the supernate thoroughly with a long beaked dropper. Add *ca.* 2 ml of α-hydroxyisobutyric acid eluting agent at pH 3.10 and transfer the slurry quantitatively with a long beaked dropper to the top of a column of the same resin (10 mm i.d. and 60 cm high) which has been equilibrated with the eluting agent. Distribute the resin evenly by stirring the surface gently with the tip of the dropper.

Run the gradient elution with the help of a fraction collector equipped with a timer, a 1-l Wolff bottle filled with 300 ml of (Note 1) *ca.* 0.5 M α-hydroxyisobutyric acid at pH 3.10 ± 0.01, and a 1-l pressure equalizing funnel filled with 400 ml of the same acid solution at pH 4.05 ± 0.01[10]. Pressurize with nitrogen gas in order to obtain an elution rate of 8–9 drops per min. The rate of dropping of the pH 4.05 solution should be 6–7 drops per min for a column-to-funnel drop weight ratio equal to 2.5.

The average weight of a drop eluted at pH 3.10 is 0.058 g (Note 2). Collect 20 drops per tube. At the Yb–Tm valley, change the funnel rate to 15 drops per min, and between Er and Ho, Ho and Dy, Tb and Gd, and Sm and Pm go successively to 20, 25, 30 and 35 drops per min (Note 3). Between the Eu and Sm peaks it is convenient to start collecting 30 drops per tube, and the elution rate may be raised at this step to 12 drops per min. At the Pr–Ce valley, stop operation, open the top of the column and add a few drops (up to 1 ml) of ammonia solution (s.g. 0.88) to speed up elution of lanthanum (Note 4). Count each test tube in a 30–130 keV window with a 1.75 × 2 in NaI(Tl) well detector (Note 5).

Transfer each fraction to a 50-ml C-tube, add 2–3 drops of 30% hydrogen peroxide, warm the solution and add enough ammonia solution to destroy the rare earth complexes and decompose any residual hydrogen peroxide. Warm further to coagulate the precipitate (Note 6), centrifuge, and discard the supernate. Dissolve the individual precipitates with a minimum of nitric acid and repeat the addition of ammonia (without peroxide), centrifugation and discarding. Dissolve the individual precipitates as before and divide the rare earths and yttrium into two groups: #1 (Lu, Yb, Er, Ho, Tb, Gd, Eu, Sm, Nd, Ce and La) and #2 (Tm, Dy–Y, and Pr).

Transfer the first group of solutions with a long beaked dropper into tared, 2-dram polyvials; the final volume should be 2–3 ml. Weigh the polyvials and pipet out *ca.* 20% of the solution volumes into clean, tared half-dram polyvials. Reweigh both polyvials to determine the amounts withdrawn and transferred. Heat-seal the polyvials. These rare earth solutions in half-dram vials and the appropriate rare earth carrier quantities are reactivated for chemical yield determinations; 15-h ^{24}Na contamination is minimized by two hydroxide precipitations (with and without peroxide; Note 7).

The remaining volume (*ca.* 80%) is counted together with the corresponding standards with either a NaI(Tl) or Ge(Li) detector coupled to a multichannel analyzer for both purity checks and calculation purposes.

Add saturated oxalic acid solution to the individual rare earths in the second group to precipitate the oxalates. Digest on a hot plate for 15 min. Filter through tared 24-mm glass fiber discs (Whatman GF/A) with gentle suction, wash the precipitates with water, alcohol, and ether, and vacuum-dry as described by SCHMITT *et al.*[14]. Count the Tm, Dy–Y and Pr oxalate precipitates with a β-counter.

To the Tm and Pr standards add about the same amount of carrier as calculated from weighing the oxalates, and precipitate and count the oxalates as described above (Note 8). To the combined Y and Dy standards, add a quantity of Dy carrier similar to that calculated from the Dy–Y oxalate precipitate obtained from the sample, and also *ca.* 0.1 μCi of ^{88}Y tracer. Count the 2.3-h ^{165}Dy decay with NaI(Tl) or Ge(Li) detectors and β-count the 64.2-h ^{90}Y. Purity is checked by decay and β-ray absorption curves. For Yb determination, the ^{174}Yb/^{169}Yb ratio may be determined by counting with a Ge(Li) detector.

Chemical yields of yttrium are simply obtained by γ-ray analysis of ^{88}Y in both sample and standard. The chemical yield of dysprosium is determined by weighing the oxalate precipitates or by reactivation. In the latter case, after measurement of ^{165}Dy, ^{90}Y, and ^{88}Y, transfer carefully the dysprosium oxalate precipitate and filter paper to a 2-dram polyvial, dissolve the precipitate with nitric acid, and remove the filter paper. Reactivate this solution together with an amount of dysprosium equivalent to the original dysprosium carrier and γ-analyze these two solutions.

Chemical yields of most of the rare earths were determined by reactivating the 20% volumes of solutions set aside in separate vials. Reference rare earth standards consisted of 1 ml each in half-dram vials. Activation periods and neutron fluxes were: Eu, Er and In, 10^9 n cm^{-2} sec^{-1} for 10 min; La, Ce, Sm, Gd, and Ho, $3\cdot10^{11}$ n cm^{-2} sec^{-1} for 10 min; and Nd, Tb, Yb, and Lu, $3\cdot10^{12}$ n cm^{-2} sec^{-1} for 5 min. Activated specimens were counted with either a 3 × 3 in NaI(Tl) detector or a 30-cm^3 Ge(Li) detector (Note 9).

The rare earths are separated in this way in about 15 h with a purity greater than 99% and a chemical yield of about 70%.

Notes. 1. This volume gave better separation than the 220 ml recommended by HASKIN *et al.*[12]. Also it was easier to control the rate of dropping of the pH 4.05 solution into the pH 3.10 solution, especially in the 6–7 drops per min range. When two samples are analyzed, the amounts of pH 3.10 and of pH 4.05 α-acid solutions are doubled.

2. A small bore tube is connected to the outlet of the pressure equalizing funnel to reduce the drop size, so as to obtain a more continuous change of pH.

3. Though successful elution curves were obtained by changing rates in 10-drop steps, it is advisable to adopt 5-drop steps in order to assure a reasonable final volume left in the Wulff bottle (80–100 ml).

4. The elution rate should not be increased before the europium peak has been observed, at which point all the remaining elements (with the possible exception of lanthanum) will have been removed from the original 1 ml of resin. An early increase in elution rate may result in peak broadening and excessive use of solutions.

5. No oxalic acid is needed for peak delimitation when the radioactivity levels of the rare earths are sufficient for this purpose.

6. The rare earths form complexes with α-hydroxyisobutyric acid, which result in precipitates of variable and unknown composition, either by using ammonia or oxalic acid. These precipitates carry down all the rare earths, but must be redissolved and reprecipitated to eliminate any residual organic acid.

7. Er, Eu and Gd do not go through this step, since they are relatively short lived. Simply transfer their solutions into clean half-dram polyvials for both counting and reactivation.

8. Though the number of molecules of crystallization water in rare earth oxalate precipitates is uncertain, precipitates are reproducible under similar conditions, and errors in the molecular composition cancel out when comparing sample and standard. Both terbium sample and standard should be counted with and without an appropriate aluminum absorber, say *ca.* 30 mg cm^{-2}; their respective ratios should be compared as a ^{170}Tm purity check.

9. In estimation of the required neutron fluxes for reactivation, the rare earth abundances in a typical basalt have been assumed and a 2-week decay period has been adopted between activation of the rock sample and reactivation for chemical yield determinations. In general, the activity levels of the pertinent rare earth radionuclides after reactivation were *ca.* 100 times the rare earth residual activities from the primary activation of the rock sample; therefore, the errors in the chemical yields from reactivation are below 1%. For lower rare earth abundances in the rock sample, compared to a typical basalt, neutron fluxes and/or activation time may be

decreased proportionately. In the analysis of a 1-g specimen of basalt or a rock with an equivalent quantity of the rare earths, small corrections of *ca.* 2% must be considered in the calculations of the cerium and neodymium chemical yields *via* the reactivation method, and corrections of *ca.* 1%, for the lanthanum chemical yield. For example, these obvious corrections for cerium and neodymium reflect the abundances (20–50 μg) of these elements in 1 g of basalt compared to 2 mg of added cerium and neodymium carriers.

RESULTS

Data for the measurement of the rare earths are shown in Table I. Peak energies are the most recently determined values[15]. Abundance values have been compiled in Table II. Available data from other studies are given for comparison.

TABLE I

NUCLEAR DATA FOR RARE EARTHS

Product nuclide(s) measured	*Half-life*	*Main energies (relative intensity) used in the determination (keV)*
^{140}La	40.2 h	1595.4(50)
^{143}Ce	33 h	293.1(60)
^{142}Pr	19.2 h	Beta counted
^{147}Nd	11.1 d	91.4(50); 531.0(20)
^{153}Sm	47 h	103.2(80)
^{152m}Eu	9.3 h	841.6(30); 963.5(30)
^{159}Gd	18.0 h	363.5(100)
^{160}Tb	72.1 d	879.4(21); 965.8(16)
^{165}Dy	2.32 h	94.6(35); 280(0.6); 361(1.1)
^{166}Ho	26.9 h	80.6(90)
^{171}Er	7.52 h	295.8(20); 308.1(50)
^{170}Tm	130 d	Beta counted
^{169}Yb	31.8 d	63.3(30); 177.0(15); 197.8(20)
^{175}Yb	101 h	396.1(50)
^{177}Lu	6.7 d	208.4(70); 113.0(30)
^{90}Y	64 h	Beta counted

Errors represent counting statistics of one measurement; total estimated overall errors are within ±5%, as indicated by decay of short-lived rare earth, yttrium, cadmium and indium radionuclides. The sensitivity of the method (3 σ) was tested in the analysis of DTS-1 and found to fluctuate between 1 and 100 p.p.b. Reproducibility was within 1–10% for most elements determined in G-2 and BCR-1. Consistently higher values were obtained in the second BCR-1 analysis for La, Ce, Nd, and Sm (light rare earth fraction), and these higher values are considered real and outside of experimental error. The higher light rare earth abundances are probably attributable to varying amounts of accessory minerals in the two analyzed fractions. If the sample that was higher in light rare earths had been enriched in plagioclase, the abundance of europium would be significantly higher than the observed 5% difference.

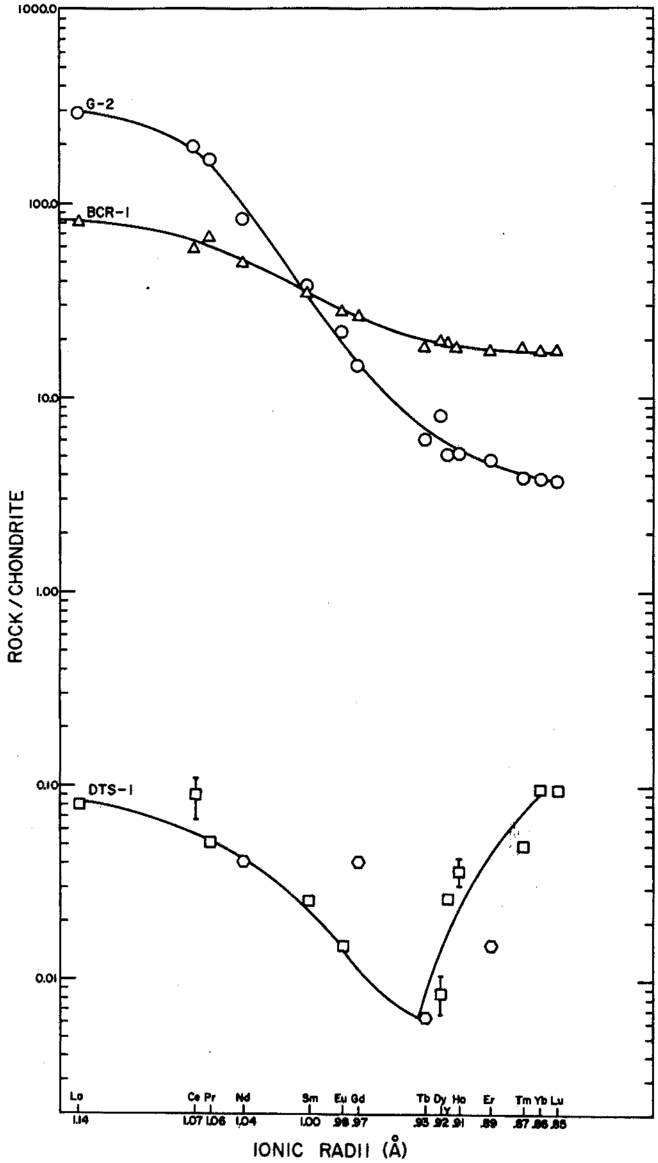

Fig. 1. Comparison plot for G-2 (○), BCR-1 (△) and DTS-1 (□,⬡). The p.p.m. rare earth elements have been divided element by element by the average values from 29 chondritic meteorites (HASKIN *et al.*[12]; SCHMITT *et al.*[11,14]). The statistical standard deviations are represented by the size of the symbols, △, ○, and □ except where otherwise indicated. Symbol ⬡ represents upper limit abundances (3 σ) of DTS-1.

DISCUSSION

Indium

This element is considered chalcophile–siderophile in meteorites and

TABLE II

ABUNDANCES IN USGS ROCK STANDARDS (p.p.m.)

G-2[a]					*BCR-1*[b]
Element	*This work*	*Others*[d]	MORRISON *et al.*[e]	HIGUCHI *et al.*[f]	*This work*
La	93 ± 7 93 ± 6	81–84(76–142)	78	87–95	23 ± 1 29 ± 1
Ce	163 ± 5 177 ± 5	144–167 (175, 180)	110	175–185	45 ± 2 57 ± 2
Pr	18.7 ± 0.2 18.7 ± 0.2	— (20)	—	—	7.4 ± 0.2 7.2 ± 0.2
Nd	48 ± 2 51 ± 2	—	67	42–51	26 ± 2 33 ± 2
Sm	7.2 ± 0.1 7.3 ± 0.1	7.3–9.1(10)	7.0	6.7–7.8	6.6 ± 0.2 7.2 ± 0.2
Eu	1.52 ± 0.02 1.53 ± 0.02	1.37–1.6	1.3	1.50–1.60	2.0 ± 0.1 2.1 ± 0.1
Gd	3.5 ± 0.1 3.9 ± 0.2	—	3	6.2–6.5	7.0 ± 0.3 6.3 ± 0.3
Tb	0.30 ± 0.02 —	0.52	0.5	0.49–0.50	0.92 ± 0.05 0.82 ± 0.02
Dy	2.5 ± 0.1 —	2.1	5.2	2.0–2.1	5.9 ± 0.4 6.4 ± 0.4
Ho	0.36 ± 0.01 0.36 ± 0.01	—	0.7	—	1.23 ± 0.02 1.40 ± 0.02
Er	0.80 ± 0.03 1.11 ± 0.06	—	—	—	3.7 ± 0.1 3.3 ± 0.1
Tm	0.12 ± 0.003 —	<0.4	0.3	<0.4	0.60 ± 0.01 0.53 ± 0.01
Yb	0.62 ± 0.02 0.81 ± 0.03	0.8(<1)	0.9	0.65–0.72	3.4 ± 0.1 3.3 ± 0.1
Lu	0.12 ± 0.01 0.13 ± 0.01	0.18	0.13	0.13	0.58 ± 0.04 0.57 ± 0.01
Y	8.1 ± 0.2 10.9 ± 0.3	—(8–<20)	—	—	36 ± 1 37 ± 1
Cd	0.072 ± 0.008 0.046 ± 0.009	— (0.01)	—	—	0.081 ± 0.0 0.20 ± 0.03 0.20 ± 0.03
In	0.028 ± 0.001 0.036 ± 0.001	0.028 (0.045)	0.04	—	0.079 ± 0.0 0.079 ± 0.0
K[h]	4.66 ± 0.05 (%)	4.0–3.9 (3.3–3.9)	—	—	—
Rb[h]	191 ± 3 177 ± 5	129–185 (108–513)	—	—	—

---

[a] Specimens were taken from Split 19, position 10.
[b] From either Split 9, position 13 and/or Split 30, position 21.
[c] From Split 31, position 21.
[d] FLANAGAN (1969); only activation analytical results are cited; values in parentheses were obtained by other techniques.

				DTS-1[c]		
hers[d]	MORRISON *et al.*[e]	HIGUCHI *et al.*[f]	HASKIN[g]	*This work*	*Others*[d]	HIGUCHI *et al.*[f]
–24(28–36)	23, 23	22–26	24–26	0.026 ± 0.002	<0.5	0.036
–53(40)	47, 39	62–63	56–66	0.076 ± 0.018	<0.1	0.039
5)	—	—	—	0.0058 ± 0.0002	—	—
–	27, 36	22–34	31–31	<0.024(3σ)	—	—
.5–7.4(10)	6, 6	7.1–7.5	7.4–7.5	0.0050 ± 0.0001	<0.1	0.0028
.0–2.3	2.1–1.8	2.35–2.42	1.93–1.96	0.0011 ± 0.0001	<0.002	0.0007
–	5, 5	6.7–7.3	6.7–8.1	<0.010(3σ)	—	—
.0	1, 1	1.14–1.20	1.17–1.19	<0.0003(3σ)	—	0.0003
.3	6	6.3	6.3–6.5	0.0026 ± 0.0006	—	—
–	1, 1	—	1.22–1.47	0.0026 ± 0.0004	—	—
–	—	—	2.5–3.9	<0.003(3σ)	—	—
.6	0.6, 0.6	0.6	—	0.0015 ± 0.0001	—	—
.2(3–5.5)	3.2, 3.0	3.5–3.7	3.5–3.5	0.018 ± 0.001	(<2)	0.0057
.60	0.62, 0.46	0.53–0.56	0.53–0.53	0.0031 ± 0.0001	(<3)	0.0014
0–60)	—	—	—	0.050 ± 0.001	(<3)	—
(0.067–<2)	—	—	—	—	(0.005)	—
0.11(0.075)	0.07, 0.08	—	—	0.0022 ± 0.0001 0.0030 ± 0.0004	0.0027 (0.004)	—
—	—	—	—	7.9 ± 0.4 7.6 ± 0.4	9	—
—	—	—	—	<0.043(3σ) <0.040(3σ)	0.23(0.5)	—

Ref. 9. Rare earth abundances are relative to abundance values in USGS standard rock W-1.
Ref. 10.
L. A. HASKIN, private communication, 1969.
K and Rb results obtained agree with FLANAGAN (1969) values for G-2. BCR-1 was not analyzed; no reliable values for comparison are in the literature for K.

essentially chalcophile in terrestrial rocks. In these it is found with preference in pyroxene-containing rocks, such as gabbros and basalts. The present results confirm this tendency, *i.e.* BCR-1 shows the highest concentration, followed by G-2, and last by DTS-1. The indium values are in excellent agreement with literature values[16].

Cadmium

This is considered a chalcophilic–lithophilic element. Because of its ionic radius in octahedral coordination (1.02 Å) it is expected to replace calcium and sodium in minerals such as the plagioclases. Cadmium has been determined in basic rocks by many investigators[17]. Abundances of cadmium determined by neutron activation range from 0.08 to 0.5 p.p.m. in ten different basic rocks[17]. Another sample of the Columbia Plateau Basalt, taken approximately from the BCR-1 site, yielded 0.33 p.p.m. of cadmium by neutron activation[14].

Rare earths

By comparison of the present data with those of MORRISON *et al.*[9] and others for available elements, it is evident that, in general, the agreement is very good, considering that the samples may have come from different batches or may have local inhomogeneities. Before this work, no significant rare earth abundances had been published for ultramafic rock standards.

Observation of the rare earth ratios in Fig. 1 indicates that BCR-1 and G-2 follow distribution patterns for basalts and granites relative to chondrites, with decreasing fractionation towards smaller ionic radii, while the heavy rare earth group shows relative abundances comparable to those in chondrites, *i.e.*, with no significant fractionation. Rare earths in DTS-1, on the other hand, do not quite follow the expected pattern characteristic of high-temperature peridotites[18] relative to chondrites, *i.e.* the high-temperature peridotites are decreasingly fractionated towards the smaller ionic radii. Rare earths in DTS-1 are depleted relative to chondrites in both groups. The observed fractionation behavior could be due either to rare earth contamination during sample preparation, *i.e.* in the rock crushing and mixing steps, or to two different kinds of partition in the light and heavy groups. It is of interest to cite that FREY AND HASKIN[19] have found a similar pattern to DTS-1 in olivines from ultrabasic rocks, and that MASUDA[20] found the same distribution in olivine minerals of the Brenham pallasite.

The authors acknowledge the assistance of T. D. COOPER and D. G. COLES, and also the OSTR reactor personnel for their cooperation. This investigation was supported by the National Aeronautics and Space Administration through NASA Grant NGL-38-002-020 and Contract NAS9-8097.

SUMMARY

Indium, cadmium, yttrium and the 14 rare earth elements were simultaneously separated in the U.S. Geological Survey standard rocks, BCR-1 (basalt), G-2 (granite), and DTS-1 (dunite), and determined by γ-spectrometry with a 3×3 in NaI(Tl) well crystal and associated electronics. This method enabled the accurate determination of all the rare earths within a short time compared with instrumental methods.

Indium and cadmium were separated in about 1.5 h and 4 h, respectively. Results for indium, cadmium and the rare earths are in excellent agreement with literature values. Indium and cadmium show decreasing concentrations in the sequence BCR-1/G-2/DTS-1. Relative to the rare earth distribution pattern in chondritic meteorites, the rare earth patterns observed in BCR-1 and G-2 are similar to other basalts and granites; however, the rare earth pattern in DTS-1 is V-shaped with a minimum at terbium and is similar to rare earth patterns observed in olivine minerals.

RÉSUMÉ

L'indium, le cadmium, l'yttrium et quatorze éléments de terres rares, ont été séparés simultanément et dosés par spectrométrie-γ. Cette méthode permet des dosages exacts et très rapides comparativement aux autres méthodes instrumentales. Indium et cadmium sont séparés en 1.30 et 4 h, respectivement. Les résultats obtenus concordent très bien avec les valeurs données dans la littérature. Les essais ont été effectués avec des roches standards de l'"U.S. Geological Survey": BCR-1 (basalte), G-2 (granit) et DTS-1 (dunite). La distribution des terres rares observée dans le BCR-1 et le G-2 relative à celle des terres rares dans les condrites est similaire à la distribution trouvée dans d'autres basaltes et dans d'autres granites; cependant la distribution dans le DTS-1 a la forme d'un V avec le minimum dans la région du terbium et elle est similaire aux distributions observées dans des minéraux à base d'olivine.

ZUSAMMENFASSUNG

Indium, Cadmium, Yttrium und die 14 Seltenerd-Elemente in den U.S. Geological Survey-Standardgesteinen BCR-1 (Basalt), G-2 (Granit) und DTS-1 (Dunit) wurden gleichzeitig durch γ-Spektrometrie mit einem 3×3 in NaJ(Tl)-Kristall und zugehöriger Elektronik bestimmt. Diese Methode ermöglichte die genaue Bestimmung aller Seltenen Erden innerhalb einer kurzen Zeit im Vergleich zu instrumentellen Methoden. Für Indium und Cadmium wurden etwa 1.5 h bzw. 4 h benötigt. Die Ergebnisse für Indium, Cadmium und die Seltenen Erden stimmen mit Literaturwerten ausgezeichnet überein. Indium und Cadmium zeigen in der Reihenfolge BCR-1/G-2/DTS-1 abnehmende Konzentrationen. Im Verhältnis zu den Seltenerd-Verteilungen in chondritischen Meteoriten sind die in BCR-1 und G-2 beobachteten Seltenerd-Verteilungen ähnlich denen anderer Basalte und Granite. Dagegen ist die Seltenerd-Verteilungskurve in DTS-1 V-förmig mit einem Minimum bei Terbium und ähnlich der in Olivin-Mineralien.

REFERENCES

1 C. C. SCHNETZLER, H. H. THOMAS AND J. A. PHILPOTTS, *Geochim. Cosmochim. Acta*, 31 (1967) 95.
2 J. C. COBB, *Anal. Chem.*, 38 (1967) 127.
3 S. R. TAYLOR, *Geochim. Cosmochim. Acta*, 29 (1965) 1243.
4 G. D. NICHOLLS, A. L. GRAHAM, E. WILLIAMS AND M. WOOD, *Anal. Chem.*, 39 (1967) 584.
5 E. ALEKSIEV AND R. BOYADJIEVA, *Geochim. Cosmochim. Acta*, 30 (1966) 511.
6 G. E. GORDON, K. RANDLE, G. G. GOLES, J. B. CORLISS, M. H. BEESON AND S. S. OXLEY, *Geochim. Cosmochim. Acta*, 32 (1968) 369.

7 K. Tomura, H. Higuchi, N. Miyaji, N. Onuma and H. Hamaguchi, *Anal. Chim. Acta*, 41 (1968) 217.
8 F. M. Graber, H. R. Lukens and J. K. MacKenzie, *Trans. Am. Nucl. Soc.*, 12 (1969) 1.
9 G. H. Morrison, J. T. Gerard, A. Travesi, R. L. Currie, S. F. Peterson and N. M. Potter, *Anal. Chem.*, 41 (1969) 1633.
10 H. Higuchi, K. Tomura, N. Onuma and H. Hamaguchi, submitted to *Geochem. J.*, July 1, 1969.
11 R. A. Schmitt, R. H. Smith and D. A. Olehy, *Geochim. Cosmochim. Acta*, 28 (1964) 67.
12 L. A. Haskin, T. R. Wildeman and M. A. Haskin, *J. Radioanal. Chem.*, 1 (1968) 337.
13 H. Nagasana and H. Wakita, *Geochem. J.*, 1 (1967) 149.
14 R. A. Schmitt, R. H. Smith and D. A. Olehy, *Geochim. Cosmochim. Acta*, 27 (1963) 577.
15 R. Dams and F. Adams, *Radiochim. Acta*, 10 (1968) 1.
16 T. A. Linn, Jr. and R. A. Schmitt, Indium, to be published in K. H. Wedepohl, K. Turekian and D. M. Shaw, *Handbook of Geochemistry*, Part II.
17 H. Wakita and R. A. Schmitt, Cadmium, to be published in K. H. Wedepohl, K. Turekian and D. M. Shaw, *Handbook of Geochemistry*, Part II.
18 L. A. Haskin, F. A. Frey, R. A. Schmitt and R. H. Smith, *Physics and Chemistry of the Earth*, Pergamon Press, 1966.
19 F. A. Frey and L. A. Haskin, oral communication at the *Annual Meeting of the American Geophysical Union, Washington, 1968.*
20 A. Masuda, *Earth and Planetary Science Letters*, 5 (1968) 59.

Analytica Chimica Acta
Elsevier Publishing Company, Amsterdam
Printed in The Netherlands

MULTI-ELEMENT ATOMIC FLUORESCENCE SPECTROSCOPY

PART I. STIMULATION OF ATOMIC FLUORESCENCE OF MIXTURES OF BISMUTH, MERCURY, SELENIUM AND TELLURIUM; CADMIUM AND ZINC; GALLIUM AND INDIUM BY MEANS OF MULTI-ELEMENT MICROWAVE-EXCITED ELECTRODELESS DISCHARGE TUBES

G. B. MARSHALL* AND T. S. WEST
Department of Chemistry, Imperial College of Science and Technology, London, S.W. 7 (England)

(Received February 20th, 1970)

Atomic absorption measurements are normally made with individual hollow-cathode lamps for each element. This is sometimes seen as a disadvantage on the grounds that each laboratory must maintain a range of hollow-cathode lamps for all the metals that have to be determined. Multi-hollow cathode lamps have been described in which several cathodes are sealed inside the same lamp envelope with variable connections to the cathodes as required[1]. Multi-element hollow cathodes have also been used in which the elements concerned are formed into a cathode alloy or in which rings of individual metals are mounted in the cathode. Neither of these devices is satisfactory, chiefly because of selective sputtering of the more volatile elements; these volatile metals predominate in the resonance line output, so that the system tends to be unsatisfactory except for the predominant metal in the group. Continuum sources have been used in atomic absorption measurements[2,3], but this is largely an academic exercise. The apparatus requirements are considerable and the sensitivity of measurement is inferior to that obtained with individual hollow-cathode lamps.

A continuum source can be used more successfully with atomic fluorescence measurements[4-7] since it is not necessary to monochromate the radiation so finely. The atoms in the flame, or other atom reservoir, absorb only those parts of the continuum that correspond to the total absorption profile of the resonance lines of the atomic species in the atom reservoir. The absorbed radiation is then re-emitted by resonance, stepwise or direct line fluorescence. Plurality of line emission by a single element, or simultaneous fluorescence by several elements, is subsequently sorted out by use of a monochromator. This system is a much more practical proposition than atomic absorption with a continuum source and our experience is that, whilst it is almost always less sensitive than flame photometry using the same apparatus, it tends to be somewhat less subject to radiation interferences[7].

The evolution of microwave-excited electrodeless discharge tubes as atomic line sources for atomic spectroscopy[8] has made possible the determination of most metals by atomic fluorescence spectroscopy. Those with resonance lines in the UV region at wavelengths shorter than 320–340 nm can be measured with a higher sensitivity than is generally possible by atomic absorption or flame photometry, because the

---

*Present address: Central Electricity Research Laboratories, Leatherhead, Surrey.

fluorescence signal is linearly related to the line intensity of the source at low atomic concentrations. In absorption, the signal is not proportional to the source intensity and line sources operated at high powers tend to suffer from line broadening, etc., which is particularly detrimental to sensitivity. In flame photometry, the sensitivity is tied to the temperature of the flame, except where thermal equilibrium does not prevail, *e.g.* in chemiluminescence.

In fluorescence, however, the energising source is external to the flame, and it is possible to optimise conditions separately. Additionally, energy can be passed to the atomic population at very energetic short wavelengths and analysed at longer wavelengths by use of stepwise and direct-line fluorescence.

However, atomic fluorescence measurements with microwave-excited electrodeless discharge tubes have hitherto been subject to the same restriction that individual sources are necessary for each element. An examination of multi-element electrodeless discharge tubes has therefore been made in an endeavour to provide multi-element analysis. Since all, or virtually all, of the material within the envelope of the electrodeless discharge tube may be maintained in the vapour phase during operation, there should be no selective volatilisation problem as in multi-element hollow-cathode lamps. Consequently, each element should produce line emissions varying in intensity according to the oscillator strength of the line.

In this paper, the construction of a multi-element electrodeless discharge tube source for Bi–Hg–Se–Te and dual-element tubes for Cd–Zn and Ga–In is described and their application to the atomic fluorescence spectroscopy of these elements in admixture in sample solutions is discussed. A comparison is made of fluorescence using the cadmium–zinc source with that from individual (single metal) spectral discharge lamps of the sodium street-lamp variety for cadmium and zinc. The sensitivity of determination of the relatively long wavelength fluorescence of gallium and indium is compared with the sensitivity for the same elements in flame photometry on the same equipment with the same instrumental settings.

The bismuth–mercury–selenium–tellurium source

The preparation of microwave-excited electrodeless discharge tubes for the individual elements, bismuth[9], mercury[10], thallium[10], antimony[11], arsenic[12], selenium and tellurium[8] has been described previously. Mercury can be used as the metal or as its iodide, but tellurium is normally used as its iodide and selenium as the metal. Bismuth may be used as its iodide, but a near coincidence of the iodine 206.163-nm non-resonance line and the bismuth resonance line at 206.170 nm allows spectral overlap excitation of bismuth by a source containing iodine or iodide at the latter wavelength. The resonance fluorescence emission of bismuth at 206.17 nm or its direct line fluorescence emission at 269.17 nm or 302.5 nm may be measured. The most sensitive determination is obtained at 302.5 nm[9], however. In the present experiments, selenium, tellurium and iodine, plus a trace of mercury which was allowed to diffuse into the tube from the mercury gauge on the vacuum line, were sealed in the envelope of the tube and the contents were heated to yield the iodides. This tube gave lines for tellurium and mercury which were similar in intensity to the corresponding lines from individual tellurium and mercury tubes, and fluorescence signals for bismuth which were also similar to those obtained with an iodine source. The sensitivity for selenium was slightly reduced because tubes for the latter are not normally made from the iodide, but from the more volatile free metal.

The cadmium–zinc dual-element source

The cadmium–zinc source was prepared from the metals since both are relatively volatile (they have vapour pressures of 1 torr at 393° and 487°, respectively). These tubes were very easily prepared and were operated in quarter wave and three-quarter wave cavities with equal facility.

Argon filler gas pressures of 0.3 torr and 3 torr were found to be optimal for the quarter wave and three-quarter wave cavities, respectively. The dual-element electrodeless discharge tube was found to have line intensities for cadmium and zinc which were of the same order of intensity as individual (single-element) tubes for cadmium or zinc prepared at the same time. Both cadmium and zinc have been determined previously by atomic fluorescence with spectral discharge lamps[13–15], and continuum sources have also been used[4,5,7]. A comparison was, therefore, made of the fluorescence signals obtained with the dual-element Cd–Zn tube and with individual discharge lamps of the type previously used.

The gallium–indium dual-element source

Both gallium and indium metals have rather low vapour pressures at elevated temperatures and they were, therefore, incorporated in the electrodeless discharge tubes as their iodides in the normal way[8]. Once again, the dual-element electrodeless discharge tube was found to give fluorescence intensities for indium and gallium which were similar to those obtained from the corresponding single-element tubes. The atomic fluorescence of indium and gallium has been studied previously with microwave-excited electrodeless discharge tubes[13]; in this study better detection limits were obtained than in the previous work, though this may be a function of the sensitivity of the measuring apparatus as well as the intensity of the source.

Both gallium and indium may be determined quite sensitively by flame photometry since their excitation potentials are sufficiently low. An investigation of the sensitivity of determination of both elements by flame photometry and atomic fluorescence with the dual-element source was therefore made for comparison.

EXPERIMENTAL

Apparatus

A "Southern Instruments" A1740 Grating Integrating Flame spectrophotometer with diffraction grating ruled at 16,000 lines per inch and blazed at 500 nm was used. Because of the blazing of the grating, most of the elements had to be determined by second-order diffraction thus reducing the sensitivity of the signals. The instrument was operated with a 0.1-mm slit with 20-sec integration under the line and with automatic background correction.

Microtron 200 Microwave Generator (Electromedical Supplies Ltd) delivering 2450 ± 50 MHz ($\lambda = 125$ mm) at up to 200 W used in conjunction with a three-quarter wave (210L) or quarter wave (214L) cavity.

An air–propane flame was used throughout these studies, burning on a Meker-type burner-head.

Standard solutions

Selenium or tellurium (1250 p.p.m.). 1.250 g of the metal was dissolved in 25 ml of a mixture of concentrated nitric and hydrochloric acids, diluted to 500 ml with distilled water, neutralised with 0.88 (sp. gr.) ammonia solution and made up to 1 l.

Bismuth (1455 p.p.m.) solution was prepared by dissolving the metal in concentrated nitric acid and diluting to an acidity of 0.4 *M*.

Mercury (1000 p.p.m.) solution was prepared from mercury(I) nitrate in 0.5 *M* nitric acid.

Cadmium (1124 p.p.m.) and *zinc* (653.7 p.p.m.) solutions were prepared by dissolving suitable amounts of the nitrate and sulphate salts, respectively, in distilled water.

Indium (1248 p.p.m.) and *gallium* (920 p.p.m.) solutions were prepared by dissolving the metal in concentrated hydrochloric acid and diluting to a final acidity of 0.2 and 0.4 *M*, respectively.

All these stock solutions were prepared from analytical-grade reagents. The solutions were diluted to the desired strength, just before use, in order to minimise errors arising from the absorption of metal ions on glassware from very dilute solutions during storage.

Preparation of electrodeless discharge tubes

The silica tubes were prepared to be *ca.* 30 mm in bulb length, from transparent silica tubing (10 mm o.d., 8 mm i.d.; Jencons) as described previously[8].

Bi–Hg–Se–Te multi-element source. Selenium, tellurium and bismuth (5 mg each) were added to the prepared bulb after it had been carefully degassed by repeated heating under vacuum and flushing with argon. The metals were also dried and degassed within the tube by partial distillation up the walls of the tube.

Iodine (5 mg) was added and this was partially sublimed, (and gently degassed) onto a cooled upper portion of the bulb. Finally the tube was hermetically sealed by strongly heating the constriction in a small oxy–propane flame and sealing in the usual way with an argon pressure of *ca.* 0.5 torr. During the sealing operation care was taken to allow sufficient mercury to diffuse back into the tube to allow subsequent mercury line emission.

Individual tubes were made for bismuth (iodine), mercury, selenium and tellurium (Te + I) in the usual way[8].

Cd–Zn dual-element source. Cadmium and zinc metals (5 mg each) were introduced into the prepared degassed bulb which was flushed with argon, and the metals were degassed by distillation onto the walls of the bulb by heating under vacuum. Those tubes for use on the quarter wave cavity were finally sealed under a pressure of 0.3 torr of argon, and those for use on the three-quarter wave cavity at 3 torr. The three-quarter cavity gave better stability because of its more uniform microwave field and its thermostatting effect.

Individual cadmium and zinc tubes were made in the same way with 5 mg of either element.

Ga–In dual-element source. Indium and gallium metals (5 mg each) were introduced and degassed as described for the Cd–Zn source. Iodine (*ca.* 5 mg) was introduced and carefully degassed as described for the Bi–Hg–Se–Te source. Finally the tube was hermetically sealed under an argon pressure of 3 torr and heated strongly to cause formation of the iodides. The Ga–In dual-element source was operated in the three-quarter wave cavity only.

Instrumental settings

The instrumental settings for the various determinations are shown in Table I.

As an alternative to setting the individual wavelengths manually, the instrument may be scanned slowly across the necessary wavelength range, while the solution is sprayed and the flame is irradiated with the appropriate multi-element source.

TABLE I

INSTRUMENTAL SETTINGS FOR MULTI-ELEMENT ELECTRODELESS DISCHARGE TUBES IN THE THREE-QUARTER WAVE RESONANT CAVITY

Source tube	*Running power (W)*	*Element*	*Wavelength (nm)*	*Scale expansion*
Bi–Hg–Se–Te	40–50	Bi	302.5	—
		Hg	253.7[a]	2
		Se	204.0[a]	2
		Te	238.3–238.6[a]	2
Cd–Zn[b]	60	Cd	228.8[a]	2
		Zn	213.9[a]	2
Ga–In	60	Ga	417.2[c]	—
		Ga	403.3	—
		In	451.1[c]	—
		In	410.18	—

[a] Used in second order because of blaze of grating.
[b] With Osram discharge lamp *via* ballast unit at 1.5 A, 18-W Cd lamp, 20-W Zn lamp.
[c] Most sensitive line.

Analytical procedures

Bi–Hg–Se–Te. Initiate the multi-element electrodeless discharge tube in the three-quarter wave cavity by means of a "Tesla" vacuum testing coil and allow the source to reach equilibrium at 40–50 W over a period of 15–20 min. Light the air–propane flame, adjust the air pressure to 15 psig and the propane flow rate at a level sufficient to obtain a non-luminous flame with stable well-defined primary cones. Spray the test solution containing $\leqq$ 40 p.p.m. Bi, $\leqq$ 50 p.p.m. Hg, $\leqq$ 125 p.p.m. Se and $\leqq$ 125 p.p.m. Te into the flame in the usual way. Use maximum line sensitivity (maximum EHT to line photomultiplier) and a 20-sec integration period under each line with the settings shown in Table I. The automatic background correction function of the apparatus is adjusted separately at each wavelength setting. Record the fluorescence intensity at each wavelength setting.

Cd–Zn. Initiate the dual-element electrodeless discharge tube in the three-quarter wave cavity as above and allow it to reach equilibrium for *ca.* 15 min at 60 W. Adjust the air–propane flame as described above, spray the test solution containing $\leqq$ 0.03 p.p.m. cadmium and $\leqq$ 0.1 p.p.m. zinc, and measure as described above.

In using the "Osram" discharge lamps, the solution should contain $\leqq$ 1 p.p.m. cadmium and $\leqq$ 1.6 p.p.m. zinc. A similar warm-up time is allowed for the lamps as for the discharge lamps.

Ga–In. Proceed as for Cd–Zn but with solutions containing $\leqq$ 12.5 p.p.m.

indium and $\leqq$ 100 p.p.m. gallium, measuring the signals at the most sensitive lines (Table I). Both gallium and indium show quite strong thermal emission at both their respective wavelengths. These were recorded with the fluorescence signals since both are d.c. in nature with the apparatus used. To obtain the signal due to the fluorescence, cut off the entry of light from the electrodeless discharge tube into the flame and subtract the thermal emission signal then obtained from the previously measured total signal. This problem does not arise with modulated sources and tuned a.c. amplifiers.

DISCUSSION

The use of automatic background correction necessitates the use of a fairly narrow slit width and this is compensated for by the use of the 20-sec integration period. This makes impossible adoption of the definition of the detection limit as twice the background noise. Accordingly, in these studies the detection limit was taken as twice the standard deviation of the analytical method as determined experimentally near the lower end of the analytical calibration curve.

The fluorescence of selenium was observed at 196.1, 204.0 and 206.3 nm. All the signals had to be examined in second-order diffraction because of the monochromator being blazed at 500 nm. The 204.0-nm line was the most sensitive and yielded a detection limit of 10 p.p.m. This is slightly greater than the detection limit obtained with a selenium (metal) electrodeless discharge tube because the somewhat involatile iodide was used in the multi-element source. The fluorescence curve is shown in Fig. 1. The presence of hundred-fold excesses of the other three elements in the solution caused no interference in the fluorimetric determination of selenium even though the multi-element electrodeless discharge tube was irradiating the flame with the lines for all four elements simultaneously.

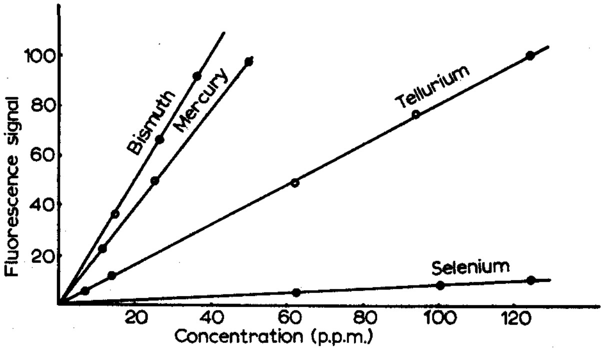

Fig. 1. Fluorescence curves for bismuth, mercury, selenium and tellurium with multi-element Bi–Hg–Se–Te source.

The fluorescence of tellurium was observed at 225.9, 238.3 and 238.6 nm in second-order diffraction. The last two lines were not resolved by the monochromator and the combined lines were found to be *ca.* five times more intense in fluorescence yield than the 225.9-nm line. In this instance no substantial difference was found between the sensitivity of the fluorescence excited by the multi-element electrodeless discharge tube and that excited by a tellurium tube. A detection limit of 1.5 p.p.m.

Te was obtained in second-order diffraction. Again there was no mutual interference from the other three elements in the solution. A calibration curve for tellurium is shown in Fig. 1.

For bismuth, the 302.5-nm fluorescence (see p. 180) gave the best detection limit (0.5 p.p.m.) and this is comparable to the sensitivity obtained by means of an iodine tube. Figure 2 shows a comparison of the fluorescence intensities of all three main bismuth lines in first- and second-order diffraction. In this particular instance, an integration time of 10 sec was used.

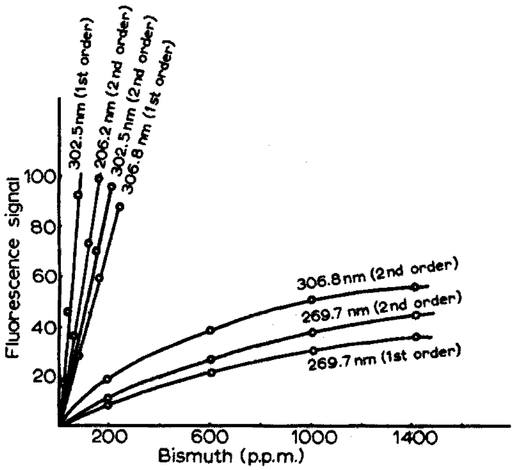

Fig. 2. Fluorescence curves for bismuth at various wavelengths and in various orders of diffraction.

Figure 1 also shows the calibration curve obtained for the most sensitive mercury line at 253.7 nm but in second-order diffraction. The curve is linear up to 50 p.p.m. and yields a detection limit of 0.6 p.p.m.; the other three elements present in the solution do not interfere.

Table II shows the results obtained when each element was determined at its own wavelength in the presence of 100-fold excesses of the other elements whose re-

TABLE II

DETERMINATION OF KNOWN AMOUNTS OF SELENIUM, TELLURIUM, MERCURY AND BISMUTH IN PRESENCE OF EACH OTHER (*ca.* 100-FOLD EXCESS) BY ATOMIC FLUORESCENCE SPECTROSCOPY WITH A MULTI-ELEMENT Bi–Hg–Se–Te SOURCE

Mercury (p.p.m.)		*Bismuth (p.p.m.)*		*Tellurium (p.p.m.)*		*Selenium (p.p.m.)*	
Taken	*Found*	*Taken*	*Found*	*Taken*	*Found*	*Taken*	*Found*
50.0	49.1	36.3	36.5	62.5	63.4	125	121
50.0	48.7	36.3	38.2	62.5	61.8	125	123
25.0	26.2	36.3	35.4	12.6	12.7	62.5	61.6
25.0	25.4	14.5	16.1	12.5	12.5	62.5	63.0
25.0	26.1	14.5	14.2	6.2	6.0		
12.5	13.0	14.5	15.0	6.2	6.3		
12.5	12.2	1.4	1.7				
5.0	5.2	1.4	1.0				
5.0	6.1	1.4	1.5				

sonance or direct line fluorescence was being simultaneously excited by the multi-element Bi–Hg–Se–Te source. These results indicate the reliability of this first multi-element electrodeless discharge tube to be devised for atomic fluorescence spectroscopy.

Cadmium exhibits strong resonance fluorescence at 228.8 nm and the signal was remarkably strong even with the second-order mode which had to be used in these experiments; a detection limit of 0.0003 p.p.m. cadmium was found. The 326.1-nm line was not detected (even though the source emits it quite strongly) because it has a very low g.f. value, and the conditions in the air–propane flame did not seem to stimulate stepwise fluorescence of cadmium at 326.1 nm. The 18-W cadmium "Osram" discharge lamp behaved similarly to the Cd–Zn dual source, but gave a detection limit of only 0.01 p.p.m. at 228.8 nm. With the dual-element source, a typical calibration graph was rectilinear over the range 0.005 to 0.025 p.p.m. cadmium with fluorescence signals ranging from 20 to 100 arbitrary scale units. When the cadmium discharge lamp was used, an analogous curve was obtained for the range 0.1–1.0 p.p.m. cadmium. The presence of zinc in the test solution and simultaneous stimulation of its fluorescence in the flame by the Cd–Zn dual source caused no interference of any kind.

The zinc fluorescence similarly examined showed no interference from cadmium. The 213.9-nm line was used and it yielded a detection limit of 0.002 p.p.m. for the dual source and 0.023 p.p.m. for the Osram discharge lamp. With the dual source, a typical calibration graph was rectilinear over the range 0.01–0.1 p.p.m. zinc with fluorescence signals ranging from 10 to 75 scale units; with the discharge lamp, analogous graphs were found over the range 0.4–1.6 p.p.m. zinc.

Both the fluorescence signals for cadmium and zinc were equally intense using the Cd–Zn dual-element source or individual cadmium or zinc electrodeless discharge tubes. The dual-element source yielded fluorescence detection limits *ca.* 40 times better for cadmium and 10 times better for zinc than those obtained using the spectral discharge lamps. The increased sensitivity comes from the greater line intensity of the electrodeless discharge tubes and probably also from their lower tendency to suffer self-reversal because of the manner of their operation.

These results obtained with the dual-element electrodeless discharge tube for Cd–Zn again exhibit freedom from mutual interference, and sensitivities comparable to those obtained using separate single-element tubes for each element. The detection limits compare favourably with those reported elsewhere[4,5,13–15], but this may be a matter of instrumental response as well as line intensity. It should of course be possible to obtain much superior detection limits by using a grating blazed much closer to the zinc/cadmium wavelengths, by the use of slightly wider slits, etc.

Figure 3 shows the relative fluorescence intensities and thermal emission sensitivities of indium at 451.1 and 410.18 nm. As explained previously, the fluorescence curve had to be obtained by subtraction of the thermal emission signal from the measured total of thermal emission and fluorescence because the instrument was not of the frequency-discriminating kind. In both cases the 451.1-nm line was the more sensitive. A detection limit of 0.2 p.p.m. indium was obtained by atomic fluorescence and 0.6 p.p.m. by flame photometry, both at 451.1 nm. Both techniques yielded a detection limit of *ca* 0.7 p.p.m. at 410.18 nm.

Similarly, Fig. 4 shows the relative fluorescence and thermal emission curves for gallium obtained as for indium. In both techniques the 417.2-nm line is more sensitive than the 403.3-nm line which is also emitted quite strongly, however. Detection limits of 1 p.p.m. and 4.6 p.p.m. were obtained at 417.2 nm by fluorescence and flame photometry respectively, whilst at 403.3 nm, the corresponding detection limits were 3 p.p.m. and 9.2 p.p.m.

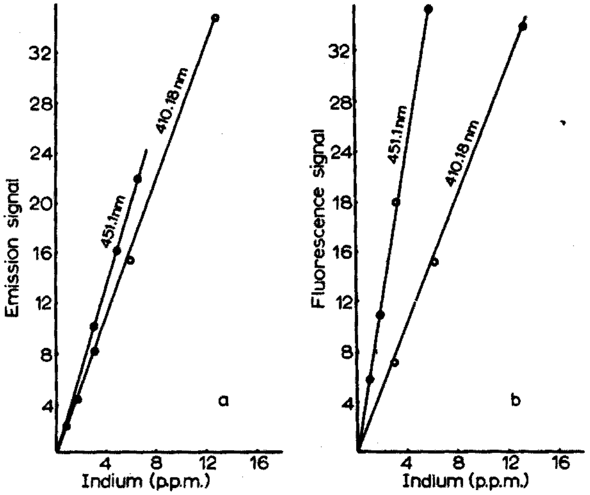

Fig. 3. Fluorescence and thermal emission curves for indium: (a) thermal emission at 451.1 and 410.18 nm; (b) fluorescence at 451.1 and 410.18 nm excited by Ga–In dual source.

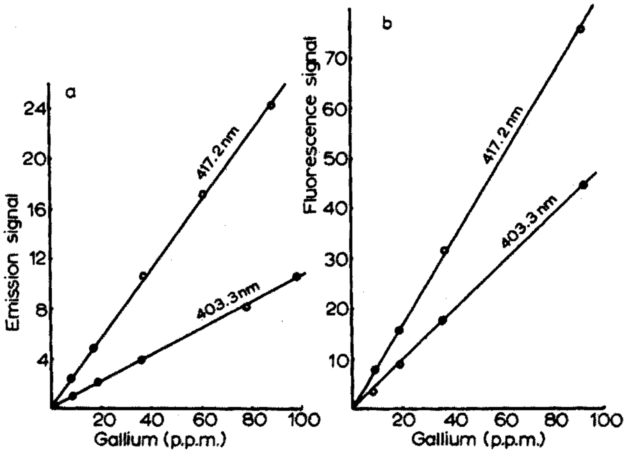

Fig. 4. Fluorescence and thermal emission curves for gallium: (a) thermal emission at 417.2 and 403.3 nm; (b) fluorescence at 417.2 and 403.3 nm excited by Ga–In dual source.

It is not possible to make comparisons of sensitivity of these determinations with those obtained for indium, gallium, cadmium, zinc, etc. with other equipment, but once again the fluorescence detection limits compare favourably with previously reported fluorescence work on indium and gallium. What is remarkable, however, is that the sensitivity of the fluorescence technique is better than that of flame photometry even at a wavelength as long as 450 nm. Better detection limits have of course been reported for indium and gallium[16, 17] than those found in this study, but this is a function of the use of lower background flames, *e.g.* air–hydrogen, which would be beneficial also in fluorescence measurements, and of the use of more sensitive equipment which would again be of benefit to fluorescence measurements.

The fluorescence signals for indium and gallium were of the same order of intensity as those obtained by the use of individual indium or gallium electrodeless discharge tubes and it was again found that each element could be determined by atomic fluorescence measurements in the presence of large excesses of the other whilst the flame was being irradiated by the dual-element source, without any radiative interference problems.

This study of these multi-element electrodeless discharge tubes for Bi–Hg–Se–Te, Cd–Zn, Ga–In has shown that the tubes can be operated over prolonged periods of time in exactly the same way as the individual (single-element) tubes and that their intensity and stability are as good as those of the single-element tubes. Furthermore, it has been demonstrated that, in the examples which have been looked at so far, there is no spectral interference introduced by the simultaneous presence of additional elements in the source and in the solution to be analysed. It is, of course, apparent that with any multi-element source a monochromator must be used which has sufficient resolution to differentiate between the lines fluoresced by the elements introduced into the flame. In this respect, it is very probable that the resolution requirement of the monochromator need not be nearly as stringent as that for thermal emission measurements because the fluorescence spectra of most elements are generally restricted to a few very intense lines. Even where there are more than one or two lines, most of the others are usually relatively weak[9].

The number of elements that may be incorporated into a single electrodeless discharge tube requires examination, but there appears to be no difficulty, from these experiments, in incorporating three or four at least. In these initial experiments care has been taken to select elements of similar vapour pressures so that the conditions for microwave excitation within the electrodeless discharge tube are similar. Care must also be taken in selecting the group of elements to be incorporated in the multi-element electrodeless discharge tube, that no two lines of the different elements that are caused to fluoresce in the flame shall fall within the bandpass of the monochromator to be used for the analysis. Similar considerations apply to the determination of elements by atomic absorption spectroscopy, and in this case it would also be necessary that no two lines emitted by the multi-element source itself should fall within the bandpass of the monochromator.

Further experiments are now in progress to permit the construction of multi-element electrodeless discharge tubes for groups of elements of quite different vapour pressures. The application of these multi-element sources to atomic absorption measurements will also be described.

We are grateful to Messrs. I.C.I. Ltd. for the award of a grant for the purchase of the spectrophotometer used in these experiments. One of us (G.B.M.) also wishes to thank the Central Electricity Generating Board for the award of a scholarship.

SUMMARY

The construction and use of multi-element electrodeless discharge tubes for excitation of the atomic fluorescence of bismuth, mercury, selenium and tellurium; cadmium and zinc; and gallium and indium, are described. The tubes are operated at *ca.* 50–60 W and 2450 MHz in a three-quarter wave resonant cavity and the fluorescence is generated in a premixed air–propane flame. The performance and fluorescence detection limits obtained with the multi-element tubes are of the same order as those obtained with the individual single-element tubes. There is no spectral interference from the presence of 100-fold excesses of the co-elements in the analyte solution. The atomic fluorescence detection limit for indium is three times better than the corresponding detection limit for flame photometry at its most sensitive wavelength of 451.1 nm, on the same apparatus at similar instrumental settings.

RÉSUMÉ

On décrit la construction et les applications de tubes à décharge multi-éléments pour l'excitation de fluorescence atomique de bismuth, mercure, sélénium et tellure; cadmium et zinc; gallium et indium. Les possibilités et limites de détection obtenues avec ces tubes sont du même ordre que celles des tubes à un seul élément. Il n'y a pas d'interférence spectrale, en présence d'un excès de 100 fois des coéléments, dans la solution à analyser. La limite de détection de l'indium par fluorescence atomique est trois fois meilleure que la limite de détection correspondante pour la photométrie de flamme, à sa longueur d'onde la plus sensible de 451.1 nm, sur le même appareil.

ZUSAMMENFASSUNG

Es werden die Konstruktion und die Verwendung von elektrodenlosen Multielement-Entladungsröhren für die Anregung atomarer Fluoreszenz von Wismut, Quecksilber, Selen, Tellur; Cadmium und Zink, und Gallium und Indium beschrieben. Die Lampen werden bei *ca.* 50–60 W und 2450 MHz in einem Dreiviertelwellen-Resonanzhohlraum betrieben. Die Fluoreszenz wird in einer vorgemischten Luft–Propan-Flamme erzeugt. Die mit den Multielement-Röhren erhaltenen Nachweisgrenzen sind von derselben Grössenordnung wie die bei den individuellen Einzelelement-Lampen. Ein 100facher Überschuss der anderen Elemente in der Analysenlösung ruft keine spektrale Störung hervor. Die Atomfluoreszenz-Nachweisgrenze für Indium ist dreimal besser als die entsprechende Nachweisgrenze bei der Flammenphotometrie bei der empfindlichsten Wellenlänge 451.1 nm, wenn dieselbe Apparatur und ähnliche instrumentelle Einstellungen benutzt werden.

REFERENCES

1 A. WALSH, in J. W. ROBINSON, *Atomic Absorption Spectroscopy*, Marcel Dekker, New York, 1966, p. 19–20.
2 J. H. GIBSON, W. E. L. GROSSMAN AND D. W. COOKE, in P. W. WEST, A. M.G. MACDONALD AND T. S. WEST, *Analytical Chemistry 1962*, Elsevier, 1963, p.288.
3 V. A. FASSEL, V. G. MOSSOTTI, W. E. L. GROSSMAN AND R. N. KNISELEY, *Spectrochim. Acta*, 22 (1966) 347.
4 C. VEILLON, J. M. MANSFIELD, M. L. PARSONS AND J. D. WINEFORDNER, *Anal. Chem.*, 38 (1966) 204.
5 R. M. DAGNALL, K. C. THOMPSON AND T. S. WEST, *Anal. Chim. Acta*, 36 (1966) 269.
6 D. W. ELLIS AND D. R. DEMERS, *Anal. Chim. Acta*, 38 (1966) 1943.

7 M. S. CRESSER AND T. S. WEST, *Spectrochim. Acta*, 25B (1970) 61.
8 R. M. DAGNALL, K. C. THOMPSON AND T. S. WEST, *Talanta*, 14 (1967) 551 and 557.
9 R. M. DAGNALL, K. C. THOMPSON AND T. S. WEST, *Talanta*, 14 (1967) 1467.
10 R. F. BROWNER, R. M. DAGNALL AND T. S. WEST, *Talanta*, 15 (1969) 75.
11 R. M. DAGNALL, K. C. THOMPSON AND T. S. WEST, *Talanta*, 14 (1967) 1151.
12 R. M. DAGNALL, K. C. THOMPSON AND T. S. WEST, *Talanta*, 15 (1968) 677.
13 J. M. MANSFIELD, J. D. WINEFORDNER AND C. VEILLON, *Anal. Chem.*, 37 (1965) 1051.
14 J. D. WINEFORDNER AND R. A. STAAB, *Anal. Chem.*, 36 (1964) 165, 1367.
15 R. M. DAGNALL, T. S. WEST AND P. YOUNG, *Talanta*, 13 (1966) 803.
16 R. HERMANN AND C. T. J. ALKEMADE, *Flame Photometry*, Interscience, New York, 1963, pp. 264–265.
17 E. E. PICKETT AND S. R. KOIRTYOHANN, *Spectrochim. Acta*, 23B (1968) 235.

Anal. Chim. Acta, 51 (1970) 179–190

Analytica Chimica Acta
Elsevier Publishing Company, Amsterdam
Printed in The Netherlands

PHOTOCHEMICAL COMPLEXATION TITRATIONS WITH FLUORIMETRIC END-POINTS

JOHN L. BECK*, J. M. FITZGERALD** AND JOHN A. BISHOP***
Department of Chemistry, Seton Hall University, South Orange, N.J. 07079 (U.S.A.)

(Received February 7th, 1970)

In previous publications work on photochemical titrations[1-4] and on fluorimetric titrations[5-7] has been reported. The present paper discusses a combination of the two methods to permit titrations in which the titrating ion for a fluorimetric displacement reaction is generated in a photochemical decomposition. Both the photolysis and fluorescence excitation are accomplished with a single u.v. source[1,3].

EXPERIMENTAL

Reagents

Reagent-grade chemicals were used without further purification with the exception of potassium trisoxalatocobalt(III) and sodium perchlorate. Deionized water was used throughout the study.

The cobalt(III) oxalate complex was prepared as described by BOOTH[8] and purified[9]. The ultraviolet spectrum of the final product agreed with the values found by COPESTAKE AND URI[10]. The air-dried solid was stored in brown bottles under refrigeration, since the compound can decompose by both photochemical reaction and a thermal reaction[10].

Stock solutions of Mg(II), Cd(II), Zn(II) and Cu(II), all 10^{-2} M, were prepared from their sulfates and were standardized by titration with standard EDTA. Solutions of 8-hydroxyquinoline-5-sulfonic acid (Aldrich Chemical Company) were prepared by weight as needed, at a concentration of $4 \cdot 10^{-3}$ M. In preparing this solution, just enough sodium hydroxide was used to cause complete dissolution, and the final pH was adjusted to 8–9.

Sodium hydrogen carbonate buffer (0.5 M) was prepared by weight and adjusted to pH 8.2 with sodium hydroxide. A 0.5 M phosphate buffer was prepared by dissolving sodium monohydrogen phosphate in water and adjusting the pH with sodium hydroxide.

In order to study the effect of electrolytes on this titration, 1 M potassium chloride was prepared (by weight), and 1 M sodium perchlorate was prepared by allowing stoichiometric amounts of sodium carbonate and hydrochloric acid to react in water. The final pH was adjusted to 8.4 with sodium hydroxide.

---

* Present address: Merck Institute for Therapeutic Research, Rahway, N.J. 07016.
** Present address: Department of Chemistry, University of Houston, Houston, Texas 77004; to whom correspondence should be addressed.
*** Present address: Department of Chemistry and Chemical Engineering, Newark College of Engineering, Newark, N.J. 07102.

Apparatus

The apparatus used was based on the single source design of SMITH[1,3] with small modifications, and is shown schematically in Fig. 1. A medium-pressure mercury arc (Hanovia Utility Quartz Lamp, type 30520, Englehard Hanovia, Inc., Newark, N. J.) served as the source of radiation for photolysis and also as the source of fluorescence excitation radiation. Voltage to the arc was regulated to help stabilize the intensity[2,3,9] (Model 1000S, Sorensen and Co., Inc., Norwalk, Conn.). The electrically operated shutter (Harvard Electric Shutter, Burke and James, Inc., Chicago, Ill.) was mounted directly on the lamp housing. Four selenium photocells (Type B-2M, International Rectifier, El Segundo, Calif.) were connected in series, to a recorder (Model SRL, Sargeant & Co., Chicago, Ill.) operated in a linear-millivolt mode. The shutter and the chart drive were coupled so that the shutter opened when the time drive started; a chart speed of 1 in/min was used. Dark current was zeroed with an external bucking current between the photocells and the recorder input.

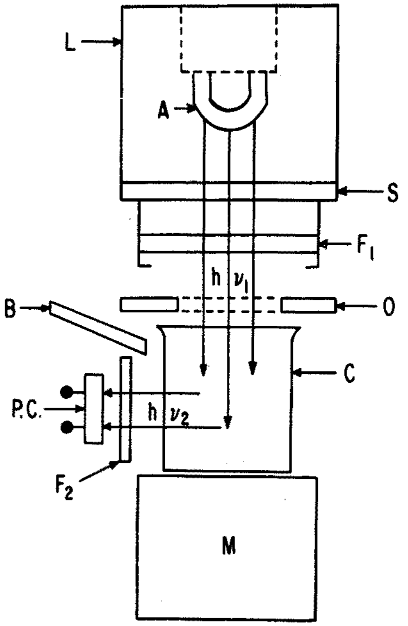

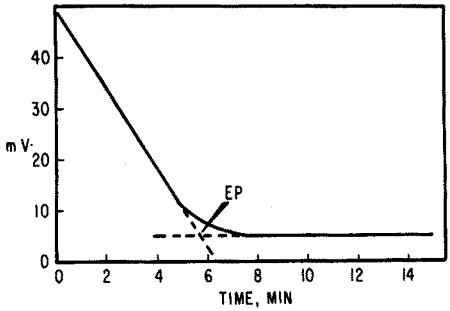

Fig. 1. Schematic design of apparatus: (A) mercury vapor arc, (L) lamp housing, (S) electrically operated shutter, (F_1) u.v. bandpass filter, photolysis and fluorescence excitation; (F_2) interference filter, fluorescence emission selection; (O) light aperture; (B) light baffle; (C) titration vessel; (P.C.) photovoltaic cells; ($h\nu_1$) path of incident radiation; ($h\nu_2$) path of emitted fluorescent light; (M) magnetic stirrer.

Fig. 2. Typical fluorescence titration curve: mV=relative fluorescence intensity; time = time from start of photolysis; EP = extrapolated end-point.

In the excitation radiation path, a u.v.-transmitting–visible-absorbing filter (#7–54, Corning Glass Works, Corning, N.Y.) was combined with a heat-absorbing filter (#6540–001, Englehard Hanovia, Newark, N.J.) to prevent cracking of the u.v. filter. A 500-nm, 2-in^2 interference filter was used in position 2 (Fig. 1) to select the radiation for fluorescence measurement.

Procedure for titration

Prepare a fresh solution of $M(HQSO_3)_2$ (8-hydroxyquinoline-5-sulfonic acid anion will be shortened to $HQSO_3$ for the remainder of the paper) from the stock solution of the desired metal sulfate and a freshly prepared solution of $HQSO_3$, to a final concentration of $1 \cdot 10^{-3}$ *M*.

Prepare a cobalt(III) oxalate solution ($5 \cdot 10^{-2}$ *M*) by weight daily. Best results are obtained when the solution is stored in an ice-bath to minimize thermal decomposition[10].

To a 250-ml graduated beaker add 20 ml of 0.5 *M* phosphate buffer (pH 9) followed by an aliquot containing 1–15 µmoles of the complex to be determined. Finally, add 4 ml of the $5 \cdot 10^{-2}$ *M* Co(III)–oxalate complex and dilute to a 200-ml mark on the beaker. After adding a stirring bar, place the vessel in the apparatus, start stirring, and throw the switch which starts the recorder drive as the shutter opens[3].

A plot of mV *vs.* time of photolysis is obtained (Fig. 2). By using different amounts of $M(HQSO_3)_2$ it is possible to prepare a standardization curve in which the extrapolated time to reach the extinction of fluorescence (EP, Fig. 2) is plotted against µmoles of complex taken (Fig. 3).

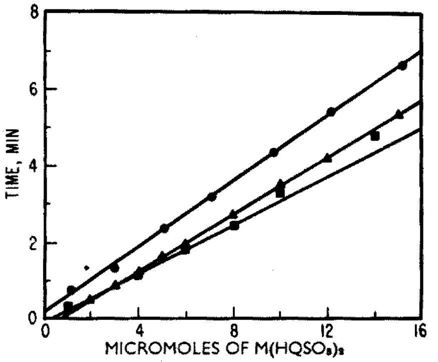

Fig. 3. Calibration titration plots for fluorescent complexes: (●)$Zn(HQSO_3)_2$ (least-squares line 1–15 µmole); (▲)$Cd(HQSO_3)_2$ (least-squares line, 2–15 µmole); (■)$Mg(HQSO_3)_2$ (least-squares line, 1–8 µmole). Concentration of photogenerator Co(III) oxalate = 10^{-3} *M*; pH range 8–9.5.

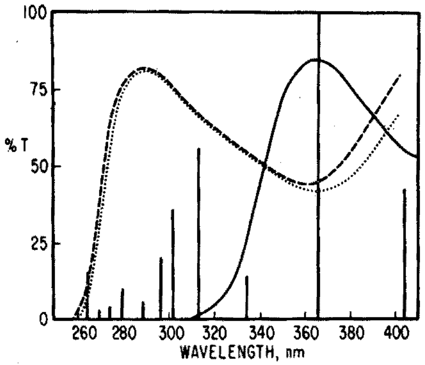

Fig. 4. Electronic absorption spectra: (——) Co(III) oxalate, $1 \cdot 10^{-3}$ *M*, pH 8.8; (------) $Mg(HQSO_3)_2$, $4 \cdot 10^{-5}$ *M*, pH 9; (.......) $Cd(HQSO_3)_2$, $5 \cdot 10^{-5}$ *M*, pH 8.5. All spectra for 1-cm path lengths. (|) Mercury emission wavelengths. Intensities relative to that at 366 nm (corrected for detector response).

A metal ion which forms a nonfluorescent species can be determined by using an excess of a fluorescent complex, followed by back-titration of the excess. Copper(II) was determined in this way by the use of excess of $Cd(HQSO_3)_2$, the excess being titrated by the photogeneration of cobalt(II). The calibration curve for the copper(II) titration was linear over the range 1–13.5 µmole of copper(II) for a photogeneration time range of 5–1 min when 15 µmole of $Cd(HQSO_3)_2$ were used under the conditions discussed above.

DISCUSSION

The combination of a photochemical decomposition and fluorescent end-point is made possible by the very favorable absorption characteristics of ultraviolet and visible light in the systems involved (Fig. 4).

The absorption of ultraviolet light by the three fluorescent species is low at wavelengths causing decomposition of the cobalt oxalate, while the cobalt complex transmits relatively well at 366 nm, which is the wavelength causing fluorescence of the $M(HQSO_3)_2$ complexes. DREW[9] found that incomplete absorption of a strong mercury emission line at 366 nm results in variations in the rate of the cobalt oxalate decomposition, and he was forced to use filters to remove this line from the photolytic path (or alternatively, concentrated solutions[4]). In the present study the $M(HQSO_3)_2$ complexes acted as "internal filters"[4] to remove this interference.

The fluorescent complexes used all have broad-band emission spectra with maxima between 495 and 515 nm[6]. There is no mercury line near 500 nm, and, in addition, the cobalt oxalate complex has a minimum in its absorption spectrum at this wavelength[10]. Consequently, a 500-nm interference filter was used to select emitted fluorescent light.

Typical data for the photochemical titration of one of the fluorescent complexes, $Cd(HQSO_3)_2$, are shown in Table I. The complex was titrated over a seven-fold range. A least-squares fit of data yielded a slope of 0.373 min/μmole with an intercept of −0.261 min. The relative standard deviation for three determinations at the 8-μmole level was 1.34%.

TABLE I

TITRATION OF CADMIUM 8-HYDROXYQUINOLINE-5-SULFONIC ACID COMPLEX

$Cd(HQSO_3)_2$ taken (μmole)	*Photolysis time to end-point obsd. (min)*	*Photolysis time to end-point calcd.[a] (min)*	*Error[b] (%)*
2.02	0.48	0.49	− 2.04
3.04	0.93	0.87	+ 6.45
4.05	1.31	1.25	+ 4.58
5.06	1.62	1.63	− 0.62
6.07	1.92	2.00	− 4.17
8.10	2.74	2.76	− 0.73
10.12	3.51	3.51	0.00
12.14	4.20	4.27	− 1.67
15.18	5.48	5.40	+ 1.46

[a] Calculated from least-squares fit of data: time to end-point = − 0.261 min + 0.373 min/μmole.
[b] Difference between observed and calculated values.

It was not possible to titrate mixtures. When one attempts the titration of a mixture of metal ion and excess $HQSO_3$, the initial species in solution are the fluorescent $M(HQSO_3)_2$ complex and free $HQSO_3$. One might expect to obtain the type of titration curve in which there is no change in the level of fluorescence until the first break at which time all of the excess $HQSO_3$ is titrated. Then one might expect the fluorescence intensity to decrease to zero as the $M(HQSO_3)_2$ complex is titrated and the second break is reached. The actual titration curve obtained from such a mixture has no initial flat portion but begins to decrease immediately, slowly at first and then more rapidly with a good deal of rounding. The reasons for this behavior may be found in the spectral properties of the various species in the solution. $HQSO_3$ and $Co(HQSO_3)_2$ as well as $M(HQSO_3)_2$ absorb fairly strongly at 366 nm. The absorbance of the $Co(HQSO_3)_2$ is stronger than that of free $HQSO_3$ at this wavelength. Since 366 nm is the excitation wavelength used to cause the $M(HQSO_3)_2$ complexes to fluoresce, one can see that a net increase in quenching results as $Co(HQSO_3)_2$ is produced during the titration of the excess of $HQSO_3$ and thus a decrease in the fluorescence intensity is observed during the first part of the titration. Quenching also occurs during the second part of the titration as $Co(HQSO_3)_2$ is produced in addition to the decrease of fluorescence as the $M(HQSO_3)_2$ complex is titrated; hence, the increasing rate of decreasing fluorescence. This stepwise nature of the formation and displacement of the various complexes with $HQSO_3$ results in a titration curve which is unusable.

Several titrations were performed on the various fluorescent complexes with complete shutdown of equipment between runs. The results of these titrations are condensed in Table II. Five titration runs for the three complexes are listed, all run on different days. These runs were made during some very hot weather in a laboratory without air-conditioning. It was noted that if a series of titrations were performed late in the evening, using a cobalt(III) oxalate solution which had been prepared in the morning, the least-squares intercepts of the calibration plots became increasingly more negative. This is due to the thermal decomposition of the reagent solution with the resulting formation of cobalt(II) impurity [9,10]. This problem can be circumvented in either of two ways. Since the cobalt(III) oxalate dissolves in aqueous solution immediately, it could be added as the solid if a conveniently reproducible way to accomplish this is available. Alternatively, the freshly prepared cobalt(III) oxalate solution can be kept in an ice-bath. At this temperature no significant change in the intercepts of the calibration plots is noted over a 24-h period.

TABLE II

TITRATION OF FLUORESCENT 8-HYDROXYQUINOLINE-5-SULFONIC ACID COMPLEXES

Metal ion complexes	*Range (μmole)*	*No. of detns.*	*Slope*[a] *(min/μmole)*	*Intercept*[a] *(min)*	*Difference*[b] *(%)*	*Rel. st. dev. (%)*
Cd	4–12	9	0.355	0.089	—	1.34[c]
Cd	2–15	9	0.373	−0.261	2.48	—
Zn	1–15	7	0.430	0.154	0.96	—
Mg	1– 8	15	0.310	−0.060	—	1.09[d]
Mg	2– 8	18	0.402[e]	−0.337	—	1.30[d]

[a] Least-squares fit of data: time to end-point = min+min/μmole.
[b] Difference between observed and calculated times averaged over all points determined.
[c] Relative standard deviation for triplicate determinations at the 8-μmole level.
[d] Relative standard deviation for triplicate determinations at the 4-μmole level.
[e] Potassium trisoxalatocobalt(III) conc. = 50% that used in other sets.

Since an arbitrary millivolt scale can be set on the recorder, the shapes of all of the titration curves are qualitatively alike (Fig. 2) and can be made as steep or as shallow as one whishes by choosing the proper full-span setting. The place at which some difference does arise in the curves is the end-point region (EP; Fig. 2). Mg(HQ-

$SO_3)_2$ exhibits the least amount of "rounding" in the end-point region, with Cd(HQ-$SO_3)_2$ next and Zn($HQSO_3)_2$ exhibiting the greatest rounding. This behavior falls in line nicely with the relative strengths of the complexes being titrated compared to the strength of the complex being formed in the titration[6], *i.e.* Co($HQSO_3)_2$. The relative strengths of the complexes are in the order Co, Zn, Cd, Mg and therefore the rounding of the end-point should be in the order Zn, Cd, Mg, which is, in fact, observed.

It can be seen in Fig. 3 that the calibration plots for the complexes do not have the same slopes nor do they have zero intercepts. Theoretically, the titration rate depends on the rate of photolysis alone[4] so that all the slopes in Fig. 3 should be identical. However, complications have been observed in previous photochemical methods. DREW[9] and SMITH AND FITZGERALD[1], in their titrations, attributed their non-zero intercepts to traces of cobalt(II) in the cobalt(III)–oxalate reagent. As has been stated above, extreme care must be taken to prevent thermal degradation of the reagent yielding cobalt(II).

DREW[9] and SMITH AND FITZGERALD[1] attributed the non-stoichiometric relationship of some of their titrations to induced reactions but this is unlikely in the present set of metal-ion chelate titrations. A more reasonable explanation is that the titrations are stoichiometric but the very similar, though not identical, shape of the electronic absorption spectra of the various complexes affects the slope of the calibration curve. The monocomplex and the dicomplex have different absorption spectra and therefore the overall spectrum changes somewhat during the titration. The relative changes in the solution as a whole depend also upon the small differences in molar absorptivity at 366 nm for a given complex, compared to the absorptivity of the Co($HQSO_3)_2$ which is being produced. These spectral changes result in the "internal filter effect"[4] for both the photolytic radiation and the fluorescence excitation radiation. In addition, the "window" for fluorescence emission is subtly altered during the course of the titration as the concentrations of the various absorbers change dramatically. The situation is obviously quite involved but qualitatively the cobalt complex exhibits the most intense absorption of 366 nm at the pH used in the titration and is followed closely by complexes of zinc, cadmium and magnesium, in that order. This is also the order of the relative slopes of the titration curve, *i.e.*, Zn, Cd, Mg.

It should also be noted that the quantum yield for cobalt(II) production is changed slightly by heavy metal ions such as mercury(II) and copper(II)[10]. It is unlikely, however, that the micromolar amounts of metal ions taken for titration could account for the differences in slopes of calibration curves.

With the Cd($HQSO_3)_2$ system, a study was made on the effect of the buffer used. Cd($HQSO_3)_2$ (5 ml) was titrated by the standard procedure with sodium acetate, sodium hydrogen carbonate or sodium phosphate buffers. Similar titration curves were obtained with all three buffers.

It has been previously reported[5] that the fluorescence for the complexes used decreases as the pH is lowered, owing to incomplete formation of the M($HQSO_3)_2$ complex, the rate of decrease with drop in pH depending on the strength of the complex. At very basic pH values the fluorescence again falls off, probably due to formation of hydroxides. pH values between 8–9.5 gave the best results (Table II).

COPESTAKE AND URI[10] found that neutral electrolytes had no effect on the photoreduction of cobalt(III) oxalate [10]. The electrolyte effect was studied by using the standard procedure with the addition of neutral electrolyte, with titrations of

$Cd(HQSO_3)_2$. Potassium chloride at 0.25 *M* and 0.5 *M* caused no change in the shape of the titration curve, but sodium perchlorate at the same concentrations curved the titration plot, and shortened the extrapolated times to end-points. However, at 0.25 *M* sodium perchlorate concentration the time was shortened only 5%, so that small concentrations of perchlorate might be tolerated.

An examination of the stability constants of the complexes of 8-hydroxyquinoline-5-sulfonic acid with bivalent cations[6] indicated that it should be possible to determine copper(II) by means of excess of a fluorescent complex which is displaced by copper (*e.g.*, $Cd(HQSO_3)_2$) and back-titrating the excess. The results of such titrations shown in Table III indicate that such is the case. These results refer to a calibration plot composed from the least-squares fit of the data. It should be possible to apply this back-titration method to other cations which are more strongly complexed than cobalt(II), but which do not form fluorescing complexes with 8-hydroxyquinoline-5-sulfonic acid. On the other hand, small differences in slopes of calibration curves may well be observed with different metal-ions used. This would again be due to the change in concentration of the various absorbing species during the course of the titration.

TABLE III

DETERMINATION OF COPPER(II) BY TITRATION OF EXCESS FLUORESCENT METAL COMPLEX WITH COBALT(III) OXALATE

Copper(II) (μmole)	*Time to end-point obsd. (min)*	*Time to end-point calcd.* [a] *(min)*	*Difference*[b] *(%)*
1.0 (0.32 p.p.m.)	5.03	5.02	+ 0.16
2.0	4.70	4.71	− 0.23
4.0	4.23	4.09	+ 3.45
6.0	3.40	3.44	− 1.23
6.0	3.38	3.44	− 1.81
8.0	2.75	2.82	− 2.45
8.0	2.66	2.82	− 5.64
8.0	2.85	2.82	+ 1.09
8.0	2.82	2.82	—
10.0	2.12	2.22	− 4.62
12.1	1.62	1.60	+ 1.22
13.5 (4.3 p.p.m).	1.23	1.34	− 8.50

[a] Calculated from least-squares fit of data: time to end point = 5.33 min − 0.311 min/μmole.
[b] Difference between observed and calculated values. Relative standard deviation for four determinations at the 8-μmole level = 3.04%.

SUMMARY

A fluorimetric end-point method has been developed for the photochemical decomposition of cobalt(III) oxalate to produce cobalt(II) ion as titrant. The method is used in titrating the fluorescent complexes formed between 8-hydroxyquinoline-5-sulfonic acid and Mg(II), Cd(II) and Zn(II) by displacement of the metal ion by cobalt(II), which forms a non-fluorescent complex. A back-titration of an excess of cadmium(II) complex is used for the determination of copper(II) which also forms a non-fluorescent complex with the ligand. A single ultraviolet source is used for photolysis and fluorescence excitation. The method is made possible by favorable u.v. absorption spectra of the various complexes involved.

RÉSUMÉ

Une méthode à point final fluorimétrique est mise au point; elle est basée sur la décomposition photochimique de l'oxalate de cobalt(III) en ion cobalt(II) utilisé comme titrant. Elle permet le titrage de complexes fluorescents formés entre l'acide hydroxy-8-quinoléine sulfonique-5 et, Mg(II), Cd(II) et Zn(II), par déplacement du métal par le cobalt(II), formant un complexe non fluorescent. Une titration en retour par un excès de complexe de cadmium permet de doser le cuivre, formant également un complexe non fluorescent avec le ligand. Une simple source ultra-violette est utilisée pour la photolyse et l'excitation de fluorescence.

ZUSAMMENFASSUNG

Es ist eine fluorimetrische Endpunktsmethode für die photochemische Zersetzung von Kobalt(III)-oxalat zum als Titrant verwendeten Kobalt(II)-ion entwickelt worden. Bei der Methode werden die zwischen 8-Hydroxychinolin-5-sulfonsäure und Mg(II), Cd(II) und Zn(II) gebildeten fluoreszierenden Komplexe titriert, indem das Metallion durch Kobalt(II) ersetzt wird, das einen nichtfluoreszierenden Komplex ergibt. Die Rücktitration eines Überschusses an Cadmium(II)-Komplex wird für die Bestimmung von Kupfer(II) benutzt, das ebenfalls mit dem Liganden einen nichtfluoreszierenden Komplex bildet. Für die Photolyse und die Fluoreszenzanregung wird eine einzige Ultraviolett-Strahlenquelle verwendet. Die Methode wird durch die günstigen u.v.-Absorptionsspektren der verschiedenen Komplexe ermöglicht.

REFERENCES

1 E. J. Smith and J. M. Fitzgerald, Abstracts, *153rd National Meeting ACS, Miami Beach, Fla., April 1965*, No. B40; Abstracts, *154th National Meeting ACS, Chicago, Ill., Sept. 1967*, No. B46.
2 H. D. Drew and J. M. Fitzgerald, *Anal. Chem.*, 38 (1966) 778.
3 R. J. Lukasiewicz and J. M. Fitzgerald, *Anal. Lttrs.*, 1 (1968) 455.
4 J. M. Fitzgerald, R. J. Lukasiewicz and H. D. Drew, *Anal. Lttrs.*, 1 (1967) 173.
5 J. A. Bishop, *Anal. Chim. Acta*, 29 (1963) 172, 178.
6 J. A. Bishop, *Anal. Chim. Acta*, 35 (1966) 224.
7 J. A. Bishop, *Anal. Chim. Acta*, 39 (1967) 189; *Anal. Lttrs.*, 2 (1969) 111.
8 H. S. Booth, *Inorganic Synthesis*, Vol. 1, McGraw-Hill, 1939, p. 37.
9 H. D. Drew, *Ph.D. Thesis*, Seton Hall University, South Orange, N. J., 1967, p. 35.
10 T. B. Copestake and N. Uri, *Proc. Roy. Soc. (London), Ser. A*, 228 (1955) 232.

Analytica Chimica Acta
Elsevier Publishing Company, Amsterdam
Printed in The Netherlands

ON THE USE OF THE PROTOLYTIC EFFECT OF COMPLEXATION REACTIONS FOR THE INDICATION OF END-POINTS IN COMPLEXIMETRIC TITRATIONS

H. POPPE, G. DEN BOEF AND F. FREESE
Laboratory for Analytical Chemistry, University of Amsterdam, Amsterdam (The Netherlands)

(Received February 14th, 1970)

A complexation reaction generally gives rise to an acid–base effect. In acidic solution protons are released from the complexing agent, and in alkaline solution hydroxyl ions are released from the metal ions. This effect is usually considered to be a nuisance, and to minimize the pH change it is necessary to add a buffer which can affect the position of different equilibria[1].

The present study was made in order to establish how useful these protolytic effects can be in the detection of the end-points of compleximetric titrations. Of course, the indication of end-points by means of pH effects was used in the very early days of compleximetry by SCHWARZENBACH AND BIEDERMANN[2]. However, they made use of the pH jump, which occurs at the end-point, whereas in this work linear plots are used. The work reported here includes the measurement of pH by potentiometric (glass electrode) or spectrophotometric (acid–base indicator) means. Attractive aspects of such systems are their generality and the high sensitivity which can be obtained in some cases. Furthermore, as the method is analogous to other kinds of linear indication, *e.g.* self-indicating photometric and amperometric titration, the main advantages of these methods would apply equally to indication via the hydrogen ion concentration instead of pH.

The theory of this type of end-point indication is discussed from different aspects, depending on the indication technique and the titration conditions used. Each case is illustrated by an experimental example. No attempt has been made to exhaust the analytical possibilities of the method.

POTENTIOMETRIC INDICATION WITH NO EXTERNAL BUFFER ADDED

The metal salt, $M(ClO_4)_2$, of a divalent metal ion is titrated with EDTA which is assumed to be dissolved as $Na_pH_{4-p}Y$, in a very concentrated solution in order to avoid dilution effects. No external buffer is added.

The following species in the solution are considered:

M^{2+}, $M(OH)_i^{2-i}$ ($i=1\ldots.6$), H_iY^{-4+i} ($i=0\ldots.4$), MY^{2-}, MHY^-, $MOHY^{3-}$,
H^+, OH^-, Na^+, ClO_4^-.

In the following paragraphs, charges will be omitted for simplicity. According to the recommendations of RINGBOM[1], the following symbols are used:

$$[M]' = \sum_{i=0}^{6} M(OH)_i = \alpha_M[M] = \left\{\sum_{i=0}^{6} \beta_i[OH]^i\right\}[M]$$

$$[Y]' = \sum_{i=0}^{4} H_iY = \alpha_Y[Y] = \left\{\sum_{i=0}^{4} \beta_i[H]^i\right\}[Y]$$

$$[MY]' = [MY]+[MHY]+[MOHY] = \alpha_{MY}[MY] =$$

$$= \{1+K^{H}_{MHY}[H]+K^{OH}_{MOHY}[OH]\}[MY]$$

where $\beta_0 = 1, \beta_i = K_1 \ldots\ldots K_i$

$$K_i = \frac{[M(OH)_i]}{[M(OH_{i-1})]\cdot[OH]} \quad \text{for the protolysis of M}$$

$$K_i = \frac{[H_iY]}{[H_{i-1}Y]\cdot[H]} \quad \text{for the protolysis of Y}$$

$$K^{H}_{MHY} = \frac{[MHY]}{[MY]\cdot[H]} \quad \text{and} \quad K^{OH}_{MOHY} = \frac{[MOHY]}{[MY]\cdot[OH]}$$

The change in pH during the titration can be derived from the charge balance of the solution. To apply this equation, the average charges for the free metal ion, the complex and the free ligand are required. The average charge of the metal, $\bar{n}_M$, is derived as an example:

$$\bar{n}_M = 2 - \frac{\sum_{i=0}^{6} i\,[M(OH)_i]}{\sum_{i=0}^{6} [M(OH)_i]} = 2 - \frac{\sum_{i=0}^{6} i\,\beta_i\,[M]\,[OH]^i}{\alpha_M[M]} =$$

$$= 2 - \frac{[OH]}{\alpha_M}\sum_{i=0}^{6} i\,\beta_i\,[OH]^{i-1} = 2 - \frac{[OH]}{\alpha_M}\frac{d\alpha_M}{d[OH]} =$$

$$= 2 - \frac{d\log\alpha_M}{dpH} \tag{1}$$

In the same way it can be derived that:

$$\bar{n}_Y = -4 - \frac{d\log\alpha_Y}{dpH} \tag{2}$$

$$\bar{n}_{MY} = -2 - \frac{d\log\alpha_{MY}}{dpH} \tag{3}$$

The results obtained here can also be easily derived from Bjerrum's expression for the ligand number.

The charge balance is:

$$[M]'\bar{n}_M + [H] - [ClO_4] + [Na] + [Y]'\bar{n}_Y + [MY]'\bar{n}_{MY} - [OH] = 0 \tag{4}$$

Writing out the subsequent terms in this equation and rearranging, we obtain:

$$-[\mathrm{H}]+[\mathrm{OH}]=[\mathrm{M}]'\left\{2-\frac{\mathrm{d}\log\alpha_{\mathrm{M}}}{\mathrm{dpH}}\right\}+[\mathrm{Y}]'\left\{-4-\frac{\mathrm{d}\log\alpha_{\mathrm{Y}}}{\mathrm{dpH}}\right\}+$$
$$+[\mathrm{MY}]'\left\{-2-\frac{\mathrm{d}\log\alpha_{\mathrm{MY}}}{\mathrm{dpH}}\right\}+pfc_{\mathrm{M}}-2c_{\mathrm{M}} \qquad (5)$$

If it is assumed that during the titration the pH remains at such values that reasonable conditions for a linear titration exist, *i.e.* that the product of the conditional constant and the concentration to be determined remains larger than 10^3, then the following approximations for the region *before* the equivalence point can be made:

$$\left.\begin{array}{r}[\mathrm{M}]'=(1-f)c_{\mathrm{M}}\\ [\mathrm{Y}]'=0\\ [\mathrm{MY}]'=fc_{\mathrm{M}}\end{array}\right\} \qquad (6)$$

This leads to the following expression for the region before the equivalence point:

$$-[\mathrm{H}]+[\mathrm{OH}]=-c_{\mathrm{M}}\frac{\mathrm{d}\log\alpha_{\mathrm{M}}}{\mathrm{dpH}}+c_{\mathrm{M}}f\left\{p-4+\frac{\mathrm{d}\log\alpha_{\mathrm{M}}}{\mathrm{dpH}}-\frac{\mathrm{d}\log\alpha_{\mathrm{MY}}}{\mathrm{dpH}}\right\} \qquad (7)$$

For the region *after* the equivalence point, analogous approximations can be made:

$$\left.\begin{array}{r}[\mathrm{M}]'=0\\ [\mathrm{Y}]'=(f-1)c_{\mathrm{M}}\\ [\mathrm{MY}]'=c_{\mathrm{M}}\end{array}\right\} \qquad (8)$$

and then:

$$-[\mathrm{H}]+[\mathrm{OH}]=+c_{\mathrm{M}}\frac{\mathrm{d}\log\alpha_{\mathrm{Y}}}{\mathrm{dpH}}-c_{\mathrm{M}}\frac{\mathrm{d}\log\alpha_{\mathrm{MY}}}{\mathrm{dpH}}+c_{\mathrm{M}}f\left\{p-4-\frac{\mathrm{d}\log\alpha_{\mathrm{Y}}}{\mathrm{dpH}}\right\} \qquad (9)$$

From eqns. (7) and (9) it is clear that a titration plot of $-[\mathrm{H}]+[\mathrm{OH}]$ against the amount of titrant added consists of two straight lines, if the differential quotients in these equations are independent of pH. If the pH is higher than 8, [H] can be neglected with respect to [OH]; for values lower than 6, [OH] can be omitted.

The end-point of the titration can be detected only if the slope of the titration curve changes at the equivalence point. The difference in slope in the two regions is:

$$+\frac{\mathrm{d}\log\alpha_{\mathrm{M}}}{\mathrm{dpH}}+\frac{\mathrm{d}\log\alpha_{\mathrm{Y}}}{\mathrm{dpH}}-\frac{\mathrm{d}\log\alpha_{\mathrm{MY}}}{\mathrm{dpH}}=-\frac{\mathrm{d}\log K'/K}{\mathrm{dpH}}=-\frac{\mathrm{d}\log K'}{\mathrm{dpH}} \qquad (10)$$

From this simple result, it follows that the end-point of a compleximetric titration can be detected by means of the protolytic effect if (*a*) the conditional constant remains large enough over the whole pH region covered by the titration, and (*b*) the value of the conditional constant, $\log K'$, varies with the pH of the solution in the pH region used. Furthermore, it is advantageous if the partial differential quotients of eqns. (7) and (9) are independent of pH in the region used. In that case perfectly linear titration plots will be obtained.

As an example, Fig. 1, taken from RINGBOM[1], shows that according to the requirements mentioned above, cadmium(II) can be titrated in the pH range 3–9, and in the pH range 11–14 at concentrations of 10^{-3} M or less. Below pH 3 and above pH 14, the product $K'c_{\mathrm{M}}$ will not be large enough even for the titration of 10^{-3} M solutions. Between pH 9 and pH 11, there is no linear relationship between log K' and pH, so that the titration plots will be difficult to interpret.

A few remarks on the pH change during the titration are necessary. In order to fulfill the two conditions, the total change of pH during the titration must not be very large (not more than 2 pH units). Therefore, the starting pH of the titration must be adapted according to the concentration to be determined. This can be done by adding acid or base to the solution; the equations derived above for the titration curves are then changed by adding a term of constant magnitude. In some cases dilution of the sample will be necessary.

On the other hand, excessive amounts of acid or base must be avoided, other-

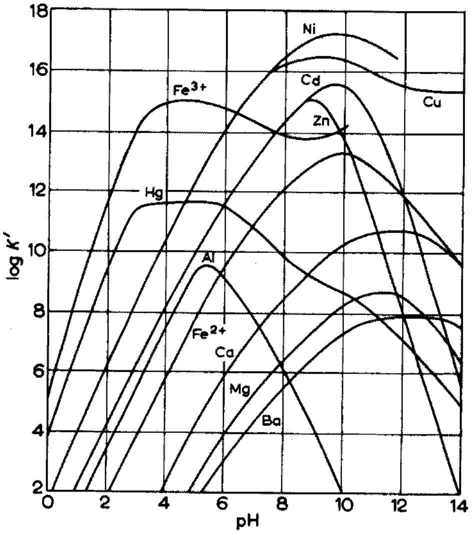

Fig. 1. Conditional stability constants, K', of various metal EDTA complexes as functions of pH. This figure is taken from ref. 1 with kind permission of the author and publisher.

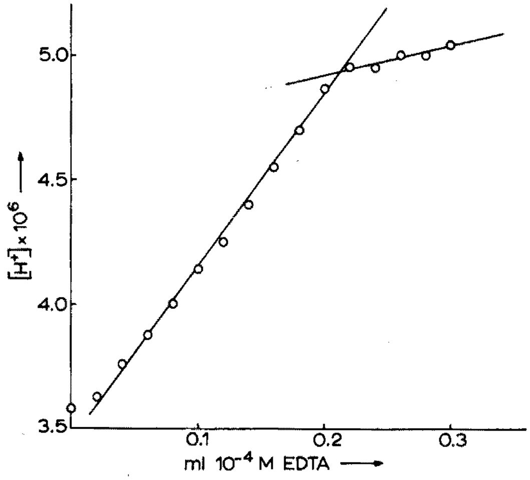

Fig. 2. Titration curve of 20 nmol of copper(II) in 25 ml of solution containing 0.1 M potassium chloride with 10^{-4} M EDTA.

wise the pH change may be too small to be readily measurable. In general, the amount of acid or base added should be of the same order of magnitude as the protolytic effect of the reaction. Moreover, it is useful if the two branches of the titration curve have slopes of different signs, so that a large difference in slope can be achieved within a small pH region. This can be realized by having a favourable value of p, the number of sodium ions per EDTA ion in the titrant solution, which can readily be obtained by adding acid or base when the titrant solution is prepared.

The sensitivity which can be obtained with potentiometric acid–base indication can readily be estimated. At pH 7 a release of protons to the amount of $5 \cdot 10^{-8}$ M will change the pH by 0.1 unit. As modern expanded-scale or compensation pH meters are readable and stable to 0.001 pH unit, such a change can be measured with a precision of about 1%. For most complexation reactions, this $5 \cdot 10^{-8}$ M change corresponds to a metal concentration of about $2.5 \cdot 10^{-8}$ M.

Titration of copper in acid solution

Figure 2 shows the curve obtained in the titration of 25 ml of solution containing $0.8 \cdot 10^{-6}$ M copper(II) and 0.08 M potassium chloride, with 10^{-4} M Na_2H_2Y. The theoretical prediction that titrations in solutions even less concentrated should be possible could not be verified experimentally, because of the interference by carbon dioxide, which always buffers the solution to a certain extent.

Titration of a mixture of mercury and cadmium

As can be seen from Fig. 1, the pH range 3–4 is suitable for the simultaneous titration of mercury and cadmium; the former has a much larger conditional constant and displaces no protons on complexing with EDTA, whereas the latter displaces two protons. Experimental results are in accordance with theoretical prediction. The titration of mercury alone gave no break-point; the titration of cadmium alone was possible. Figure 3 shows a typical titration curve for the simultaneous titration of mercury and cadmium.

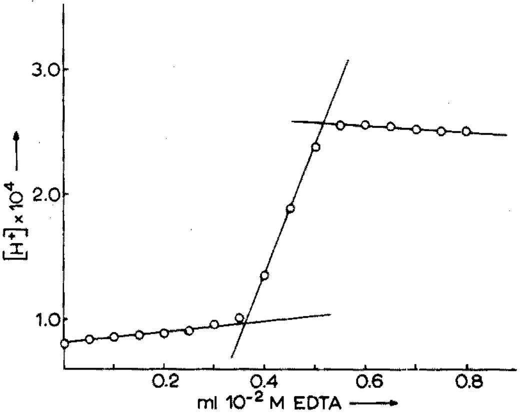

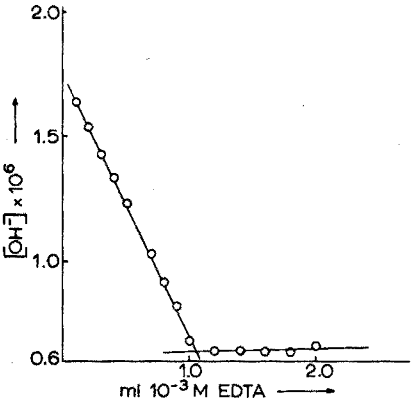

Fig. 3. Titration curve of 4 μmol of mercury(II) and 2 μmol of cadmium(II) in 25 ml of solution containing 0.1 M potassium nitrate with 10^{-2} M EDTA.

Fig. 4. Titration curve of 1 μmol of calcium(II) in 25 ml of solution containing 0.1 M potassium chloride, 10^{-4} M ammonia and 10^{-3} M ammonium chloride with 10^{-3} M EDTA.

POTENTIOMETRIC INDICATION WITH EXTERNAL BUFFER ADDED

It is sometimes necessary to carry out the titration in approximately neutral solution in order to achieve a suitable conditional constant or in order to avoid precipitation of the metal ion. When the buffer index of this neutral solution is inadequate to limit the pH change to reasonable values, an external buffer must be added. The simplest case is when the buffer does not react with the metal ion or the complex. The case of a buffer consisting of a weak acid (HB) and its salt (NaB), with a total concentration c_B, is discussed. In the equation for the charge balance (eqn. 4), $[H]-[OH]$ must be replaced by $[H]-[OH]-[B]$. The function plotted against the amount of titrant added is then:

$$-[H]+[OH]+\frac{K_a}{K_a+[H]}c_B \tag{11}$$

If the buffer reacts with the metal ion, the complex or both, the situation is more complicated. If the total amount of sodium ions added before the titration (as part of the buffer) is denoted as $q\,c_B$ and the total concentration of the buffer as c_B, then:

(a) before the equivalence point:

$$-[H]+[OH]+\frac{K_a}{K_a+[H]}c_B=-c_M\left(\frac{\partial \log\alpha_M}{\partial \text{pH}}\right)_{c_B}+q\,c_B+$$

$$+c_M f\left\{p-4+\left(\frac{\partial \log\alpha_M}{\partial \text{pH}}\right)_{c_B}-\left(\frac{\partial \log\alpha_{MY}}{\partial \text{pH}}\right)_{c_B}\right\} \tag{12}$$

(b) after the equivalence point:

$$-[H]+[OH]+\frac{K_a}{K_a+[H]}c_B=-c_M\left(\frac{\partial \log\alpha_{MY}}{\partial \text{pH}}\right)_{c_B}+c_M\left(\frac{\text{d} \log\alpha_Y}{\text{d pH}}\right)+q\,c_B+$$

$$c_M f\left\{p-4-\left(\frac{\text{d} \log\alpha_Y}{\text{d pH}}\right)\right\} \tag{13}$$

Fortunately, in nearly all important cases, the equations can be simplified, [H] and [OH] being small in comparison with $K_a c_B/(K_a+[H])$. It is then possible to plot $K_a/(K_a+[H])$ against the amount of EDTA added. The curves are not perfectly straight lines, because the partial differential quotients in eqns. (12) and (13) cannot be constant with changing pH, if the buffer reacts with the metal or the complex.

The expressions given above for a bivalent metal ion, EDTA as titrant and a buffer derived from a weak acid, are also applicable for metals of other valencies, other chelating titrants and other types of buffer.

Titration of calcium in a solution buffered by ammonia–ammonium chloride

Figure 4 shows the plot obtained in the titration of $8\cdot10^{-5}\,M$ calcium in a solution buffered with $1.6\cdot10^{-4}M$ ammonia and $1.6\cdot10^{-3}M$ ammonium chloride; the titrant was a $10^{-3}\,M$ solution of Na_3HY. In order to avoid the absorption of carbon dioxide from the air, the solution was covered with a layer of petroleum ether. Because of the very small pH change it was possible to plot [OH].

PHOTOMETRIC INDICATION

For the discussion of the photometric acid–base indication method, it is assumed that a buffer is present in concentration c_B with an acidity constant K_a^B, and an indicator in concentration c_I with an acidity constant K_a^I.

The expression

$$-[H]+[OH]+c_B\frac{K_a^B}{K_a^B+[H]}+c_I\frac{K_a^I}{K_a^I+[H]} \tag{14}$$

will vary linearly with the amount of titrant added in both branches of the titration curve, as long as the conditions mentioned above, *i.e.* $K'c_M > 10^3$ and a not too large pH change are valid.

Actually, the absorbance

$$A=b([I]\varepsilon_I+[HI]\varepsilon_{HI})=b\,c_I\left(\frac{K_a^I\,\varepsilon_I}{K_a^I+[H]}+\frac{[H]\,\varepsilon_{HI}}{K_a^I+[H]}\right) \tag{15}$$

is measured. Calculation of the hydrogen ion concentration from the absorbance and substitution in eqn. (14), is possible but rather cumbersome. Moreover, such a calculation depends on an exact knowledge of the two acidity constants. Therefore, direct plotting of the absorbance is the most practicable method. This will yield straight lines if (*a*) the pH change is very small, and (*b*) the acidity constants of the buffer and the indicator are the same. Equation (14) then simplifies to one which is linearly related to the absorbance.

It is interesting to compare the sensitivity of the potentiometric and the photometric method. In the previous paragraphs, it was assumed that 0.001 is the smallest detectable pH change. For the smallest detectable absorbance change, 0.0001* can be taken, provided that the absorbance does not exceed 0.5. As an example, a solution with a buffer of total concentration c_B and equal concentrations of acid and base is considered. For the indicator added, a total concentration c_I and $K_a^I=K_a^B$ are assumed. The smallest amount of acid or base which then can be detected potentiometrically appears to be equivalent to $0.00058\ c_B$. For the photometric method, calculation yields $0.0002\ (c_B+c_I)$. In view of the uncertainties in the assumptions, it can be concluded that the two methods have essentially the same sensitivity in buffered solution. However, for the highest sensitivity, the potentiometric method is superior, because of the finite value of c_I needed for precise photometric measurement. Moreover, a suitable indicator for the photometric method may be difficult to find in some cases.

Titration of zinc

Figure 5 shows the curve obtained in the titration of 10 ml of solution containing $5\cdot10^{-4}$ *M* zinc, $2\cdot10^{-3}$ *M* acetic acid–sodium acetate buffer and $9\cdot10^{-6}$ *M* methyl

---

* These estimates of the smallest detectable values may seem optimistic. However, these figures do not apply to accurate measurement of different solutions, but only to a change in one solution during a relatively short time. The value of 0.0001 for the photometric measurement is obtainable only when a filter instrument is used based on the substitution principle.

red. Almost perfectly linear plots are obtained because the pH changes only very slightly as a result of the presence of the buffer. The pH was 5.78 at the start and 5.98 at the end of the titration. In such a narrow region the change of absorbance of methyl red is linearly related to the amount of protons released, especially because the acidity constants of the indicator and the buffer differ only slightly. It must be emphasized that such an approximation to linear plots with maintenance of a reasonable precision was possible only because of the very high stability of the photometer used.

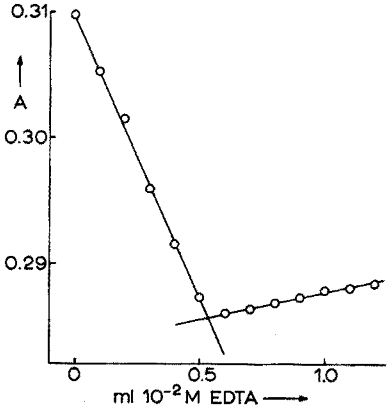

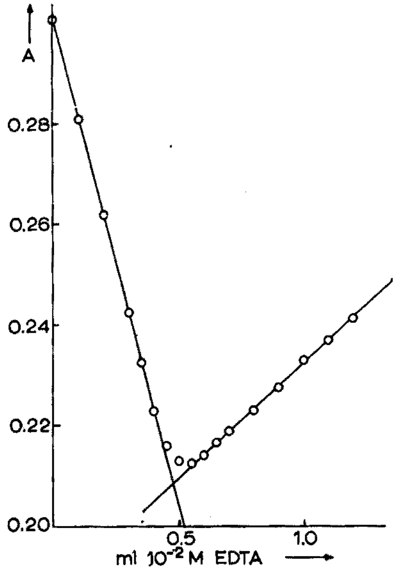

Fig. 5. Titration curve of 5 μmol of zinc(II) in 10 ml of solution containing $2 \cdot 10^{-3}$ *M* acetic acid–sodium acetate buffer and $9 \cdot 10^{-6}$ *M* methyl red.

Fig. 6. Titration curve of 5 μmol of aluminium(III) in 10 ml of solution containing 10^{-2} *M* formic acid–sodium formate buffer and $9 \cdot 10^{-6}$ *M* methyl orange.

The total change in absorbance in this titration was only 0.02, which corresponds to 10 % of the methyl red present. Another possibility for measuring relatively small changes in the absorbance of the indicator could be the use of differential methods with deflection-type photometers.

Titration of aluminium

Figure 6 shows the curve obtained in the titration of 10 ml of solution containing $5 \cdot 10^{-4}$ *M* aluminium, 0.01 *M* formate–formic acid buffer and $9 \cdot 10^{-6}$ *M* methyl orange.

EXPERIMENTAL

Reagents

All reagents used were pro analysi. The potassium chloride used in the potentiometric measurements was Merck "Suprapur" grade.

Apparatus

The potentiometric measurements were carried out with glass and calomel electrodes (Radiometer G 202 B and K 401) and a compensation pH meter (Radiometer PHM 4). The photometric measurements were carried out with a substitution photometer (Zeiss Elko II).

Procedures

No attempt was made to eliminate systematic errors from the pH measurements, because only the changes in pH were of importance.

Potassium chloride in about 0.1 *M* concentration was added to the solutions for the potentiometric experiments, in order to obtain more stable readings. For the same reason, the saturated potassium chloride solution in the calomel electrode was replaced by a 0.1 *M* solution. The instability which was otherwise obtained is attributed to an unstable liquid junction potential at the capillary tip of the reference electrode.

The photometric titrations were carried out without a reference solution, because this is easier and more precise for the apparatus used.

SUMMARY

Almost every complexation reaction gives rise to a protolytic effect, whose influence is usually decreased by adding a buffer. The use of the protolytic effect for locating the end-points of compleximetric titrations is discussed. Expressions are given for the linear titration graphs which can be obtained by photometric or potentiometric methods under different conditions. Examples of each case are described. The advantages of the method are its general applicability and high sensitivity.

RÉSUMÉ

La formation d'un chélate en solution aqueuse s'accompagne généralement d'un effet protolytique, qu'on peut diminuer par addition d'un tampon. On examine les possibilités d'utilisation de cet effet protolytique pour déterminer les points d'équivalence de titrages compleximétriques. Des courbes de titrage linéaires sont obtenues dans diverses conditions, soit par méthodes photométriques, soit par potentiométrie. Ce procédé présente l'avantage d'être très sensible et très généralement applicable.

ZUSAMMENFASSUNG

Die meisten Komplexbildungsreaktionen sind mit einem protolytischen Effekt verbunden, dessen Einfluss üblicherweise durch Zugabe eines Puffers klein gehalten wird. Es wird die Anwendung des protolytischen Effektes zur Endpunktsanzeige bei komplexometrischen Titrationen erörtert. Die linearen Titrationskurven, die durch photometrische oder potentiometrische Methoden unter verschiedenen Bedingungen erhalten werden, werden theoretisch behandelt; praktische Beispiele werden vorgelegt. Die Vorteile der Methode sind die allgemeine Anwendbarkeit und hohe Empfindlichkeit.

REFERENCES

1 A. Ringbom, *Complexation in Analytical Chemistry*, Interscience–Wiley, New York, 1963.
2 G. Schwarzenbach and H. Biedermann, *Helv. Chim. Acta*, 31 (1948) 459.

Analytica Chimica Acta
Elsevier Publishing Company, Amsterdam
Printed in The Netherlands

COPPER(I) SULFIDE CERAMIC MEMBRANES AS SELECTIVE ELECTRODES FOR COPPER(II)

HIROSHI HIRATA, KENJI HIGASHIYAMA AND KENJI DATE
Wireless Research Laboratory, Matsushita Electric Industrial Co., Ltd., Kadoma (Japan)

(Received January 5th, 1970)

Several types of solid-state membranes have been applied for ion-selective electrodes[1]. Glass electrodes are available for alkali and alkali-earth metal ions. FRANT AND ROSS[2] developed fluoride-selective membranes with a single crystal of lanthanum fluoride doped with europium. Fused silver sulfide membranes have been developed for sulfide-selective electrodes[1], and a copper(II)-selective electrode has been prepared from fused silver and copper(I) sulfides by Orion Research Inc.[1]. Copper(II)-selective electrodes of the liquid–liquid membrane type are also available[1] but these electrodes have the disadvantages of rather low sensitivity and of requiring frequent change of the ion-exchange solution.

So far as is known, no electrodes have previously been prepared from ceramic membranes made by an annealing process. The present work was directed towards the development of a ceramic membrane which would show a selective response towards copper(II) ion. The electrode developed has short response times even in low concentrations and can be produced at lower cost than the silver sulfide membrane by annealing of copper(I) sulfide powder. The effects of various conditions on the potential properties of the copper(I) sulfide membrane were examined and the results have proved that the membrane has a satisfactory response and selectivity for copper(II).

EXPERIMENTAL

Apparatus and reagents

An Orion Model 801 digital pH meter was used to make the potential measurements. Copper powder was Merck high-purity grade and all other reagents were Nakarai Chemical reagent grade.

Preparation of copper(I) sulfide ceramic membrane

A fine powder of copper(I) sulfide was obtained by heating a mixture of copper powder and sulfur in the molar ratio 2:1, at 400–800° for 2 h in an atmosphere of hydrogen sulfide. The heated mixture was ground to give a particle size of less than 10 μm. The copper(I) sulfide powder was compressed at a pressure of 150 kg cm^{-2}, so as to form a tablet with a diameter of 15 mm and a thickness of 2–3 mm, and was then heated at 500–900° for 1–5 h in an atmosphere of hydrogen sulfide or nitrogen. After the tablet had cooled, its surfaces were polished and washed with an ultrasonic wave cleaner. The structure of copper(I) sulfide was analysed by X-ray diffractometry.

Measurement of the potentials

Figure 1 shows the cross-section of copper(I) sulfide ceramic membrane electrode. The potentials developed in the test solution by the electrode were measured with a saturated calomel electrode as the reference electrode at 25.0 ± 0.1°.

RESULTS AND DISCUSSION

The internal electrode and solution which are commonly used in the usual selective electrodes, were eliminated by attaching the leading wire to the membrane directly as shown in Fig. 1; this avoids any internal contamination of the membrane and the need for careful preservation and change of an internal solution. Moreover, the elimination of the internal electrode simplifies the structure of the electrode.

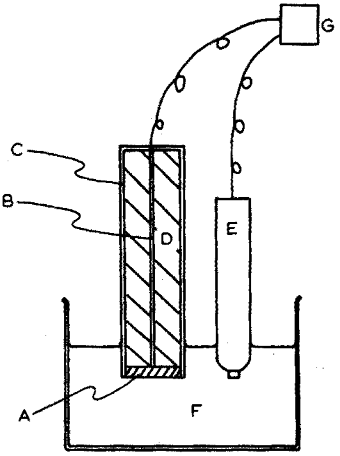

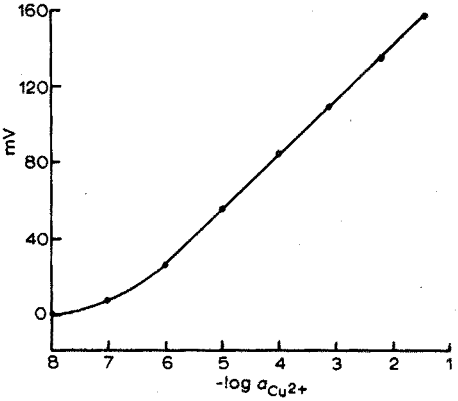

Fig. 1. Cross-section of copper(I) sulfide ceramic membrane electrode. (A) Copper(I) sulfide ceramic membrane, (B) leading wire, (C) cover (plastics), (D) insulator (epoxy resin), (E) reference electrode (S.C.E.), (F) test solution, (G) pH meter.

Fig. 2. Potential responses of copper(I) sulfide ceramic membrane in solutions of copper(II) sulfate.

Preparation of copper(I) sulfide ceramic membrane

When pores appeared on the surfaces of the copper(I) sulfide membrane, the response time became longer and the lower limit of the concentration range which could be determined became higher than those of non-porous membranes. The appearance and the amount of pores depended on the distribution of particle size of the copper(I) sulfide powder, the pressure at the press, the temperature and the atmosphere during the annealing process, the technique of polishing, etc.

When x in $Cu_{2-x}S$, which describes the composition of the copper(I) sulfide ceramic, increased, the response time became shorter and at the same time it became more difficult to make non-porous ceramic. When x decreased, the response time became longer and the slope of the potential response, *i.e.*, mV *vs.* $-\log a_{Cu^{2+}}$, decreased. Here, x varied from 0 to 0.21. Accordingly, great care must be taken in the preparation of the copper(I) sulfide ceramic in order to obtain a non-porous ceramic which contains excess of sulfur beyond the stoichiometric ratio for copper(I) sulfide, *e.g.*, $Cu_{1.79}S$.

Potential responses in solutions of copper(II) sulfate

The potential responses of the copper(I) sulfide ceramic membrane in solutions of copper(II) sulfate are shown in Fig. 2. The activity was corrected from the concentration using the ion activity coefficients tabulated by KIELLAND[3]. A Nernstian slope was obtained in the concentration range of 10^{-1}–10^{-6} *M* of copper(II) ion and the analytical range was 10^{-1}–10^{-8} *M*. The potentials were steady and stable. The response time was short, being only a few seconds for 10^{-1} *M* copper(II) and about 2 min for 10^{-8} *M* copper(II) ion as shown in Fig. 3.

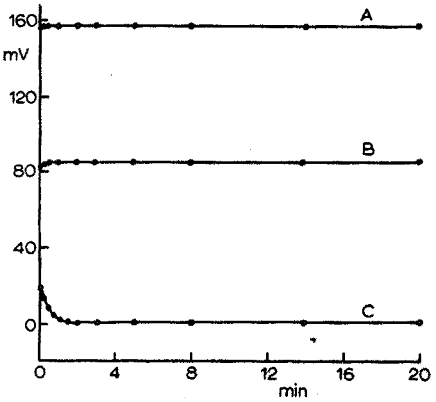

Fig. 3. Variation of potential of the membrane with time in (A) 10^{-1} *M*, (B) 10^{-4} *M* and (C) 10^{-8} *M* solutions of copper(II) sulfate.

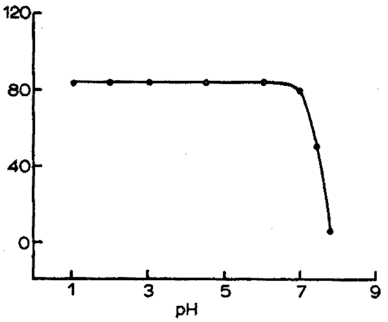

Fig. 4. Influence of pH on the potentials of the membrane in 10^{-4} *M* copper(II) solution.

Influence of pH

Figure 4 shows the influence of pH on the potentials of the copper(I) sulfide ceramic membrane in a 10^{-4} *M* copper(II) solution. The potentials did not change over the pH range 1–7, but they decreased sharply when the pH increased above 7, because of precipitation of copper(II) hydroxide. Of course the pH at which the precipitation begins depends on the concentration of copper(II) present.

Influence of foreign ions

The influence of foreign ions on the determination of copper was examined by adding various salts to 10^{-4} *M* solutions of copper(II). Ammonium ion at pH above 7, and silver and mercury(II) interfered, for ammonium ion forms the stable complex $Cu(NH_3)_4^{2+}$ ion with copper(II) in basic solution, whereas silver and mercury deposit on the membrane as their ionization potential is smaller than that of copper. A 10^{-3} *M* solution of iodide interfered because of the formation of copper(I) iodide. Iron(III) at the 10^{-3} *M* level interfered, but 10^{-4} *M* solutions of iodide or iron(III) did not interfere. Of course, sulfide interfered and the membrane can also be used as a selective electrode for sulfide ion. Other common cations and anions could be tolerated and the selectivity ratios for copper(II) were about 10^3.

Effect of temperature

The copper(I) sulfide ceramic membrane electrode was safely used at temperatures in the range 0–80° and the potentials of the membrane satisfied the Nernstian equation within the experimental error.

The authors thank Dr. S. KISAKA and Dr. K. SUGIHARA for their encouragement in this work. Thanks are also due to Mr. T. MIYAZAWA for X-ray analysis of copper(I) sulfide.

SUMMARY

A new type of copper(II)-selective electrode has been developed, based on copper(I) sulfide ceramic membranes prepared by an annealing process. The response time was very short even at low concentrations and the potentials were steady and reproducible. The Nernst equation was obeyed in the concentration range of 10^{-1}–10^{-6} M copper(II) and the analytical range was 10^{-1}–10^{-8} M. Among the common ions, silver, ammonium, iron(III) and iodide interfered.

RÉSUMÉ

On propose un nouveau type d'électrode sélective de cuivre(II), basée sur des membranes sulfure de cuivre(I) céramique. Le temps de réponse est très court, même pour de faibles concentrations; les potentiels sont stables et reproductibles. L'équation de Nernst s'applique pour des concentrations allant de 10^{-1} à 10^{-6} M. Parmi les ions communs, argent, ammonium, fer(III) et iodure gênent.

ZUSAMMENFASSUNG

Es ist ein neuer Typ einer kupfer(II)selektiven Elektrode entwickelt worden, die aus einer durch einen Glühprozess hergestellten Kupfer(I)-sulfid–Keramik-Membran besteht. Die Ansprechzeit war sogar bei niedrigen Konzentrationen sehr kurz, und die Potentiale waren beständig und reproduzierbar. Die Nernstsche Gleichung war gültig im Konzentrationsbereich 10^{-1}–10^{-6} M Kupfer(II), der analytische Bereich war 10^{-1}–10^{-8} M. Von den üblichen Ionen störten Silber, Ammonium, Eisen(III) und Jodid.

REFERENCES

1 See R. A. DURST (Editor), *Ion-Selective Electrodes*, N.B.S. Monograph 314, U.S. Govt. Printing Office, Washington, 1969.
2 M. S. FRANT AND J. W. ROSS, JR., *Science*, 154 (1966) 1553.
3 J. KIELLAND, *J. Am. Chem. Soc.*, 59 (1937) 1675.

Analytica Chimica Acta
Elsevier Publishing Company, Amsterdam
Printed in The Netherlands

THE BEHAVIOUR OF ION-SELECTIVE SILICONE-RUBBER MEMBRANE ELECTRODES IN SOME NON-AQUEOUS SOLVENTS

N. A. KAZARJAN* AND E. PUNGOR
Department of Analytical Chemistry, University of Chemical Industries, Veszprém (Hungary)
(Received April 3rd, 1970)

During the last decade, ion-selective silicone-rubber electrodes have played an increasingly important role in analytical chemistry[1-6]. The high selectivity of the electrodes makes possible the determination of various anions and cations in the presence of other ions. Until now the behaviour of these ion-selective electrodes has only been examined in aqueous solutions, and the potential behaviour of the ion-selective electrodes has been interpreted for solutions containing only the ion to which the electrode is reversible[1,5], or for solutions which contain other ions besides the required ion. This other ion can also take part in the formation of the electrode potential[2], which can be described with a modified Nernst equation as follows:

$$E = E_0' + \frac{RT}{zF} \ln (a_{is} + K_{ik}\, a_{ks} + K_{il}\, a_{ls}) \tag{1}$$

where a_i is the activity of ion i, to which the electrode is reversible (required ion); a_k and a_l are the activities of ions k and l, which also can take part in the formation of the electrode potential; K_{ik} and K_{il} are selectivity constants; and s denotes the aqueous solution phase.

The theoretical examination of the lower range of the potential–log a_i function has led to the interesting conclusion that the lower detection limit of a precipitate-based ion-selective electrode is determined by the solubility of the precipitate composing the membrane layer of the electrode[7]. Accordingly, the lower detection limit of the halide-selective electrodes is within the concentration range of 10^{-5}–10^{-8} *M*.

The aim of this paper was to study how the application of non-aqueous solvents alters the correlations valid for the ion-selective electrodes in aqueous media, and furthermore, to what extent these alterations can be used for analytical purposes.

EXPERIMENTAL

Solvents and chemicals

Water-miscible, non-aqueous solvents such as methanol, ethanol, *n*-propanol and isopropanol were used in this study. The solvents were of *pro analysi* grade or were purified before use. The experiments were carried out in mixtures of distilled water and the appropriate non-aqueous solvent.

The amounts of the two solvents generally were changed in 10 or 20 % steps.

---

* Permanent address: Mendeleev Institute of Chemical Technology, Moscow.

All chemicals used were of *pro analysi* grade. Before measurements the chemicals were dissolved in the appropriate solvent mixture in the concentration desired.

Examination of the dissolution of the membrane layer

For this study silver iodide-based silicone-rubber membrane disks were used. The membrane disks were weighed and immersed in the appropriate solvent mixture for a certain period of time. After soaking, the membrane disks were dried between filter paper (2–3 sec) and weighed on an analytical balance. Parallel to this, the colour change of the solvent mixture was observed.

Potential measurement

A precision pH meter (Model OP 205, Radelkis, Budapest) with an expanded scale was employed. The input resistance of the pH meter is greater than 10^{12} Ω.

The potential measurements were carried out in the following measuring cell: Ag/AgCl electrode–aqueous chloride solution/silicone-rubber membrane/ the appropriate halide dissolved in a solvent mixture–KNO_3 salt bridge–S.C.E.

Determination of the solubility product of silver halide salts in various solvent mixtures

The data given in the literature for the solubility products of the silver halide salts in various solvent mixtures[8-11] were insufficient for drawing theoretical conclusions about the behaviour of the precipitate-based silicone-rubber membrane electrodes. For this purpose, it was necessary to determine the solubilities of the silver halide salts in every solvent in which the electrodes were used.

The solubility products were determined on the basis of the potentiometric titration curves since great accuracy was not required. For titration a solution containing the appropriate alkali halide salt in the appropriate solvent mixture was prepared and titrated with an aqueous silver nitrate solution. The concentration of the titrant was two orders of magnitude higher than that of the solution to be titrated. As an indicator electrode an appropriate halide-selective electrode was used. The solubility products were calculated from the titration curves by neglecting the dilution of the solution caused by the addition of the silver nitrate titrant.

Determination of the lower detection limit of an ion-selective electrode

From the determinations of the solubility products, it became clear that in a solvent mixture containing 90 % methanol and 10 % distilled water, the solubility of the silver iodide precipitate decreases to a great extent. Consequently, it seemed interesting to study how the lower detection limit of an iodide ion-selective electrode changes in this solvent mixture. For the study, solutions were freshly prepared by the dilution of a 10^{-3} M potassium iodide solution in 90 % methanol with 90 % methanol. The potential was read after attaining equilibrium. This took about 2–5 min in the lower concentration ranges at or below 10^{-5} M.

Determination of the selectivity constants of an iodide-selective electrode in mixtures of various aqueous and non-aqueous solvents

The determination of the selectivity constants was carried out by two different methods in every solvent mixture[5,6]. In the direct method, direct potential measurements were carried out in the appropriate non-aqueous solution containing a constant amount of potassium iodide and various amounts of the ion for which the selectivity constant of the electrode was being examined. In the indirect method (potentiometric titration method), a non-aqueous solution containing potassium iodide and another salt in the same concentration, was titrated with an aqueous silver nitrate solution; the concentration of the titrant was two orders of magnitude higher than that of the solution to be measured. In the former case, the concentrations measured at the break-point of the potential *vs.* $-\log c_I$ curve, while in the latter case the concentrations obtained when coprecipitation starts in the solution, were used for the experimental determination of the selectivity constants. The concentration of the iodide at the coprecipitation point was calculated with the help of the Nernst equation by considering the initial iodide concentration and the potential fall.

The selectivity constants were calculated as given in the literature[5,6], with the solubility products determined experimentally.

RESULTS AND DISCUSSION

On the basis of the experiments carried out in mixtures of distilled water and alcohols, the concentration ratios of the solvents could be determined at which noticeable changes were observed either in the weight of the membrane disks or in the colour of the solvent mixtures studied[12]. The results clearly showed that a silicone-rubber membrane electrode can be used without any harm in mixtures containing up to 90 % (v/v) alcohol for methanol or ethanol with distilled water. In mixtures of isopropanol or *n*-propanol with distilled water, the limit of applicability lies at a content of 40 % propanol.

When the membrane layers were soaked in the latter two solvent mixtures, then besides swelling, a colour change of the solvent mixtures was also observed. The colour change may indicate that part of the precipitate in the boundary layers of the membrane dissolves colloidally. This suggestion was proved experimentally by precipitating silver iodide in the same solvent mixtures; the freshly precipitated silver iodide was highly dispersed and the particle size did not decrease with time. The colour of the solvent mixtures used was similar to that obtained by soaking the silver iodide electrodes in these mixtures.

The solubility products of the silver halide salts were determined in the solvent mixtures chosen on the basis of preliminary experiments. Table I shows the solubility data for each silver halide salt determined potentiometrically[12], as well as some values taken from the literature[9-11,13]. It can be seen that the application of methanol and ethanol in relatively high concentrations offers possibilities for extending the lower detection limits of the iodide- and bromide-selective electrodes. In aqueous solutions, the lower detection limit of a monovalent ion-selective electrode is given by the following equation:

$$E = E_0' + \frac{RT}{zF} \ln \frac{S^{\frac{1}{2}} + (S + 4(a_1)_s{}^2)^{\frac{1}{2}}}{2} \tag{2}$$

where E_0' is the normal potential of the electrode; S is the solubility product of the precipitate in the membrane layer; a_1 is the activity of the ion, to which the electrode is reversible; and s denotes the aqueous solution phase.

A calibration curve for iodide in an aqueous 90 % methanol solution is shown

TABLE I

SOLUBILITY PRODUCTS OF SILVER HALIDE SALTS IN AQUEOUS–ALCOHOLIC SOLVENT MIXTURES

Solvent	*Ratio of solvents (v/v %)*	*Mole fraction of solvents*	*Solubility products*		
			AgI	*AgBr*	*AgCl*
H_2O	100	0	15.96 (15.96[a])	12.36 (12.36[a])	9.82 (9.81[a])
CH_3OH	10	0.047	16.12	12.48	10.10
	40	0.228	16.48	13.00	10.40
	60	0.400	16.72	13.38	10.74
	90	0.802	17.42	14.40	11.50
	100	1.00	17.84[a]	14.91[a]	12.69[a]
C_2H_5OH	10	0.032	16.16	12.54	10.20
	40	0.162	16.40	12.90	10.58
	60	0.298	16.60	13.26	10.82
	90	0.677	17.30	14.30	10.32
	100	1.00	18.96[a]	—	13.77[a]
n-C_3H_7OH	10	0.026	16.20	12.50	9.90
	20	0.056	16.24	12.66	9.92
	30	0.092	16.32	12.74	9.92
	40	0.137	16.40	12.82	10.00
iso-C_3H_7OH	10	0.026	16.04	12.30	9.88
	20	0.056	16.12	12.48	10.16
	30	0.092	16.20	12.64	10.20
	40	0.137	16.28	12.78	10.28

[a] Values taken from the literature.

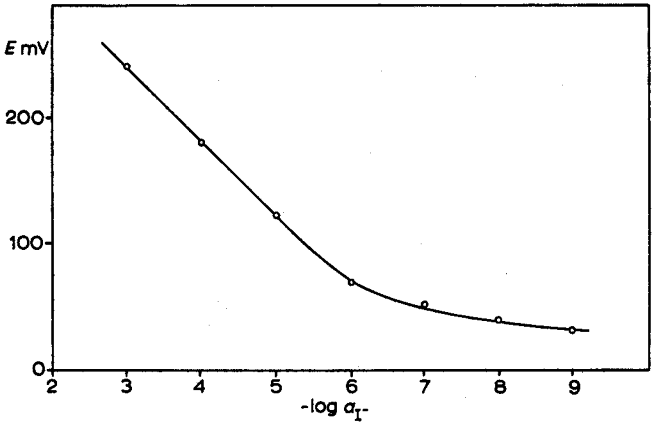

Fig. 1. Calibration curve for iodide in aqueous 90 % (v/v) methanol solution.

in Fig. 1. It can be seen that iodide even in 10^{-8}–10^{-9} *M* concentration gives rise to an electrode potential. However, these experimental results did not prove completely the validity of eqn. (2) in non-aqueous media. The correlation in non-aqueous media is more complicated and experiments to elucidate the matter further are in progress.

It is extremely interesting from the analytical point of view, that the iodide ion can be determined with an iodide-selective electrode even in 10^{-9} *M* concentration in mixtures of ethanol or methanol and distilled water, the alcohol concentration of which is 90 %. The reproducibility of the results is shown in Table II. The iodide solutions used for the measurements were prepared by dilution and the results were evaluated with the help of a calibration curve.

TABLE II

DETERMINATION OF IODIDE IN VERY LOW CONCENTRATIONS

(Total volume 10 ml)

I^- *taken* (*ng*)	I^- *found* (*ng*)	*Av. error* (Δ*ng*)
13	13.0, 16.0, 10.0, 7.5, 7.5	± 3.4
1.3	2.5, 2.0, 1.3, 1.3, 1.3	± 0.38

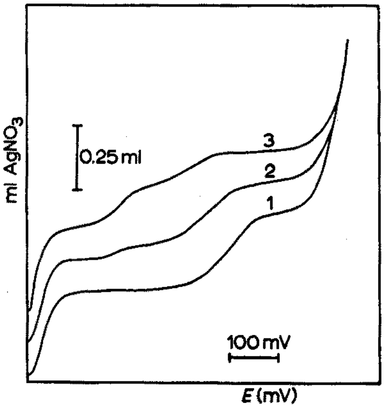

Fig. 2. Determination of the selectivity constant of an iodide-selective electrode in methanol–water mixtures. (1) 10^{-3} *M* I^- + 10^{-3} *M* Cl^- in water, (2) 10^{-3} *M* I^- + 10^{-3} *M* Cl^- in 20 % methanol–80 % water, (3) 10^{-3} *M* I^- + 10^{-3} *M* Cl^- in 90 % methanol–10 % water.

The application of these ion-selective electrodes in non-aqueous media also creates the problem of selectivities. For the determination of the selectivity constants both methods described in the literature[5,6] were employed. From the results shown in Fig. 2, it is clear that the application of the indirect method causes problems in non-aqueous media. An additional potential jump, which interferes with the evaluation of the results, appears in solutions of high alcohol concentrations. Parallel to this, the grain size of the precipitate in the solution becomes finer. The interfering potential jump may be due to the silver chloride precipitate formed in the reaction of the titrant with chloride being in the primary adsorbed chloride layer on the surface of the silver iodide precipitate. The solubility product of this silver chloride is lower than that of silver chloride formed in the absence of silver iodide. This phenomenon is analogous to that obtained when the solubility products of slightly soluble silver halide salts adsorbed on the surface of a silver iodide precipitate were studied[14]. Consequently, the indirect potentiometric method is not recommended for the determination of selectivity constants in non-aqueous media. The application of this method can be recommended only if the negative logarithm of the selectivity constant is relatively high, although it can always serve to give approximate results[5,6].

However, the selectivity constants of the electrodes in non-aqueous media were determined successfully by the direct method[12]. The reproducibility of the results was checked at two different iodide concentrations. From Table III, it can be seen that the results are in good agreement with each other.

TABLE III

REPRODUCIBILITY OF THE RESULTS OBTAINED FOR THE SELECTIVITY CONSTANTS IN MIXTURES OF DISTILLED WATER AND ISOPROPANOL

Alcohol %	*pBr*[b]		*pK_c (−log K)*[a]	
	$pI = 5$	*$pI = 6$*	*$pI = 5$*	*$pI = 6$*
10	1.22	2.22	3.78	3.78
20	1.40	2.40	3.60	3.60
30	1.50	2.52	3.50	3.48
40	1.86	2.82	3.14	3.18

[a] pK_c is the value of the selectivity constant calculated.
[b] Measured values.

TABLE IV

SELECTIVITY CONSTANTS OF AN IODIDE-SELECTIVE ELECTRODE IN MIXTURES OF DISTILLED WATER AND AN ALCOHOL

Solvent	*Ratio of solvent (v/v %)*	*Mole fraction of solvent*	*pK*		
			Theor.	*Calcd.*	*ΔpK*
CH_3OH	10	0.047	3.64	3.78	−0.14
	40	0.228	3.48	3.60	−0.12
	60	0.400	3.34	3.38	−0.04
	90	0.802	3.02	3.02	−0.00
	100	1.00	2.93	—	—
C_2H_5OH	10	3.20	3.62	3.70	−0.08
	40	16.20	3.50	3.55	−0.05
	60	29.80	3.34	3.30	−0.04
	90	67.70	3.00	2.76	+0.24
	100	100	—	—	—
n-C_3H_7OH	10	2.60	3.70	3.74	−0.04
	20	5.60	3.58	3.54	+0.04
	30	9.20	3.58	3.46	+0.12
	40	13.70	3.58	3.42	+0.16
iso-C_3H_7OH	10	2.60	3.74	3.78	−0.04
	20	5.60	3.64	3.60	+0.04
	30	9.20	3.56	3.49	+0.06
	40	13.70	3.50	3.16	+0.36

The selectivity constants measured in mixtures of distilled water and an alcohol are summarized in Table IV. It can be seen that the selectivity constants measured and calculated on the basis of the solubility products are in good agreement with each other. It can also be seen that the selectivity constants of an iodide-selective electrode for other halide ions become worse in alcoholic media compared to the values obtained in aqueous media.

In conclusion, it can be said that it is valuable from the theoretical point of view that eqn. (1) derived for aqueous media, is also valid in non-aqueous media. However, the use of mixtures of distilled water and an alcohol is not recommended for the determinations of individual halides in the presence of each other with halide-selective silicone-rubber membrane electrodes, because the selectivities of the halide-selective electrodes decrease in non-aqueous media.

The authors thank K. Tóth for her help in carrying out this work.

SUMMARY

The applicability of silicone-rubber ion-selective electrodes was studied in mixtures of distilled water with methanol, ethanol, propanol, or isopropanol. The limit of applicability of the electrodes lies at a 90 % alcohol concentration in aqueous methanol or ethanol solutions, and at 40 % alcohol concentration in aqueous *n*-propanol or isopropanol solutions. The solubility products of the silver halide salts and the selectivity constants of an iodide-selective electrode for other halide ions were measured in aqueous alcohol solutions. The equation previously derived for potentials in aqueous media involving selectivity constants is also valid in non-aqueous media.

RÉSUMÉ

Une étude est effectuée sur le comportement des électrodes ioniques sélectives silicone–caoutchouc en milieux méthanol, éthanol, propanol ou isopropanol. La limite de concentration possible est de 90% pour les solutions aqueuses de méthanol ou d'éthanol et 40% pour le propanol ou l'isopropanol. Les produits de solubilité des halogénures d'argent et les constantes de sélectivité d'une électrode au iodure pour les autres halogénures ont été mesurés en solution aqueuse d'alcohol. L'équation précédemment établie pour les potentiels en milieu aqueux, comprenant les constantes de sélectivité peut s'appliquer également en milieu non-aqueux.

ZUSAMMENFASSUNG

Die Anwendbarkeit ionenselektiver Silicon–Gummi-Elektroden in Mischungen von destilliertem Wasser mit Methanol, Äthanol, Propanol oder Isopropanol wurde untersucht. Die Grenze der Anwendbarkeit liegt bei 90% Alkoholkonzentration in wässrigen Methanol- oder Äthanollösungen und bei 40% Alkoholkonzentration in wässrigen *n*-Propanol- oder Isopropanollösungen. Die Löslichkeitsprodukte der Silberhalogenide und die Selektivitätskonstanten einer jodidselektiven Elektrode für andere Halogenidionen in wässrigen Alkohollösungen wurden gemessen. Die früher abgeleitete Gleichung für die Potentiale in wässrigem Medium mit samt den Selektivitätskonstanten ist auch im nichtwässrigen Medium gültig.

REFERENCES

1 E. Pungor, *Anal. Chem.*, 39 (1967) No. 13, 28A.

2 E. Pungor and K. Tóth, *Analyst*, in press.
3 A. Covington, *Ion-Selective Electrodes*, N.B.S. Spec. Publ. No. 314, p. 89.
4 G. J. Moody, R. B. Ohe and J. D. R. Thoms, *Lab. Pract.*, 18 (1969) 1056.
5 K. Tóth, *Candidate's Thesis*, 1969, Veszprém.
6 E. Pungor and K. Tóth, *Anal. Chim. Acta*, 47 (1969) 291.
7 E. Pungor, J. Havas and K. Tóth, *Acta Chim. Acad. Sci. Hung.*, 48 (1966) 17.
8 W. F. Linke, *Solubilities of Inorganic and Metal Organic Compounds*, Vol. I, 4th Edn., D. Van Nostrand Co., Princeton, N. J.–Toronto–London–New York, 1958.
9 P. S. Buckley and H. Hartley, *Phil. Mag.*, 8 (1929) 320.
10 F. K. Koch, *J. Chem. Soc.*, (1930) 1551, 2385.
11 J. Neustadt, *Z. Elektrochem.*, 16 (1910) 866.
12 N. A. Kazarjan and E. Pungor, in preparation.
13 J. Bjerrum, G. Schwarzenbach and L. G. Sillén, *Stability Constants. II. Inorganic Ligands*, The Chemical Soc., London, 1958.
14 E. Pungor and I. Konkoly Thege, *Talanta*, 10 (1963) 1211.

Analytica Chimica Acta
Elsevier Publishing Company, Amsterdam
Printed in The Netherlands

DETERMINATION OF CYANIDES WITH ION-SELECTIVE MEMBRANE ELECTRODES

KLÁRA TÓTH AND ERNŐ PUNGOR
Department of Analytical Chemistry, Umiversity of Chemical Industries, Veszprém (Hungary)

(Received April 3rd, 1970)

The determination of cyanides is often necessary in pharmaceutical industry, biochemistry, and in various other fields. It is especially important, for example, in effluents originating from anodic plating plants and pharmaceutical production processes where cyanide is used.

Numerous chemical and physicochemical methods for the determination of cyanides in various concentration ranges can be found in the literature. However, only the potentiometric determination of cyanides will be referred to here, because this offers a possibility for use in automatic systems of controlling the cyanide content.

Apart from gold, mercury and amalgam electrodes, the most widely used electrode for cyanide determination is the silver rod electrode. When the silver electrode is immersed in a cyanide solution, a potential arises on its surface which is dependent on the concentration of the cyanide[1]. However, the correlation between the electrode potential and the cyanide concentration is disturbed by various reactions which take place on the electrode surface, *e.g.* complex formation between the silver and cyanide ions. Other complications may arise when organic solvents are used[2]. To exclude these phenomena, GERCHMAN AND RECHNITZ[3] suggested the use of a cation-sensitive glass electrode for the potentiometric titration of cyanide with silver nitrate. The cation-sensitive glass electrode indicates the presence of silver ions[4-6], and cannot be used for the direct determination of cyanide.

The development of heterogeneous[7,8] and homogeneous[9] ion-selective electrodes has offered new possibilities for cyanide determinations. Cyanide-sensitive electrodes have been developed as a result of research on ion-selective membrane electrodes. The membrane layer, the sensing part of these electrodes, is composed either of a silver halide salt incorporated in a suitable supporting material such as silicone rubber[10], or of a mixture of inorganic silver salts[11].

The electrochemical behaviour of both types of ion-selective electrodes can be interpreted in the same way, *i.e.* on the basis of the precipitate ion-exchange reaction taking place at the boundary phases of the membrane layer[12,13]. Recently, BUCK[14,15] has also used the ion-exchange interpretation to describe the behaviour of homogeneous (solid-state) membrane electrodes.

EXPERIMENTAL

Apparatus

An expanded-scale pH meter (Model OP 205, Radelkis, Budapest, Hungary) was used for all potentiometric measurements. A Radelkis iodide-selective (Model OP-I-711) and a bromide-selective (Model OP-Br-711) electrode were used as indicator electrodes, while a Radelkis refill-type (Model OP 811) saturated calomel electrode was used as reference electrode. Before measurements, the indicator electrodes were pretreated by soaking in a 0.1 M potassium nitrate solution at pH 11 for about 6 h. After careful washing of the electrodes with distilled water, they were standardized. Between measurements the electrodes were kept in the pretreating solution, with exclusion of carbon dioxide, but they were stored dry.

The response of the silver halide-based ion-selective electrodes to cyanide ion activity was measured with a Polymetron Poly-Recorder Model 120.2.

Reagents

All chemicals used were of *pro analysi* grade.

The standardizing solutions were made by serial dilution of a 10^{-1} M potassium cyanide stock solution with a 10^{-1} M potassium nitrate solution of pH 11. The pH of the solution was adjusted to 11 with sodium hydroxide. The stock solution was stored in a polythene bottle and renewed weekly, while the standardizing solutions were renewed daily.

For studies of the theoretical behaviour of the silver iodide-based membrane electrodes in cyanide solutions, another series of potassium cyanide solutions was made by dilution of a 2 M potassium cyanide solution with a 2 M sodium hydroxide solution.

Solutions (10^{-2} M) of silver nitrate, copper(II) sulphate, nickel sulphate, zinc sulphate and mercury(II) nitrate were prepared by weight and were standardized by titrations with EDTA solution.

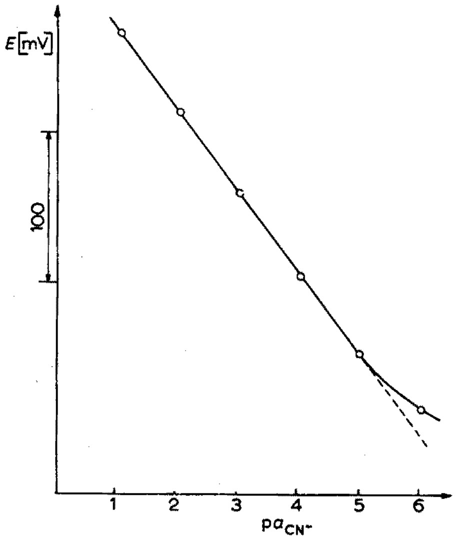

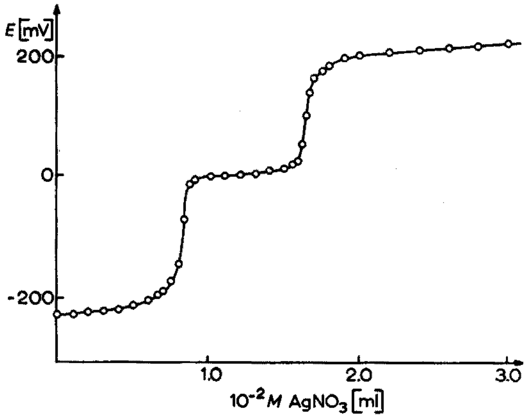

Fig. 1. Calibration curve for determination of cyanide. Silver iodide-based membrane electrode *vs.* S.C.E.

Fig. 2. Potentiometric titration curve of 2 ml of 10^{-2} M cyanide with 10^{-2} M silver nitrate. Silver iodide-based membrane electrode *vs.* S.C.E.

Procedures

Direct method. The direct determination of cyanide was carried out with the help of a calibration curve (Fig. 1), which was prepared by inserting the appropriate silver halide-based electrode and the reference electrode into the standardizing solutions and reading the stable potential values obtained on the pH meter. The millivolt reading measured in an unknown solution of the same pH and ionic strength as that of the standardizing solutions, is converted to sample activity or concentration by means of the calibration curve.

Indirect method (potentiometric titration). Besides direct measurements, the silver halide-based membrane electrodes were used as indicator electrodes in the titrimetric determination of cyanide. The shape of the titration curve obtained when silver nitrate is used as titrant is shown in Fig. 2. There are two inflection points on the titration curve, either of which can be used for the evaluation of the results.

Response time measurement. For studying the response of a silver iodide-based electrode to cyanide activity, the S.C.E. with a potassium nitrate salt bridge was immersed in the appropriate cyanide solution and the potential *vs.* time curve was recorded as soon as the indicator electrode had been inserted into the solution.

RESULTS AND DISCUSSION

Determination of cyanide

All halide ion-selective electrodes respond to cyanide ion activity (Fig. 3), and this was examined from both theoretical and practical points of view. First of all, it was necessary to know whether the silver halide-based cyanide-sensitive electrode can discriminate between cyanide ions and hydrocyanic acid molecules or not. For these measurements, a silver iodide-based membrane electrode and $10^{-2}\ M$ potassium cyanide solutions of various pH values were used. The ionic strength of the solutions was maintained at 0.1 with potassium nitrate. The results are summarized in Fig. 4. In addition to the experimental results, Fig. 4 also shows the theoretical curve which was

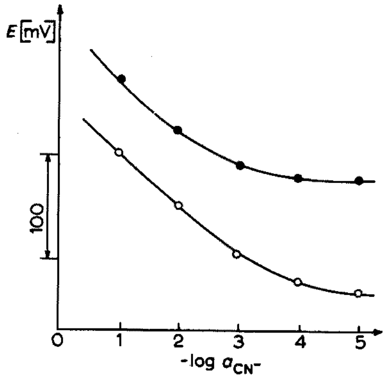

Fig. 3. The behaviour of a silver iodide-based and a silver bromide-based electrode in a solution containing iodide + cyanide, and bromide + cyanide ions, respectively. (●) In the presence of $10^{-3}\ M$ KI$^-$, (○) in the presence of $10^{-4}\ M$ KBr.

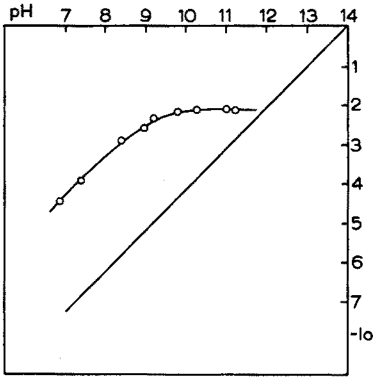

Fig. 4. Effect of pH on $-\log a_{CN^-}$ values. (○) Values measured by a silver iodide-based electrode, (———) theoretical curve calculated from the dissociation constant.

calculated on the basis of the following equation:

$$-\log a_{\mathrm{CN}} = \mathrm{p}K - \log c_{\mathrm{t}} + \log(c_{\mathrm{H}} + K) \tag{1}$$

where K is the dissociation constant of hydrocyanic acid; c_{t} is the total cyanide concentration in the solution *i.e.* $[\mathrm{CN}^-] + [\mathrm{HCN}]$; and c_{H} is the hydrogen ion concentration.

The good agreement between the calculated and measured values demonstrates unambiguously that the silver iodide-based membrane electrodes measure only the cyanide activities in cyanide solutions. It can be concluded from these results that the pH of the cyanide solutions is important in the potentiometric determination of cyanide with halide-based electrodes and that the pH should be kept higher than 11 if the total cyanide content of the sample has to be measured. At the same time, the potentiometric results allow the calculation of the dissociation constant of hydrocyanic acid (pK = 9.21 at 25°).

The cyanide content of a sample can be determined by either the direct or the indirect method.

Potential behaviour

The sensing part of a halide-selective electrode is the silver halide salt, which composes the membrane layer of the electrode. Cyanide ions react with the silver halide salt by complex formation, and halide ions are released[11]:

$$\mathrm{AgX} + 2\mathrm{CN}^- \rightleftharpoons \mathrm{Ag(CN)_2} + 2\mathrm{X}^- \tag{2}$$

Consequently, the cyanide ions determine the potential of any halide-selective electrodes through the halide ions liberated. Thus in a solution containing the appropriate halide and cyanide ions, the halide and cyanide ions together—through the total halide concentration—determine the potential of a silver halide-based electrode according to the following equation, which is deduced by considering the stationary dissolution equilibrium (eqn. (2)):

$$E = E_0' + \frac{RT}{F} \ln\,(a_{\mathrm{X_t}} + K_{\mathrm{CN,X}}\, a_{\mathrm{CN}}{}^2) + d \tag{3}$$

where E_0' is the standard electrode potential; $a_{\mathrm{X_t}}$ is the total halide ion activity on the surface of the electrode; a_{CN} is the cyanide ion activity; $K_{\mathrm{CN,X}}$ is the dissolution constant of the AgX electrode, the value of which was found to be 0.1 for the AgI-based membrane electrode; and d is a constant, which depends on the ionic diffusion.

The total halide activity is composed of two parts: $a_{\mathrm{X}}{}^*$ represents the actual activity of halide ion released by the cyanide from the membrane layer, while a_{X} is the appropriate halide activity in the solution.

Thus

$$a_{\mathrm{X_t}} = a_{\mathrm{X}} + a_{\mathrm{X}}{}^* \tag{4}$$

$$a_{\mathrm{X_t}} = a_{\mathrm{X}} + \tfrac{1}{2}\, a_{\mathrm{CN}} \tag{5}$$

Naturally, if the solution contains only cyanide ions, then eqn. (3) is simplified.

$$E = E_0' + \frac{RT}{F} \ln\,(\tfrac{1}{2}\, a_{\mathrm{CN}} + K_{\mathrm{CN,X}}\, a_{\mathrm{CN}}{}^2) + d \tag{6}$$

Figure 3 shows the behaviour of a bromide-selective and an iodide-selective membrane electrode in solutions containing cyanide and the appropriate halide ions. From this, it follows that all halide ion-selective electrodes can be used for the determination of cyanides. For an iodide-selective electrode, Table I shows a comparison between the potential values measured in a solution containing iodide and cyanide ions (Fig. 3) and the potential values calculated by means of eqn. (3). The agreement between the results proves the validity of eqn. (3).

TABLE I

COMPARISON OF THE CALCULATED AND MEASURED POTENTIAL CHANGES IN SOLUTION CONTAINING CYANIDE AND IODIDE IONS

(Iodide membrane electrode *vs.* S.C.E.)

$[CN^-]$ (M)	$[I^-]$ M	$\Delta E_{meas.}$ (mV)	$\Delta E_{calcd.}$ (mV)
10^{-4}	10^{-3}	51	50
	10^{-4}	19	24
	10^{-5}		

The effect of the dissolution constant on the cyanide determination was studied; relatively high concentrations of cyanide were used, and the pH and total ionic strength were kept constant. The results obtained experimentally and calculated from eqn. (6) are shown in Fig. 5.

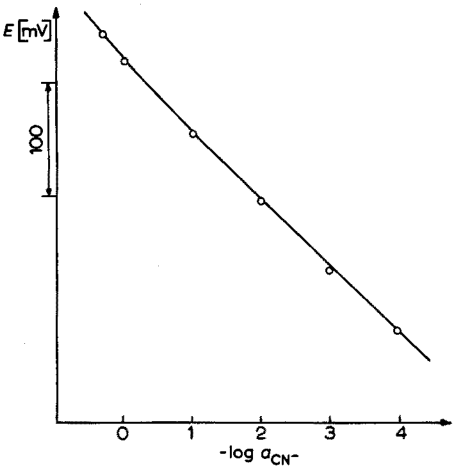

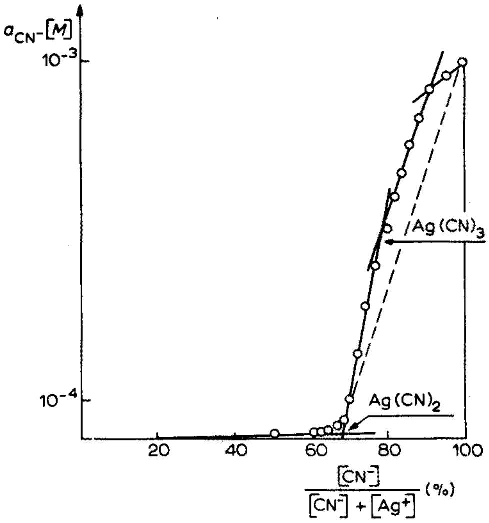

Fig. 5. The behaviour of a silver iodide-based electrode in cyanide solutions of higher concentrations.

Fig. 6. Effect of silver on the activity of cyanide measured.

Selectivity of the silver halide-based cyanide electrodes to other ions

Table II gives a comparison between the selectivity constants of a silver iodide-based iodide-selective electrode, which were measured in the presence of cyanide and iodide ions, respectively. The results show that the selectivity of an iodide electrode to other ions is essentially the same in the presence of iodide as in the presence of cyanide ions. This means that every halide ion-selective electrode keeps its original selectivity to other ions in the presence of cyanide ions, also. Consequently, the silver iodide-based electrode is suggested for the determination of the cyanide because of its high selectivity for iodide and cyanide ions in the presence of other ions.

TABLE II

SELECTIVITY CONSTANTS OF A SILVER IODIDE-BASED MEMBRANE ELECTRODE TO VARIOUS ANIONS

Ion	*Selectivity constants in the presence of*	
	CN^-	*I^-*
Cl^-	10^{-5}–10^{-6}	10^{-6}
Br^-	10^{-3}–10^{-4}	10^{-4}
I^-	1	
CN^-		1
NH_4^+	10^{-5}–10^{-6}	10^{-6}
SO_4^{2-}	10^{-5}–10^{-6}	10^{-6}

Effect of metal ions

The direct measurement of cyanide contents is especially important for determining cyanide in trade effluents, which often contain, besides cyanide, metal ions which can form complexes with the cyanide. This gave rise to the question of how the metal cyanide complexes influence the response of the silver halide-based electrode to cyanide ions. A systematic study of these complexes was carried out to examine the behaviour of the cyanide-sensitive electrodes in solutions containing various metal complexes. The nickel, mercury, copper, silver, cadmium and zinc cyanide complexes were investigated. The study was carried out at a pH 11, at which hydroxo complexes of metals are also formed. However, the problem has been considered only from the point of view of the determination of cyanides. The detailed chemical study of these complexes was outside the scope of the present work.

The results are presented as graphs in which the cyanide activity measured by a silver iodide-based electrode is plotted against the mole fraction of the cyanide ions in solutions containing both cyanide and metal ions being examined. The results for silver are shown in Fig. 6, which has two breaks in the curve corresponding to complexes of composition $Ag(CN)_3$ and $Ag(CN)_2$, respectively. The differing slopes of the curve show that the latter complex influences the measurement of cyanide. The curve also shows that the electrode does not respond to cyanide bound in $Ag(CN)_2$ or silver complexes of lower coordination number.

Figures 7–9 show the behaviour of the silver iodide-based electrode in the presence of mercury, copper and nickel, respectively. It can be concluded that in these complexes the cyanide is tightly bound, so that a high concentration of free cyanide is not available in the solution. The β values of the appropriate complexes, which were found to have no effect on the silver iodide-based electrode, are all greater than the β_2 value of $Ag(CN)_2$.

In the literature only a few cyanide complexes have been reported, the stability constants of which are lower than that of the $Ag(CN)_2$ complex. In the book on *Stability Constants* by SILLÉN AND MARTELL[16], only two complexes were found to have lower

β values than $Ag(CN)_2$. These were the cadmium and zinc complexes, the β_4 values of which differed by 3 and 4 orders of magnitude from that of the $Ag(CN)_2$ complex. These complexes were found to have less influence on the measured cyanide concentration than the other complexes discussed above. The results are shown in Figs. 10 and 11, from which it can be seen that even when the concentration of the metal was

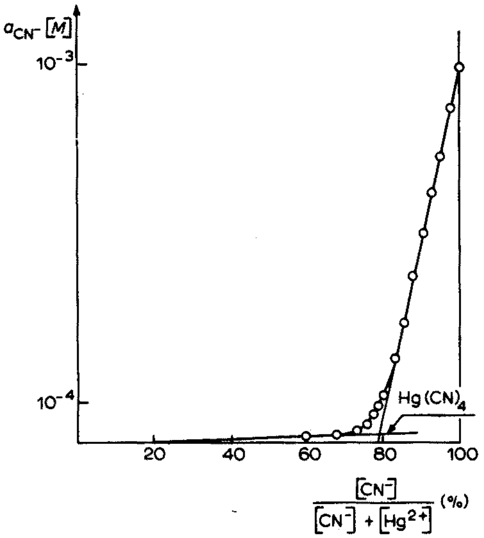

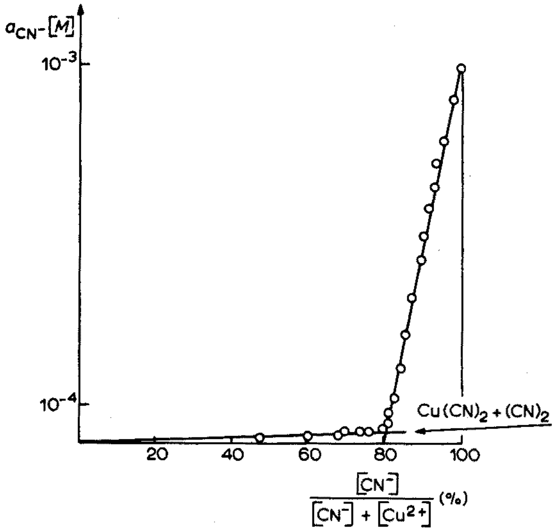

Fig. 7. Effect of mercury(II) on the activity of cyanide measured.

Fig. 8. Effect of copper(II) on the activity of cyanide measured.

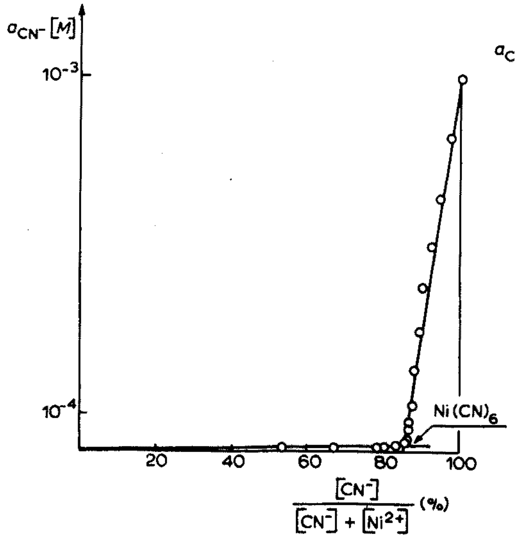

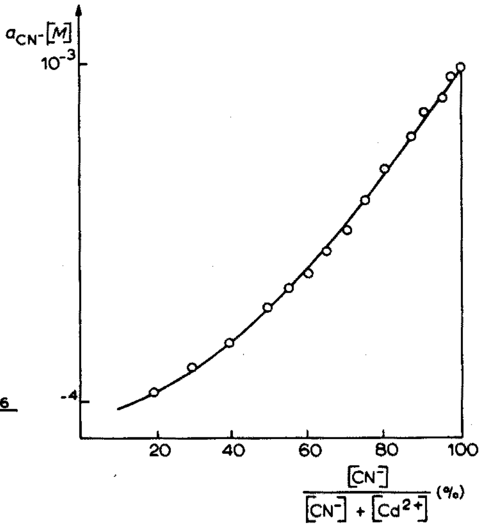

Fig. 9. Effect of nickel on the activity of cyanide measured.

Fig. 10. Effect of cadmium on the activity of cyanide measured.

in great excess, the measured cyanide activity decreased only to a small extent. This can be interpreted by assuming that these complexes can participate in the exchange reaction in the membrane layer analogously to free cyanide. This may be of importance for the application of the membrane electrodes to complex chemistry.

The assumption that cyanide complexes of lower stability than silver dicyanide are also sensed by a silver iodide-based membrane electrode was proved by measuring the slope of the cadmium tetracyanide complex at different dilutions, but at constant ionic strength. Figure 12 shows that the slope of the calibration curve of the cadmium tetracyanide complex is initially the same as that of the cyanide ions; the potential measured is lower than that corresponding to the total cyanide content of the cadmium tetracyanide complex, which means that all the cyanide bound in the complex cannot take part in the electrode reaction.

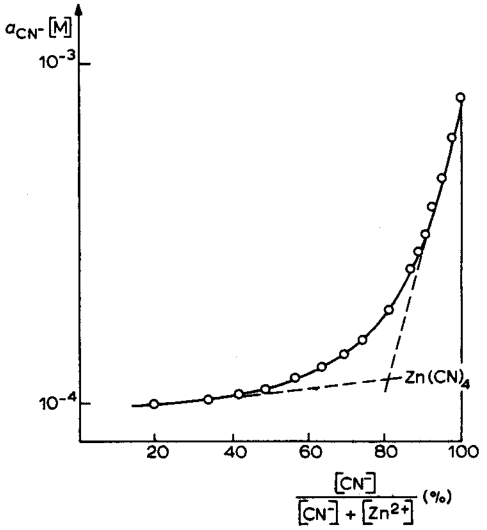

Fig. 11. Effect of zinc on the activity of cyanide measured. (---) Curve expected for formation of Zn(CN)$_4$ if the electrode is not influenced by the complex.

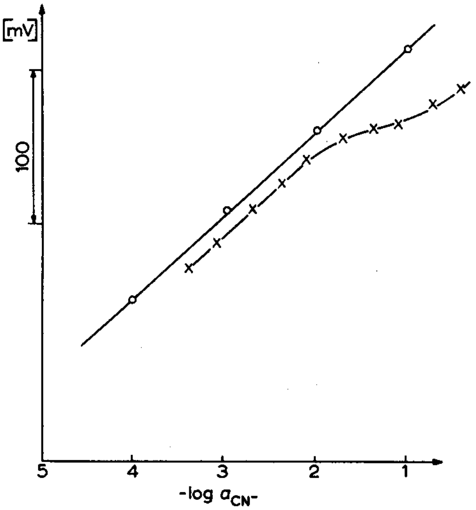

Fig. 12. The behaviour of a silver iodide-based electrode in diluted Cd(CN)$_4$ solutions. (×) Values measured in Cd(CN)$_4$ solutions, (o) values measured in KCN solutions.

To summarize the experimental results, it can be stated that all free cyanide and a part of the cyanide complexes of lower β values than the silver dicyanide complex can be measured by a halide-based cyanide-sensitive electrode.

Elimination of cyanides with hypochlorite

The potential of the cyanide electrode can be used as a signal in automatic process control for the elimination of cyanides with hypochlorite. However, the stronger metal cyanide complexes, which are not measured by the electrode, produce an error in such control. This can be overcome by setting a potential which is much lower than the potential measured under the same conditions in a 10^{-6} or 10^{-7} *M* cyanide solution. Thus, if the potential which is due to the cyanide concentration produced by the dissociation of metal cyanide complexes is higher in the system than the potential used for the process control, the metal cyanide complexes will also be eliminated.

Response time

With stirring, the response of a silver iodide-based cyanide-sensitive electrode reaches equilibrium within 5–20 sec; even in very dilute solutions, the response time does not exceed 1 min. Response is more rapid when going from dilute to concentrated solutions than in the other direction.

Reproducibility

The reproducibility of the results determined by the direct method with a silver iodide-based electrode is within ±0.05 pa_{CN} (pa_{CN} = $-\log a_{CN^-}$) in the range of 10^{-1}–10^{-5} *M* potassium cyanide (Table III).

TABLE III

REPRODUCIBILITY OF THE RESULTS MEASURED WITH A SILVER IODIDE-BASED ELECTRODE

CN⁻ (M)	E_{mean} *(mV)*	*Reproducibility* pa_{CN}
10^{-1}	357	± 0.02
10^{-2}	300	± 0.04
10^{-3}	242	± 0.02
10^{-4}	187	± 0.02
10^{-5}	130	± 0.05
10^{-6}	100	± 0.4

The authors thank ERIKA SCHMIDT for her valuable experimental assistance.

SUMMARY

The direct and indirect determination of cyanides can be carried out with a silver iodide-based ion-selective electrode. The electrode measures only cyanide ions and does not respond to hydrocyanic acid. A detailed study of metal–cyanide complexes shows that the cadmium and zinc cyanide complexes can participate in the exchange reaction on the membrane surface, but that metal cyanide complexes of higher stability than silver dicyanide have no effect on the electrode. The cyanide-sensitive electrodes can be employed for continuously recording the cyanide content of effluents.

RÉSUMÉ

Le dosage direct et indirect des cyanures peut s'effectuer à l'aide d'une électrode ionique-sélective à l'iodure d'argent. Une telle électrode ne mesure que les ions cyanures et non l'acide cyanhydrique. Une étude détaillée montre que les complexes cyanurés de cadmium et de zinc peuvent participer à la réaction d'échange à la surface de la membrane; cependant, les complexes métalliques plus stables que le dicyanure d'argent n'ont pas d'influence sur l'électrode. On peut utiliser ces électrodes pour l'enregistrement en continu de la teneur en cyanure des caux résiduaires.

ZUSAMMENFASSUNG

Die direkte und indirekte Bestimmung von Cyaniden kann mit einer ionenselektiven Silberjodidelektrode durchgeführt werden. Die Elektrode misst nur Cyanidionen und spricht nicht auf Cyanwasserstoffsäure an. Eine genaue Untersuchung von Metallcyanid-Komplexen zeigt, dass die Cadmium- und Zink-Cyanid-Komplexe an der Austauschreaktion auf der Membranoberfläche teilnehmen können, dass jedoch Metall-Cyanid-Komplexe von grösserer Stabilität als Silberdicyanid keinen Einfluss auf die Elektrode haben. Die cyanidempfindliche Elektrode kann für die kontinuierliche Aufzeichnung des Cyanidgehalts von Abwässern benutzt werden.

REFERENCES

1 E. Raub and H. Wiegand, *Metalloberflaeche*, 19 (1965) 273.
2 E. Bishop and R. G. Dhaneshwar, *Analyst*, 88 (1963) 433.
3 L. Gerchman and G. A. Rechnitz, *Z. Anal. Chem.*, 230 (1967) 265.
4 G. Mattock and R. Uncles, *Analyst*, 87 (1962) 977.
5 R. Geyer, K. Chojnacki and C. Stief, *Z. Anal. Chem.*, 200 (1964) 326.
6 J. E. McClure and G. A. Rechnitz, *Anal. Chem.*, 38 (1966) 136.
7 E. Pungor and E. Hollós-Rokosinyi, *Acta Chim. Acad. Sci. Hung.*, 27 (1961) 63.
8 E. Pungor and K. Tóth, *Mikrochim. Acta*, (1964) 565.
9 M. S. Frant and J. W. Ross, *Science*, 154 (1966) 1553.
10 J. Havas, K. Tóth, I. Szabó and E. Pungor, *Proc. Analytical Chemical Conference, Budapest, 1966*, p. 159.
11 *Instruction Manual on Cyanide Ion Activity Electrode (Model 94-06)*, Orion Research Incorporated, 11, Blackstone Str., Cambridge, Mass., U.S.A.
12 E. Pungor, *Anal. Chem.*, 39 (13) (1967) 28A.
13 E. Pungor and K. Tóth, *Anal. Chim. Acta*, 47 (1969) 291.
14 R. P. Buck, *Anal. Chem.*, 40 (1968) 1432.
15 R. P. Buck, *Anal. Chem.*, 40 (1968) 1439.
16 L. G. Sillén and A. E. Martell, *Stability Constants*, The Chemical Society, London, 1964.

Analytica Chimica Acta
Elsevier Publishing Company, Amsterdam
Printed in The Netherlands

PREPARATION AND SOME ANALYTICAL APPLICATIONS OF A NEW SULFIDE-SELECTIVE HETEROGENEOUS MEMBRANE ELECTRODE

MARCO MASCINI AND ARNALDO LIBERTI
Istituto di Chimica Analitica, Università di Roma, Roma (Italy)

(Received February 3rd, 1970)

Sulfide ion membrane electrodes have been described by PUNGOR[1] and by FRANT AND ROSS[2]. The membrane made by PUNGOR is obtained by incorporating silver sulfide into a silicone rubber matrix, whereas in the Orion electrode a homogeneous polycrystalline silver sulfide membrane is used; both electrodes are selective to sulfide and to silver ions. The electrochemical behaviour of the Orion electrode has been thoroughly investigated[3-4].

This paper deals with the preparation of a new type of heterogeneous silver sulfide membrane electrode, which is selective to sulfide and to silver ions. The evaluation and application of this electrode is discussed.

EXPERIMENTAL

Preparation of membrane electrode

The procedure used was similar to that previously described for silver halide electrodes[5]; it consisted of the moulding of a mixture of silver sulfide and thermoplastic polymer at a suitable temperature. The thermoplastic polymer used was polythene but successful results can also be obtained with methacrylic esters.

The silver sulfide was precipitated in three different ways: (*a*) by mixing a silver sulfide solution with an excess of silver nitrate, (*b*) by mixing a silver nitrate solution with an excess of sulfide, and (*c*) by bubbling hydrogen sulfide into a solution, which was 0.1 M in silver nitrate, and $10^{-2} M$ in perchloric acid.

Electrodes prepared from membranes which contained silver sulfide precipitated by these methods behaved in the same way towards $[Ag^+]$ but exhibited different behaviours towards $[S^{2-}]$.

The membranes, which were 1–2 mm thick and 12 mm in diameter, were thermosealed in a suitable mould to a rigid polythene tube[6]; this procedure made it possible to obtain electrodes with good mechanical properties and chemical durability as neither adhesive nor sealing of any material is used. The internal solution was 10^{-3} M silver nitrate; a silver wire, which dipped into it, was thermosealed to the polythene tubing.

Method of measurement

Potentiometric measurements were carried out in the conventional manner by using the sulfide electrode and a saturated calomel electrode (Beckman 39170) as a reference electrode with a Beckman Research pH meter 1019. The reference electrode was separated from the tested solution by a 1 *M* sodium nitrate liquid bridge.

RESULTS AND DISCUSSION

A set of 20 electrodes was tested. All the electrodes yielded reproducible results, the behaviour of any single electrode deviating from the average value by not more than 5–6 mV.

Response of electrode to silver ion activity

To evaluate the response of the sulfide electrode towards change in silver ion activity, the following cell was used:

$$\text{S.C.E.}|1\ M\ \text{NaNO}_3|\text{Ag}^+\ \mu=1\ (\text{NaNO}_3)|\text{Ag}_2\text{S electrode}$$

The e.m.f. at 25° is given by:

$$E=E^0+0.059\log[\text{Ag}^+]$$

where the E^0 term includes the potentials of the internal electrode, the reference electrode, and the liquid junction, and the activity coefficient for silver(I). The plot of the e.m.f. *versus* $\log[\text{Ag}^+]$ is shown in Fig. 1: the slope is 59 mV per decade change in concentration. Extrapolation to $[\text{Ag}^+]=1$ gives 553 mV, which is in good agreement

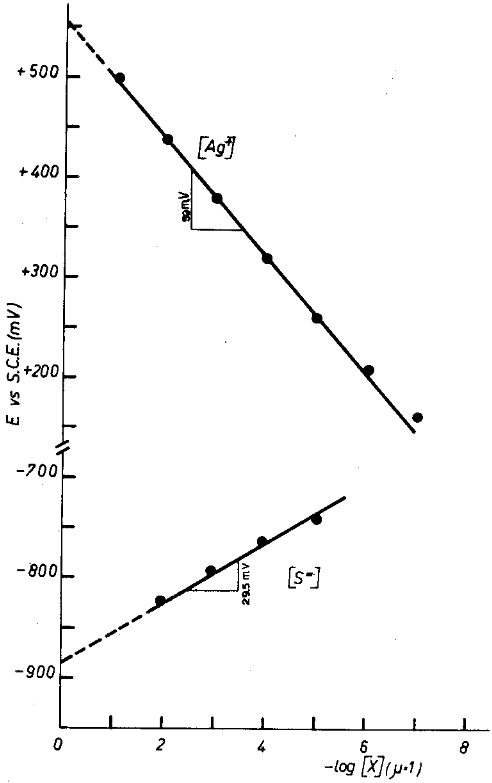

Fig. 1. Response of a silver sulfide membrane electrode at ionic strength 1 *M versus* $-\log[\text{Ag}^+]$ or $-\log[\text{S}^{2-}]$.

with the e.m.f. of a cell consisting of a standard silver and a saturated calomel electrode.

Response of electrode to sulfide ion activity

To study the electrode response to sulfide ion, the test solution in the above cell was prepared at various sulfide concentrations. These were obtained by adding a 0.1 *M* sodium sulfide solution in 0.1 or 1 *M* sodium hydroxide to 50 ml of 0.1 or 1.0 *M* sodium hydroxide under a stream of nitrogen in a closed vessel. The high and constant hydroxide concentration provides a constant fraction of the total sulfide concentration; the $[S^{2-}]$ can be calculated by means of the following expression:

$$[S^{2-}] = \frac{[S^{2-}]_T}{1+[H^+]/K_2}$$

where $K_2 = 10^{-14.2}$ (calculated at 0.1 *M* ionic strength) and $[S^{2-}]_T$ is the total concentration of sulfide present $[S^{2-}]_T = [S^{2-}] + [HS^-]$.

The membrane electrodes which contained silver sulfide prepared by procedures (*b*) and (*c*), *i.e.* with excess of sulfide, displayed an electrode response which was rapid and stable with time. The plot of e.m.f. *versus* $-\log [S^{2-}]$ at 0.1 *M* sodium hydroxide is shown in Fig. 1; the slope is 29.5 mV per decade change in concentration.

The potential intercept obtained by extrapolating to $[S^{2-}] = 1$, gives a value from which it is possible to calculate the solubility product of silver sulfide, as the intercept potential is:

$$E_{\mathrm{int}} = E^0_{\mathrm{Ag}} + \frac{0.059}{2} \log K_{\mathrm{Sp}}$$

A value of 10^{-49} was obtained. The solubility product calculated from the results obtained with the Orion polycrystalline silver sulfide membrane[3] is $1.5 \cdot 10^{-51}$ whereas a value of $6.2 \cdot 10^{-52}$ has been reported from e.m.f. measurement[7] and a value of $7 \cdot 10^{-50}$ has been calculated from free energy data[8].

The membrane electrodes which contained silver sulfide prepared by adding an excess of silver nitrate to a sodium sulfide solution, were sluggish in response and yielded potential values higher than the electrodes prepared with the other precipitates. This erratic behaviour can probably be attributed to the nature of the precipitate which is contaminated by silver oxide. This procedure for the preparation of silver sulfide is not recommended and these electrodes have been disregarded.

Electrode selectivity

The effect of various anions on the response of the silver sulfide membrane electrode was determined by the e.m.f. value of the cell with the indicator electrode placed in a 0.1 *M* solution of the tested anion and of the same cell when the electrode was dipped into a solution where $[S^{2-}] = (0.1)^{2n}$ (where n is the valence of the interfering ion). With the aid of the Nernst equation as modified by GARRELS *et al.*[9], the selectivity constants $K_{S\text{-}X}$ were found to be about 10^{-8}–10^{-10} for the more common anions such as Cl^-, Br^-, I^-, CN^- and $S_2O_3^{2-}$.

In a similar way, the selectivity for some cations was calculated from the results obtained when the electrode response was measured in a solution which was 0.1*M* in the interfering cation and in a solution where $[Ag^+] = (0.1)^{1/n}$: a low value (10^{-5}–

10^{-6}) was obtained for various cations (Na^+, K^+, Ca^{2+}, Mg^{2+}, Pb^{2+}, Cu^{2+}, etc.). Only mercury(II) interfered: $K_{Ag^+-Hg^{2+}} = 0.01$. The selectivity constants for this electrode have the same order of magnitude as those for the Orion homogeneous membrane electrode.

The behaviour of the electrode was studied in mixed solvents made of water–ethanol and water–acetone containing up to 80% of the organic solvent. The slope of the curve E–pAg was found to be about 60 mV per decade change in concentration in all cases.

APPLICATIONS

A sulfide electrode can be used as a specific indicator in any reaction where the sulfide concentration should be determined. It can therefore be used in potentiometric titrations in aqueous and in mixed solvents. As an example, the potentiometric titration of a natural water containing sulfide and chloride with silver nitrate is shown (Fig. 2). Since the electrode acts as an indicator for both sulfide and silver ions, two breaks are observed; the former is due to the less soluble silver sulfide and the latter to the formation of silver chloride. As the concentration of sulfide in natural waters is usually much smaller than that of chloride, after the first break obtained by titration with 10^{-3} M silver nitrate, the titration should be completed with a more concentrated solution *e.g.* 10^{-2} M silver nitrate.

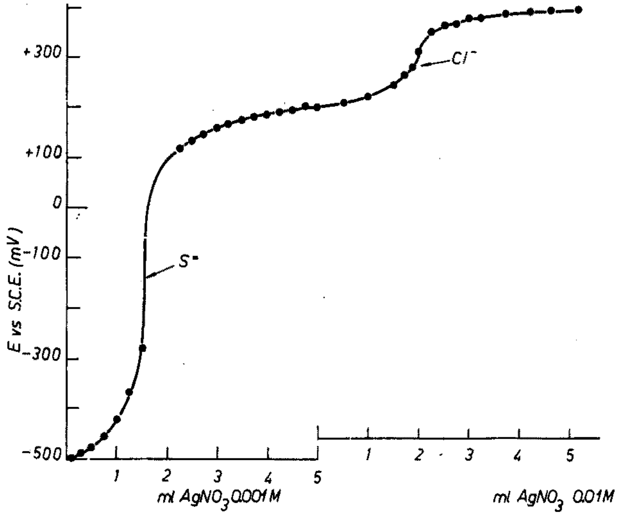

Fig. 2. Potentiometric titration of a natural water containing sulfide and chloride ions. Titration carried out with standard 10^{-3} M $AgNO_3$; after the first equivalence point a 10^{-2} M $AgNO_3$ solution was used.

A useful application is found in the study of hydrolytic reactions where sulfide ions are produced. The hydrolysis of thioacetamide carried out at room temperature was followed with this electrode. Two sets of measurements were made, at a constant thioacetamide concentration of 0.02 M by varying the hydroxide concentration, and at a constant 0.01 M hydroxide concentration by changing the thioacetamide concentration. The experimental arrangement was simply realized by connecting the in-

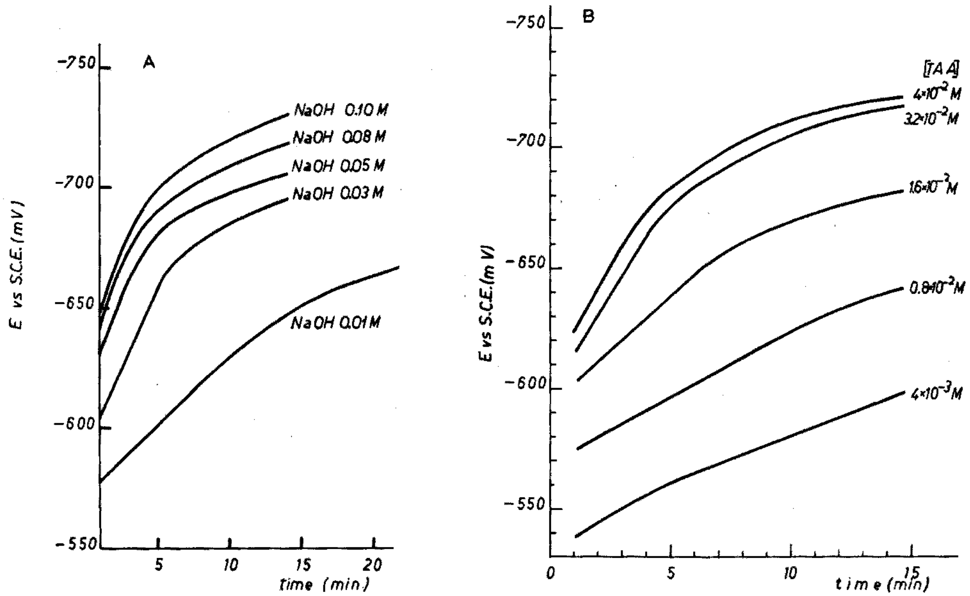

Fig. 3. Hydrolysis of thioacetamide measured with a silver sulfide membrane electrode and a saturated calomel electrode. (A) Thioacetamide = 0.02 M; (B) NaOH = 0.01 M.

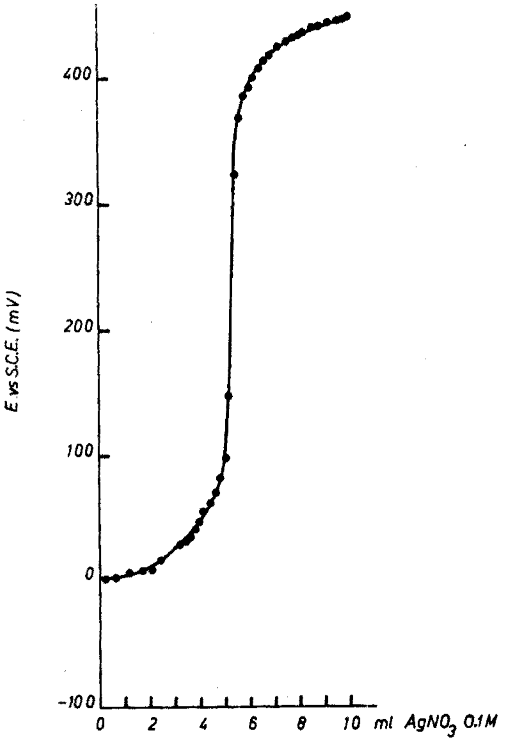

Fig. 4. Potentiometric titration of about 80 mg of mercaptobenzothiazole dissolved in aqueous 80% acetone with 0.1 M $AgNO_3$ and a silver sulfide membrane electrode.

dicator and the reference electrodes to a recorder by means of an impedance adaptor device (Fig. 3A and B). The experimental results can be described by the following equations:

at [OH⁻] = constant: $E = E' - K' \log[\text{TAA}]$ where $K' = 3.5$
at [TAA] = constant: $E = E'' - K'' \log[\text{OH}^-]$ where $K'' = 2.5$

An interesting feature of this electrode is that no adhesive or heterogeneous connections are necessary in its preparation. Since the body of the electrode is made of polythene, it can be used extensively in all solvents which do not affect this material. As an example, the potentiometric titration of mercaptobenzothiazole with silver nitrate was carried out in aqueous 80% acetone, with the sulfide indicator electrode and a saturated calomel electrode connected through a potassium nitrate liquid bridge (Fig. 4).

The general results indicate that the polymeric material used to prepare the heterogeneous membrane of this electrode does not affect the electrode potential as the plots of potential *vs.* logarithmic concentration for both anion and cation follow the Nerst law. The reproducibility of the potential of these electrodes made from the silver sulfide–polythene membranes in different preparations appears to exclude any effect from the polymeric material. On the other hand, the purity of the silver sulfide strongly affects the selectivity of the electrode. If the precipitate is contaminated by silver oxide, the electrode is less selective; it is very sluggish and there is no linear relationship between electrode response and log $[S^{2-}]$.

SUMMARY

A new sulfide-selective heterogeneous membrane electrode has been developed by thermomoulding a mixture of silver sulfide and a thermoplastic polymer such as polythene. The membrane is attached to a rigid polythene tubing by suitable treatment without any adhesive. The electrodes show a rapid and stable response and follow the Nernst equation for both silver and sulfide ions. Some applications of these electrodes are discussed.

RÉSUMÉ

Une nouvelle électrode, sulfure, à membrane est préparé par thermomoulage d'un mélange de sulfure d'argent et d'un polymère thermoplastique, tel que le polythène. La membrane est fixée à un tube rigide de polythène par un traitement approprié, sans aucun adhésif. L'électrode présente une réponse rapide et stable; elle obéit à l'équation de Nernst soit pour l'argent, soit pour les ions sulfures. On examine quelques applications de ces électrodes.

ZUSAMMENFASSUNG

Es wurde eine neue sulfidselektive heterogene Membranelektrode entwickelt. Sie besteht aus einer bei geeigneter Temperatur geformten Mischung von Silbersulfid und einem thermoplastischen Kunststoff wie Polythene. Die Membran wird ohne Klebmittel in geeigneter Weise mit einem stabilen Polythene-Rohr verbunden. Die

Elektroden sprechen schnell und zeitlich beständig an und folgen der Nernstschen Gleichung sowohl für Silber- als auch Sulfid-Ionen. Einige Anwendungen dieser Elektroden werden diskutiert.

REFERENCES

1 E. Pungor, *Anal. Chem.*, 39 (13) 1967) 28 A.
2 *Instruction Manual, Sulfide ion electrode, model 94-16*, Orion Research, Inc., 11 Blackstone Street, Cambridge, Mass., 1967.
3 Tong-Ming Hseu and G. A. Rechnitz, *Anal. Chem.*, 40 (1968) 1054.
4 T. S. Light and J. L. Swartz, *Anal. Lttrs.*, 1 (13) (1968) 825.
5 M. Mascini and A. Liberti, *Anal. Chim. Acta*, 47 (1969) 339.
6 M. Mascini and A. Liberti, patent pending.
7 J. R. Coates, A. G. Cole, E. L. Gray and N. D. Faux, *J. Am. Chem. Soc.*, 73 (1951) 707.
8 J. R. Coates, M. B. Gordon and N. D. Faux, *J. Am. Chem. Soc.*, 74 (1952) 835.
9 R. M. Garrels, M. Sato, M. E. Thompson and A. H. Truesdell, *Science*, 135 (1962) 1045.

Analytica Chimica Acta
Elsevier Publishing Company, Amsterdam
Printed in The Netherlands

APPLICATIONS ANALYTIQUES DE L'ELECTRODE-METAL COMPLEXE ARGENT-IMIDAZOLE

G. BERTHON ET C. LUCA

Laboratoire de Thermodynamique Chimique et Electrochimie, Faculté des Sciences, Université de Poitiers, 40, Avenue du Recteur Pineau, 86-Poitiers (France)

(Reçu le 2 mars, 1970)

L'étude de la stabilité des complexes formés en solution à partir d'un ion métallique M* et d'un coordinat A, dont l'équilibre peut être décrit[1] par la loi d'action de masse

$$[MA_n]=\beta_n[M]\,[A]^n=k_n\,[MA_{n-1}]\,[A] \qquad (1)$$

(où [A] représente la concentration de coordinat à l'équilibre;
[M] celle de l'ion métallique à l'équilibre;
$[MA_n]$ celle du complexe d'ordre n en solution;
$[MA_{n-1}]$ celle du complexe d'ordre inférieur;
n le nombre de coordinats du composé MA_n;
β_n la constante globale de stabilité du complexe d'ordre n rapporté à ses constituants initiaux A et M;
k_n la constante étagée de stabilité de ce même complexe, rapportée au complexe d'ordre inférieur, ces différentes constantes étant définies dans un milieu de force ionique prépondérante[2])
est généralement accessible expérimentalement par la mesure de la concentration [A] et par la connaissance d'une grandeur physique reliant directement [A] aux constantes β_n ou k_n, que l'on cherche à déterminer[2,3].

La méthode utilisée dans le présent mémoire fait intervenir des mesures statopotentiométriques, au moyen de l'électrode métal–complexe[4] Ag/Ag^+–imidazole, dont nous discuterons tout d'abord les équilibres électrochimiques.

Ayant dès lors mis en évidence la possibilité d'utiliser cette électrode pour doser le coordinat considéré, nous établirons, par concurrence avec un tel intermédiaire, les constantes des équilibres de complexation de l'ion cadmium(II) avec l'imidazole.

PARTIE THÉORIQUE

Considérons l'équilibre électrochimique d'un métal M^0 avec une solution contenant des ions M de ce métal et un coordinat A, c'est à dire l'électrode:

$M^0/M,A$

dont le potentiel peut être exprimé par la relation de Nernst:

$$E=E_{M^0}+(RT/zF)\ln[M] \qquad (2)$$

La concentration en ion métallique libre étant reliée à celle du coordinat par

---

* Pour alléger l'écriture, nous n'affecterons pas l'ion M de sa charge $z+$ que nous utiliserons ensuite pour celui-ci dans les équations de Nernst.

la relation (1), il est possible, en considérant pour celle-ci la réaction globale de complexation, d'écrire l'équation (2) sous la forme:

$$E = E_M{}^0 + (RT/zF) \ln \frac{[MA_{\bar{n}}]}{\beta_{\bar{n}}\,[A]^{\bar{n}}} \tag{3}$$

où $\bar{n}$ represente le nombre moyen de coordination.

Lorsque la concentration initiale d'ions métalliques est négligeable par rapport à celle du coordinat, tous ces ions peuvent être considérés comme transformés en complexes; de plus, la concentration [A] du coordinat à l'équilibre est pratiquement équivalente à C_A, la concentration totale de coordinat.

L'équation (3) s'écrit dans ces conditions:

$$E = E_M{}^0 + (RT/zF)\ln\,[MA_{\bar{n}}] - (RT/zF)\ln\,\beta_{\bar{n}} - (\bar{n}RT/zF)\ln\,C_A \tag{4}$$

ou encore

$$E = E^0_{MA\bar{n}} - (\bar{n}RT/zF)\ln C_A \tag{5}$$

la concentration du complexe et la constante $\beta_{\bar{n}}$ entrant dans le terme constant.

L'électrode métallique devient alors réversible par rapport au coordinat, ce qu' évoque la dénomination "électrode métal–complexes"[4], correspondant au schéma général

$$M^0/[MA], [MA_2], \ldots, [MA_N], [A]$$

Si N complexes coexistent en solution (N représente le nombre de coordination maximum), la concentration totale des ions M peut s'exprimer par la relation:

$$C_M = [M] + \sum_1^N [MA_n] \tag{6}$$

soit

$$C_M = [M] + \sum_1^N \beta_n\,[M]\,[A]^n \tag{7}$$

et, après réarrangement des termes, si C_M est toujours négligeable par rapport à C_A,

$$\frac{C_M}{[M]} = 1 + \sum_1^N \beta_n\,[A]^n = \sum_0^N \beta_n\,[A]^n = \sum_0^N \beta_n\,C_A{}^n \tag{8}$$

Le rapport $C_M/[M]$ peut être mesuré en partant d'une cellule de concentration du type

$$M^0|M,A|\,|M|M^0$$

pour laquelle on peut écrire

$$\varepsilon = E - E' = (RT/zF)\ln \frac{C_M}{[M]} \tag{9}$$

si la concentration C_M est la même dans les deux demi-cellules.

Des relations (8) et (9), on tire l'expression

$$\psi\,(C_A) = \exp \frac{E - E'}{RT/zF} = \sum_0^N \beta_n\,C_A{}^n \tag{10}$$

soit $E = E' + (RT/zF)\ln\,(\beta_0 + \beta_1\,C_A + \beta_2\,C_A{}^2 + \ldots + \beta_N\,C_A{}^N)$ (11)

L'électrode étant réversible par rapport au coordinat, l'expression (11) peut être utilisée pour déterminer sa concentration en solution[5,6].

Cette détermination est, a priori, subordonnée à la connaissance préalable du potentiel E' et des constantes de stabilité β_n. Elle peut cependant être effectuée par une méthode graphique[4] qui n'implique pas la connaissance préalable des constantes β_n.

Lorsque la concentration C_M n'est pas pratiquement négligeable par rapport à C_A, il demeure possible d'accéder à [A] au moyen d'une suite d'approximations successives basées sur la définition, selon BJERRUM[1] de l'indice de coordination moyen

$$\bar{n} = \frac{\sum_{0}^{N} n\,\beta_n\,[A]^n}{\sum_{0}^{N} \beta_n\,[A]^n} \tag{12}$$

et, à tour de rôle les valeurs affinées

$$\begin{cases} [A] = C_A - \bar{n}.C_M & (13) \\ \psi\,([A]) = \sum_{0}^{N} \beta_n\,[A]^n & (14) \end{cases}$$

jusqu'à convergence effective.

ÉTUDE DU SYSTÈME Ag^+–IMIDAZOLE

Détermination des constantes β_n

L'étude des équilibres successifs entre l'ion Ag^+ et l'imidazole définissant l'électrode métal–complexe

$$Ag/[Ag\,(imid)_n]^+,\ imid \tag{15}$$

a été effectuée en milieu nitrate de potassium pris à la force ionique prépondérante $\mu = 0.5$ et à la température constante de $25 \pm 0.1°$ au moyen des cellules

$$\underset{}{Ag}|\underset{(C_0)}{Ag^+},\ \underset{(0.5\,M)}{KNO_3}\ ||\ \underset{(sat)}{KNO_3}\ ||\ \underset{(sat)}{KCl}\ |\ Hg_2Cl_2\text{–}Hg \tag{16}$$

$$Ag\ |\ \underset{(C \sim C_0)}{[Ag\,(imid)_n]^+},\ \underset{(C_1)}{imid},\ \underset{(0.5\,M)}{KNO_3}\ ||\ \underset{(sat)}{KNO_3}\ ||\ \underset{(sat)}{KCl}|Hg_2Cl_2\text{–}Hg \tag{17}$$

La molarité initiale C_0 de l'ion Ag^+ est identique dans ces deux cellules: la molarité globale C_1 du coordinat est en excès par rapport à C_0 et la molarité C de l'ensemble des complexes formés est ainsi sensiblement égale à C_0.

Nous avons ainsi calculé par la méthode de LEDEN[7] les constantes de stabilité des complexes formés par l'imidazole avec l'argent dans le milieu considéré, grâce à deux séries de cellules (16) et (17) contenant des rapports de concentration différents entre métal et coordinat.

Pour la première série de mesures, la molarité initiale d'argent C_0 était égale à $4 \cdot 10^{-6}\,M$ dans les cellules (16) et (17).

TABLEAU I

FONCTIONS DE LEDEN DU SYSTÈME Ag^+–IMIDAZOLE

$C_{imid} \cdot 10^4$ (M)	ε (mV)	ψ(imid)	ψ_1(imid)	ψ_2(imid) $\cdot 10^{-6}$	$C_{imid} \cdot 10^4$ (M)	ε (mV)	ψ(imid)	ψ_1(imid)	ψ_2(imid) $\cdot 10^{-6}$
0	0	1	500	7.64	12.281	66.15	13.127	9875.4	7.63
1.961	9.40	1.4417	2252.4	—	13.793	71.55	16.197	11017.9	7.62
3.846	22.20	2.3727	3569.1	—	15.254	76.40	19.562	12168.6	7.65
5.660	34.10	3.7705	4894.8	—	16.666	80.60	23.036	13222.1	7.63
7.407	44.20	5.5863	6191.8	7.68	18.032	84.50	26.812	14314.5	7.66
9.091	52.70	7.7768	7454.4	7.65	19.354	87.80	30.487	15235.6	7.61
10.714	59.90	10.292	8672.7	7.63	20.634	91.35	35.003	16479.1	7.74

Le Tableau I consigne les molarités C_1 du coordinat, les différences de tensions ε existant entre les cellules (17) et (16) exprimées par la relation (9), et les valeurs correspondantes des fonctions ψ(imid), ψ_1(imid), ψ_2(imid).

La méthode de LEDEN[7] conduit ainsi aux valeurs numériques des constantes, exprimées par leurs logarithmes:

$$\log \beta_1 = 2.70 \qquad \log \beta_2 = 6.88$$

Les mêmes mesures traitées numériquement de manière différente, par une des méthodes d'élimination mises au point par SILLÉN[8] (Fig. 1) permettent de vérifier exactement les constantes obtenues au moyen de la méthode précédente, puique l'on trouve alors à nouveau les mêmes valeurs.

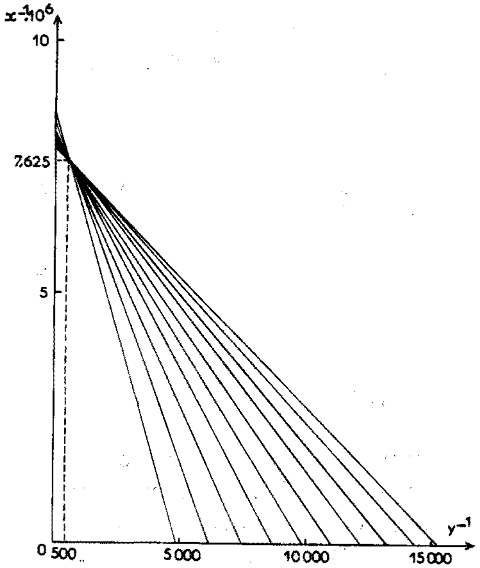

Fig. 1. Calcul des constantes β_1 et β_2 du système Ag^+–imidazole par la méthode de SILLÉN.

Pour la deuxième série de mesures, la molarité initiale d'argent C_0 était égale à $1 \cdot 10^{-5}$ M. La méthode de LEDEN nous a permis (Fig. 2) d'obtenir dans ce cas $\log \beta_2 =$ 6.89.

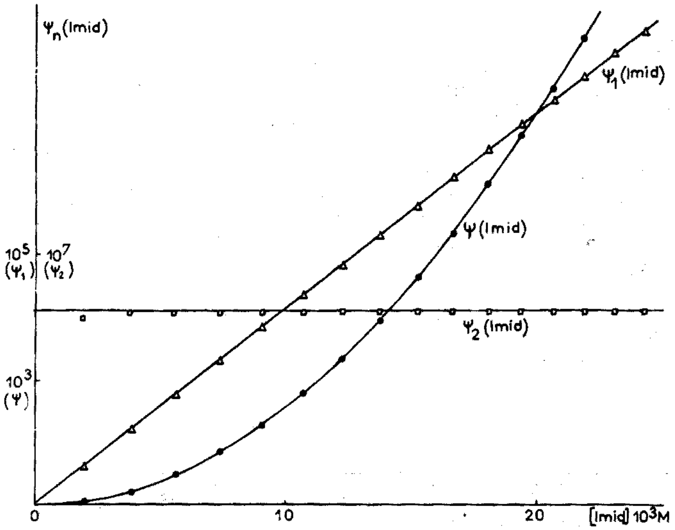

Fig. 2. Calcul des constantes β_1 et β_2 du système Ag^+–imidazole par la méthode de LEDEN.

Bien qu'il soit impossible d'extrapoler la valeur de β_1 avec quelque précision, la reproductibilité est cependant satisfaisante quant à celle de β_2. De plus, nos résultats recoupent suffisamment bien les valeurs trouvées dans la littérature pour ces mêmes constantes, déterminées au moyen de méthodes et dans des conditions nettement différentes:

En milieu KNO_3 1 *M* à 25°: $\log \beta_1 = 3.11$, $\log \beta_2 = 6.84$ (ref. 9).
En milieu KNO_3 0.1 *M* à 25°: $\log \beta_1 = 3.17$, $\log \beta_2 = 6.93$ (ref. 10).
En milieu KNO_3 1 *M* à 25°: $\log \beta_1 = 3.05$, $\log \beta_2 = 6.88$ (ref. 11).

Dosage de l'imidazole

Dans la deuxième série de mesures faites précédemment, il apparaît que le deuxième complexe est nettement prédominant par rapport au premier, ce qui autorise, dans de telles conditions, l'application à l'imidazole de deux méthodes rapides de dosage déjà utilisées pour d'autres coordinats[5,6].

La remarque mentionnée ci-dessus permet d'écrire, après une suite d'approximations:

$$\log [\text{imid}] = \varepsilon/0.11831 - \tfrac{1}{2} \log \beta_2 \qquad (\text{à } 25°) \tag{18}$$

Ayant donc déterminé $\log \beta_2 = 6.894$, au moyen de la relation (18) écrite sous la forme

$$\log \beta_2 = \frac{\varepsilon}{0.05916} - 2 \log [\text{imid}] \tag{19}$$

nous avons recalculé les concentrations en imidazole.

Le Tableau II consigne les concentrations connues, le rapport $\varepsilon/0.11831$, les concentrations recalculées par la relation (18) auxquelles sont affectées leurs incertitudes absolues et relatives. La précision obtenue est meilleure que 1%.

TABLEAU II

DOSAGE DE L'IMIDAZOLE (1° MÉTHODE)

$[imid]_{connu}$ $\cdot 10^3$	$\frac{\varepsilon}{0.11831}$	$[imid]_{calc}$ $\cdot 10^3$	$\Delta[imid]$ $\cdot 10^3$	$\frac{\Delta[imid]}{[imid]}$ (%)	$[imid]_{connu}$ $\cdot 10^3$	$\frac{\varepsilon}{0.11831}$	$[imid]_{calc}$ $\cdot 10^3$	$\Delta[imid]$ $\cdot 10^3$	$\frac{\Delta[imid]}{[imid]}$ (%)
5.660	1.199	5.65	−0.010	0.18	18.032	1.705	18.113	+0.081	0.45
7.407	1.316	7.396	−0.011	0.15	19.354	1.735	19.409	+0.055	0.28
9.091	1.405	9.078	−0.013	0.14	20.634	1.762	20.654	+0.020	0.10
10.714	1.476	10.690	−0.024	0.22	21.875	1.786	21.827	−0.048	0.22
12.281	1.535	12.246	−0.035	0.28	23.076	1.810	23.067	−0.009	0.04
13.793	1.86	13.772	−0.021	0.15	24.242	1.830	24.154	−0.088	0.36
15.254	1.630	15.242	−0.012	0.08	25.373	1.851	25.351	−0.022	0.09
16.666	1.669	16.672	+0.006	0.04					

TABLEAU III

DOSAGE DE L'IMIDAZOLE (2° MÉTHODE)

$[imid]_{connu}$ $\cdot 10^3$	$E_s - E_x$ (mV)	$[imid]_{calc}$ $\cdot 10^3$	$\Delta[imid]$ $\cdot 10^3$	$\frac{\Delta[imid]}{[imid]}$ (%)	$[imid]_{connu}$ $\cdot 10^3$	$E_s - E_x$ (mV)	$[imid]_{calc}$ $\cdot 10^3$	$\Delta[imid]$ $\cdot 10^3$	$\frac{\Delta[imid]}{[imid]}$ (%)
5.660	55.65	5.642	−0.018	0.32	18.032	4.15	18.068	+0.036	0.20
7.407	41.85	7.381	−0.026	0.35	19.354	7.75	19.379	+0.025	0.13
9.091	31.25	9.072	−0.019	0.21	20.634	10.90	20.604	−0.030	0.14
10.714	22.85	10.683	−0.031	0.29	21.875	13.85	21.822	−0.053	0.24
12.281	15.85	12.242	−0.039	0.32	23.076	16.65	23.044	−0.032	0.14
13.793	9.90	13.745	−0.048	0.35	24.242	19.05	24.146	−0.096	0.39
15.254	4.60	15.239	−0.015	0.10	25.373	21.45	25.301	−0.072	0.28
16.666 $= C_s$	0	16.666	0	0					

La deuxième méthode fait appel à l'utilisation d'une solution standard et ne nécessite pas la connaissance préalable de la constante β_2.

On écrit ainsi:

$$\log C_x = \log C_s - (E_s - E_x)/0.11831 \qquad (20)$$

les indices x et s se rapportant respectivement aux solutions inconnues et standard.

Le Tableau III donne les concentrations connues, les différences de tensions $E_s - E_x$, les concentrations calculées affectées de leurs incertitudes absolue et relative. La précision, cette fois encore est meilleure que 1%.

APPLICATION DE L'ÉLECTRODE $Ag/[Ag(imid)_n]^+$,imid À LA DÉTERMINATION DES CONSTANTES DU SYSTÈME Cd^{2+}–IMIDAZOLE

L'étude de la complexation du cadmium par l'imidazole est effectuée à partir de la mesure des f.e.m. d'une série de cellules de type:

$$\begin{array}{llllll} Ag \,|\, [Ag\,(imid)_n]^+, imid, & Cd^{2+}, & KNO_3 \,\|\, & KNO_3 \,\|\, & KCl \,|\, Hg_2Cl_2\text{–}Hg & (21) \\ \quad (C \sim C_0) & (C_2 < C_1) & (10^{-2}\,M) & (0.5\,M) & (sat) \quad (sat) & \end{array}$$

où la molarité C_2 du coordinat à l'équilibre est inférieure à la molarité globale C_1 laquelle demeure la même que dans les cellules (16) et (17); par contre, la concentration initiale d'argent C_0 est différente et égale à $4 \cdot 10^{-4}\,M$.

Les concentrations en coordinat libre dans les cellules (21) sont mesurées soit en utilisant l'expression (18) (pour les valeurs élevées où l'influence de β_1 est négligeable), soit après avoir calculé la fonction ψ(imid) par la relation

$$E_{[16]}-E_{[21]}=(RT/F)\ln \psi(\mathrm{imid}) \tag{22}$$

en lisant sur la courbe d'étalonnage (Fig. 2) les valeurs des concentrations correspondantes qui permettront de définir

$$\bar{\mathrm{n}}_{\mathrm{Cd}} = \frac{C_{\mathrm{imid}}-[\mathrm{imid}]-\bar{\mathrm{n}}_{\mathrm{Ag}}\cdot C_0}{C_{\mathrm{Cd}}} \tag{23}$$

les valeurs de $\bar{\mathrm{n}}_{\mathrm{Ag}}$ étant obtenues par la relation (12).

La courbe $\bar{\mathrm{n}}_{\mathrm{Cd}}$/[imid], [imid] est ensuite utilisée pour déterminer par intégration graphique la fonction de FRONAEUS[12]:

$$\varphi(\mathrm{imid})=\exp\int_0^{[\mathrm{imid}]} (\bar{\mathrm{n}}_{\mathrm{Cd}}/[\mathrm{imid}])\,\mathrm{d}[\mathrm{imid}] \tag{24}$$

dont le développement en série permet de calculer, par la méthode de LEDEN[7], les constantes β_n d'équilibre du système Cd^{2+}–imidazole.

Le Tableau IV consigne les concentrations du coordinat à l'équilibre [imid], le nombre moyen de coordination $\bar{\mathrm{n}}_{\mathrm{Cd}}$, les valeurs de p[imid] et celles de la fonction $\bar{\mathrm{n}}_{\mathrm{Cd}}$/[imid].

TABLEAU IV

FONCTIONS DE CONCENTRATION DU SYSTÈME Cd^{2+}–IMIDAZOLE

[*imid*] $\cdot 10^3$	$\bar{n}_{Cd}$	*p*[*imid*]	$\bar{n}_{Cd}$/[*imid*]
0.326	0.1306	3.487	400.61
0.644	0.2737	3.191	425.00
1.024	0.4219	2.989	412.01
1.479	0.5662	2.830	382.83
2.002	0.7034	2.698	351.35
2.584	0.8330	2.588	322.34
3.238	0.9525	2.490	294.16
3.953	1.0628	2.403	268.86
4.726	1.1633	2.325	246.15
5.527	1.2576	2.257	227.54
6.335	1.3477	2.198	212.74
7.222	1.4249	2.141	197.30
8.098	1.5000	2.091	185.23
9.027	1.5649	2.044	173.36
9.895	1.6339	2.004	165.12
10.830	1.6908	1.965	156.12
11.785	1.7411	1.929	147.74
12.740	1.7876	1.895	140.31
13.695	1.8303	1.863	133.65
14.629	1.8721	1.835	127.97
15.565	1.9099	1.808	122.70
16.468	1.9488	1.783	118.34
17.372	1.9838	1.760	114.19
18.288	2.0135	1.738	110.10
19.190	2.0417	1.717	106.39
20.150	2.0573	1.696	102.10
21.885	2.1060	1.670	96.23
23.408	2.1749	1.631	92.91
25.125	2.1996	1.610	87.55
26.775	2.2220	1.572	82.99
30.77	2.338	1.512	75.98
37.34	2.436	1.428	65.24
44.27	2.565	1.354	57.94
48.28	2.600	1.316	53.85
58.54	2.721	1.232	46.48
73.08	2.835	1.136	38.79

Le Tableau V contient, pour les valeurs des concentrations à l'équilibre [imid] choisies entières pour faciliter les calculs, les valeurs correspondantes de log ψ(imid), ψ(imid), ψ_1(imid), ψ_2(imid), ψ_3(imid), ψ_4(imid).

TABLEAU V

FONCTIONS DE LEDEN DU SYSTÈME Cd^{2+}–IMIDAZOLE

[*imid*] $\cdot 10^3$	*log* ψ*(imid)*	ψ*(imid)*	ψ_1*(imid)*	ψ_2*(imid)* $\cdot 10^{-3}$	ψ_3*(imid)* $\cdot 10^{-6}$	ψ_4*(imid)* $\cdot 10^{-6}$
0	0	1	500	71.0	1.427	13.85
1	0.19825	1.5785	578.50	78.500	—	—
2	0.36415	2.3128	656.40	78.200	—	—
3	0.50639	3.2091	736.37	78.790	—	—
4	0.63038	4.2695	817.37	79.342	—	—
5	0.74025	5.4986	899.72	79.944	—	—
6	0.83949	6.9102	985.03	80.838	—	—
7	0.93047	8.5206	1074.37	82.053	—	—
8	1.01462	10.342	1167.75	83.469	1.559	—
9	1.09301	12.388	1265.33	85.037	1.560	—
10	1.16640	14.669	1366.90	86.690	1.569	14.20
11	1.23535	17.193	1472.09	88.372	1.579	13.81
12	1.30049	19.975	1581.25	90.104	1.592	13.75
13	1.36227	23.029	1694.54	91.888	1.607	13.85
14	1.42101	26.364	1811.71	93.693	1.621	13.86
15	1.47703	29.994	1932.93	95.529	1.635	13.87
16	1.53056	33.928	2058.00	97.375	1.648	13.81
17	1.58191	38.186	2187.41	99.259	1.662	13.82
18	1.63121	42.777	2320.94	101.163	1.676	13.83
19	1.67854	47.702	2458.00	103.053	1.687	13.68
20	1.72414	52.984	2599.20	104.960	1.698	13.55

Nous avons, par cette méthode, obtenu les constantes suivantes exprimées par leurs logarithmes:

$\log \beta_1 = 2.70 \quad \log \beta_2 = 4.85 \quad \log \beta_3 = 6.15 \quad \log \beta_4 = 7.14.$

Celles-ci ont été vérifiées grâce à un calcul basé sur la méthode des moindres carrés[13], effectué sur ordinateur IBM 1620, ce qui a conduit aux résultats

$\log \beta_1 = 2.67 \pm 0.01 \quad \log \beta_2 = 4.87 \pm 0.02 \quad \log \beta_3 = 6.01 \pm 0.12$
$\log \beta_4 = 7.14 \pm 0.14.$

Enfin nous avons établi la courbe de formation $\bar{n}_{Cd} = f\,(p[\text{imid}])$, dont l'extrapolation[14] nous a fourni, au moyen de la méthode de BJERRUM[1] spécialement mise au point[15], des constantes

$\log \beta_1 = 2.72 \quad \log \beta_2 = 4.83 \quad \log \beta_3 = 6.22 \quad \log \beta_4 = 7.0$

De ces trois séries de valeurs, la plus significative est certainement celle qui provient de la méthode la plus objective, c'est à dire celle des moindres carrés, la méthode de FRONAEUS[12] n'étant utilisée que pour déterminer le nombre maximum de coordination de l'ion Cd^{2+} dans l'intervalle de concentrations considéré, et la méthode de BJERRUM[1] ne vérifiant ici que l'ordre de grandeur[14] des constantes ainsi calculées.

Ces valeurs sont assez voisines de celles trouvées dans la littérature et déterminées de manière différente dans d'autres conditions:

pour $\mu = 0.15$ à 25°[16]
$\log \beta_1 = 2.80 \quad \log \beta_2 = 4.90 \quad \log \beta_3 = 6.45 \quad \log \beta_4 = 7.58$
et[17] $\log \beta_2 = 5.07 \quad \log \beta_3 = 6.46 \quad \log \beta_4 = 7.48$

pour $\mu = 0.1$ à 25° [18]

$\log \beta_1 = 3.03 \quad \log \beta_2 = 5.14 \quad \log \beta_3 = 6.48 \quad \log \beta_4 = 7.27$

L'incertitude assez importante affectant, dans la deuxième série de nos résultats, les valeurs des deux constantes globales β_3 et β_4 provient de la relation (23) définissant des valeurs de $\bar{n}_{Cd}$ de moins en moins précises au fur et à mesure que la concentration en imidazole à l'équilibre augmente. Les mêmes difficultés avaient d'ailleurs été rencontrées par de précédents auteurs[16], utilisant l'ion H^+ comme référence.

CONCLUSION

La détermination quantitative des équilibres de complexation de l'électrode $Ag/[Ag\,(imid)_n]^+$, imid permet d'envisager deux applications intéressantes pour cette dernière.

La première réside dans la possibilité de calculer toute concentration d'imidazole dans une solution de teneur inconnue supérieure à 10^{-4} M, soit, algébriquement, lorsque les concentrations sont inférieures à $5 \cdot 10^{-3}$ M, en utilisant les deux constantes β_1 et β_2 définies dans le milieu considéré (ou aussi graphiquement); soit, plus rapidement encore, par le seul intermédiaire de la constante β_2 lorsque le deuxième complexe est largement prédominant ($[\text{imid}] > 5 \cdot 10^{-3}$ M).

La deuxième application, suscitée par la première, consiste, une fois connues les concentrations à l'équilibre [A] du coordinat en présence d'un deuxième ion métallique introduit dans la solution, en la détermination du nombre moyen de coordination $\bar{n}$ de ce dernier, ce qui permet de calculer les constantes de ses équilibres de complexation.

L'étude ici présentée à titre d'exemple concerne le système cadmium(II)–imidazole, dont tous les complexes[17] ont pu être ainsi caractérisés dans les conditions adoptées.

RÉSUMÉ

L'étude quantitative des équilibres de complexation de l'ion Ag^+ par l'imidazole à 25° et à la force ionique KNO_3 0.5 M conduit à la possibilité de doser rapidement ce coordinat, et permet ainsi d'accéder aux constantes de stabilité des complexes d'un deuxième ion métallique mis en concurrence avec Ag^+ dans les mêmes conditions. Le principe a été appliqué ici à la détermination des constantes d'équilibre du système cadmium(II)–imidazole.

SUMMARY

A quantitative study of the equilibria in the complex formation between silver(I) and imidazole at 25° in 0.5 M potassium nitrate has made it possible to determine this ligand very rapidly. Moreover, the stability constants of the complexes of a second metal which is in competition with silver(I) under the same conditions can be established. The principle has been applied to the determination of the stability constants of the cadmium(II)–imidazole system.

ZUSAMMENFASSUNG

Eine quantitative Untersuchung der Gleichgewichte bei der Komplexbildung zwischen Silber(I) und Imidazol bei 25° in 0.5 *M* Kaliumnitrat hat es ermöglicht, sehr schnell diesen Liganden zu bestimmen. Darüberhinaus können die Stabilitätskonstanten der Komplexe eines zweiten Metalls, das bei denselben Bedingungen mit Silber(I) konkurriert, ermittelt werden. Das Prinzip ist auf die Bestimmung der Stabilitätskonstanten im Cadmium(II)–Imidazol-System angewendet worden.

BIBLIOGRAPHIE

1 J. Bjerrum, *Metal Ammine Formation in Aqueous Solution*, 2° Edn., P.Haase, Copenhague, 1957.
2 F. J. C. Rossotti, dans J. Lewis et R. G. Wilkins, *Modern Coordination Chemistry*, Interscience, New-York, 1960.
3 F. J. C. Rossotti et H. Rossotti, *The Determination of Stability Constants*, Mc Graw-Hill, New-York, 1961.
4 C. Luca, *Bull. Soc. Chim. France*, 7 (1967) 2556.
5 G. Berthon et C. Luca, *Chim. Anal. (Paris)*, 49, 9 (1967) 452.
6 G. Berthon et C. Luca, *Chim. Anal. (Paris)*, 51,8 (1969) 385.
7 I. Leden, *Z. Phys. Chem.*, 188 A (1941) 160.
8 L. G. Sillén, *Acta Chem. Scand.*, 10 (1956) 186.
9 D. H. Gold et H. P. Gregor, *J. Phys. Chem.*, 64 (1960) 1461.
10 S. P. Datta et A. K. Grzybowski, *J. Chem. Soc.*, (1966) 1059.
11 J. E. Bauman et J. C. Wang, *Inorg. Chem.*, 3 (1964) 368.
12 S. Fronaeus, *Komplexsystem hos Koppar*, Gleerupska Universitets Bokhandeln, Lund, 1948.
13 G. Berthon et C. Luca, *Chim. Anal. (Paris)*, 52, 4 (1970) 391.
14 A. Sirieix, G. Berthon et C. Luca, *Bull. Soc. Chim. France*, 3 (1970) 899.
15 G. Berthon, A. Sirieix et C. Luca, *Bull. Soc. Chim. France*, 2 (1970) 509.
16 C. Tanford et M. L. Wagner, *J. Am. Chem. Soc.*, 75 (1953) 434.
17 N. C. Li, J. M. White et E. Doody, *J. Am. Chem. Soc.*, 76 (1954) 6219.
18 A. C. Andrews et J. K. Romary, *Trans. Kansas Acad. Sci.*, 67 (1964) 4.630.

Analytica Chimica Acta
Elsevier Publishing Company, Amsterdam
Printed in The Netherlands

METAL–PYRIDINE-2-ALDEHYDE-2′-PYRIDYLHYDRAZONE COMPLEXES AS VISUAL ACID–BASE INDICATORS

PART I. INDICATOR CONSTANTS, COLOUR CHANGES AND TITRATIONS

A. J. CAMERON* AND N. A. GIBSON
Chemistry School, Sydney University, Sydney, N.S.W. (Australia)

(Received November 21st, 1969)

The use of metal complexes as visual indicators in acid–base titrations has received little attention. HIRSCH[1] used the formation and extraction of the red dithizone complex of lead to indicate the end-point of aqueous acid–base titrations. In 1962, SCHILT[2] used the complexes dicyanobis(1,10-phenanthroline)iron(II) and dicyanobis(2,2′-dipyridyl)iron(II) as indicators for the titration of weak organic bases in nonaqueous solvents.

CAMERON *et al.*[3] suggested that certain complexes of the tridentate ligand 1,3-bis(2′-pyridyl)-1,2-diazoprop-2-ene (pyridine-2-aldehyde-2′pyridylhydrazone; PAPHY; I) should prove useful as acid–base indicators.

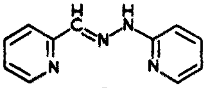

I

These cationic complexes (*e.g.*, $[Ni(PAPHY)_2]^{2+}$; IIa) can be deprotonated at the imino group with alkalis to give intensely coloured neutral complexes (*e.g.*, $[Ni(PAPY)_2]^0$; IIb).

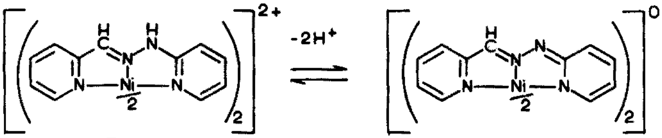

IIa IIb

It is evident from the above publication[3] that the complexes with the most favourable light absorption properties for use as indicators are those of Cu(II), Fe(II), Ni(II), Zn(II) and Cd(II). This paper is concerned with the pH intervals and colour changes of these complexes, and their application in acid–base titrations.

Titrations were generally of strong alkali against strong acid (HCl), the alkali being selected as the titrant, because the basic forms of the complexes are highly coloured. Thus, with the Cu, Ni, Zn and Cd complexes, the end-points were signalled

---

* Present address: The N.S.W. Institute of Technology, Sydney, N.S.W., Australia.

by the appearance of yellow colour and with the Fe–PAPHY complex, a colour change from pink to yellow resulted.

EXPERIMENTAL

Apparatus

Visible absorption spectra were measured with a Perkin-Elmer Spectracord (Model 4000) and 4-cm cells. The blank cell contained water. The pH values were determined with a Radiometer pH meter 4, standardised against 0.05 *M* potassium hydrogen phthalate (pH 4.005).

Reagents

Aqueous solutions of the metal complex indicators (0.1%) were prepared from the complex salts $[Cu(PAPHY)Cl]ClO_4$, $[Fe(PAPHY)_2](ClO_4)_2 \cdot 2H_2O$, $[Ni(PAPHY)_2](ClO_4)_2 \cdot H_2O$, $[Zn(PAPHY)_2](ClO_4)_2 \cdot 1.5H_2O$ and $[Cd(PAPHY)_2](ClO_4)_2 \cdot 2H_2O$. The preparation of all these compounds has been reported by LIONS *et al.*[4].

Freshly prepared 0.1 *M* solutions of hydrochloric acid and sodium hydroxide were used for titrations.

Procedure for establishment of indicator constants

For each complex, series of aqueous solutions containing the same concentration of complex and different values of pH were prepared. The visible absorption spectra of the solutions were measured and the apparent indicator constants found (see below for details). Visual comparisons of the colour intensities of the solutions afforded the pH ranges over which the complexes changed colour.

Titration procedure

Samples of hydrochloric acid (20.00 ml) were pipetted into a 250-ml conical flask, indicator was added and the solutions were titrated with 0.1 *M* sodium hydroxide. End-points were taken at the first appearance of yellow colour, permanent for at least 20 sec. Recommended amounts of indicator are shown in Table II.

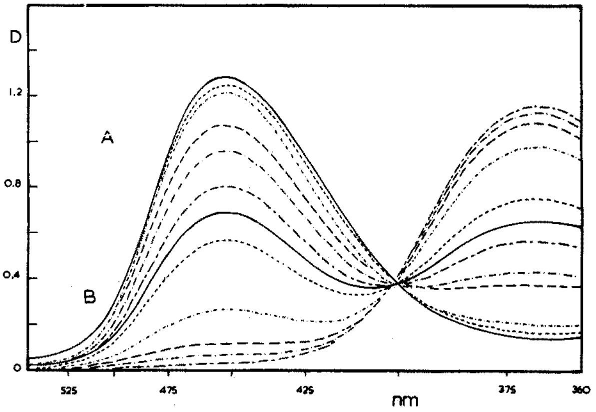

Fig. 1. Visible absorbance spectra of the Cu (II)–PAPHY complex in aqueous solution. (————) pH 11.2 (A), pH 5.8 (B); (-----) pH 9.3 (A), pH 5.7 (B); (-.-.-.-.-.) pH 7.2 (A), pH 5.1 (B); (— — —) pH 6.4 (A), pH 4.6 (B); (—.—.—.) pH 6.3 (A), pH 4.2(B); (— — — —) pH 6.0 (A), pH 3.1 (B).

INDICATOR PROPERTIES

Apparent indicator constants

A selected number of the spectra measured for the copper(II)- and nickel(II)-PAPHY complexes are shown in Figs. 1 and 2. Similar spectra were obtained for the zinc(II)- and cadmium(II)-PAPHY complexes. These spectra clearly demonstrate the change in absorbance, and therefore intensity of colour, with change in pH. As the pH is raised, deprotonation occurs, resulting in an increase in the degree of possible conjugation of the double chelate ring system (see formulae II). This is associated with a decrease in the height of the absorption peak at *ca.* 360 nm and an increase in the height of the peak in the 430–450 nm region. A direct consequence of this increase in absorbance is an increase in the visually observable yellow colour intensity of the indicators. A plot of optical density at this absorbance peak (452 nm for Cu(PAPY)OH, 431 nm for $Ni(PAPY)_2$, 428 nm for $Zn(PAPY)_2$ and 431 nm for $Cd(PAPY)_2$) against pH gives a measure of the change in yellow colour intensity with change in pH. From the resulting curves (*e.g.* Fig. 3) the pH values corresponding to one-half colour development, *i.e.* the apparent indicator constants, may be obtained. The indicator constants obtained are listed in Table I.

TABLE I

pH INTERVALS OF COLOUR CHANGE

Indicator	*Aqueous solution concn. (%)*	*Apparent indicator constant*	*pH colour change interval*	*Colour change*	*Middle tint pH*
Cu complex	0.0006	5.8	4.4– 6.8	Very pale yellow–yellow	
Fe complex	0.0006		5.6– 8.2	Pink–yellow	6.4
Ni complex	0.0004	8.6	6.4– 9.5	Colourless–yellow	
Zn complex	0.0006	8.7	6.7– 9.8	Colourless–yellow	
Cd complex	0.001	9.7	7.8–10.4	Colourless–yellow	

Whereas the visible spectra of the PAPHY complexes of Cu(II), Ni(II), Zn(II) and Cd(II) are characterised by two regions of strong absorbance, the iron(II)–PAPHY spectra have no definite absorbance peaks to which can be solely attributed the visually observable pink and yellow colours. A plot of optical density at an absorption peak against pH was not attempted for this complex.

Colour change intervals

Full development of the yellow colour with the PAPHY complexes of Fe(II), Ni(II), Zn(II) and Cd(II) involves the loss of two protons from the "acid" forms of the indicators:

$$[M(PAPHY)_2]^{2+} \overset{-H^+}{\rightleftharpoons} [M(PAPHY)(PAPY)]^{+} \overset{-H^+}{\rightleftharpoons} [M(PAPY)_2]^{0}$$

With the copper (II)–PAPHY complex, although the added complex cation has the formula $[Cu(PAPHY)Cl]^+$, in dilute aqueous solution the chloride ion in the fourth coordination position is presumably replaced by a water molecule. The deprotonation reactions may therefore be written thus:

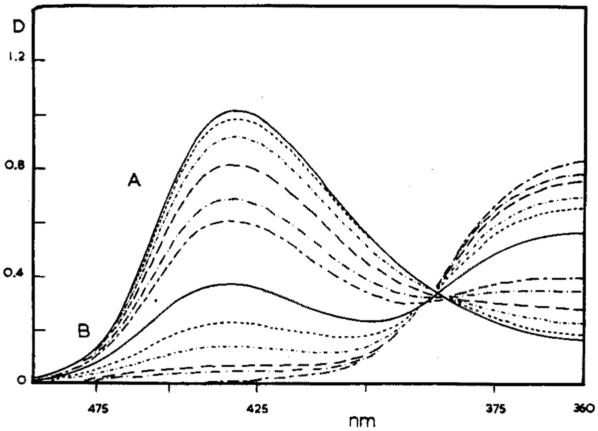

Fig. 2. Visible absorbance spectra of the Ni(II)–PAPHY complex in aqueous solution. (————) pH 11.2 (A), pH 8.2 (B); (------) pH 10.3 (A), pH 7.7 (B); (-.-.-.-.-.-) pH 9.7 (A), pH 7.1 (B); (———) pH 9.3 (A), pH 6.6 (B); (—.—.—) pH 9.1 (A), pH 6.3 (B); (————)pH 8.8 (A), pH 3.1 (B).

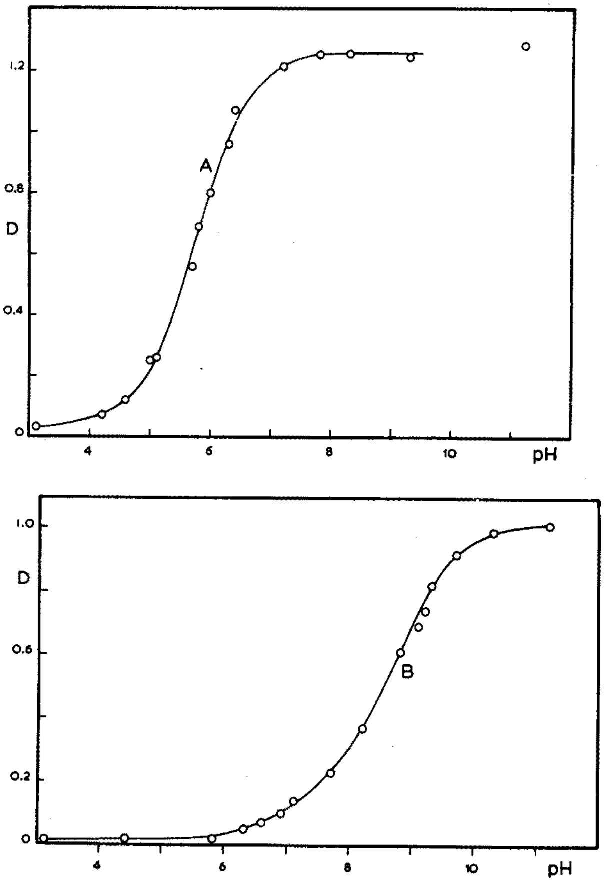

Fig. 3. Absorbance plotted against pH for aqueous solutions of the complexes. (A) Cu(II)–PAPHY at 452 nm, (B) Ni(II)–PAPHY at 431 nm.

$$[Cu(PAPHY)H_2O]^{2+} \overset{-H^+}{\rightleftharpoons} [Cu(PAPY)H_2O]^{+} \overset{-H^+}{\rightleftharpoons} [Cu(PAPY)OH]^{0}$$

Although two deprotonation steps are needed to form a neutral complex, only the first step involving the deprotonation of the PAPHY residue[5] results in an intensification of colour. The pH interval over which this indicator changes colour would therefore be expected to be shorter than the corresponding intervals for the other four indicators. An inspection of Table I shows this to be the case.

It is evident from Table I that the longest interval of colour change is only 3.1 pH units, for the PAPHY complexes of nickel and zinc. Consequently, for each of the Fe–, Ni–, Zn– and Cd–PAPHY complexes, the two acid dissociation steps overlap sufficiently for an acceptable interval of colour change to be obtained.

It should be noted that the iron(II)–PAPHY complex, unlike the other complexes in this study, behaves as a two-colour indicator, changing from pink to yellow with increase in pH. The "middle tint" of this indicator occurs at pH 6.4.

It is evident from Table I that with this series of PAPHY complexes, it is possible to select indicators having different pH intervals of colour change merely by changing the nature of the coordinated metal.

APPLICATION AS ACID–BASE INDICATORS

The recommended quantities of indicator solutions for use in acid–base titrations are shown in Table II. These quantities are suited to solution volumes at the end-point of 50–75 ml, the range obtained in the present study.

TABLE II

RECOMMENDED QUANTITY OF 0.1% INDICATOR SOLUTION

Indicator	*Amount added*
Cu complex	4 drops (0.2 ml)
Fe complex	6 drops
Ni complex	4 drops
Zn complex	5 drops
Cd complex	7 drops

TABLE III

PRECISION OF TITRATION

(Individual titration results were *ca.* 20.0 ml)

Indicator	*Maximum deviation from the mean*		*Average deviation from the mean*	
	(ml)	*(%)*	*(ml)*	*(%)*
Cu complex	0.02	0.1	0.02	0.1
Fe complex	0.03	0.15	0.02	0.1
Ni complex	0.02	0.1	0.01	0.05
Zn complex	0.03	0.15	0.01	0.05
Cd complex	0.02	0.1	0.01	0.05

Precision of titration

The ability of the indicators to change colour sharply, thereby clearly signifying titration end-points, was tested by performing eight titrations with each indicator (Table III). The precision obtained for each set is excellent, clearly demonstrating the worth of the PAPHY complexes as acid–base indicators.

The effect of using different quantities of indicators

For a one-colour indicator, changing the concentration of the indicator alters slightly the pH range over which the visually observable variation in colour intensity occurs. Therefore, the effect of indicator concentration on the position of the end-point was tested. Titrations were performed with 1 drop of indicator solution (except with the Fe and Cd complexes where 2 drops were used) and 20 drops, *i.e.* 1.0 ml, of indicator solution. The results obtained were compared with the mean titration results found with the recommended quantities of indicators (Table IV).

TABLE IV

DEVIATION FROM THE MEAN TITRATION OBTAINED WITH THE RECOMMENDED QUANTITY OF INDICATOR

Indicator	*1 or 2 drops of indicator*	*20 drops of indicator*
Cu complex	+0.04 ml	−0.02 ml
Fe complex	0.00 ml	+0.01 ml
Ni complex	+0.03 ml	−0.01 ml
Zn complex	+0.01 ml	−0.01 ml
Cd complex	−0.02 ml	−0.03 ml

As expected, the observed end-points generally tended to be a little late when small amounts of indicator were used, as a high pH was needed for the yellow colour to be seen. Conversely, end-points tended to be a little early when large quantities of indicator were used. As the iron(II) complex is a two-colour indicator, it was the least affected by changes in indicator concentration; titrations carried out with 2, 6 and 20 drops of this indicator gave essentially identical results.

Although sharp end-point colour changes were not obtained when only 1 drop of the iron or cadmium complex was used, the sensitivity of all five complexes as indicators could still be classed as good.

With the less stable zinc and cadmium complexes ($\log \beta_1 = 5.7$ and $\log \beta_2 = 11.2$ for the Zn–PAPHY complexes, and $\log \beta_1 = 4.8$ and $\log \beta_2 = 10.1$ for the Cd–PAPHY complexes^5), varying the quantity of indicator solution has an additional effect on the amount of complexes present. The PAPHY complexes of these metals are only partly formed at low concentrations, and any increase in concentration results in an increase in the degree of complex formation. Thus, increasing the quantity of indicators from, say, 1 drop to 20 drops results in a greater than 20-fold increase in the concentration of PAPHY complexes.

Boiling the solutions during titrations

Carbon dioxide introduced either from the reagents or the atmosphere, can have a large effect on the titration result if the indicator used shows its "base" colour above *ca.* pH 4.5. As the indicators under investigation all have apparent indicator constants in excess of this figure, the effect of boiling out carbon dioxide was studied. Titrations were performed by adding sodium hydroxide solution to within 0.1–0.2 ml of the end-points. The acidic solutions were then boiled to remove carbon dioxide and immediately cooled in an ice-bath, and the titrations were continued in the normal way.

Depending on the indicator used, the results were 0.02–0.08 ml lower than those obtained without boiling. The greatest difference (0.08 ml) was obtained for the cadmium(II) complex, for this indicator changes colour at the highest pH.

Reversibility of the indicator

The reversibility of the indicators was demonstrated for titrations with the recommended quantities of indicators present. At the end-points, successive 1-drop additions of 0.1 *M* acid and alkali resulted in the solutions changing from yellow to colourless (or pink in the case of the iron(II) complex) and back to yellow again.

Indicator errors

The 0.1% indicator solutions were prepared from complex salts which contained the indicators in the charged or acid forms. To convert 1 ml of these solutions to the fully deprotonated or basic forms of the indicators theoretically would require *ca.* 0.03 ml of 0.1 *M* sodium hydroxide. However, with the recommended quantities of indicators, the indicator error should in no case exceed 0.01 ml of 0.1 *M* solution. To ensure experimentally that the indicator errors were in fact small, 1 ml of indicator solution in 20–30 ml of water was titrated dropwise with 0.1 *M* acid or alkali. Indicator errors were found to be no greater than 0.05 ml (1 drop) when such a large quantity of indicator was used.

The solution of the iron(II) complex had to be diluted considerably, since the basic form of the complex was found to be dichroic. The solution changed from red to yellow on dilution. When the iron(II) complex is employed as an indicator, it must not be used in large amounts.

Titrations with acid as the titrant

To investigate the clarity of the end-point for titrations to the disappearance of the yellow colour rather than to its appearance, four titrations were performed with each of the nickel, zinc or iron(II) complexes as indicators with hydrochloric acid as titrant. The precision obtained was exactly the same as that found for these indicators in titrations with sodium hydroxide (Table III). However, the end-points were more distinct when alkali was added to acid.

Titrations of weak acid or weak base

It was shown that the indicators could be used for titrations of strong acid with weak base and weak acid with strong base. Ammonia (0.1 *M*) was titrated against hydrochloric acid (0.1 *M*) with the copper complex as indicator, and sodium hydroxide (0.1 *M*) was titrated against acetic acid (0.1 *M*) with the cadmium complex as indicator. In both cases sharp end-points were obtained, requiring less than one drop of titrant.

Stability of stock solutions of the indicators

Freshly prepared aqueous stock solutions of the indicators (0.1 %) were stored for 3 weeks in colourless glass bottles exposed to diffused daylight and artificial light but not to direct sunlight. Visible absorption spectral measurements before and after storage showed solutions of the Ni, Zn and Cd complexes to be stable. Similar measurements indicated that the acid form of the Cu complex, $[Cu(PAPHY)H_2O]^{2+}$, underwent some deprotonation on storage; this would not affect the efficiency of the indicator. The spectra demonstrated the relative instability of aqueous solutions of the iron(II) complex, optical densities decreasing by about 20% over the three weeks period. Stock solutions of this indicator should therefore be prepared at fairly frequent intervals, *e.g.*, weekly.

SUMMARY

The PAPHY complexes of certain metals are suggested as acid–base indicators. The colour change intervals of aqueous solutions of the complexes of Cu(II), Fe(II), Ni(II), Zn(II), and Cd(II) have been studied. Apparent indicator constants have been determined. The performance of the indicators in titrations of weak and strong acid and bases is excellent.

RÉSUMÉ

Les complexes PAPHY (pyridine-2-aldéhyde-2′-pyridylhydrazone) de certains métaux sont proposés comme indicateurs acide–base. On a examiné l'intervalle de virage de complexes de cuivre(II), fer(II), nickel(II), zinc(II) et cadmium(II) en solutions aqueuses. On a déterminé les constantes apparentes d'indicateur. Les résultats obtenues à l'aide de ces indicateurs pour des titrages d'acides et de bases forts et faibles sont excellents.

ZUSAMMENFASSUNG

Die PAPHY-Komplexe einiger Metalle werden als Säure–Base-Indikatoren vorgeschlagen. Die Farbwechsel-Bereiche von wässrigen Lösungen der Komplexe von Cu(II), Fe(II), Ni(II), Zn(II) und Cd(II) sind untersucht und die scheinbaren Indikatorkonstanten ermittelt worden. Die Indikatoren eignen sich ausgezeichnet für Titrationen starker und schwacher Säuren und Basen.

REFERENCES

1 W. Hirsch, *Analyst*, 73 (1948) 160.
2 A. A. Schilt, *Anal. Chim. Acta*, 26 (1962) 134.
3 A. J. Cameron, N. A. Gibson and R. Roper, *Anal. Chim. Acta*, 29 (1963) 73.
4 F. Lions and K. V. Martin, *J. Am. Chem. Soc.*, 80 (1958) 3858; J. F. Geldard and F. Lions, *Inorg. Chem.*, 2 (1963) 270; 4 (1965) 414.
5 R. W. Green, P. S. Hallman and F. Lions, *Inorg. Chem.*, 3 (1964) 376.

Analytica Chimica Acta
Elsevier Publishing Company, Amsterdam
Printed in The Netherlands

METAL–PYRIDINE-2-ALDEHYDE-2'-PYRIDYLHYDRAZONE COMPLEXES AS VISUAL ACID–BASE INDICATORS

PART II. EXTRACTIVE END-POINT TITRATIONS AND pH OF EXTRACTION

A. J. CAMERON* AND N. A. GIBSON
Chemistry School, Sydney University, Sydney, N.S.W. (Australia)
(Received November 21st, 1969)

In a recent publication[1] the use of metal complexes of the tridentate ligand 1,3-bis(2'-pyridyl)-1,2-diazaprop-2-ene (pyridine-2-aldehyde-2'-pyridylhydrazone; PAPHY) as visual indicators in acid–base titrations was described. In this paper, an extension of the work is presented. The PAPHY complexes of copper(II), iron(II) and nickel(II) are examined as extraction indicators in titrations of strong alkali against strong acid. Although the PAPHY complexes of zinc(II) and cadmium(II) were shown to be satisfactory indicators in aqueous solution, their relative instability[2] renders them unsuitable as extraction indicators. The end-points of the titrations are signalled by extraction of the intensely coloured deprotonated forms of the indicators (*e.g.* $[\mathrm{Ni(PAPY)_2}]^0$)into organic solvents.

An extractive method of end-point detection is useful if unreactive coloured species are present in the aqueous phase, provided of course that such species are not extracted by the organic solvent employed.

The pH values at which the complexes signal the end-points are also discussed. QUDDUS AND BELL[3] have recently reported distribution coefficients for the extraction of metal–PAPHY complexes.

EXPERIMENTAL

Apparatus

Titrations were performed in a glass-stoppered 250-ml conical flask fitted near the base with a horizontal closed side-arm approximately 3 cm long and 2 cm in diameter. The appearance of colour at the end-point is more easily seen when the organic layer is run into this closed side-arm.

For the absorbance measurements in the extraction studies, a Unicam SP. 600 spectrophotometer with 4-cm cells was used. The blank cell contained the organic solvent. Aqueous solution pH values were determined with a Radiometer pH Meter 4, standardised against 0.05 *M* potassium hydrogen phthalate (pH 4.005).

Reagents

Solutions of the complex salts $[\mathrm{Cu(PAPHY)Cl}]\mathrm{ClO_4}$, $[\mathrm{Fe(PAPHY)_2}](\mathrm{ClO_4})_2\cdot 2\mathrm{H_2O}$ and $[\mathrm{Ni(PAPHY)_2}](\mathrm{ClO_4})_2\cdot\mathrm{H_2O}$ were prepared as described previously[1].

---

* Present address: The N.S.W. Institute of Technology, Sydney, N.S.W., Australia.

Aqueous 0.1 % solutions were used for the indicator studies and aqueous 0.004 % solutions for the extraction studies.

Buffer solutions were prepared from A.R. quality reagents. Disodium hydrogen phosphate and citric acid solutions were used to adjust aqueous phase pH values when extracting the iron and nickel complexes. To buffer aqueous solutions of the copper complex, a solution containing boric acid and potassium chloride was used in conjunction with sodium hydroxide solution.

Titration method

With the exception of the iron complex, the quantities of indicators recommended for use in aqueous solution acid–base titrations[1] were also used here. Since end-points were sharper when relatively small amounts of the iron complex were used, 4 drops of this indicator are recommended for extractive end-points. The recommended amounts are suitable for aqueous volumes at the end-point of 50–75 ml. Carbon tetrachloride was used for extraction of the copper complex, the colour at the end-point being pink. The iron and nickel complexes were extracted into chloroform, giving a yellow extract at the end-point.

The wavelengths of maximum absorbance in the visible region for the neutral complexes of copper(II) and nickel(II) are higher when the complexes are dissolved in organic solvents than when dissolved in water (Table I). The bathochromic shifts on extraction are quite large and with the copper(II) complex the shift results in a change of colour from yellow to pink.

TABLE I

ABSORBANCE MAXIMA IN DIFFERENT SOLVENTS

Neutral complex	λ_{max} *in* H_2O *(nm)*	λ_{max} *in* $CHCl_3$ *(nm)*
$Ni(PAPY)_2$	431	473
Cu(PAPY)OH	452	508 (520 nm in CCl_4)
$Fe(PAPY)_2$	(see ref. 1)	395

Procedure. Samples of 0.1 *M* hydrochloric acid (20.00 ml) were pipetted into the titration flask. Indicator was added, followed by *ca.* 10 ml of organic solvent. Titrations were then performed with 0.1 *M* sodium hydroxide. Near the end-point, the flask was stoppered and shaken after each addition of titrant. End-points were taken when the organic layer first remained coloured after 20-sec shaking.

Procedure for extraction measurements

Indicator solution (3.00 ml of the copper complex, or 2.00 ml of the iron or nickel complex) was added to a 100-ml separating funnel followed by the appropriate buffer solutions. Chloroform (or carbon tetrachloride with the copper complex) (20.00 ml) was then added, together with distilled water to achieve a total aqueous solution volume of 50 ml. The funnel was stoppered and shaken for 20 sec and the layers allowed to separate. The organic layer was then run off and its absorbance was measured at the wavelength of maximum absorbance (see above). The pH of the remaining aqueous phase was also measured. Absorbances were plotted against pH for

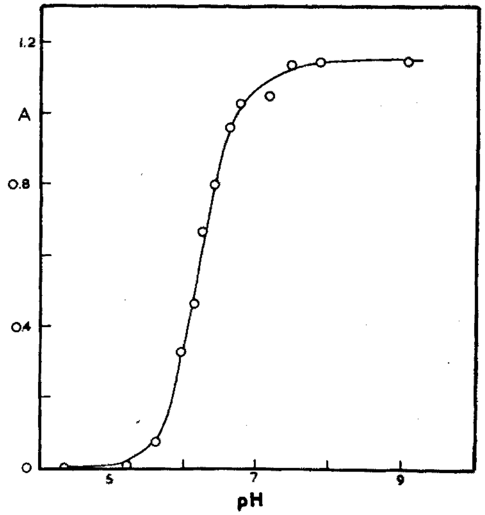

Fig. 1. Extraction of the nickel complex into chloroform. Absorbance at 473 nm of bis(PAPY)–nickel(II) in chloroform plotted against the pH of the aqueous phase.

each of the complexes; Fig. 1 shows a typical curve. The temperature of the extractions was 25 ± 1°.

RESULTS AND DISCUSSION

Titration precision and amount of indicator

Eight titrations were performed with each indicator; the results are shown in Table II. These deviations are similar to those obtained in the normal aqueous titrations[1], and clearly demonstrate the sharpness of the end-points obtained.

TABLE II

PRECISION OF TITRATIONS

(Individual titration results were *ca.* 20 ml)

Indicator	*Maximum deviation from the mean*		*Average deviation from the mean*	
	(ml)	*(%)*	*(ml)*	*(%)*
Cu complex	0.03	0.15	0.02	0.1
Fe complex	0.03	0.15	0.01	0.05
Ni complex	0.02	0.1	0.01	0.05

The effect of using different quantities of indicators

Titrations were also done with 1 drop or 20 drops (*ca.* 1.0 ml) of indicator. When only 1 drop was used, the deviations from the mean result obtained when the recommended quantities of indicators were used, was +0.03 ml for the copper complex and +0.02 ml for the iron complex, whereas the deviation was, unexpectedly, −0.01 ml for the nickel complex. When 20 drops of indicator were used, the deviation from the mean obtained for the recommended indicator quantities was −0.01 to −0.02 ml in all cases.

With the nickel complex, the colour of the chloroform layer is one-half developed at pH 6.2 (see below), which is relatively close to the equivalence point of the strong alkali–strong acid titration (pH 7). Consequently, this complex gave a very sharp end-point. The titration result was little affected by the amount of nickel complex used.

In the present study, end-points were clearly defined when only 1 drop of the iron complex solution was added. This demonstrates the added sensitivity obtained with extractive end-points, for when normal titrations[1] were attempted with this small amount of indicator, it was almost impossible to detect colour change. With large quantities of the iron complex solution (1.0 ml) the end-points were not sharp, the chloroform layer appearing pale yellow some 3–4 drops (of alkali) before the sudden intensification of the yellow colour at the end-point (*cf.* p. 258).

Variation in the time of shaking

The effect of the length of shaking on titration results was studied. Titrations were performed with the recommended quantities of indicators, the shaking time being varied between 2 sec and 100 sec after each addition of alkali. Since it was possible to establish separate end-points for different shaking times in any one titration, accurate determination of the effect of the length of the shaking was obtained.

A reduction in shaking time from 20 to 2 sec had no effect on results with the iron complex but decreased the result by 0.03 ml with the copper complex, and by 0.01 ml with the nickel complex. The pH values at which these complexes indicate titration end-points decrease in the order Cu > Ni > Fe (see below). Thus, the higher the pH at the indicated end-point, the more shaking that is required to establish equilibrium, but with all three complexes, equilibrium was apparently established within 20 sec. An increase in shaking time from 20 to 100 sec had no effect on the titration results and did not produce any visible decrease in the colour intensity of the organic layers.

Boiling the solutions during titrations

The effect of carbon dioxide on the results was investigated. Titrations were performed by addition of sodium hydroxide to within 0.1–0.2 ml of the end-points; the solutions were then boiled to remove carbon dioxide and immediately cooled in an ice-bath. The organic solvent was then added and the titrations were continued in the normal way.

The titration results were 0.02–0.04 ml lower than those obtained without boiling. The greatest difference (0.04 ml) was obtained with the copper complex, the basic form of which is extracted at the highest pH (see below). The least difference (0.02 ml) was obtained with the iron and nickel complexes; since the end-points are signalled at slightly acidic pH values, carbon dioxide has little effect.

Reversibility of the indicator colour changes

The reversibility of the indicator action was demonstrated for the recommended quantities of indicators. At the end-point, addition of one drop of 0.1 *M* hydrochloric acid resulted in the organic layer turning colourless on shaking, and addition of one drop of alkali reproduced the coloured organic layer.

Indicator errors

As stated previously[1], *ca.* 0.03 ml of 0.1 M sodium hydroxide is theoretically required to deprotonate 1 ml of a 0.1 % solution of the acid form of any of the indicators. Subsequent extraction of the deprotonated form should not add to the indicator error. This was confirmed by adding 10 ml of the recommended organic solvent to aqueous solutions containing 1.0 ml of the 0.1 % indicator solutions, and titrating dropwise with 0.1 M acid or alkali. For example, with the nickel complex the chloroform layer went from yellow to colourless with the addition of 1 drop of acid.

pH values at one-half colour development

The pH values corresponding to one-half colour development of the organic phase ($\mathrm{pH}_{\frac{1}{2}}^{*}$) can be taken as the approximate pH at which the extraction indicators signal titration end-points. These $\mathrm{pH}_{\frac{1}{2}}^{*}$ values were found, by inspection of absorbance *versus* pH graphs (see, *e.g.* Fig. 1) to be 7.6 for the copper complex, 6.2 for the nickel complex and 4.7 for the iron complex. The results quoted for the copper complex are approximate only; for the neutral form of this complex was not very stable in the organic solvent, as evidenced by colour fading.

The effect of altering indicator concentrations and solvent volumes

It can be shown[4] from a mathematical study of the extraction equilibria involved, that changes in indicator concentrations and solvent volumes must be large before $\mathrm{pH}_{\frac{1}{2}}^{*}$ values are affected sufficiently to alter titration results. For example, reducing the volume of organic solvent from 20 ml (the quantity found convenient for these measurements) to 10 ml (the quantity recommended for extractive end-points) increases $\mathrm{pH}_{\frac{1}{2}}^{*}$ values by approximately 0.2.

With regard to indicator concentrations, the complexes were essentially completely formed at the concentrations used in this study. Any increase (as recommended for the extractive end-points)[2] would therefore have a negligible effect on the $\mathrm{pH}_{\frac{1}{2}}^{*}$ values.

Colour change intervals

Estimates of the pH intervals of colour change, or more precisely, intervals of change in colour intensity, were obtained (Table III). The extreme pH values of these colour change intervals were chosen to correspond to 1/11 and 10/11 of the total colour development of the organic phase, as read from the curves of absorbance *versus* pH.

TABLE III

ESTIMATED pH INTERVALS OF COLOUR CHANGE

Indicator	*pH interval of colour change*	$\mathrm{pH}_{\frac{1}{2}}^{*}$	*Apparent indicator constant*[a]
Cu complex	6.5–8.6	7.6	5.8
Fe complex	4.1–5.5	4.7	6.4[b]
Ni complex	5.7–6.9	6.2	8.2

[a] Values in aqueous media[1].

[b] Estimated visually[1].

With the exception of the copper complex, these colour change intervals are much shorter than those observed for the indicators in aqueous solution[1]. This would indicate sharper end-points for the extractive titrations than for the normal aqueous acid–base titrations[1]. With the copper complex, this decrease is quite small, consistent with the extraction of the suggested species [Cu(PAPY)OH].

A comparison of the above pH intervals with the indicator constants established previously for aqueous solutions[1] shows that when the iron or nickel complex is used as indicator, the end-points appear at a lower pH for extractive titrations than for normal aqueous titrations[1]. This is only to be expected as extraction of the neutral species $M(PAPY)_2$ displaces eqn. (1)

$$[M(PAPHY)_2]^{2+} \rightleftharpoons [M(PAPY)_2]^0 + 2H^+ \qquad (1)$$

to the right, so that deprotonation is half complete at the lower pH when extraction is employed.

With the copper complex, the deprotonation reaction may be written thus[1]:

$$[Cu(PAPHY)H_2O]^{2+} \overset{-H^+}{\rightleftharpoons} [Cu(PAPY)H_2O]^+ \overset{-H^+}{\rightleftharpoons} [Cu(PAPY)OH]^0 \qquad (2)$$

For extractive end-points, the indicator must undergo both deprotonation steps to produce its neutral extractable form. However, in normal aqueous solution titrations, the indicator need undergo only the first deprotonation step to produce its highly coloured form, as the loss of a proton from the co-ordinated water molecule does not result in any further intensification of colour.

Visible absorbance spectra

Conditions similar to those described above were used for measurement of the visible absorbance spectra of chloroform solutions after extraction of the neutral complex $Ni(PAPY)_2$ from aqueous solutions of various pH. The spectra (Fig. 2) clearly demonstrate the sharpness of absorbance change, and therefore the change in colour intensity with increase in pH.

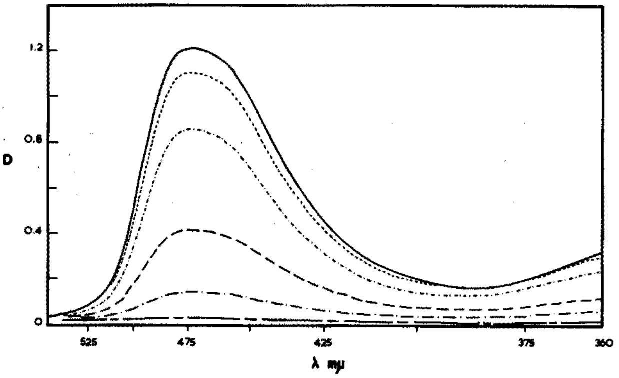

Fig. 2. Visible absorption spectra of bis(PAPY)–nickel(II) in chloroform after extraction from aqueous solutions of various pH. (————) pH 7.50; (– – – – – –) pH 6.76; (–.–.–.–.–.–.) pH 6.38; (— — —) pH 5.97; (—.—.—) pH 5.63; (— – — –) pH 5.20.

SUMMARY

The PAPHY complexes of copper(II), iron(II) and nickel(II) are shown to be very good indicators for extractive end-points in acid–base titrations. The pH ranges for extraction of the complexes have been established, and their relevance to the extractive end-points is discussed.

RÉSUMÉ

Les complexes PAPHY (pyridine-2-aldéhyde-2′-pyridylhydrazone) constituent de très bons indicateurs pour des titrages acide–base, par extraction. On a examiné les zones de pH pour l'extraction des complexes.

ZUSAMMENFASSUNG

Die PAPHY-Komplexe von Kupfer(II), Eisen(II) und Nickel(II) sind sehr gute Indikatoren für die extraktive Endpunktsbestimmung bei Säure–Base-Titrationen. Die pH-Bereiche für die Extraktion der Komplexe sind festgelegt worden; deren Anwendbarkeit auf die extraktive Endpunktsbestimmung wird diskutiert.

REFERENCES

1 A. J. Cameron and N. A. Gibson, *Anal. Chim. Acta*, 51 (1970) 249.
2 R. W. Green, P. S. Hallman and F. Lions, *Inorg. Chem.*, 3 (1964) 376.
3 M. A. Quddus and C. F. Bell, *Anal. Chim. Acta*, 42 (1968) 503.
4 A. J. Cameron, *Ph. D. Thesis*, Sydney University, 1966.

Analytica Chimica Acta
Elsevier Publishing Company, Amsterdam
Printed in The Netherlands

STABILITY CONSTANTS OF METAL COMPLEXES OF BITHIONOL, FENTICLOR AND HEXACHLOROPHENE

A. G. FOGG, A. GRAY AND D. THORBURN BURNS
Department of Chemistry, Loughborough University of Technology, Loughborough, Leics. (England)

(Received February 9th, 1970)

o,o'-Dihydroxydiphenyl sulphides and methanes are important compounds pharmaceutically. In general, one or more halogen atoms (preferably chlorine) must be present in each benzene ring for the compound to be pharmaceutically active, and, in addition, one of these halogen atoms must be in the *para* position to the hydroxyl group[1]. Hexachlorophene (I) is particularly active and has found widespread use. Other compounds including bithionol (II) and fenticlor (III) are available commercially for use as bacteriostats, etc.

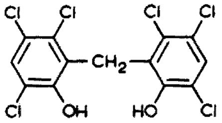

I

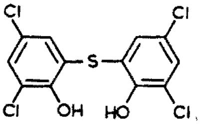

II

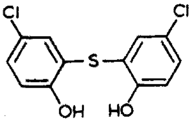

III

The mechanism of the pharmaceutical activity of certain drugs is known to involve complexation of metal ions; either the metal complex formed *in vitro* is potent to the infecting organism or the organism is deprived of essential trace metals by complexation[2]. ADAMS[3] made a semi-quantitative study of metal complexes of bithionol and hexachlorophene potentiometrically and colorimetrically as a means of demonstrating that their pharmacological action could involve complexation of trace metals.

The present authors have been investigating methods of determining *o,o'*-dihydroxydiphenylsulphides and methanes, and also have investigated the utilisation of compounds of this type as analytical reagents for metals. Procedures for the determination of iron(III) with bithionol have been described[4]. As part of this investigation the stability constants of several metal complexes of bithionol, fenticlor and hexachlorophene have been determined potentiometrically. As these compounds are only sparingly soluble in water—the solubility of bithionol is 0.0004% (w/v) at 25°[5]—the stability constants were determined in 3 + 1 (v/v) ethanol–water solution.

EXPERIMENTAL

Reagents

Analytical-reagent grade chemicals were used where available. Water was double distilled in silica apparatus, and was purged with nitrogen before use. Absolute ethanol of British Pharmacopoeia quality was used.

Sodium perchlorate solution 6.47 M. This was prepared from analytical-reagent grade sodium perchlorate, and was filtered before use.

Standard metal solutions, ca. 0.01 M in metal ion and 0.0403 M in nitric acid. These were prepared by dissolving the appropriate metal nitrate in 25.0 ml of 0.8 *M* nitric acid solution (microanalytical-reagent grade), and diluting to exactly 500 ml. The solutions of Mn, Ni, Cu, Zn, Mg, Cd, Fe(III) and Co were standardised by EDTA titration, and the silver solution was standardised by potentiometric titration with potassium chloride.

Bithionol, fenticlor or hexachlorophene, 0.00647 M solution in ethanol. Bithionol (Cyclo Chemicals Ltd.; m.p. 188–190°, lit. value[6] 186–189°) and hexachlorophene (Koch-Light Ltd., m.p. 156–160°, lit. value[6] 161–167°) were used as received. Fenticlor (Calmic Ltd.) was recrystallised from toluene (m.p. 167–169°, lit. value[7] 175°). In all cases, the purity was confirmed by potentiometric titration.

Standard carbonate-free sodium hydroxide solution. A 0.1 *M* solution in 3 + 1 (v/v) ethanol–water was prepared from an ampoule of B.D.H. concentrated volumetric solution and was made 1 *M* in sodium ion by the addition of sodium perchlorate. The hydrogen ion molarity of the solution was confirmed by titration against potassium hydrogen phthalate, and the solution was kept under nitrogen.

pH measurements

pH measurements were made with a Pye 290 pH meter, an E.I.L. GHSN33 screened glass electrode and a saturated calomel reference electrode at 25 ± 0.01° in an ionic background of 1 *M* $NaClO_4$. The initial standardisation of the pH meter was made at all times with a 0.05 *M* aqueous solution of potassium hydrogen phthalate (B.D.H. primary pH standard grade), the meter being set at pH 4.005. The reproducibility of the response of the electrode was checked daily with this buffer and with a 0.01 *M* borax A.R. solution. On the British Standard scale this latter buffer solution has a pH of 9.18 at 25°, but a pH meter reading of 9.12 was obtained consistently.

The response of the glass electrode in 3 + 1 (v/v) ethanol–water was checked by potentiometric titration of a standard nitric acid solution with standard sodium hydroxide solution. The stoichiometric pH, *i.e.* ($-\log [H^+]$), was calculated at various points on the titration curve from the known amounts of sodium hydroxide and nitric acid added. A plot of stoichiometric pH against pH meter reading was linear, and was of the form: stoichiometric pH = (pH meter reading · 0.94) + 0.03. For the calculation of stability constants all pH meter readings were converted to stoichiometric pH values.

Potentiometric titrations

Potentiometric titrations were carried out in a 100-ml glass vessel. Gentle stirring and exclusion of carbon dioxide was achieved by bubbling oxygen-free nitrogen through the solution; the nitrogen was first scrubbed with 0.1 *M* sodium hydroxide solution to remove carbon dioxide, and then passed through two scrubbers containing 3 + 1 (v/v) ethanol–water, to saturate the gas with solvent.

In order to evaluate the proton–ligand and metal–ligand stability constants by the IRVING AND ROSSOTTI procedure[8], solutions prepared from the following amounts of reagents were titrated with standard sodium hydroxide: (*a*) 5 ml of 0.0403 *M* nitric acid solution, 37.5 ml of ethanol, and 7.5 ml of 6.47 *M* sodium perchlorate solution;

(*b*) 5 ml of 0.0403 *M* nitric acid solution, 37.5 ml of 0.00647 *M* solution of ligand in ethanol and 7.5 ml of 6.47 *M* sodium perchlorate solution; and (*c*) 5 ml of 0.01 *M* standard metal solution, 37.5 ml of 0.00647 *M* solution of ligand in ethanol, and 7.5 ml of 6.47 *M* sodium perchlorate solution.

Each titration was performed at least twice to check reproducibility, and in the case of bithionol–nickel and fenticlor–nickel, the titration was also carried out at a nickel concentration one-half of that used previously in order to confirm the absence of polymeric species. Some contraction of the ethanol–water occurred on mixing. The initial volume of titrand was shown experimentally and by calculation to be 48.5 ml, and the initial concentrations of sodium perchlorate, nitric acid, ligand and metal were therefore 1.00, 0.00415, 0.005 and (*ca.*) 0.001 *M*, respectively.

Calculation of stability constants

For the formation of the protonated and complex species HL, H_2L, ML and ML_2, the following equations apply[8].

(*a*) The degree of formation of ligand–proton species,

$$\bar{n}_A = 2 - \frac{(V_2 - V_1)(N + E_0)}{(V_0 + V_1) T_L{}^0},$$

where N = molarity of the standard sodium hydroxide solution, E_0 = initial molarity of nitric acid, $T_L{}^0$ initial total concentration of ligand, and V_0 = initial volume. V_1, V_2 and V_3 are the volumes of sodium hydroxide solution giving the same pH-meter reading in the three titrations above.

(*b*) The degree of formation of ligand–metal complexes,

$$\bar{n} = \frac{(V_3 - V_2)\,[N + E_0 + T_L{}^0\,(2 - \bar{n}_A)]}{(V_0 + V_2)\,\bar{n}_A\,T_M{}^0},$$

where $T_M{}^0$ = initial total concentration of metal.

$$(c)\ \mathrm{pL} = -\log\,[\mathrm{L}] = \log\left[\frac{(V_0 + V_3)\,(\beta_{H1}\,10^{-\mathrm{pH}} + \beta_{H2}\,(10^{-\mathrm{pH}})^2)}{V_0(T_L{}^0 - \bar{n} T_M{}^0)}\right]$$

where β_{H1} and β_{H2} are the first and second overall formation constants of the ligand–proton species.

For the ligands studied here, the values of K_{H1} and K_{H2} (the stepwise proton–ligand stability constants) were sufficiently different to allow the assumption that in solutions with $\bar{n}_A$ between 0 and 1, only L and HL are present, and in solutions with $\bar{n}_A$ between 1 and 2, only HL and H_2L are present.

Thus when $0 < \bar{n}_A < 1$,

$$\bar{n}_A = \frac{C_H - [H]}{C_L} = \frac{[HL]}{[H] + [HL]} = \frac{K_{H1}\,[H]}{1 + K_{H1}[H]}$$

and, therefore, $\log K_{H1} = \mathrm{pH} + \log\left(\frac{\bar{n}_A}{1 - \bar{n}_A}\right)$

When $1 < \bar{n}_A < 2$,

$$\bar{n}_A = \frac{[HA] + 2[H_2A]}{[HA] + [H_2A]} = \frac{K_{H1}\,[H] + 2K_{H1}\,K_{H2}\,[H]^2}{K_{H1}\,[H] + K_{H1}\,K_{H2}\,[H]^2}$$

and, therefore, $\log K_{H2} = \mathrm{pH} + \log\left(\frac{\bar{n}_A - 1}{2 - \bar{n}_A}\right)$

Values of K_{H1} and K_{H2} were calculated at several points on the ligand–proton formation curve; the values obtained for K_{H1} at points where $0.2 < \bar{n}_A < 0.8$ were in good agreement, as were those for K_{H2} at points where $1.2 < \bar{n}_A < 1.8$. The results given in Table I were obtained by averaging these values of K_{H1} and K_{H2}.

Preliminary values for the ligand–metal stability constants were obtained from the formation data by means of a computer program devised by Thun *et al.*[9] based on Fronaeus' graphical integration method. The formation curves were then recalculated from the preliminary values of the stability constants and these values were then refined to give the closest fit to the experimental curve. The results are given in Table I. The possible errors given were estimated from the closeness of fit of the calculated and experimental curves.

TABLE I

VALUES OF STABILITY CONSTANTS

	Bithionol		*Fenticlor*		*Hexachlorophene*	
	log K_{H1}	*log* K_{H2}	*log* K_{H1}	*log* K_{H2}	*log* K_{H1}	*log* K_{H2}
H^+	9.05 ± 0.03	5.33 ± 0.02	10.38 ± 0.03	7.68 ± 0.02	11.50 ± 0.05	5.10 ± 0.03
	log K_1	*log* K_2	*log* K_1	*log* K_2	*log* K_1	*log* K_2
Mn^{2+}	5.32 ± 0.05	4.02 ± 0.04	5.98 ± 0.05	$\simeq 4.5$		
Co^{2+}	7.80 ± 0.03	6.56 ± 0.03	8.86 ± 0.02	6.29 ± 0.02		
Ni^{2+}	8.06 ± 0.02	7.75 ± 0.02	8.86 ± 0.02	7.52 ± 0.02	$\simeq 6.7$	
Cu^{2+}	9.75 ± 0 03	7.05 ± 0.02	10.73 ± 0.05	6.20 ± 0.05	9.55 ± 0.05	
Zn^{2+}	8.08 ± 0.03	5.86 ± 0.02	9.07 ± 0.02	4.87 ± 0.02		
Cd^{2+}	6.76 ± 0.02	5.21 ± 0.02				
Ag^+	4.55 ± 0.05	2.60 ± 0.05				
Fe^{3+}		$\simeq 11.1$				
Mg^{2+}	$\simeq 2.6$					

DISCUSSION

Examination of the ligand–proton stability constants for bithionol and fenticlor shows the effect of the extra electron-withdrawing chlorine atom in each benzene ring of bithionol, which results in bithionol being the stronger acid. The three chlorine atoms in each benzene ring of hexachlorophene cause it to be an even stronger acid than bithionol, although the second proton is more difficult to remove. The ease of combination of ligands with metal ions often follows the same order as the ease of combination with protons, and indeed the 1:1 metal complexes of fenticlor are more stable than those of bithionol. The values of log K_2 for bithionol, however, are slightly greater than those for fenticlor.

Values of log K_1 for complexes of bithionol and fenticlor with the divalent ions of the first transition series metals follow the Irving–Williams' order[10], *viz.* $Mn^{2+} < Co^{2+} < Ni^{2+} < Cu^{2+} > Zn^{2+}$. (Log K_1 values for iron(II) were not determined owing to the ready oxidation of iron(II)–bithionol solutions[4]). Values of log K_2 for nickel(II) were greater than those for copper. This effect has been noted previously for several ligands[10,11].

Jørgensen[12] has commented on the probability that thio-ether groups in many multidentate ligands such as thenoyltrifluoroacetonate and methionine do not participate in complexation. The formation of a distorted octahedral configuration for the 1:2 copper–bithionol complex, if the bithionol acts as a tridentate ligand, would probably be difficult. Thus, either the formation of six coordinate copper(II) with tridentate bithionol or fenticlor, or the formation of a square-planar complex with bidentate bithionol or fenticlor (in which the sulphur is non-coordinating), could explain why the values of log K_2 for complexes of these ligands are smaller for copper than for nickel. The formation of the square-planar complex with bidentate bithionol or fenticlor, however, would involve the formation of an eight-membered ring, and this is unlikely.

JØRGENSEN[13] has shown from u.v. and visible spectra, that 2,2′-diaminodiethylsulphide gives high-spin octahedral complexes with nickel. The 1:2 complex of nickel with bithionol in solution has an absorbance maximum at 650 nm ($\varepsilon = 25$), compared with that of 2,2′-diaminodiethylsulphide at 553 nm ($\varepsilon = 15$), and is similarly octahedral. The much lower approximate value of log K_1 obtained for the nickel–hexachlorophene complex compared with the corresponding values for bithionol and fenticlor, appears to indicate that in the case of the nickel complexes the coordination of the sulphur atom has a considerable stabilising effect.

Hexachlorophene would be expected to act as a bidentate ligand, but, in this case, the complex formed would contain an eight-membered ring. Hydrolysis, as well as complex formation, was evident in the copper- and nickel–hexachlorophene systems, but it is uncertain if mixed hexachlorophene–hydroxo metal complexes were formed. At an apparent pH of 5.5, the copper–hexachlorophene system was dark brown, and the volume of sodium hydroxide solution consumed, after formation of the singly charged hexachlorophene ion, corresponded to the ionisation of one proton per copper ion. The method of continuous variations, applied at 440 and 470 nm, also indicated a 1:1 complex, but the complex formed could be either CuL or $(Cu(OH)HL)_n$. At higher apparent pH values, the solution became much paler in colour, and a blue precipitate formed on standing, indicating extensive hydrolysis.

The method of continuous variations was also applied to the copper–bithionol system. At an apparent pH of 4.3, where the sodium hydroxide consumed, after formation of HL^-, corresponded to the ionisation of one proton per copper ion, the formation of a 1:1 copper–bithionol complex was indicated. At an apparent pH of 8.0 (two extra protons per copper ion beyond HL^-) the formation of a 1:2 copper–bithionol complex was indicated. The method of continuous variations was used earlier[4] to confirm that a 1:2 iron(III)–bithionol complex was formed.

The authors wish to thank Dr. H. THUN for making available to them a copy of his computer program and Dr. W. J. EILBECK for much helpful discussion. One of us (A.G.) is indebted to the S.R.C. for financial support.

SUMMARY

The stability constants of several metal complexes of bithionol, fenticlor and hexachlorophene in 3+1 (v/v) ethanol–water at ionic strength 1 have been determined. Values of log K_1 for complexes of bithionol and fenticlor follow the IRVING–WILLIAMS' order, but the values of log K_2 for nickel are greater than those for copper.

RÉSUMÉ

On a déterminé les constantes de stabilité de divers complexes métalliques de bithionol, fenticlor et hexachlorophène dans un mélange éthanol–eau 3+1 (v/v), à une force ionique de 1. Les valeurs de log K_1 pour les complexes bithionol et fenticlor suivent l'ordre de IRVING–WILLIAMS; cependant les valeurs de log K_2 du nickel sont plus grandes que celles du cuivre.

ZUSAMMENFASSUNG

Es sind die Stabilitätskonstanten verschiedener Metallkomplexe von Bithionol, Fenticlor und Hexachlorophen in Äthanol–Wasser (3 Vol. +1 Vol.) bei Ionenstärke 1 bestimmt worden. Die log K_1-Werte für die Bithionol- und Fenticlor-Komplexe folgen der IRVING–WILLIAMS-Regel, jedoch sind die log K_2-Werte für Nickel grösser als die für Kupfer.

REFERENCES

1 W. S. GUMP AND G. R. WALTER, *J. Soc. Cosmetic Chemists*, 11 (1960) 307.
2 A. ALBERT, *Selective Toxicity*, Methuen, London, 1965.
3 J. B. ADAMS, *J. Pharm. Pharmacol.*, 10 (1958) 507.
4 A. G. FOGG, A. GRAY AND D. THORBURN BURNS, *Anal. Chim. Acta*, 45 (1969) 196; 47 (1969) 151.
5 R. S. SHUMARD, D. J. BEAVER AND M. C. HUNTER, *Soap and Sanitary Chemicals*, 29 (1953) 34.
6 *Remington's Pharmaceutical Sciences*, 13th Edn., Mack Publ. Co., 1965.
7 *The Merck Index of Chemicals and Drugs*, 7th Edn., Merck and Co., Inc., 1960.
8 H. M. IRVING AND H. S. ROSSOTTI, *J. Chem. Soc.*, (1954) 2904.
9 H. THUN, F. VERBEEK AND W. VANDERLEEN, *J. Inorg. & Nucl. Chem.*, 29 (1967) 2109.
10 H. IRVING AND R. J. P. WILLIAMS, *J. Chem. Soc.*, (1953) 3192.
11 E. GONICK, W. C. FERNELIUS AND B. E. DOUGLAS, *J. Am. Chem. Soc.*, 76 (1954) 4671.
12 C. K. JØRGENSEN, *Inorganic Complexes*, Academic Press, London, 1963, p. 142.
13 C. K. JØRGENSEN, *J. Inorg. & Nucl. Chem.*, 24 (1962) 1571.

Analytica Chimica Acta
Elsevier Publishing Company, Amsterdam
Printed in The Netherlands

AN EXTRACTION–SPECTROPHOTOMETRIC METHOD FOR THE DETERMINATION OF ZINC WITH 1-[(5-CHLORO-2-PYRIDYL)AZO]-2-NAPHTHOL

SHOZO SHIBATA, MASAMICHI FURUKAWA AND SHOZO SASAKI
Government Industrial Research Institute, Nagoya Kita-ku, Nagoya (Japan)

(Received February 10th, 1970)

Several spectrophotometric methods are available for the determination of small amounts of zinc (see Table I). Although dithizone has been extensively employed as the most sensitive reagent for this determination[2], the conditions for its use are critical. During an investigation of several organic compounds, selected as possible analytical reagents because of their structure, the compound 1-[(5-chloro-2-pyridyl)azo]-2-naphthol (5-Cl-β-PAN) was observed to give a red precipitate with zinc[1]. This complex is extractable into various organic solvents. A brief discussion of the complex formation with zinc has already been presented[1]. With 5-Cl-β-PAN, a sensitive and selective determination of microgram amounts of zinc is possible under the optimum conditions established in this study.

TABLE I

SENSITIVITY OF SOME METHODS FOR ZINC

Reagents	*Molar absorptivity (10^4 l mole^{-1} cm^{-1})*
Di-β-naphthylthiocarbazone[3]	4.0 at 650 nm
α,α′-Dipyridyl[4]	1.77 at 306 nm
Dithizone (CCl_4)[2]	9.4 at 535 nm
β-PAN[5]	5.6 at 550 nm
5-Br-β-PAN[6]	6.7 at 570 nm
5-Cl-β-PAN	8.4 at 564 nm

TABLE II

EFFECT OF SOLVENTS

(Zinc(II) = $1 \cdot 10^{-6}$ *M*)

Solvents	λ_{max} *(nm)*	*Absorbance*[a]
Carbon tetrachloride	570	0.770
Chloroform	568	0.700
Benzene	568	0.745
Isopropyl ether	565	0.510
Ether	564	0.850
Methyl isobutyl ketone	564	0.735

[a] Values uncorrected for solubility of each solvent in water.

Solvent for extraction

The effect of solvents on the absorbance of the extracted complex was studied. The results obtained are shown in Table II with the maximum absorbance wavelength of each extract. The zinc complex could be extracted with ether, carbon tetrachloride, chloroform, benzene or methyl isobutyl ketone, but the ether extraction method was preferred because of its high effective molar absorptivity.

Absorbance curve

Addition of 5-Cl-β-PAN to a zinc sample solution causes immediate formation of a red water-insoluble precipitate. The absorbance curves of the reagent and its zinc complex in ether are shown in Fig. 1. It can be seen that the absorbance of the reagent alone is very small at the wavelength of maximum absorbance (564 nm) of its zinc complex.

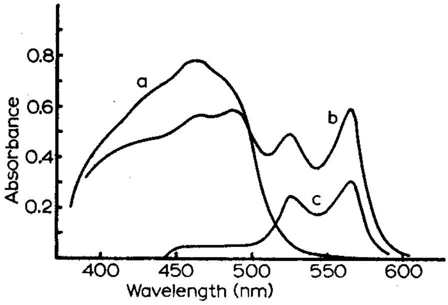

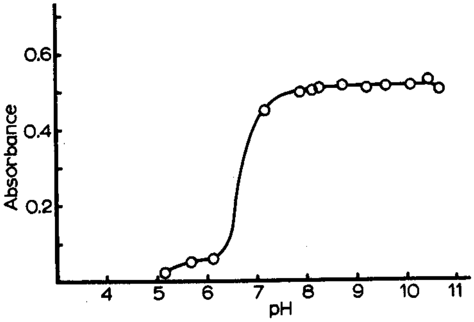

Fig. 1. Absorbance curves of 5-Cl-β-PAN and its zinc complex in ether. (a) 5-Cl-β-PAN (8.5 p.p.m.) *vs.* ether; (b) 5-Cl-β-PAN (8.5 p.p.m.) + 0.39 p.p.m. Zn *vs.* ether; (c) 5-Cl-β-PAN (56.8 p.p.m.) + 0.19 p.p.m. Zn *vs.* reagent blank.

Fig. 2. Effect of pH on ether extraction of the zinc–5-Cl-β-PAN complex. Reagent 56.8 p.p.m., Zn 0.32 p.p.m., $\lambda = 564$ nm.

Optimum pH and amount of reagent

Standard amounts of zinc and 5-Cl-β-PAN solution were buffered at varying pH values. The final pH of each aqueous solution was measured after extraction and the absorbance was measured at 564 nm. A plot of absorbance against pH showed that maximum absorbance was obtained at pH 8–11.0 (Fig. 2); subsequent determinations were carried out at pH 8.5.

The absorbance of a series of solutions containing known amounts of zinc and 0.5–4 ml of $1 \cdot 10^{-3}$ *M* dye solution at pH 8.5 were measured. It was found that 1.5 ml of this dye solution sufficed to complex 5 μg of zinc; with higher concentrations the absorbance was essentially constant.

Colour development, stability and effect of temperature

The minimum time for complete colour development of the complex was found to be 5–10 min at room temperature. The absorbance was then stable for at least 1 h.

Beer's law and sensitivity

The calibration graph proved to be linear over the range 0.05–0.5 p.p.m. of zinc. The effective molar absorptivity for the zinc complex in ether was $8.4 \cdot 10^4$ l mole^{-1} cm^{-1} at 564 nm.

Effect of foreign ions

Numerous cations and anions were examined by applying the method to fixed amounts of zinc in the presence of increasing quantities of the ion being studied (Table III). It is evident that most ions have no effect at the levels studied. Among the cations, interference was caused by cadmium, but amounts about equal to that of zinc did not interfere. The presence of potassium cyanide prevented the reaction of large amounts of metal ions with 5-Cl-β-PAN, so that the proposed method becomes one of the most selective available for the determination of zinc.

TABLE III

EFFECT OF FOREIGN IONS

(3.27 μg zinc taken)

Ion	*Amount added (μg)*	*Zn found (μg)*	*Error (μg)*	*Ion*	*Amount added (μg)*	*Zn found (μg)*	*Error (μg)*
Ag^+	4	3.27	± 0.00	Mn^{2+}	4.7	3.27	± 0.00
	20	3.38	+ 0.11		54	3.57	+ 0.30
Al^{3+}	10	3.22	− 0.05	Ni^{2+}	4	3.74	+ 0.47
	100	2.80	− 0.33		10	3.81	+ 0.54
Bi^{3+}	2	3.24	− 0.03	Pb^{2+}	100	3.27	± 0.00
	10	3.35	+ 0.08		400	3.27	± 0.00
Cd^{2+}	0.2	3.30	+ 0.03	Th^{4+}	2	3.27	± 0.00
	2.2	3.69	+ 0.42		20	3.20	− 0.07
Ce^{3+}	8	3.25	− 0.02	Zr^{4+}	20	3.30	+ 0.03
	40	2.64	− 0.57	NaCl	500 mg	3.27	± 0.00
Co^{2+}	4	3.70	+ 0.43	NaBr	500 mg	3.27	± 0.00
	20	2.23	− 1.04	KI	100 mg	3.27	± 0.00
Cr^{3+}	0.4	2.97	− 0.30		500 mg	3.24	− 0.03
Cu^{2+}	0.3	3.30	+ 0.03	NaF	40 mg	3.27	± 0.00
	3	5.06	+ 1.79		100 mg	3.10	− 0.17
Fe^{3+}	4	3.35	− 0.08	KCN	0.13 mg	3.27	± 0.00
	20	2.78	− 0.49	$Na_2S_2O_3$	100 mg	3.27	± 0.00
Hg^{2+}	4	3.33	+ 0.06		200 mg	3.06	− 0.21
La^{3+}	10	3.10	− 0.17				
Mg^{2+}	100	3.34	+ 0.07	Citric acid	3 mg	3.27	± 0.00
	400	3.45	+ 0.18				
				Tartaric acid	10 mg	3.27	± 0.00

Although potassium cyanide also prevented the formation of the zinc–5-Cl-β-PAN complex, the zinc cyanide complex was readily demasked by addition of formaldehyde. When potassium cyanide was added to zinc(II) and 2 ml of $1 \cdot 10^{-3}$ M reagent solution, it was found that 3 ml of 5% formaldehyde solution was satisfactory for demasking up to 5 μg of zinc; larger amounts of formaldehyde should not be used because of the possibility of demasking interfering ions. Results for zinc in the presence of various ions that normally interfere are shown in Table IV.

Nature of complex

The empirical formula of the complex was studied by the continuous variations and mole ratio methods. A typical plot showed quite unequivocally that a 1:2 Zn:L complex is formed (Fig. 3). Similar results were obtained from mole ratio plots. The apparent stability constant of the 1:1 complex can be estimated by the HILDEBRAND–REILLEY method[7]. The apparent stability constant was thus found to be 7.04 (at 25° in aqueous 50%(v/v) dioxane, $\mu = 0.2$).

TABLE IV

ELIMINATION OF INTERFERENCES BY MASKING

(3.27 μg zinc taken, 2 ml of 10% KCN solution, 3 ml of 5% formaldehyde)

Ion	*Amount added (μg)*	*Zinc found (μg)*	*Error (μg)*
Ag^{+}	2000	3.32	+ 0.05
	3000	3.34	+ 0.07
Cd^{2+}	2.8	3.39	+ 0.12
	5.6	4.64	+ 1.37
Co^{2+}	10	3.38	+ 0.11
	40	3.51	+ 0.24
Cu^{2+}	200	3.27	± 0.00
	400	3.36	+ 0.09
Fe^{3+}	50	3.27	± 0.00
	100	3.09	− 0.18
Hg^{2+}	4000	3.27	± 0.00
	8000	3.36	+ 0.09
Mn^{2+}	15	3.27	± 0.00
	30	3.10	− 0.17
Ni^{2+}	1000	3.27	± 0.00
	2000	3.36	+ 0.09

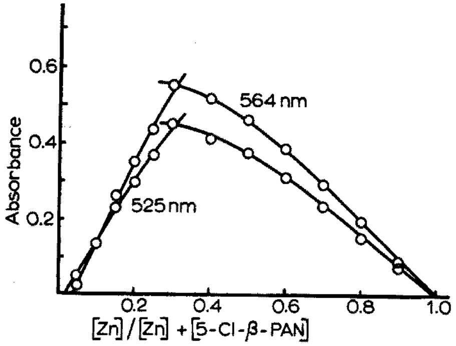

Fig. 3. Composition of the Zn–5-Cl-β-PAN complex. [Zn] + [5-Cl-β-PAN] = $2 \cdot 10^{-5}$ M, pH 8.5.

EXPERIMENTAL

Reagents

5-Cl-β-PAN solution. A methanolic 10^{-3} M solution was prepared from the pure material[1]. This solution was stable for at least three months when stored in an amber bottle.

Buffer solutions. Mixtures of 0.1 M acetic acid–0.1 M sodium acetate, 0.05 M borax–0.2 M boric acid–0.05 M sodium chloride, 0.2 M borax–0.1 M hydrochloric acid, and 0.2 M borax–0.1 M potassium hydroxide were used for pH adjustment.

Standard zinc solution. 0.1309 g of 99.99% zinc metal was dissolved in hydrochloric acid; the solution was fumed with 10 ml of (1+1) perchloric acid solution, cooled and diluted to 250 ml in a volumetric flask with water.

Organic solvents were purified by the usual methods. All other reagents used, including metal solutions and formaldehyde were prepared from high-purity metals or purified chemicals, and all solutions were prepared with twice-distilled water.

Apparatus

Absorbance curves were measured with a Model EPS-3T Hitachi recording spectrophotometer with 1-cm cells; absorbances were measured with a Model 139 Hitachi spectrophotometer with 1-cm cells. A Hitachi M 5 type pH meter was used.

Recommended procedure for the determination of zinc

Transfer an aliquot of the slightly acidic sample solution containing 0.5–5.0 μg of zinc to a 50-ml separatory funnel and dilute to about 20 ml with water. Add 1 ml of 10% (w/v) potassium cyanide solution, mix well, and then add 3 ml of 5% formaldehyde solution. Add 2 ml of methanolic 10^{-3} *M* 5-Cl-β-PAN solution and 5 ml of pH 8.5 buffer solution. Mix and allow the solution to stand for 10 min. Add 10.0 ml of ether, and shake vigorously for 2–3 min. Transfer the organic phase into a glass-stoppered conical flask and dehydrate with anhydrous sodium sulfate. Measure the absorbance at 564 nm in 1-cm cells against a reagent blank carried through the same procedure.

SUMMARY

Zinc(II) reacts with 1-[(5-chloro-2-pyridyl)azo]-2-naphthol (5-Cl-β-PAN) in aqueous solution; the complex can be extracted with various organic solvents at pH 8–11.0 to give a red solution with an absorbance peak at 564–570 nm. The colour in ether is stable and the system conforms to Beer's law; the optimal range for measurement in 1.00-cm cells is 0.05–0.5 p.p.m. zinc in the ether layer. Common anions and cations do not interfere. Large amounts of some cations can be masked by potassium cyanide, the zinc cyanide complex being demasked by formaldehyde. The proposed method is one of the most sensitive and selective procedures for the determination of zinc. The molar absorptivity in the ether extract is $8.4 \cdot 10^4$ l mole^{-1} cm^{-1} at 564 nm.

RÉSUMÉ

Le zinc réagit avec le 1-[(5-chloro-2-pyridyl)azo]-2-naphtol (5-Cl-β-PAN) en solution aqueuse. Le complexe formé peut être extrait dans divers solvants organiques aux pH 8 à 11.0 en donnant une coloration rouge, avec un pic d'absorption à 564–570 nm. La couleur est stable dans l'éther et obéit à la loi de Beer (0.05–0.5 p.p.m. zinc). Les anions et cations communs ne gênent pas. Certains cations peuvent être masqués par le cyanure de potassium; le cyanure complexe de zinc est décomposé par le formaldehyde. Cette méthode est l'une des plus sensibles et sélectives pour le dosage du zinc. Le coefficient d'extinction molaire dans l'éther est de $8.4 \cdot 10^4$ l mole^{-1} cm^{-1}, à 564 nm.

ZUSAMMENFASSUNG

Zink(II) reagiert mit 1-[(5-Chlor-2-pyridyl)azo]-2-napthol (5-Cl-β-PAN) in wässriger Lösung; der Komplex kann mit verschiedenen organischen Lösungsmitteln bei pH 8–11.0 extrahiert werden und ergibt eine rote Lösung mit einem Absorptionsmaximum bei 564–570 nm. Die Färbung in Äther ist stabil; das System gehorcht dem Beerschen Gesetz; der optimale Bereich für Messungen in 1.00 cm-Küvetten ist 0.05–0.5 p.p.m. Zink in der Ätherphase. Die üblichen Anionen und Kationen stören nicht. Grosse Mengen einiger Kationen können mit Kaliumcyanid maskiert werden, wobei der Zinkcyanid-Komplex durch Formaldehyd demaskiert werden muss. Die vorgeschlagene Methode ist eine der empfindlichsten und selektivsten für die Zinkbestimmung. Der molare Extinktionskoeffizient im Ätherextrakt beträgt $8.4 \cdot 10^4$ l mol^{-1} cm^{-1} bei 564 nm.

REFERENCES

1 S. Shibata, M. Furukawa, E. Kamata and K. Goto, *Anal. Chim. Acta*, in press.
2 IUPAC, *Spectrophotometric Data for Colorimetric Analysis*, Butterworths, London, 1963, p. 594.
3 IUPAC, *Spectrophotometric Data for Colorimetric Analysis*, Butterworths, London, 1963, p. 589.
4 W. Berger and H. Elvers, *Z. Anal. Chem.*, 171 (1959) 255.
5 S. Shibata, *Anal. Chim. Acta*, 23 (1960) 367.
6 S. Shibata, K. Goto and E. Kamata, *Anal. Chim. Acta*, 45 (1969) 279.
7 G. P. Hildebrand and C. N. Reilley, *Anal. Chem.*, 29 (1957) 258.

Analytica Chimica Acta
Elsevier Publishing Company, Amsterdam
Printed in The Netherlands

DETERMINATION OF THE MINIMUM SOLUBILITY OF THE NEW CHROMOGENIC REAGENT PALLADIAZO BY A SPECTROPHOTOMETRIC METHOD BASED ON ISOSBESTIC POINTS*

J. A. PÉREZ-BUSTAMANTE AND F. BURRIEL-MARTÍ

Consejo Superior de Investigaciones Científicas, Departamento de Química Analítica, Universidad de Madrid, Facultad de Ciencias, Ciudad Universitaria, Madrid (3) (Spain)

(Received February 5th, 1970)

In connection with the experimental determination of the protonation constants[1] of 1,8-dihydroxynaphthalene-3,6-disulphonic-2,7-bis[azophenyl-*p*-arsonic] acid, which has been synthesized and investigated in detail as a reagent ("palladiazo") for palladium(II)[2-4], it was found that the reagent exhibits unexpectedly complicated behaviour in perchloric acid media of intermediate acidity.

The main difficulties connected with the spectrophotometric study of the protonation behaviour of palladiazo in concentrated perchloric acid[1] derived from the following facts. The reagent absorbance (λ_{max} at 540 and 630 nm) *vs.* acidity functions showed sharp breaks in the $1 \geq$ pH, $H_0 \leq -3$ acidity interval (*ca.* 0.1–6 *M* $HClO_4$). Depending on the order of addition of palladiazo, water and perchloric acid, clear or colloidal solutions were obtained. The colloidal solutions precipitated extensively during 4–24 h whereas the stability of clear solutions was very variable. The formation and stability of colloidal solutions was critically related to the overall reagent concentration, which was always kept very low ($1.25–3.37 \cdot 10^{-5}$ *M*).

It was found that the reagent exhibited "amphoteric" properties, passing through a point of minimum solubility located in the $-0.70 \leq H_0 \leq -2$ (1.6–4.5 *M* perchloric acid) interval; on coagulation of the colloidal solutions, the precipitated reagent could be easily dissolved in both less acidic or more acidic solutions. Outside these acidity limits, the palladiazo solutions showed excellent stability over very long periods within the 0.5–13 pH interval. In different perchloric acid media, the reagent underwent considerable interaction after a few days, and different side-reactions occurred over long periods (>6 months).

The palladiazo molecule forms an octaprotic acid (I).

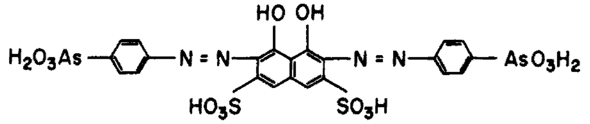

(I)

In addition to the 8 obvious protons, the two azo groups could also bind 2 additional protons in concentrated acid media. The present investigation was aimed at determining the minimum solubility of the palladiazo reagent in perchloric acid media by

---

* Communication presented at the XIV Biennial Meeting of the Spanish Royal Society of Physics and Chemistry, Seville, September–October 1969.

spectrophotometric means exclusively, taking advantage of the isosbestic points shown by the reagent as the acidity of the medium increased.

EXPERIMENTAL

Reagents and apparatus

Aqueous solutions were prepared from palladiazo which was synthesized and purified as described elsewhere[2,5]. The overall purity of the palladiazo was established as 97.2 % by potentiometric titration of the first 4 protons, and as 98.1% from ion-exchange experiments[2]. Infrared spectra[6] and u.v. and visible[2] absorption spectra have been reported.

Merck and U.C.B. 70 % perchloric acid solutions were used without further purification.

A Martin Christ mod. UJ 1 (3,200 r.p.m.) centrifuge with 10-ml Pyrex tubes was used to obtain the clear supernates for spectrophotometric measurements, which were done with a single-beam Beckman Model DU spectrophotometer with 10-mm glass cells.

TABLE I

SUMMARY OF OBSERVATIONS WITHIN THE ACID REGION OF INSTABILITY OF PALLADIAZO–PERCHLORIC ACID SOLUTIONS

Series no.	$c_L \cdot 10^{-5}$	*Order of addition*[a]	*t (°)*	*Remarks*
1	3.37	$HClO_4 + P^b + H_2O$	20–25	Heavy precipitation after 2–3 h in the $-0.1 \leq H_0 \leq -0.4$ (*ca.* 0.7–1.15 *M* $HClO_4$) range
2	2.50	$HClO_4 + H_2O + P$	10–15	Heavy precipitation before 8 h in the $-0.30 \leq H_0 \leq -3.0$ (*ca.* 0.9–6 *M* $HClO_4$) range
3	2.50	$HClO_4 + P + H_2O$	20–25	Occasional precipitation of some samples in the $-0.8 \leq H_0 \leq -1$ (*ca.* 1.85–2.3 *M* $HClO_4$) range in 24 h. No precipitation was observed after 1 month in the $-1 \leq H_0 \leq -3$ (*ca.* 2.3–6 *M* $HClO_4$) range
4[c]	2.50	$HClO_4 + H_2O + P$	20–25	Samples in the $0.1 \leq H_0 \leq -0.6$ range remained stable for 48 h. Samples of acidity $-0.7 \leq H_0 \leq -1.25$ were very unstable particularly for the first 4 h, after which they became colloidal; after 24 h heavy precipitation occurred.
5	1.25	$HClO_4 + P + H_2O$	20–25	No precipitation was observed in the $0.1 \leq H_0 \leq -3$ (*ca.* 0.5–6 *M* $HClO_4$) range during the first 12 days or indeed for several months.

[a] 25–50 ml volumetric flasks were used. The necessary amount of $HClO_4$ was first added followed by H_2O or aqueous 0.1 %palladiazo solution, as stated. Finally the mixture was diluted to volume with water, after cooling and thorough mixing. The process was repeated until the volume remained constant with time.

[b] P = Palladiazo.

[c] Within the first 4 h, anomalous spectra were recorded (see p. 284).

Preliminary investigation of the instability characteristics shown by the palladiazo–perchloric acid–water system

A series of solutions of different overall palladiazo concentrations was prepared in order to study the effect of the order of addition of reagents on the stability of the resultant solutions.

From the summarized observations shown in Table I, the following conclusions can be drawn. The colloidal and precipitation phenomena are particularly pronounced when the solutions are prepared at 10–15°, when the reagent concentration exceeds $1.25 \cdot 10^{-5}$, and when water, acid and palladiazo are added in that order.

Stable palladiazo solutions are pink in moderately acidic media (pH 1) and deep green (different tints) in concentrated perchloric acid ($H_0 \geq -3$). Within the $1 \geq$ pH, $H_0 \leq -3$ range, the solutions progressively change colour from pink through indigo and blue to bluish-green as the acidity increases. After several months, the original colours fade considerably or even disappear, and lilac or yellowish solutions are formed as a result of interaction between palladiazo and perchloric acid to form adducts and/or oxidation products[2].

All the above-mentioned instability factors are due, in our opinion, to the unusual solubility characteristics of the reagent. The colloidal transition phase before appreciable precipitation occurs, can be related to the voluminous structure of the reagent which can undergo self-association through its numerous functional groups to build molecular associates of very high molecular weight as its concentration increases. The semicolloidal nature of various organic reagents, some of which are closely related to palladiazo, has been unequivocally established as a function of their concentration by different physicochemical techniques, *e.g.* thoron[7], alizarin[8], chromotropic acid[9], arsenazo III[10], etc. A knowledge of the colloidal behaviour of a reagent under different conditions is important from both physicochemical and analytical points of view, since self-association and/or colloidal phenomena could lead to erroneous metal : ligand stoicheiometries in fundamental studies.

A detailed spectrophotometric investigation of the system showed the presence of several isosbestic points, indicating the occurrence of successive stepwise protolytic equilibria of the general type:

$$[\mathrm{H}_{8-n}\,\mathrm{L}]^{n-} + \mathrm{H}^+ \rightleftharpoons [\mathrm{H}_{8-n+1}\,\mathrm{L}]^{(n+1)-} \tag{1}$$

(L = fully deprotonated palladiazo molecule)
provided that the spectrophotometric measurements were made under optimal kinetic conditions with regard to solution preparation and time elapsed. The spectra shown in Fig. 1 were obtained under the optimal conditions (see legend) as inferred from many preliminary observations[1]. Figure 1 shows clearly the appearance of a pronounced bathochromic shift (from 630 to 665 nm) accompanied by an intense hyperchromic effect, as the acidity increases from $H_0 \geq -0.4$ to $H_0 \leq -5.25$. These spectral changes are directly related to the protonation of the azo groups[1].

The following points are of importance in the interpretation of the phenomena discussed in this paper. The protonation of the two sulphonic acid groups of the palladiazo molecule can be represented by apparent stability constants $pK_7 \cong 0$ and $pK_8 = -1.46$. By means of tests at extended acidity intervals (in concentrated sulphuric acid media up to an acidity of $H_0 \leq -9$) with a spectrophotometric method

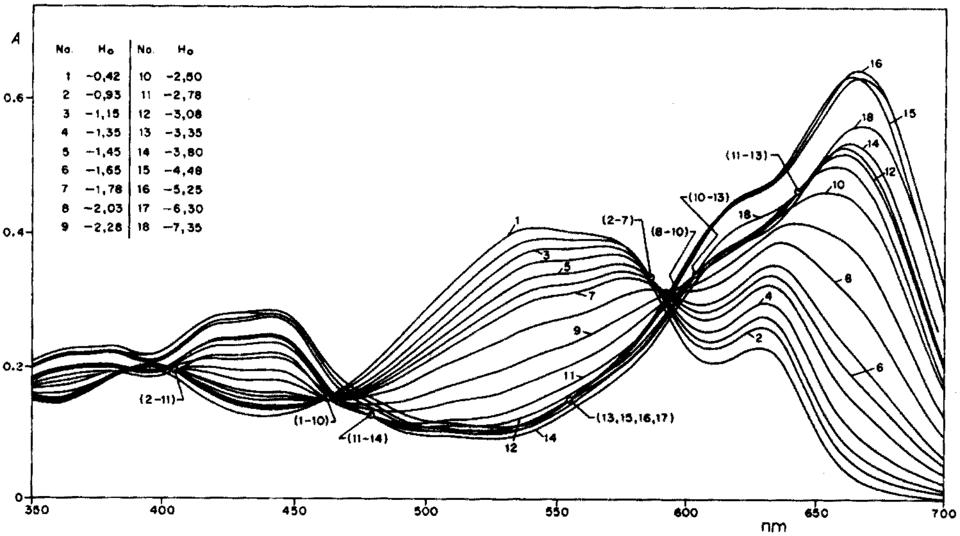

Fig. 1. Absorbance spectra and isosbestic points shown by the palladiazo–perchloric acid–water system. $c_L = 1.25 \cdot 10^{-5}$ M; $\Delta t = 96$ h; 21°; 1-cm cells.

proposed by MUK *et al.*[11], it was concluded that only one of the two azo groups is clearly protonated, the stability constant being $pK_9 = -(2.2 \pm 0.2)$. According to BUDEŠÍNSKÝ[12], the pK_9 and pK_{10} values corresponding to the protonation of the two azo groups in this type of reagent may be so close that the graphical method used to assess the average number of bound protons in very strong acid media cannot distinguish between the successive protonation equilibria. The observed region of instability of the palladiazo solutions lies within the isoelectric acidity interval where the following equilibria take place:

$$[H_7L]^- \underset{-H^+}{\overset{+H^+}{\rightleftharpoons}} [H_8L]^0 \underset{-H^+}{\overset{+H^+}{\rightleftharpoons}} [H_9L]^+ \qquad (2)$$

All the palladiazo–perchloric acid solutions in the acidity interval $-0.7 \leq H_0 \leq -1.8$ show a neat isosbestic point at a wavelength of 580 nm (Fig. 1).

In view of these various observations, an attempt was made to carry out a quantitative spectrophotometric study of the solubility of palladiazo in this acidity interval, in order to decide on the nature of the "amphoteric" palladiazo precipitate.

Spectrophotometric procedure

Two series of palladiazo–perchloric acid solutions containing a ligand concentration of $2.5 \cdot 10^{-5}$ in the acidity interval $-0.4 \leq H_0 \leq -2.7$ were prepared. The solutions were left for 8 days at room temperature to allow establishment of equilibrium between the precipitated phases and the supernates; 10-ml portions of each solution were then centrifuged for 30 min at 2,300 r.p.m., and the absorbances of the supernates were measured at 580 nm against corresponding perchloric acid blank solutions.

The H_0 values were calculated from the analytical c_{H_3O} values (determined by potentiometric titration of the palladiazo–perchloric acid solutions with 1 M sodium

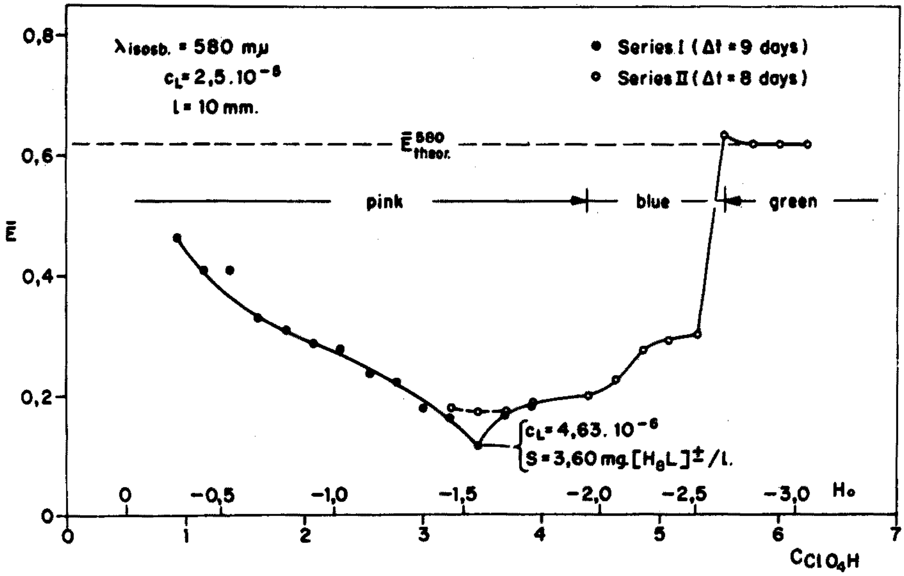

Fig. 2. Graphic determination of the minimum solubility of palladiazo in perchloric acid media, assessed from spectrophotometric measurements at the wavelength of a characteristic isosbestic point. $\lambda_{isosb} = 580$ nm; $c_L = 2.5 \cdot 10^{-5}$ *M*; 1-cm cells. (●) Series I for $\Delta t = 9$ days; (○) Series II for $\Delta t = 8$ days.

hydroxide) by interpolation in the experimental perchloric acid–acidity function[13] established as described by YATES AND WAI[14].

RESULTS

Figure 2 shows the results obtained from the plot of the measured absorbance values of the clear supernates *vs.* the acidity of the medium used. The trend of palladiazo to pass through a region of minimum solubility is clearly evident. Considering the complicated nature of the precipitation and colloidal phenomena involved, the agreement of the results in the two experimental series is reasonably good. The minimum solubility point of palladiazo is located at $H_0 = -1.55$; the solubility of the reagent at this point was calculated as $4.63 \cdot 10^{-6}$ *M*, equivalent to 3.60 mg of palladiazo per l.

Other measurements made in sulphuric acid medium[1] showed that the reagent has then minimum solubility at $H_0 = -1.6 \pm 0.1$, which is further evidence for the unequivocal nature of the process involved.

It is of interest to note that PIŠTĚK *et al.*[10] attempted to determine the solubility of arsenazo III, which is a structural isomer of palladiazo with its phenylarsonic groups in *o,o′*-position to the azo groups, but concluded that the reagent has no defined solubility because of its semicolloidal behaviour.

The minimum solubility value found for palladiazo in perchloric acid media is well below the value $1.25 \cdot 10^{-5}$ *M* which was initially considered as a "safe" concentration to prevent the appearance of the disturbing phenomena described above, for the spectrophotometric studies shown in Fig. 1; it is also much smaller than some of the overall reagent concentrations used for the experiments summarized in

Table I. This seems to indicate clearly the semicolloidal nature of the palladiazo solutions which become increasingly metastable (or quite unstable, depending on the experimental conditions) as the acidity value of minimum solubility is approached.

DISCUSSION

Before sufficient experimental data had been accumulated, it seemed tempting to interpret the observed phenomena by considering the palladiazo species involved in the precipitation processes as a zwitterion, $[H_8L]^{\pm}$, assuming a betaine structure from which hybrid molecules could be formed, as discussed by KÜSTER[15] for methyl orange. The minimum of solubility could then be interpreted in terms of the isoelectric or isoionic point of the zwitterion. The detailed protolytic study of the palladiazo–perchloric acid system[1] showed that the minimum solubility occurs in an acidity interval where neutral $[H_8L]^0$ palladiazo species predominate over the $[H_7L]^-$ and $[H_9L]^+$ complexes. Thus, the extreme instability of the reagent in this acid range and under incorrectly chosen experimental conditions could be understood—at least qualitatively—as derived from the neutralization of the positive and negative formal charges carried by the reagent micelles, to yield hybrid $[H_8L]^{\pm}$ molecules of zero charge, which could undergo the "amphoteric" behaviour implied by the ready dissolution of the precipitated species in either more or less acidic media. However, this interpretation would apply only if the protonation of the two azo groups occurred before the protonation of the sulphonic groups, as was initially thought to be the case. Since palladiazo has two phenolic groups in the *o,o'*-positions to the azo groups, the general azo–hydrazone tautomerism[16] characteristic of *o*-hydroxyazo compounds must also be considered. If all these assumptions apply, the structure of the hypothetical hybrid $[H_8L]^{\pm}$ zwitterion could be described by the tautomeric equilibrium:

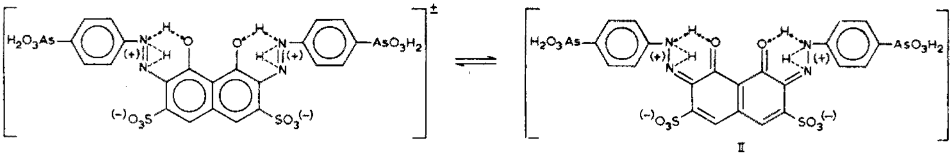

II

implying the formation of an "inner salt".

However, this explanation had to be rejected, because it was later proved that the sulphonic groups are protonated before the azo groups[1]. This indicates that the precipitated reagent molecules cannot be considered as betaine (zwitterion) species but simply as neutral palladiazo molecules, $[H_8L]^0$, whose structure may be expressed by the tautomeric equilibrium

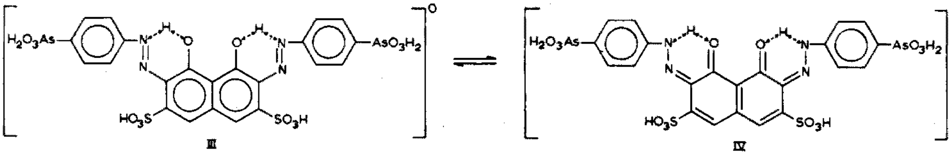

III IV

In this scheme, it is assumed that the protonation of the azo groups occurs stepwise as the acidity of the medium increases, as postulated by SAWICKI[17] for a number of bisazobenzene derivatives. However, the formation of hybrid molecular structures postulated by SAWICKI as a result of the net positive charges of the azo groups after protonation, cannot apply to palladiazo because of the previous protonation of the sulphonic groups, which would lead to neutralization of the corresponding net negative charges.

In the tautomeric equilibria III$\rightleftharpoons$IV, the protonation of the azo groups implies the formation of non-localized hydrogen–azo bonds, as has been concluded by JAFFÉ *et al.*[18–21] to be the case for a number of azobenzene derivatives. JAFFÉ *et al.* postulate that the conjugate acids of azobenzene derivatives formed by protonation do not give rise to a mixture of tautomeric species exhibiting $-NH^+{=}N-$ and $-N{=}NH^+-$ localized bonds, but the proton combines with both nitrogen atoms of the azo group simultaneously. However, the real nature of the hydrogen bonds in these types of compound cannot be considered as definitely established, as implied by the conclusions of GERSON AND HEILBRONNER[22], but rather as a problem awaiting complete elucidation.

Apart from the elucidation of the minimum solubility phenomenon, it is of interest that the semicolloidal nature of this type of reagent can be established solely from spectrophotometric methods based on the properties of protonation step-equilibria (isosbestic points). This finding complements the interpretation of the proton-complex species formed by the reagent in acidic media inferred from other experimental data, such as ion exchange, chromatography, etc.

An immediate practical application of the acidity conditions for minimum solubility for the palladiazo reagent, is in the purification process. Repeated precipitation of synthesized palladiazo from aqueous 3.5 *M* perchloric acid solutions, after redissolution in aqueous sodium hydroxide or carbonate solutions should free the reagent from undesirable monoazo components, structural isomers, degradation products from the coupling process and other impurities which are more soluble than the reagent itself in 3.5 *M* perchloric acid. The purification process can be followed by means of paper or thin-layer chromatography with suitable eluents.

Finally, it is of interest to refer to the fact that, despite earlier statements[23] that *p,p'*-phenyl derivatives of bisazochromotropic acid are of limited analytical utility because of the unsatisfactory stability of their complexes with cations, such reagents have recently been extensively studied [24–26]; some of these reagents exhibit unusual reaction behaviour and can react by three different reaction mechanisms with various elements. The most interesting of these reactions, which might give rise to the formation of complex species (for the alkaline-earth elements) with very high molar absorptivities (*ca.* $2\cdot10^5$) and strong bathochromic shifts (*ca.* 120–160 nm), compared to other bisazo chromotropic acid reagents, are found with *p,p'*-phenyl derivatives containing coplanar substituents; the lack of steric hindrances leads to the formation of very stable dimeric sandwich-type complex ML_2 species[25]. Curiously, some of these *p,p'*-phenyl derivatives homologous to palladiazo show[25,26] the same peculiar qualitative phenomena described in detail here for the palladiazo reagent. From the preliminary qualitative testing for such reagents in the minimum solubility acidity interval, SAVVIN *et al.*[25,26] arrived at conclusions similar to those presented here.

As regards the possibility of the formation of sandwich-type complexes by palladiazo, the predictions of SAVVIN *et al.* appear to be confirmed. No complex species of this kind has so far been found for the different palladiazo reactions investigated (Pd, Ca, Li, Th, rare-earths, Mo(VI), Fe(III), etc.). Seemingly, the bulky non-planar nature of the $-AsO_3H_2$ substituents, *p,p'* to the phenyl groups of palladiazo, rules out the possibility of the reagent forming sandwich-type metal complexes.

However, the appearance of "anomalous" spectra referred to explicitly by SAVVIN *et al.*[24-26] in the acidity region of minimum reagent solubility, was observed early in the palladiazo work[2], and complicated the spectrophotometric studies under these conditions. As a result, the work described above was done in order to establish experimental conditions which would allow stable palladiazo–perchloric acid solutions to be obtained.

The authors express their warmest thanks to the Directorate of Chemistry and Isotopes of the Spanish Atomic Energy Commission for their kind interest in the preparation of the diagrams connected with this work.

SUMMARY

The instability characteristics of various 1,8-dihydroxynaphthalene-3,6-disulphonic-2,7-bis[azophenyl-*p*-arsonic] acid (palladiazo) solutions in different perchloric acid media have been studied in detail. Isosbestic points corresponding to stepwise protonation equilibria were utilized in a spectrophotometric method for determining the minimum solubility of palladiazo. The minimal solubility ($4.63 \cdot 10^{-6}$ *M*; 3.6 mg l^{-1}) was found at an acidity value $H_0 = -1.55$ (*ca.* 3.5 *M* perchloric acid). The semicolloidal nature of the reagent was established. The most probable nature and structure of the precipitated palladiazo species are discussed. The experimental conditions for minimal solubility are valuable for purification of the reagent.

RÉSUMÉ

Une étude détaillée est effectuée sur diverses solutions d'acide 1,8-dihydroxynaphtalène-3,6-disulfonique-2,7-bis[azophényl-*p*-arsonique] (palladiazo), en milieu acide perchlorique. La solubilité minimale du palladiazo $4.63 \cdot 10^{-6}$ *M* (3.6 mg l^{-1}) est obtenue à une acidité de -1.55 (H_0), correspondant environ à un $HClO_4$ 3.5 *M*. Les conditions expérimentales pour une solubilité minimale sont très intéressantes pour la purification du réactif.

ZUSAMMENFASSUNG

Die Instabilitätseigenschaften verschiedener 1,8-Dihydroxynaphthalin-3,6-disulfon-2,7-bis[azophenyl-*p*-arson]-säure-(Palladiazo)-Lösungen in perchlorsaurem Medium sind im einzelnen untersucht worden. Die zu den stufenweisen Protonisierungsgleichgewichten gehörenden isosbestischen Punkte wurden bei einer spektrophotometrischen Methode zur Bestimmung der minimalen Löslichkeit von Palladiazo benutzt. Diese betrug $4.63 \cdot 10^{-6}$ *M* (3.6 mg l^{-1}) bei einem Aciditätswert $H_0 = -1.55$ (*ca.* 3.5 *M* Perchlorsäure). Es wurde festgestellt, dass das Reagenz semikolloid ist. Beschaffenheit und Struktur des gefällten Palladiazo werden diskutiert. Die experimentellen Bedingungen für minimale Löslichkeit sind für die Reinigung des Reagenzes wichtig.

REFERENCES

1 J. A. PÉREZ-BUSTAMANTE AND F. BURRIEL-MARTÍ, *Talanta*, to be published.
2 J. A. PÉREZ-BUSTAMANTE AND F. BURRIEL-MARTÍ, *Anal. Chim. Acta*, 37 (1967) 49; J. A. PÉREZ-BUSTAMANTE, *Doctoral Thesis*, Madrid, 1967.
3 J. A. PÉREZ-BUSTAMANTE, C. MORELL GARCÍA AND F. BURRIEL-MARTÍ, *Anal. Chim. Acta*, 44 (1969) 95.
4 L. BOCANEGRA SIERRA, *Doctoral Thesis*, Madrid, 1969.
5 J. A. PÉREZ-BUSTAMANTE AND F. BURRIEL-MARTÍ, *Inform. Quím. Anal. (Madrid)*, 22 (1968) 25, 31.
6 J. A. PÉREZ-BUSTAMANTE AND R. PARELLADA BELLOD, *An. Quím.*, 64B (2) (1968) 213.
7 S. P. SANGAL AND A. K. DEY, *J. Sci. Ind. Res. (India)*, 21B (12) (1962) 600.
8 A. K. MUKHERJI AND A. K. DEY, *Kolloid.-Z.*, 158 (2) (1958) 147.
9 S. P. SANGAL, *Bull. Chem. Soc. Japan*, 36 (1963) 1349.
10 P. PIŠTĚK, J. RAIS AND M. KYRŠ, *Z. Phys. Chem.*, 232 (1966) 103.
11 A. MUK AND R. T. RADOSAVLJEVIĆ, *Bull. Boris Kidrich Inst. Nucl. Sci.*, 17 (1) (1966) P/370.
12 B. BUDĚŠÍNSKÝ, personal communication.
13 L. P. HAMMETT AND A. J. DEYRUP, *J. Am. Chem. Soc.*, 54 (1932) 2721.
14 K. YATES AND H. WAI, *J. Am. Chem. Soc.*, 86 (1964) 5408.
15 F. W. KÜSTER, *Z. Anorg. Chem.*, 13 (1897) 135; *Jahrb. Chem.*, 7 (1898) 64.
16 H. ZOLLINGER, *Chemie der Azofarbstoffe*, Birkhäuser Verlag, 1958.
17 E. SAWICKI, *J. Org. Chem.*, 23 (1958) 532.
18 J. H. COLLINS AND H. H. JAFFÉ, *J. Am. Chem. Soc.*, 84 (1962) 4708.
19 H. H. JAFFÉ AND R. W. GARDNER, *J. Am. Chem. Soc.*, 80 (1958) 319.
20 SI-YUNG YEH AND H. H. JAFFÉ, *J. Am. Chem. Soc.*, 81 (1959) 3279, 3283.
21 M. ISAAKS AND H. H. JAFFÉ, *J. Am. Chem. Soc.*, 86 (1964) 2209.
22 F. GERSON AND E. HEILBRONNER, *Helv. Chim. Acta*, 41 (1958) 1444.
23 S. B. SAVVIN AND YU. M. DEDKOV, *Zh. Analit. Khim.*, 19 (1964) 21.
24 S. B. SAVVIN AND T. V. PETROVA, *Zh. Analit. Khim.*, 24 (1969) 177, 490.
25 S. B. SAVVIN, E. L. KUZIN, T. V. PETROVA AND N. KHAKIMKHODZHAEV, *Zh. Analit. Khim.*, 24 (1969) 1325.
26 S. B. SAVVIN, T. V. PETROVA AND N. KHAKIMKHODZHAEV, *Zh. Analit. Khim.*, 24 (1969) 1460.

Analytica Chimica Acta
Elsevier Publishing Company, Amsterdam
Printed in The Netherlands

THE DETERMINATION OF INDIUM IN SEA WATER

A. D. MATTHEWS* AND J. P. RILEY
Department of Oceanography, The University, P.O. Box 147, Liverpool L69 3BX (England)

(Received March 2nd, 1970)

The crustal abundance of indium is very low and has been estimated by SHAW[1] to be *ca.* 0.11 p.p.m. Little is known about its occurrence in natural waters. IKEDA[2] has claimed that he has found 0.1–1.0 μg l^{-1} in spring waters spectrographically—a figure which seems suspiciously high when its low abundance and its geochemical properties are considered. Indium has been determined fluorimetrically in subterranean waters after concentration by coprecipitation with iron(III) hydroxide[3]. The element does not yet appear to have been detected in sea water, although SHAW[1] has attempted unsuccessfully to detect it spectrographically in the residues from the evaporation of sea water. BARIĆ AND BRANICA[4] have used pulse polarography and anodic stripping polarography to study the concentration of indium remaining in supernates from the precipitation of indium hydroxide at various pH values. They have concluded that the concentration of indium in sea water of pH 8 should be *ca.* 10^{-10} M.

In view of the very low concentration at which indium is likely to occur in sea water, it is necessary to carry out a preliminary concentration before determining it. Even so, since it is often inconvenient to collect samples greater than 15 l it is necessary to use a method for the determination which is capable of detecting 0.5 ng or less. A review of the literature suggested that only neutron activation analysis[5–12] and perhaps isotope dilution[13] techniques would have the required sensitivity. The present paper describes a neutron activation procedure for the determination of indium in sea water.

The irradiation with thermal neutrons of indium-115, which constitutes 95.7% of natural indium, simultaneously produces two short-lived nuclides, ^{116m}In and ^{116}In. Since the capture cross-section of ^{115}In in the reaction ^{115}In(n, γ)^{116m}In is very great (145 barns) a very high sensitivity could be attained by means of the activation product of this nuclide. However, the half-life of ^{116m}In is too short (54 min) to permit the use of the lengthy radiochemical separations which would be necessary in the analysis of sea water. In contrast, irradiation of indium-113 (isotopic abundance 4.3%) gives rise to a comparatively long-lived nuclide ^{114m}In ($T_{\frac{1}{2}}$ 49 days), which undergoes an internal transformation to ^{114}In ($T_{\frac{1}{2}}$ 72 sec). When equilibrium has been established, indium can be determined by counting the 1.98-MeV β-radiation of this daughter. Counting of this nuclide was used in the present work, although the sensitivity is less than 1/20 of that which can be attained if the activity of the short-lived indium-116m is measured.

---

*Present address: Unilever Research Limited, Greyhope Road, Aberdeen.

Preconcentration of indium

The concentration of indium in sea water is so low that even with the highly sensitive neutron activation technique a preconcentration stage is essential. In order to obviate the need for storage of samples, with the attendant risk of contamination or losses by adsorption[14], the method of concentration should be suitable for use on board ship. For this reason ion-exchange procedures were investigated.

Tests showed that the retention of indium from acidified sea water medium by the strongly basic anion exchanger Deacidite FF (100–200 mesh) was far from quantitative. Indeed, the maximum uptake (80%) by a 0.6 × 7.5 cm column of the resin only occurred from sea water which was 6 *M* with respect to hydrochloric acid. For this reason, work on the use of anion exchange for the preconcentration of indium was abandoned.

RILEY AND TAYLOR[15] have shown that many trace metals can be quantitatively concentrated from sea water by adsorption onto chelating ion-exchange resins, from which they can be removed by elution with dilute nitric or hydrochloric acid. The possibility of using a resin of this type for the preconcentration of indium was therefore investigated. Dowex A1 (50–100 mesh) was selected for this purpose; this resin is cross-linked polystyrene substituted with iminodiacetic acid groups. The uptake of indium from 1-l aliquots of sea water by 17 × 1.2 cm columns of the sodium form of this resin was therefore investigated radiochemically using ^{114m}In as tracer. It was found that only *ca.* 20% of the indium was retained at pH 7.0, but that the efficiency of retention increased rapidly as the pH was raised; 99% being absorbed at pH 9.2 (Table I). Adsorbed indium could be eluted quantitatively with 150 ml of 3 *M* hydrochloric acid, the element being present in the final 100-ml fraction of the acid. Further radiochemical tests showed that retention of indium was still quantitative, even when 20-l samples of sea water were used. Chelating ion exchange was therefore adopted for the preliminary concentration of indium.

TABLE I

ADSORPTION OF INDIUM FROM SEA WATER BY DOWEX A1 AS A FUNCTION OF pH

pH	7.0	8.1	8.5	9.0	9.2
Percentage adsorbed	21	30	70	95	99

It was found that the hydrochloric acid eluate from the Dowex A1 column contained milligram amounts of sodium, potassium, magnesium and calcium. Since this made it impossible to evaporate the eluate to a sufficiently small volume to permit it to be transferred quantitatively to a silica irradiation ampoule, it proved necessary to remove these elements before carrying out the neutron activation. It was thought that their removal might be readily achieved by anion exchange from a hydrochloric acid medium. Under these conditions indium tends to form a chloro-anion and is somewhat weakly retained by strongly basic anion exchangers; the maximum distribution coefficient (10) occurring in 3 *M* hydrochloric acid solution[16]. In contrast, neither the alkali nor alkaline earth elements are held by such exchangers as they do not form chloro-anions. Experiments showed that indium could be completely retained by a 30×0.4 cm column of Dowex AG2-X8 (200–400 mesh) during the passage of the 100 ml of 3 *M* hydrochloric acid eluate from the Dowex A1 column, followed by washing with a further 50 ml of 3 *M* hydrochloric acid. The percolate and washings contained 98% of the alkali and alkaline earth elements present in the original eluate. Indium could then be recovered quantitatively by elution of the anion exchanger with 120 ml of 0.1 *M* hydrochloric acid. This anion-exchange separation scheme was therefore adopted for use in conjunction with the preliminary concentration stage with Dowex A1. It was observed radiochemically that the overall recovery of indium from 20-l samples exceeded 98% at concentration levels of the order of nanograms per litre.

Neutron activation of the indium concentrate

Following the preconcentration stage the indium is submitted to irradiation with thermal neutrons. Since the amount of indium is very small (*i.e.* 1–3 ng) the activation must be carried out for several weeks even at a flux of $5 \cdot 10^{12}$ n cm^{-2} sec^{-1} in order to obtain sufficient induced activity for precise counting, and to enable the radiochemical purity of the indium-114 to be checked.

Radiochemical separation scheme

The two ion-exchange procedures used in the preconcentration stage suffice to separate indium from all the major elements in the sea water. Many minor elements are also separated from it, including uranium which, on irradiation with thermal neutrons, undergoes fission to a wide range of radionuclides. However, some trace elements (*e.g.* zinc and silver) which are not only adsorbed by Dowex A1, but which also form relatively stable chloro-anions, are also concentrated to some extent along with the indium. Most of these elements, and others which are contaminants in the reagents used, are present in amounts several orders of magnitude greater than the indium. This has necessitated the use of a rather complicated multistage process to separate the low level of indium-114 activity from the activities arising from these impurities. The most important stages in the separation process are carried out by solvent extraction methods which have been shown by other workers to give very favourable decontamination factors for indium. Following the work of SUNDERMAN *et al.*[17], indium is separated by extraction of its bromide from 4.5 *M* hydrobromic acid with diethyl ether, and also by extraction of its complex with thenoyltrifluoroacetone using benzene. In addition, an iodide extraction stage is also included in the scheme since this has been shown to be highly selective for indium[18,19]. The indium is finally precipitated as its 8-hydroxyquinoline derivative for determination of the chemical yield, and for β-counting. The overall yield of the separation process averages $60 \pm 3\%$. The decontamination factor of the process is high, since no trace of β- or γ-activities other than those of indium-114 were detected in the final precipi tate, even when the procedure was used for the separation of indium-114 activity from irradiated deep sea sediments.

EXPERIMENTAL

Neutron activation of samples was carried out in the Dido reactor at Harwell in a flux of $5 \cdot 10^{12}$ n cm^{-2} sec^{-1}. β-Counting of the 8-hydroxyquinoline derivative of indium was performed using an end-window Geiger Muller counter coupled to an Ekco scaler (Type N530F).

All water and acids used in the analysis were purified by distillation through a silica still. Ammonia solution (1 *M*) was prepared by dilution of 6 *M* ammonia solution which had been purified by isothermal distillation.

Ion-exchange columns

Chelating ion-exchange column. Pack a 1.2-cm diameter ion-exchange column to a depth of 17 cm with Dowex A1 (50–100 mesh) and wash it successively with 150 ml of 3 *M* hydrochloric acid, 100 ml of distilled water, 100 ml of 2 *M* sodium hydroxide and 100 ml of distilled water.

Anion exchanger. Pack a 4-mm diameter ion-exchange column to a depth of 30 cm with Dowex AG2-X8 (200–400 mesh), wash it with 50 ml of 0.1 *M* hydrochloric acid, and then with 50 ml of 3 *M* hydrochloric acid.

Reagents

Potassium hydrogen phthalate buffer. Mix 40 ml of 0.1 *M* hydrochloric acid with 50 ml of 0.1 *M* potassium hydrogen phthalate and dilute to 100 ml. The buffer has a pH value of 2.4.

Acetate buffer. Dissolve 272 g of sodium acetate trihydrate in distilled water, add 60 ml of acetic acid and dilute to 1 l.

Procedure

Preconcentration of indium. It is probably preferable not to filter clear oceanic water samples, but inshore waters should be filtered through a 0.45-μm membrane filter immediately after collection. Commence the analysis within an hour of collecting the sample by adjusting the sample to pH 9.2 by cautious addition of 1 *M* ammonia solution and then allowing it to flow at a rate of 4–5 ml min^{-1} through the column of Dowex A1. Wash the column with 100 ml of water and elute the indium and other adsorbed ions with 150 ml of 3 *M* hydrochloric acid. Reject the percolate, washings and the first 50 ml of the 3 *M* hydrochloric acid. Collect the next 100 ml of eluate and pass it through the column of Dowex AG2-X8. Wash the column with 50 ml of 3 *M* hydrochloric acid and reject the percolate and washings. Elute indium with 120 ml of 0.1 *M* hydrochloric acid. Discard the first 25 ml of eluate, and collect the remaining 95 ml in a silica conical flask. Place a bulb-stopper in the neck of the flask and slowly evaporate the liquid to *ca.* 1.5 ml on a hot plate. Transfer the remaining liquid quantitatively to a 5 × 0.4 cm silica irradiation ampoule having a constriction at its open end. Place the ampoule in an oven at 90° and evaporate its contents to *ca.* 0.2 ml, taking care to avoid contamination. Run a blank in the same manner through the whole process but omitting the sample.

Irradiation. Irradiate the sealed ampoule in a flux of $5 \cdot 10^{12}$ n cm^{-2} sec^{-1} for 4 weeks. Irradiate along with it a silica ampoule containing the blank and others containing known weights of indium (1.0 and 2.0 ng) dissolved in 0.2 ml of 1 *M* nitric acid. After irradiation allow the ampoules and their contents to cool for 2 days before commencing the radiochemical separation.

Radiochemical separation. Cool the ampoules in liquid nitrogen and open them at the constriction. Allow them to come to room temperature and transfer their contents quantitatively to 50-ml silica beakers using small volumes of concentrated hydrochloric acid. Add 3 ml of indium carrier solution (15 mg In) to each and heat to boiling to bring about equilibration. After cooling, dilute to *ca.* 30 ml and precipitate the hydroxides by addition of a slight excess of 4 *M* ammonia solution. Separate the precipitate by centrifugation and wash it with 0.5% (w/v) ammonium nitrate solution. Discard the supernatant liquid and washings. Dissolve the precipitate in 2 *M* hydrochloric acid and repeat the ammonia precipitation.

Dissolve the hydroxide precipitate in 11 ml of 48%(w/w) hydrobromic acid and add 9 ml of water. Extract the solution, which should now be 4.5 *M* with respect to hydrobromic acid, with two 25-ml aliquots of diethyl ether. Wash the combined organic extracts with two 5-ml portions of 4.5 *M* hydrobromic acid and discard the acid phases. Back-extract indium from the ether phase by equilibrating with three successive 5-ml aliquots of 6 *M* hydrochloric acid. Add 10 mg of iron in the form of iron(III) chloride as a carrier to the hydrochloric acid and extract with three 15-ml aliquots of diethyl ether. Discard the organic layer. Evaporate the lower layer to *ca.* 1 ml, bring the pH to 2–3 by cautious addition of 2 *M* sodium hydroxide and add potassium hydrogen phthalate buffer to a final volume of 20 ml. Extract indium from this solution by shaking for 5 min with 20 ml of a 0.5 *M* solution of thenoyltrifluoroacetone in benzene. Discard the aqueous phase and back-extract indium from the benzene phase using three 5-ml aliquots of 0.01 *M* hydrochloric acid. Combine the aqueous extracts and add a slight excess of 1 *M* ammonia solution. Separate the precipitated indium hydroxide by centrifugation and wash it with 0.5% ammonium nitrate solution.

Dissolve the precipitate in 20 ml of 1.5 *M* hydriodic acid and extract indium with 20 ml of diethyl ether. Wash the ether phase with two 5-ml aliquots of 1.5 *M* hydriodic acid. Transfer the ether phase to a beaker containing 10 ml of 0.1 *M* hydrochloric acid and evaporate the ether on the water bath. Add a slight excess of 2 *M* ammonia to the solution. Separate the precipitated indium hydroxide by centrifugation and wash it with 0.5% ammonium nitrate solution. Dissolve the precipitate in 4 drops of concentrated hydrochloric acid and dilute to 15 ml with water. Add 2 ml of a 5% (w/v) alcoholic solution of 8-hydroxyquinoline, heat to 50–60° and add gradually 5 ml of the acetate buffer. Filter the precipitated indium–8-hydroxyquinoline complex on a tared 1.5-cm Whatman GF/B filter pad. Place the filter and precipitate on a tared planchette and dry at 110°. Weigh the filter and planchette to determine the chemical yield of the separation process. Measure the activities of the sample and blank with a low-background Geiger counter fitted with anti-coincidence circuitry, and compare its activity with that of the standards. Confirm the identity and purity of the separated indium-114 activity by plotting its decay and aluminium absorption curves, and by γ-spectrometry.

RESULTS

The precision of the method was tested by carrying out 5 replicate analyses on 10-l samples of sea water from the Menai Straits. These were found to contain 1.20 ± 0.06 ng of indium per litre, corresponding to a coefficient of variation of *ca.* ±5%. The accuracy of the procedure was checked by analysing 20-l aliquots of sea water, both alone and after spiking with 25 ng of indium. This showed an indium re-

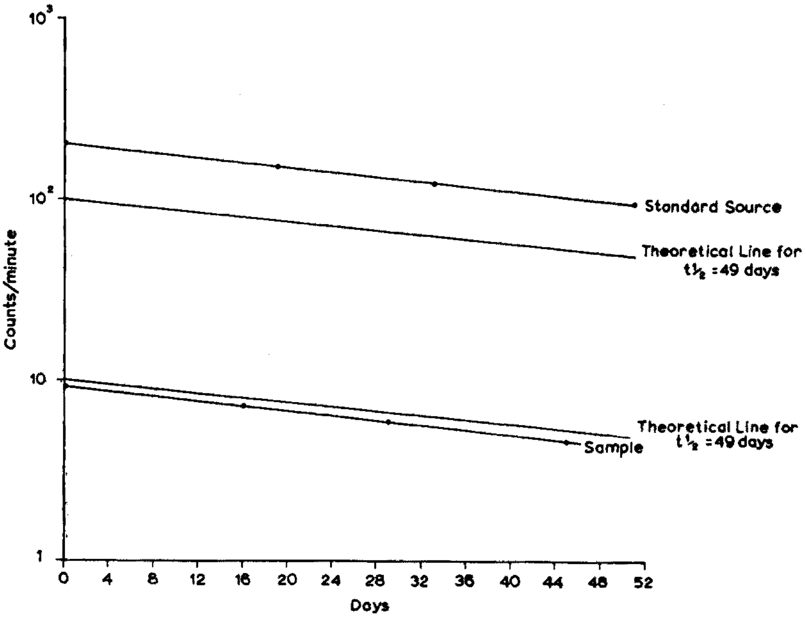

Fig. 1. Half-life determination for separated indium-114 activity from sea water taken at a depth of 2 m at Discovery Station 6917.

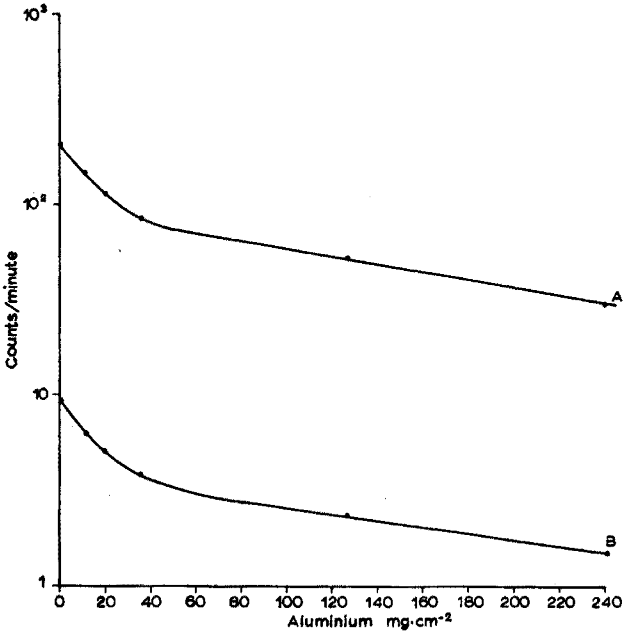

Fig. 2. Aluminium absorption curves for separated indium-114 activity. (A) Indium standard; (B) sea water from a depth of 2 m at Discovery Station 6917.

covery of 94%. The blank for the method amounted to 0.03 ng. If the sensitivity of the method is defined as the weight (in ng) of indium which will give a count of 10 d.p.m. above background then the sensitivity of the present procedure is 0.01 ng.

In order to establish the concentration level of indium in ocean waters, 15-l samples were collected at four depths at a station off the west coast of Africa during a cruise of R.R.S. Discovery in April 1969. The analyses of these samples are shown in Table II. The average concentration of indium (*ca.* 0.1 ng/l) is only about 1/100 of that predicted by BARIĆ AND BRANICA[4], which suggests that the solubility of indium hydroxide is not the factor limiting the indium concentration in sea water*.

Tests were made to confirm the identity and purity of the indium-114 activity separated from one of the activated samples. The decay curve (Fig. 1) showed the half-life to be 49±2 days; this agrees well with the literature value of 49 days[20]. The aluminium absorption curve of the separated activity was identical with that of indium-114 (Fig. 2) showing that there was no gross contamination of the isolated activity by pure β-emitters. The γ-spectrum of the separated activity was determined with a Ge(Li) detector associated 1024-channel analyzer. It showed peaks at 0.192 and 0.556 MeV arising from indium-114; no other peaks were present, demonstrating the absence of other γ-emitting radionuclides.

TABLE II

DETERMINATION OF INDIUM IN SEA WATER AT DISCOVERY STATION 6917 (23°00'N, 18°42'W; depth 3100 m)

Sampling depth (m)	2	500	1000	2000
Indium concentration (ng l^{-1})	0.31	0.12	0.10	0.11

SUMMARY

A chelating ion-exchange technique is used for the concentration of indium from sea water. After purification by chloro-anion exchange, the separated indium is determined by neutron activation analysis. The concentration of indium in Atlantic Ocean water was found to be *ca.* 0.1 ng l^{-1}. The method has a sensitivity of 0.006 ng l^{-1}.

RÉSUMÉ

Une technique par échangeur d'ions, complexant, est proposée pour concentrer l'indium de l'eau de mer. Après purification par échangeur chloroanionique, l'indium séparé est dosé par analyse par activation neutronique. La concentration en indium de l'eau de l'Océan Atlantique est d'environ 0.1 ng l^{-1}. La sensibilité de cette méthode est de 0.006 ng l^{-1}.

---

* Note added in proof. CHOW AND SNYDER (*Earth Planet. Sci. Lttrs.*, 7 (1969) 221) have very recently found an average of 4 ng of indium per litre in water from the Pacific Ocean using an isotope dilution technique. The reason for the discrepancy between the two sets of results is not known. However, it may be significant that the isotope dilution technique was being used very near to its estimated detection limit (2 ng l^{-1}), and in fact *ca.* 40 ng of ^{115}In l^{-1} was being added in the ^{113}In-enriched spike used in the analysis.

ZUSAMMENFASSUNG

Für die Anreicherung von Indium in Seewasser wird ein Verfahren des chelatisierenden Ionenaustausches angewendet. Nach Reinigung durch Anionenaustausch wird das abgetrennte Indium durch Neutronenaktivierungsanalyse bestimmt. Die Indiumkonzentration in Wasser des Atalantischen Ozeans wurde zu *ca.* 0.1 ng l^{-1} ermittelt. Die Methode hat eine Empfindlichkeit von 0.006 ng l^{-1}.

REFERENCES

1 D. M. Shaw, *Geochim. Cosmochim. Acta*, 2 (1952) 185.
2 N. Ikeda, *J. Chem. Soc. Japan, Pure Chem. Sect.*, 74 (1953) 91.
3 E. P. Mulikovskaya, *Zh. Khim. Abstr.*, No. 21G164 (1967).
4 A. Barić and M. Branica, *Limnol. Oceanog.*, 14 (1969) 796.
5 T. B. Pierce and P. F. Peck, *Analyst*, 86 (1961) 580.
6 A. A. Smales, J. R. Smith and H. Irving, *Analyst*, 82 (1957) 539.
7 O. Johansen and E. Steinnes, *Talanta*, 13 (1966) 1177.
8 H. Jaskólska and J. Minzewski, *Acta Chim. Acad. Sci. Hung.*, 32 (1962) 9.
9 H. Hamaguchi, *Japan Analyst*, 16 (1967) 1233.
10 F. E. Gleit, P. A. Benson and W. D. Holland, *Anal. Chem.*, 36 (1964) 2067.
11 A. A. Abdullaev, *Zh. Analit. Khim.*, 15 (1960) 70.
12 J. Ruzicka and J. Stary, *Talanta*, 10 (1963) 981.
13 J. Ruzicka and J. Stary, *Talanta*, 11 (1964) 691.
14 D. E. Robertson, *Anal. Chim. Acta*, 42 (1968) 533.
15 J. P. Riley and D. Taylor, *Anal. Chim. Acta*, 40 (1968) 479.
16 K. A. Kraus, F. Nelson and G. W. Smith, *J. Phys. Chem.*, 58 (1954) 11.
17 D. N. Sunderman, I. B. Ackerman and W. W. Meinke, *Anal. Chem.*, 31 (1959) 40.
18 S. Kitahara, *Bull. Inst. Phys. Chem. Res. (Tokyo)*, 24 (1948) 454.
19 H. M. Irving and F. J. C. Rossotti, *Analyst*, 82 (1952) 549.
20 G. Friedlander and J. W. Kennedy, *Nuclear and Radiochemistry*, Wiley, New York, 1955, p. 426.

Analytica Chimica Acta
Elsevier Publishing Company, Amsterdam
Printed in The Netherlands

A STUDY OF SUGAWARA'S METHOD FOR THE DETERMINATION OF IODINE IN SEA WATER

A. D. MATTHEWS AND J. P. RILEY
Department of Oceanography, The University, P.O. Box 147, Liverpool L69 3BX (England)

(Received March 2nd, 1970)

Iodine appears to occur in the sea mainly in the form of iodate and iodide ions[1,2], but minor amounts of organo-iodine compounds may also be present. There are considerable variations in the published figures for the total concentration of the element in sea water, values ranging from 7–118 μg l^{-1} having been reported[3,4] in the last 15 years. It is not known whether these differences are real and arise from processes occurring in the oceans, or whether they reflect inadequacies in the analytical methods used. As a preliminary to an investigation of the problem, it was thought to be desirable to develop accurate methods for the determination of iodide- and iodate-iodine in sea water.

A survey of the literature suggested that the procedures which have been described for the direct estimation of these ions in sea water[4-11] were unlikely to give the ±1% precision sought. It was thought that the method described by SUGAWARA AND TERADA[3,12] would give a greater prospect of success. In this process, iodide is concentrated from a fairly large volume of sea water by coprecipitation with silver chloride. The precipitate is digested with bromine water; this leads to the oxidation of the iodide to iodate. After an intermediate stage, designed to remove any hypobromite, the iodate is allowed to react under acidic conditions with excess iodide ion and the iodine thus produced (6 atoms per atom present in the original sample) is determined photometrically as the starch–iodine chromogen. Total inorganic iodine can be determined in the same way if iodate is reduced to iodide before carrying out the coprecipitation. In order to assess the potentialities of this method the efficiency of the various processes involved in it were investigated.

Coprecipitation of iodide

In the method of SUGAWARA AND TERADA the coprecipitation is carried out by treating the sea water sample (500 ml) with sufficient silver nitrate solution to precipitate 2% of the chloride present. The sample is then acidified with 2 ml of 3 *M* sulphuric acid to assist coagulation. The efficiency of this process was tested radiochemically using iodide labelled with ^{125}I. It was found that even with vigorous agitation and slow addition of silver nitrate the coprecipitation of iodide never exceeded 90%, and that the recovery could not be increased above this value, even if sufficient silver nitrate was added to precipitate 4% of the chloride present (Fig. 1).

Although this mode of coprecipitation proved unsatisfactory, it was considered that quantitative coprecipitation might be achieved if the silver ions could be added sufficiently slowly for them to be homogeneously distributed. It was thought that one way of doing this would be to add to the water a slightly soluble silver salt. The use of silver citrate (solubility 0.28 g l^{-1} at 18°) for this purpose was therefore investigated. Aliquots (500 ml) of sea water were spiked with *ca.* 0.2 μCi of carrier-free iodide-125, and sufficient finely powdered (< 180 mesh) silver citrate was added to precipitate various proportions of the chloride. The samples were agitated both mechanically and ultrasonically for 30 min. Each sample was acidified with 2 ml of 3 *M* sulphuric acid to assist the precipitate to coagulate. After 24 h, the precipitate was separated by centrifugation and the recovery of iodine was assessed by comparison of the γ-activity of the precipitate with that of an appropriate standard. It was found (Table I) that iodide was completely coprecipitated even when the amount of silver citrate added was only sufficient to precipitate 0.25% of the chloride present. This coprecipitation technique was therefore adopted for all subsequent work, sufficient silver citrate (0.23 g per 500 ml) being added to precipitate 0.5% of the chloride present in the sample. Tests showed that less than 0.1% of the iodate-iodine present in the sea water was coprecipitated under these conditions. Iodate-iodine could be coprecipitated with an efficiency of 99.5±0.3% if, before the addition of

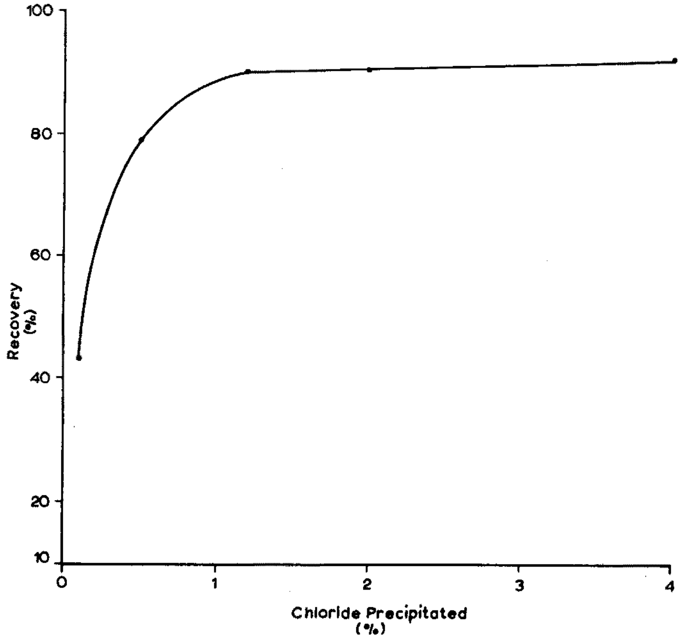

Fig. 1. Percentage coprecipitation of iodide from sea water by silver chloride as a function of the percentage of chloride precipitated.

TABLE I

COPRECIPITATION OF IODIDE FROM SEA WATER USING SILVER CITRATE

Chloride precipitated (%)	0.25	0.5	1.0	2.0
Iodide precipitated (%)	99.7	99.0	99.9	99.7

silver citrate, it was reduced to iodide by means of 4 ml of a saturated solution of hydrazine sulphate.

Oxidation of coprecipitated iodide to iodate

In the method of SUGAWARA AND TERADA the coprecipitated iodide is oxidized to iodate by stirring the silver chloride precipitate in a chloride medium with 15 ml of bromine water, and then warming to remove the excess of bromine. However, radiochemical tests showed that precipitates treated in this manner still retained a considerable proportion (5–20%) of their original iodine. Some, but not all, of this could be removed by repeated digestion of the precipitates with bromine water. Experiments showed that a consistent recovery of 98.5 ± 0.3% could be obtained if the digestion with bromine water was carried out using ultrasonic agitation instead of stirring, and if the precipitate was subsequently washed with two 5-ml aliquots of water. The *ca.* 1.5% of iodine remaining in the precipitate could only be removed by repeated ultrasonic treatment with bromine water. Since a consistent and almost quantitative recovery could be obtained by a single digestion with bromine water and ultrasonics, this technique was adopted for the analysis.

Small amounts of silver may be produced by photochemical decomposition of the silver chloride precipitate. This silver reacts with the bromine water and leads to the production of hypobromous acid which will cause serious errors in the analysis, as it oxidizes iodide ion to iodine. SUGAWARA AND TERADA reduce it with sodium sulphite, and this procedure was followed in the present method. Iodate ion is reduced to iodide during this process and must be reoxidized with bromine water before the analysis can be concluded.

Determination of iodine

In the final stage of their method SUGAWARA AND TERADA allowed the iodate ion, produced as described above, to react in acidic solution with cadmium iodide. The iodine which was produced was determined photometrically as the starch–iodine complex. This photometric method is known to lack precision because of the complex nature of the chromogen. Two alternative methods of determining the iodine liberated by reaction with iodide ion were therefore investigated and found to be equally satisfactory.

(*a*) Spectrophotometry using the 353-nm absorption band of the I_3^- ion which is produced by the reaction of the iodine with excess of iodide ion. It was found that this system obeyed Beer's law up to an original iodine (*i.e.* IO_3^-–I) concentration of more than 50 μg per 50 ml (1-cm cell). A coefficient of variation of 0.4% was found at the 25 μg IO_3^-–I level.

(*b*) Photometric micro-titration of the iodide with 0.004 *N* thiosulphate, using the disappearance of the tri-iodide absorption band at 353 nm to detect the end-point. This procedure showed a coefficient of variation of 0.2% at the 25 μg IO_3^-–I level.

EXPERIMENTAL

Apparatus

A Unicam spectrophotometer was used for spectrophotometric measurements. The end-point in the titration with thiosulphate was detected with an EEL Quantitator that had been modified by substitution of an AV90 phototube with appropriate circuitry for the normal barrier-layer cell which is insensitive to 353-nm radiation. A Wratten 18A filter having its maximum transmission at 360 nm was used to isolate the desired wavelength.

Reagents

Silver citrate. Dissolve 15.8 g of trisodium citrate (A.R.) in 50 ml of water and gradually add, with vigorous stirring, a solution of 9.1 g of silver nitrate in 50 ml of water. Filter off the precipitated silver citrate, wash it with water and dry *in vacuo*. Grind it to pass an 180-mesh sieve and store in an amber glass bottle.

Procedure

Place 500 ml of the sea water into a 750-ml conical flask which has been painted black on the outside. Add 0.23 g of silver citrate, and stir mechanically for 30 min while agitating ultrasonically. Allow the solution to stand in the dark for 24 h to permit the precipitated silver halides to settle. Siphon off most of the supernatant liquid into another 750-ml conical flask. Transfer the remainder, together with the precipitate, to a 50-ml centrifuge tube. Centrifuge, wash the precipitate with 5 ml of water and centrifuge again; combine the centrifugates with the main supernatant fraction and reserve for the determination of iodate.

Treat the washed precipitate with 15 ml of saturated bromine water and 2 ml of 0.1 *M* sodium chloride solution. Place the centrifuge tube in an ultrasonic agitator for 30 min and then in a bath of boiling water for 15 min. Centrifuge, and decant the supernatant liquid into another centrifuge tube. Wash the precipitate with two 5-ml aliquots of water. Combine the washings with the main centrifugate and evaporate on the waterbath to *ca.* 5 ml. After cooling, add 2.5 ml of a freshly prepared 0.2% solution of sodium sulphite to reduce any hypobromite ions. Reoxidize iodide to iodate by addition of 15 ml of saturated bromine water. Allow the solution to stand for 30 min, remove excess of bromine by bubbling nitrogen through the solution, and as a precaution add 0.2 g of phenol in case any traces of bromine remain. Determine the iodate-iodine in the resultant solution either titrimetrically or photometrically.

For the reagent blank, mix 2 ml of 0.1 *M* sodium chloride solution with 0.23 g of silver citrate in 30 ml of water using sonic agitation, centrifuge and discard the supernatant liquid. Treat the precipitate with 15 ml of bromine water and proceed as described in the previous paragraph.

Titrimetric determination of iodine. Transfer the solution quantitatively to the 25-ml titration cell of the photometric titration apparatus. Add 1 ml of 0.1 *M* sulphuric acid and 1 ml of freshly prepared 25%(w/v) potassium iodide solution. Close the titration cell immediately with a closely fitting perspex lid. Titrate the solution with *ca.* 0.004 *N* sodium thiosulphate (standardized with potassium iodate) using a 0.5-ml syringe microburette. Observe the titration visually until the iodine colour is almost discharged. Then add increments of 0.4 μl of thiosulphate, reading the meter of the titrimeter after each addition. Plot a graph of the percentage transmission against volume of thiosulphate added. The end-point of the titration is the intercept of the two straight lines thus obtained. Titrate the reagent blank in the same fashion.

Spectrophotometric determination of iodine. Transfer the solution containing iodate quantitatively to a 50-ml graduated flask. Add 0.25 g of potassium iodide and 1 ml of 0.1 *M* sulphuric acid and dilute to volume. Measure the absorbance of the resultant solution at 353 nm in a covered 1-cm cell after 4 min. Standardize the procedure in the same manner using 1.5 ml of 0.002 *M* potassium iodate (38.07 μg I) instead of the sample. Carry out corresponding reagent blanks in the same fashion.

Determination of iodate. Treat the supernatant liquid from the coprecipitation of iodide with 4 ml of a saturated solution of hydrazine sulphate. This reduces iodate to iodide which is then determined as described above. For the reagent blank, mix 4 ml of saturated hydrazine sulphate solution with 2 ml of 0.1 *M* sodium chloride solution, 0.23 g of silver citrate and 30 ml of water and agitate ultrasonically. Proceed as described above for the preparation of the iodide blank.

RESULTS

Accuracy and precision of the method

The accuracy and precision of the proposed method were checked by carrying out replicate analyses on 500-ml aliquots of an artificial sea water containing known amounts of iodide- and iodate-iodine. This test water was prepared according to the formula of LYMAN AND FLEMING[13], except that sodium fluoride and potassium bromide were omitted, since even the analytical-grade chemicals were found to contain appreciable amounts of iodine. The results of the analyses are presented in Tables II and III. They show that the spectrophotometric procedure gave a coefficient of variation of *ca.* 1.0% with an average iodine recovery of 98.5 ± 0.6%, a figure in close agreement with that found radiochemically (98.4 ± 0.4%). The titrimetric procedure gave an average iodine recovery of 99.0 ± 0.4%. A coefficient of variation of ± 0.4% was found at an iodate-iodine level of 40 μg l^{-1}. It is suggested that the empirical factor 1.015 should be applied to the observed iodine concentrations to correct for losses occurring during processing.

TABLE II

RECOVERY OF ADDED IODIDE- AND IODATE-IODINE FROM 500 ml OF IODIDE-FREE ARTIFICIAL SEA WATER BY THE SPECTROPHOTOMETRIC METHOD

μg of iodide-iodine added	5	10	15	—	—	—
μg of iodate-iodine added	—	—	—	10	20	40
μg of iodine found (average)	4.87	9.81	14.8	9.85	19.8	39.6
Recovery (%)	97.4	98.1	98.7	98.5	99.0	99.0
Coefficient of variation (%)	0.8	0.8	1.1	0.8	0.8	0.5

TABLE III

RECOVERY OF ADDED IODIDE- AND IODATE-IODINE FROM 500 ml OF IODIDE-FREE ARTIFICIAL SEA WATER BY THE TITRIMETRIC METHOD

μg of iodide-iodine added	5	10	15	—	—	—
μg of iodate-iodine added	—	—	—	10	20	40
μg of iodine found	4.98	9.92	14.76	9.91	19.72	39.56
Recovery (%)	99.6	99.2	98.4	99.1	98.6	98.9

SUMMARY

Several sources of error have been found in SUGAWARA's method for the determination of iodine in sea water. These are minimized in the modified procedure which has been developed. Iodide is coprecipitated quantitatively with silver chloride by silver ions slowly liberated into the water by the dissolution of silver citrate. The iodide present in the precipitate is oxidized to iodate by means of bromine under the influence of ultrasonic agitation. After destruction of hypobromite, iodine is determined either by photometric titration, or by spectrophotometry. Iodate is not coprecipitated by silver chloride, but can be determined after reduction with hydrazine sulphate. The titrimetric and spectrophotometric methods give recoveries of iodide- and iodate-iodine of 99.0 ± 0.4% and 98.5 ± 0.6% respectively, and have coefficients of variation of ±0.4% and ±0.8%.

RÉSUMÉ

Plusieurs sources d'erreur ont été trouvées dans la méthode de Sugawara pour le dosage de l'iode dans l'eau de mer. On propose de modifier ce procédé comme suit: l'iode est coprécipité quantitativement avec le chlorure d'argent, par les ions argent lentement libérés dans l'eau par dissolution du citrate d'argent. L'iodure présent dans la précipité est oxydé en iodate, au moyen de brome, sous l'influence d'une agitation ultrasonique. Après destruction de l'hypobromite, l'iode est dosé soit par titrage photométrique, soit par spectrophotométrie. L'iodate ne coprécipite pas avec le chlorure d'argent; il peut être dosé après réduction au moyen de sulfate d'hydrazine. Ces méthodes titrimétrique et spectrophotométrique donnent un rendement en iodure et iodate-iode respectivement de 99.0±0.4% et 98.5±0.6%, avec un coefficient de variation de ±0.4% et ±0.8%.

ZUSAMMENFASSUNG

Bei der Sugawara-Methode zur Bestimmung von Jod in Seewasser sind verschiedene Fehlerquellen gefunden worden. Diese werden bei dem neuentwickelten, modifizierten Verfahren weitestgehend vermindert. Jodid wird quantitativ durch Silberchlorid mitgefällt, wobei die Silberionen langsam durch Auflösung von Silbercitrat freigesetzt werden. Das im Niederschlag befindliche Jodid wird durch Brom unter Ultraschalleinwirkung zu Jodat oxidiert. Nach Zerstörung von Hypobromit wird Jod entweder durch photometrische Titration oder durch Spektrophotometrie bestimmt. Jodat wird durch Silberchlorid nicht mitgefällt, kann jedoch nach Reduktion mit Hydrazinsulfat bestimmt werden. Bei dem titrimetrischen und spektrophotometrischen Verfahren werden 99.0±0.4% des Jodid-Jods und 98.5±0.6% des Jodat-Jods wiedergefunden, die Variationskoeffizienten sind ±0.4% und ±0.8%.

REFERENCES

1 K. SUGAWARA AND K. TERADA, *Nature*, 182 (1958) 250.
2 K. K. JOHANNESSON, *Nature*, 182 (1958) 251.
3 K. SUGAWARA, T. KOYAMA AND K. TERADA, *Bull. Chem. Soc. Japan*, 28 (1955) 494.
4 A. VOIPIO, *Rapp. Cons. Explor. Mer*, 149 (1961) 38.

5 J. F. REITH, *Rec. Trav. Chim.*, 49 (1930) 142.
6 B. A. SKOPINTSEV AND L. A. MICHAILOVSKAYA, *Tr. Inst. Oceanog., Moscow*, 3 (1933) 79.
7 M. DUBRAVČIC, *Analyst*, 80 (1955) 295.
8 R. A. BARKLEY AND T. G. THOMPSON, *Anal. Chem.*, 32 (1960) 154.
9 A. N. KAPPANNA, G. T. GADRE, H. M. BHAVNAGARY AND J. M. JOSHI, *Current Sci.*, 31 (1962) 273.
10 N. YONEHARA, *Bull. Chem. Soc. Japan*, 37 (1964) 1101.
11 J. REVEL, *Cah. Oceanogr.*, 21 (1969) 273.
12 K. SUGAWARA AND K. TERADA, *J. Earth Sci. Nagoya Univ.*, 5 (1957) 81.
13 J. LYMAN AND R. H. FLEMING, *J. Marine Res.*, 3 (1940) 134.

Analytica Chimica Acta
Elsevier Publishing Company, Amsterdam
Printed in The Netherlands

A RAPID METHOD FOR RESIDUE ANALYSIS BY COLUMN LIQUID CHROMATOGRAPHY WITH POLAROGRAPHIC DETECTION

APPLICATION TO THE DETERMINATION OF PARATHION AND METHYLPARATHION ON CROPS

J. G. KOEN AND J. F. K. HUBER
Laboratory for Analytical Chemistry, University of Amsterdam, Nieuwe Achtergracht 125, Amsterdam (The Netherlands)

(Received February 28th, 1970)

Since the use of chemical pesticides is increasing greatly, and the number of available pesticide compounds is also constantly expanding, there is also a growing need for rapid, simple and reliable analytical methods for these poisons.

Recently, the application of polarographic detection to high-speed, high-efficiency column liquid chromatography has been described. As an example the quantitative analysis of mixtures of *p*-nitrophenol, methylparathion and parathion has been discussed[1]. For these compounds a limit of analysis of $2 \cdot 10^{-8}$ mole l^{-1} has been found, which value is small enough to promise useful applications in residue analysis. Classical polarography has a poor selectivity for mixtures of nitro compounds and has a limit of analysis about a hundred times higher, hence it can only be used with success in the analysis of commercial parathion products[2].

Extraction of the plant material must be carried out with solvents in which the pesticides have an excellent solubility. A broad range of solvents has been applied in extraction procedures[3,4]. In this work ethanol has been used, because it is also one of the components of the eluant mixture. In other methods of residue analysis, alcohol is a less suitable solvent[3] because much plant material dissolves in it so that highly colored extracts which are difficult to clean up are obtained, and because concentration by evaporation is accompanied by excessive loss of pesticide. These disadvantages, however, are of minor importance in column liquid chromatography with polarographic detection because of its selectivity and its low limit of detection. It is not necessary to carry out a clean up or concentration procedure. When plant material with a high water content has to be analysed, anhydrous magnesium sulphate can be added to the alcohol in order to remove the water and obtain a better solubility of the pesticides.

EXPERIMENTAL

Reagents

Magnesium sulphate. Dried for 1 h at 900° and ground.

Acetate buffer. 15 g of acetic acid and 4 g of sodium hydroxide in 1 l of water.

Eluant mixture. 60.1 % water, 38.8 % ethanol, 0.80 % acetic acid, 0.21 % sodium hydroxide and 0.09 % potassium chloride (w/w) saturated with 2,2,4-trimethylpentane (iso-octane).

Apparatus

A high-speed food mixer (Kenwood-Kenmix), and an electric centrifuge (10-ml and 40-ml tubes) were used.

Liquid chromatograph with polarographic detection. A diagram is shown in Fig. 1.

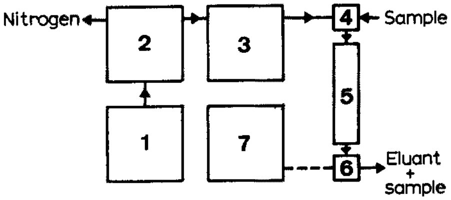

Fig. 1. Block diagram of a liquid chromatograph with polarographic detection. (1) Supply of nitrogen gas for the deaeration of the eluant, (2) eluant stock, (3) pump (Orlita DMP-1515) with damping device to obtain a constant flow rate, (4) sampling device, (5) separation column, (6) detector, (7) electronic equipment.

An extensive description of the apparatus has been given recently[1]. The separation column is made from thick-walled glass tube (length 18 cm, i.d. 2.7 mm). The tube is filled with silanised diatomaceous earth (Merck, ground and sieved to a particle size range of 28–40 μm) which is coated with iso-octane. Between the dropping mercury electrode and the mercury pool of the polarographic detector, a constant potential difference of 1100 mV is applied, and the current is recorded as a function of time.

Injection syringes (10 μl and 100 μl; Hamilton 701NCH and 1710N) were used.

Procedure

All experiments were carried out on lettuce.

Take 50 g of the coarse cut plant material and add a known amount of parathion and methylparathion dissolved in ethanol. Set the mixture aside open to the air for 1 h in order to evaporate the ethanol and to allow the pesticides to become well absorbed by the plant material. Macerate during 4 min in a high-speed food mixer with 100 ml of ethanol and 50 g of anhydrous magnesium sulphate. Then set the mixture aside for 1 h in a closed beaker so that most of the water is removed from the solution. Separate the solvent and solid material from each other in a centrifuge. (The resulting dark green solution appeared to have an ethanol content of 92 ±2%(v/v) as was found by gas-chromatographic analysis of five different extracts. It may be calculated therefore that the whole volume of the solution, of which a fraction is included in the solid sediment, amounts to 109 ml.)

Transfer 5 ml of the extract to a centrifuge tube and add 5 ml of the acetate buffer. Remove the green precipitate which is formed, by means of centrifugation. The resulting clear sample solution has a pale yellow-green color and has about the same composition as the eluant. Inject 100 μl of the clear sample solution, *i.e.* 0.046 % of the whole volume, into the liquid chromatograph by means of a syringe. The chromatogram is obtained in 5 min. The colored compounds in the sample solution are completely retained by the column, but this does not interfere with further chromatographic separations. When the column is reloaded with the stationary phase iso-octane, which has to be done once a day by injecting a few hundred μl of iso-octane, the colored substances are removed by the excess of iso-octane.

The sensitivity was measured by means of a test mixture of the pesticides; the precision can be better than 2%[1].

RESULTS

Figure 2 shows examples of chromatograms of a test mixture, a pesticide-containing plant extract and a pesticide-free plant extract. The results of the quantitative analysis of five crop extracts are included in Table I. The recovery was found to be about 95% for parathion and about 85% for methylparathion. A precision of better than 10% can be obtained in quantitative residue analysis.

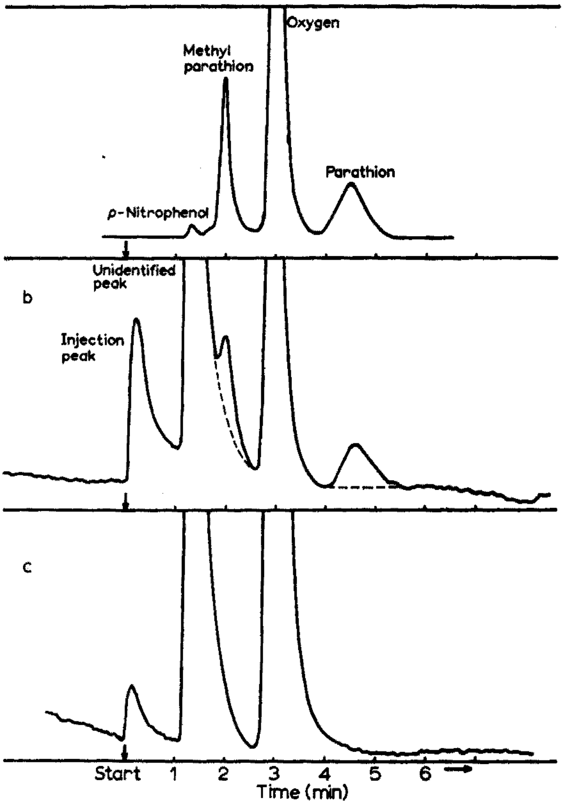

Fig. 2. Determination of methylparathion and parathion. Eluant flow rate 34 ml h^{-1}; sampling with a syringe; column length 18 cm. (a) Chromatogram of a test mixture of methylparathion and parathion. Methylparathion, 200 mg l^{-1}; parathion, 265 mg l^{-1}. Injection volume 0.90 μl. Full scale sensitivity $2 \cdot 10^{-7}$ A. Oxygen not removed from the sample solution. (b) Chromatogram of extract. Methylparathion, 0.8 p.p.m.; parathion, 1.0 p.p.m. Injection volume 100 μl. Full scale sensitivity $2.5 \cdot 10^{-8}$ A. Oxygen removed from the sample solution by a nitrogen stream. (c) Chromatogram of extract without pesticides. Same conditions as for (b).

TABLE I

RESULTS OF A PESTICIDE RESIDUE ANALYSIS OF LETTUCE

(Each extract was analysed 4 times by liquid chromatography)

Amount pesticide added (p.p.m.)		*Found (p.p.m.)*		*Standard deviation (%)*		*Recovery (%)*	
Methyl-parathion	*Parathion*	*Methyl-parathion*	*Parathion*	*Methyl-parathion*	*Parathion*	*Methyl-parathion*	*Parathion*
0	0	0	0	—	—	—	—
0.20	0.27	0.16	0.22	14	20	78	82
0.40	0.51	0.36	0.51	18	16	90	100
0.80	1.06	0.64	0.93	7	10	80	88
1.60	2.02	1.43	1.95	5	9	90	97

It has been shown previously[1] that the limit of analysis for the two pesticide compounds is $2 \cdot 10^{-8}$ mole l^{-1}. This value corresponds to amounts of about 0.03 p.p.m. on crops. The chromatograms shown in Fig. 2 were obtained under conditions where the limits of analysis were slightly higher. For parathion, a limit of analysis of 0.05 p.p.m. was found, owing to a relative low injection volume. With an injection volume of 200 μl the limit of analysis was 0.03 p.p.m. For methylparathion the limit of analysis appeared to be 0.1 p.p.m., which was due to the poor separation of its peak from a large unidentified peak in the chromatogram, which was less retarded. Complete separation and thus a limit of analysis of 0.03 p.p.m. could also be obtained for methylparathion, when a longer separation column and a valve injection system (Valco VSV 6 HP) were used. The separation time was almost twice as long in that case (Fig. 3). Sampling with a valve had advantages over sampling with a syringe: there was very little oscillation of the base line at the start of the chromatogram, and a much smaller oxygen peak was observed.

DISCUSSION

The special feature of the method described above is the short analysis time. A total analysis takes up 2 h. More than 10 samples can be analysed, however, on one chromatograph in that time, if the samples are prepared simultaneously.

The performance of the method has been proved for methylparathion and para-

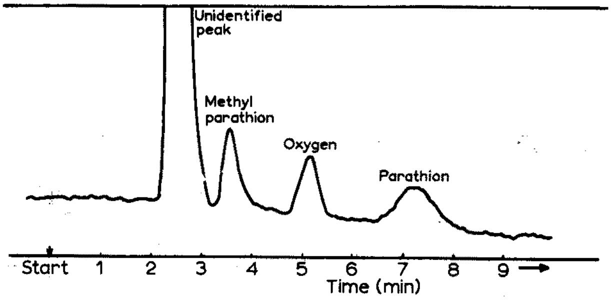

Fig. 3. Determination of methylparathion and parathion. Conditions as for Fig. 2b, except that the column length was 27 cm, and a valve injection system was used.

thion on lettuce, but the method can also very well be applied to residue analysis for other pesticide compounds and on other crops if the pesticides can be detected polarographically. In many cases, however, another eluant and stationary phase composition must be chosen to obtain a proper separation in a short time.

The authors are grateful to Mr. T. MENSONIDES for his assistance with the measurements.

SUMMARY

A rapid, sensitive, selective and simple method for the determination of residues of methylparathion and parathion on crops is described. Extraction is carried out with ethanol. The extract is diluted with an aqueous acetate buffer solution and immediately analysed by means of column liquid chromatography with polarographic detection. For lettuce the recovery is about 90%. The limit of analysis is about 0.03 p.p.m. Quantitative measurements of residue traces on crops can be carried out with a precision of better than 10%.

RÉSUMÉ

Une méthode rapide, sensible, sélective et simple est décrite pour le dosage de résidus de méthylparathion et parathion. On effectue une extraction dans l'éthanol. L'extrait, après dilution avec une solution aqueuse tampon à l'acétate est immédiatement analysé par chromatographie sur colonne et détection polarographique. La limite de l'analyse est d'environ 0.03 p.p.m.

ZUSAMMENFASSUNG

Es wird ein schnelles, empfindliches, selektives und einfaches Verfahren für die Bestimmung von Methylparathion- und Parathionrückständen auf Ernteerträgen beschrieben. Es wird mit Äthanol extrahiert, der Extrakt mit wässriger Acetat-Pufferlösung verdünnt und unmittelbar durch Säulen-Flüssig-chromatographie mit polarographischem Detektor analysiert. Bei Salat beträgt der wiedergewonnene Anteil etwa 90%. Die Nachweisgrenze beträgt etwa 0.03 p.p.m. Quantitative Bestimmungen von Rückstandsspuren können mit einer Genauigkeit besser als 10% ausgeführt werden.

REFERENCES

1 J. G. KOEN, J. F. K. HUBER, H. POPPE AND G. DEN BOEF, *J. Chromatog. Sci.*, 8 (1970) 192.
2 C. V. BOWEN AND F. I. EDWARDS, JR., *Anal. Chem.*, 22 (1950) 706.
3 P. R. AVERELL AND M. V. NORRIS, *Anal. Chem.*, 20 (1948) 753.
4 B. J. GUDZINOWICZ, *Gas-chromatographic Analysis of Drugs and Pesticides*, Dekker, New York, 1967.

Analytica Chimica Acta
Elsevier Publishing Company, Amsterdam
Printed in The Netherlands

CHARACTERISATION OF AMIDINES AS PICRATES THROUGH THIN-LAYER CHROMATOGRAPHY

STIG VEIBEL
Department of Organic Chemistry, Technical University, DK2800 Lyngby (Denmark)
(Received January 19th, 1970)

Picrates of amidines are usually easily precipitated by adding an aqueous or aqueous–ethanolic solution of the amidine to a hot aqueous 1–1.5% solution of picric acid. They are easily purified by recrystallisation from water or dilute ethanol, and can be characterised through their melting points. In this paper, an additional complementary method of characterisation, by thin-layer chromatography, is described and the titration of the picrates in non-aqueous medium is discussed.

Amidines examined

The compounds examined with their melting points, and where possible the literature values, are listed in Table I. The melting points found are sometimes lower than the values given in the literature; this is partly because the present melting points are all uncorrected, and partly because the melting points are in fact destruction points and are therefore heavily dependent on the rate of increase of temperature. Accordingly, differences of 3–10° have been found between the melting points measured in capillary tubes at a temperature rise of 4° min^{-1}, and the instantaneous melting points measured with a metal block.

Microanalyses of the picrates which have not previously been described in the literature are given in Table II.

The picrates of the guanidinoacetic acid, 4-aminopyridine and 3,6-bis-(dimethylamino)-4-methylpyridazine, require special comment.

KING[1] found that the picrate of guanidinoacetic acid, when recrystallised from 25 volumes of boiling water, was converted into a semipicrate with higher melting point and lower solubility in water than the normal picrate. The semipicrate was most easily prepared by mixing solutions of picric acid and of guanidinoacetic acid in the mole ratio 1:2. This was confirmed in the present work.

It is well known that some amino acids may form salts with hydrochloric acid both in 1:1 and in 2:1 mole ratios. For example, the structure of leucinium semichloride has been indicated by HADŽI AND MARCISZEWSKI[2] to be

$$(H_3N^+C_5H_{10}COO^-\ldots H\ldots {}^-OOCC_5H_{10}N^+H_3)^+Cl^-$$

where the hydrogen bond connecting the two amphoteric ions is close to the symmetric type. According to the infrared spectrum* of the semipicrate of guanidinoacetic

---

* The infrared spectrum was taken on a recording Perkin-Elmer 421 spectrometer using potassium bromide technique.

TABLE I

MELTING POINTS, EQUIVALENT WEIGHTS AND R_{Pi} VALUES FOR PICRATES

(R_{Pi} values in parentheses uncertain. When 2 values are indicated the last one is for the uncoloured spot)

	Picrate of	*M.p. (°) found*	*M.p. (°) lit.*	*E found*	*E calcd.*	R_{Pi}
1.	Guanidine	>300	333[a]	287.5	288.2	0.76
2.	Aminoguanidine	181–83	182–85[b]	301.2	303.2	0.80
3.	1,2-Diphenylguanidine	167–68	168[c]	435.8	440.4	1.09
4.	Acetamidine	243–44	252 k[d]	285.2	287.2	0.79
5.	Guanidinoacetic acid	201–03	210 k[e]	342.1	346.2	0.78
6.	Guanidinoacetic acid, semipicrate	228–30	237 k[e]	232.0	231.7	0.77
7.	Creatine	205–07	—	355.3	360.3	0.83
8.	Malonamideamidine	228–30	—	330.5	330.2	0.73
9.	2-Aminopyridine	218–20	224–25 k[f]	323.1	323.2	0.72
10.	4-Aminopyridine·H_2O	209–10	216–17 k[g]	338.3	341.2	(0.83)(0.04)
11.	4-Aminopyridine, anhydrous	209–10	—	324.5	323.2	(0.90)(0.04)
12.	2-Amino-4,6-dimethylpyridine	205–07	—	347.9	351.3	0.92
13.	2-Aminopyrimidine	231–33	237–38[h]	325.8	324.2	0.82
14.	2-Aminothiazole	215–16	—	328.4	329.2	0.77
15.	2-Amino-6-methylbenzothiazole	261–63	280–81[i]	391.9	393.3	0.72
16.	4-Dimethylaminopyridazine	210–11	—	353.3	352.3	(0.0) (0.0)
17.	3-Dimethylamino-5-methylpyridazine	181–82	—	366.7	366.3	(0.92)(0.03)
18.	3,6-Bis(dimethylamino)-pyridazine	179.5–80.5	—	393.3	395.4	(0.88)(0.06)
19.	3,6-Bis(dimethylamino)-4-methylpyridazine	144–45	—	410.2	409.4	(0.89)(0.04)

[a] H. J. LIDHOLM, *Ber.*, 46 (1913) 160. [b] L. E. A. GODFREY AND F. KURZER, *J. Chem. Soc.*, (1961) 5137. [c] C. P. JOSHUA AND V. K. VERMA, *Indian J. Chem.*, 2 (1964) 194. [d] R. G. FARGHER, *J. Chem. Soc.*, 117 (1920) 674. [e] H. KING, *J. Chem. Soc.*, (1930) 2374. [f] J. P. WIBAUT AND L. M. F. VAN DE LANDE, *Rec. Trav. Chim.*, 48 (1929) 1005. [g] P. A. DE VILLIERS AND H. J. DEN HERTOG, *Rec. Trav. Chim.*, 76 (1957) 647. [h] E. BÜTTNER, *Ber.*, 36 (1903) 2227. [i] R. F. HUNTER, E. R. PARKEN AND E. M. SHORT, *J. Chem. Soc.*, (1959) 784.

acid, the structure of this salt is similar to that suggested for leucinium semichloride, thus

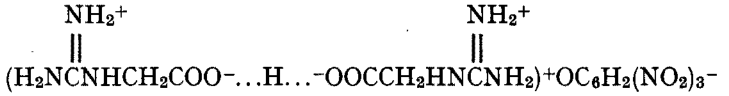

$$(H_2N\overset{\overset{NH_2^+}{\parallel}}{C}NHCH_2COO^-\ldots H\ldots {}^-OOCCH_2HN\overset{\overset{NH_2^+}{\parallel}}{C}NH_2)^+OC_6H_2(NO_2)_3^-$$

In view of this result, a similar behaviour was expected for creatine. However, neither by recrystallisation of creatinium picrate from much hot water nor by precipitating it from mixtures of creatine and picric acid in the mole ratio 2:1, was it possible to trace the slightest indication of the formation of a semipicrate. The search for semipicrates was extended to all the amidines examined, including those without a carboxylate ion which was thought to be responsible for the leucinium semichloride, but in no case was there any indication of semipicrate formation.

The picrate of 4-aminopyridine crystallised in long, yellow needles with a very definite melting point. On titration, however, the equivalent weight was found to be too high, corresponding to a content of between 0.5 and 1.0 mole of water.

TABLE II

MICROANALYSES OF PICRATES AND PERCHLORATES

No.	*Picrates of*	*%C*		*%H*		*%N*	
		Calcd.	*Found*	*Calcd.*	*Found*	*Calcd.*	*Found*
7.	Creatine $C_{10}H_{12}N_6O_9 = 360.3$	33.34	33.44	3.36	3.34	23.33	23.49
8.	Malonamideamidine $C_9H_{10}N_6O_8 = 330.2$	32.74	32.84	3.05	3.11	25.45	25.63
12.	2-Amino-4,6-dimethylpyridine $C_{13}H_{13}N_5O_7 = 351.3$	44.43	44.54	3.73	3.66	19.94	20.08
14.	2-Aminothiazole $C_9H_7N_5O_7S = 329.2$	32.84	33.18	2.14	2.18	21.28	21.21
16.	4-Dimethylaminopyridazine $C_{12}H_{12}N_6O_7 = 352.3$	40.92	40.86	3.43	3.26	23.86	23.76
17.	3-Dimethylamino-5-methylpyridazine $C_{13}H_{14}N_6O_7 = 366.3$	42.62	42.74	3.85	3.63	22.95	23.02
18.	3,6-Bis(dimethylamino)pyridazine $C_{14}H_{17}N_7O_7 = 395.4$	42.54	42.62	4.34	4.39	24.81	24.74
19.	3,6-Bis(dimethylamino)-4-methylpyridazine $C_{15}H_{19}N_7O_7 = 409.4$	44.04	44.16	4.68	4.51	23.96	24.02

	Perchlorates of	*% Cl*	
		Calcd.	*Found*
16.	4-Dimethylaminopyridazine $C_6H_{10}ClN_3O_4 = 223.6$	15.85	15.63
17.	3-Dimethylamino-5-methylpyridazine $C_7H_{12}ClN_3O_4 = 237.7$	14.92	14.87
18.	3,6-Bis(dimethylamino)pyridazine $C_8H_{15}ClN_4O_4 = 266.7$	13.30	18.76
	$C_8H_{16}Cl_2N_4O_8 = 367.2$	19.33	
19.	3,6-Bis(dimethylamino)-4-methylpyridazine $C_9H_{17}ClN_4O_4 = 280.7$	12.63	
	$C_9H_{18}Cl_2N_4O_8 = 381.2$	18.60	18.72

After drying for 1 h at 120°, a sample weighing 0.2892 g lost 0.0158 g, corresponding to 5.46% of water (calculated for $C_{11}H_9N_5O_7 \cdot H_2O$ 5.28%). In no other instances was any water of crystallisation found.

Titration in anhydrous acetic acid

All the picrates investigated can be titrated in anhydrous acetic acid with perchloric acid in the same solvent, potentiometrically or visually. However, the picrates are only slightly soluble in anhydrous acetic acid whereas they are soluble in anhydrous formic acid. Formic acid, unfortunately, is a poor solvent for titrations with perchloric acid, because of indistinct end-points. This difficulty may be overcome by diluting the solution of the picrate in formic acid with anhydrous acetic acid, for the picrates, once dissolved, do not precipitate immediately when the solution is diluted; if precipitation does occur, the precipitate is so microcrystalline that it easily redissolves during the titration. This is the method recommended by TOENNIES AND CALLAN[3] for the titration of amino acids, which are also sparingly soluble in glacial acetic acid but easily soluble in anhydrous formic acid.

The results obtained for the equivalent weights by this method are shown in Table I.

As 2-amino-substituted N-heterocycles (*e.g.* pyridine, pyrimidine, thiazole) can be regarded as amidines, such substances were included in the investigation, and the titration method was perfectly satisfactory for the 2-amino heterocycles.

Some dimethylamino-substituted pyridazines, *viz.* 4-dimethylaminopyridazine, 3-dimethylamino-5-methylpyridazine, 3,6-bis(dimethylamino)pyridazine and 3,6-bis(dimethylamino)-4-methylpyridazine, were also examined. 4-Dimethylaminopyridazine is a vinylogue to an amidine, the second substance is an amidine, the last two substances are diamidines. All of them formed titratable monopicrates with reproducible melting points. The picrate of 3,6-bis(dimethylamino)-4-methylpyridazine could be titrated visually like the other picrates, the end-point being obtained after addition of 1 equivalent of perchloric acid. By potentiometric titration, however, it could be seen that the substance was able to take up one more proton. From Fig. 1, it can be seen that 3-dimethylamino-5-methylpyridazinium picrate and 3,6-bis(dimethylamino)pyridazinium picrate require only one equivalent of acid, whereas 3,6-bis(dimethylamino)-4-methylpyridazinium picrate can take up two protons on titration with a strong acid such as perchloric acid. An attempt was made to prepare dipicrates by adding the substituted pyridazines to a large excess of picric acid, but even with compound 19 only the monopicrate precipitated.

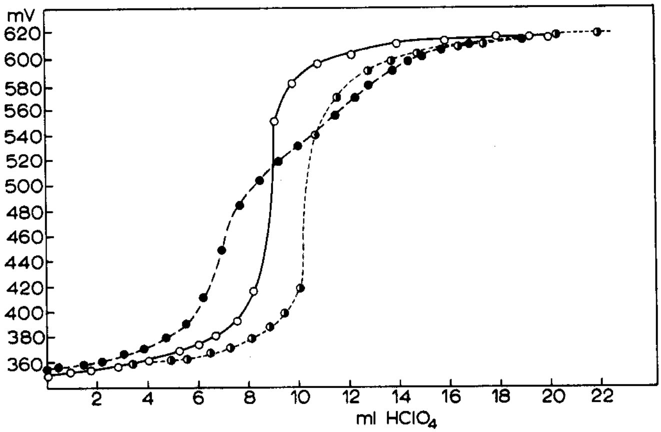

Fig. 1. Titration of amidinium picrates with perchloric acid. (○) 3-Dimethylamino-5-methylpyridazinium picrate, (●) 3,6-bis(dimethylamino)-4-methylpyridazinium picrate, (◑) 3,6-bis(dimethylamino)pyridazinium picrate.

When the solutions of the picrates after titration with perchloric acid (more than 2 equivalents of perchloric acid per mole of picrate) were precipitated with ether, the corresponding pyridazinium perchlorates could be isolated. As can be seen from Table II, only compound 19 gave a pure diperchlorate. Compound 18 gave a perchlorate which contained less than the amount of chlorine calculated for a diperchlorate; this corresponds to the shape of the titration curve which shows that when 1 proton has been taken up, the basic properties of the remaining amidine function are extremely weak. Compounds 16 and 17 only formed monoperchlorates.

Thin-layer chromatography

In order to obtain a characterisation of the individual picrates which would supplement the melting points and would perhaps be more easily reproducible, the behaviour of the picrates in thin-layer chromatography was examined. Silica gel PF254 was used as the stationary phase. A yellow fluorescence was obtained on irradiation with ultraviolet light at 254 nm, the fluorescence being quenched by aromatic compounds, thus making the spots visible as brown or blue spots on a yellow background.

Owing to the polar nature of the picrates, ethanol was first considered for the mobile phase, but all the picrates then moved so quickly that a difference in R_F values could hardly be observed.

Ethyl acetate was then examined, and a tolerably good separation was obtained, the time required for the solvent front to arrive at the top of the plate (an ordinary microscope slide) being about 10 min. As the picrates are yellow, it was possible to observe the location of the spots directly, but as a control the plates were illuminated in ultraviolet light in order to check if other spots were formed. For the picrates of the aliphatic amidines and most of the amino-substituted N-heterocycles, there was no difference between the R_F values directly observed and those observed in ultraviolet light, *i.e.* the picrates did not dissociate to picric acid and the amidine.

A spot of picric acid was always developed together with the spots of 3 or 4 amidinium picrates on one plate, in order to have a standard run to eliminate small changes caused by differences in temperature when different slides were compared. For this reason, the results given in Table I are not the directly found R_F values but the R_{Pi} values relative to the R_F value of picric acid which arbitrarily was accorded the value 1.00. (Relative to the solvent front, the R_F value of picric acid was in several parallel runs found to be between 0.72 and 0.74, the differences being due to small differences in temperature.)

It can be seen from Table I that the only amidinium picrate which moved faster than picric acid was the 1,3-diphenylguanidinium picrate; the R_{Pi} values of the other picrates varied from 0.72 to 0.92.

However, some of the aromatic amidines, *viz.* 4-aminopyridine and the amino-substituted pyridazines, behaved differently. Illumination of the developed plates in ultraviolet light showed that dissociation had taken place. In daylight yellow spots with the R_{Pi} values indicated in Table I were observed; these spots were also observed in ultraviolet light, but near the start line other spots, colourless in daylight, could also be seen.

In order to establish if the dissociation of the picrate was complete, 1 g of 4-aminopyridinium picrate was chromatographed on a 30-cm silica-gel column. When the chromatogram was developed with ethyl acetate, it could be seen that the yellow substance did not move unchanged, but spread over a length of 15 cm. About 1 l of ethyl acetate was necessary to wash the yellow substance completely off the column. By thin-layer chromatography, it was found that the first few millilitres of yellow eluate contained only picric acid (nothing remained on the start line), but when the yellow substance from the first 250 ml of eluate was isolated, it showed a very indistinct melting point between 170° and 200°, indicating that the picrate had been partially destroyed on passing through the column.

As all the picrates of the pyridazine derivatives behaved analogously in TLC, the R_{Pi} values observed are not regarded as sufficiently reproducible for the characterisation of amidinium picrates of this type.

However, all the 2-amino-substituted mono-N-heterocycles examined could be chromatographed without dissociation, and, considering the rapidly growing use of such substances, the procedure described should be useful for the rapid characterisation and estimation of such substances.

EXPERIMENTAL

Preparation of picrates

The amidinium picrates were prepared by adding 0.002 mole of the amidine dissolved in water, aqueous ethanol or ethanol to a solution of 0.5 g of picric acid in 50 ml of hot water. The picrates crystallised on cooling. They were filtered off and recrystallised from water or aqueous ethanol.

Parallel experiments with 0.004 mole of amidine to 0.5 g of picric acid or 0.002 mole of amidine to 1 g of picric acid gave picrates identical with the first prepared with the exception of guanidinoacetic acid which with a ratio of 2:1 between amidine and picric acid gave the semipicrate.

Recommended titration procedure

Weigh accurately about 1 mmole of the amidine picrate and dissolve in 5 ml of anhydrous formic acid. When the picrate has completely dissolved, dilute with 25 ml of anhydrous acetic acid. (Remove traces of water in the ordinary commercial product by adding 10 ml of acetic anhydride to 1 l of acetic acid. This greatly improves the sharpness of the end-point.) If the picrate does not dissolve in 5 ml of formic acid, 10 ml may be used, but the solution should then be diluted with 50 ml of glacial acetic acid, the ratio 5:1 between glacial acetic acid and formic acid being the minimum for obtaining a distinct end-point. Titrate with 0.1 *M* perchloric acid in anhydrous acetic acid, using crystal violet as indicator, or potentiometric indication.

Thin-layer chromatography

Plates of silica gel PF254 (Merck) were prepared in the usual way and ethyl acetate was used as eluent.

Thanks are due to Mr. I. CROSSLAND, M.Sc., for placing the substituted pyridazines at our disposal, and to Mrs. S. REFN, M.Sc., for assistance with the infrared spectra.

SUMMARY

Picrates of a series of amidines, including some 2- and 4-amino-substituted N-heterocycles, have been prepared. All were titratable with perchloric acid in glacial acetic acid. All the amidines investigated formed only monopicrates except guanidinoacetic acid which formed both a monopicrate and a semipicrate. Thin-layer chromatography on silica gel showed that aliphatic amidines and most 2-amino-substituted N-heterocycles could be characterised through their R_{Pi} values (with reference to picric acid) with ethyl acetate as the mobile phase. With 4-amino-substituted N-heterocycles and with three 2-amino-substituted pyridazines investigated, the mobile phase caused partial dissociation, thus invalidating the use of TLC for these substances. Perchlorates of the amino-substituted pyridazines were isolated. One of the diaminopyridazines formed a stable diperchlorate, another diaminopyridazine gave an unstable diperchlorate. The monoamino-substituted pyridazines formed only monoperchlorates.

RÉSUMÉ

On a préparé des picrates d'une série d'amidines, comprenant des hétérocycles-N, 2 et 4 aminosubstitués. Ils peuvent tous être titrés par l'acide perchlorique en milieu acide acétique glacial. Toutes les amidines examinées ne forment que des monopicrates, à l'exception de l'acide guanidinoacétique, formant un monopicrate et un semipicrate. On a utilisé la chromatographie sur couche mince de gel de silice pour caractériser ces différents composés.

ZUSAMMENFASSUNG

Es sind die Picrate einer Reihe von Amidinen einschliesslich einiger 2- und 4-aminosubstituierter N-Heterocyclen dargestellt worden. Alle waren mit Perchlorsäure in Eisessig titrierbar. Alle untersuchten Amidine bildeten nur Monopicrate, ausser Guanidinoessigsäure, die sowohl ein Monopicrat als auch ein Semipicrat bildete. Dünnschichtchromatographie auf Silicagel mit Äthylacetat als mobiler Phase ergab, dass aliphatische Amidine und die meisten 2-aminosubstituierten N-Heterocyclen durch ihre R_{Pi}-Werte (bezogen auf Picrinsäure) charakterisiert werden konnten. Bei den 4-aminosubstituierten N-Heterocyclen und drei 2-aminosubstituierten Pyridazinen verursachte die mobile Phase eine partielle Dissoziation, wodurch die Dünnschichtchromatographie für diese Substanzen unbrauchbar wurde. Es wurden Perchlorate der aminosubstituierten Pyridazine isoliert. Eines der Diaminopyridazine ergab ein stabiles, ein anderes ein instabiles Diperchlorat. Die monoaminosubstituierten Pyridazine bildeten nur Monoperchlorate.

REFERENCES

1 H. King, *J. Chem. Soc.*, (1930) 2374.
2 D. Hadži and H. Marciszewski, *Chem. Commun.*, (1967) 2.
3 B. G. Toennies and T. P. Callan, *J. Biol. Chem.*, 125 (1938) 259.

Analytica Chimica Acta
Elsevier Publishing Company, Amsterdam
Printed in The Netherlands

ANALYSIS OF BINARY MIXTURES OF HEXAALKYLDITIN COMPOUNDS BY A DIFFERENTIAL RATE METHOD

PAOLO ZAIA, VALERIO PERUZZO AND GUALTIERO PLAZZOGNA
Istituto di Chimica Analitica, Università di Padova, Padova (Italy)

(Received February 25th, 1970)

Coulometric titrations with biamperometric end-point detection have been applied to the determination of several organoditin compounds by generation of iodine, bromine or silver ions[1]. The conditions for a selective titration of one species in the presence of another have also been studied, and suitable titrations for the binary mixture hexaphenylditin–trimethyltriphenylditin have been developed[1]. In this case selective titration is possible because the rate of oxidation of triphenyltrimethylditin is much greater than that of the hexaphenylditin compound. The procedure previously adopted is not useful for the analysis of mixtures of the other examined ditin compounds, their oxidation rates being very similar[2,3].

Among those organotin compounds only hexaphenylditin can be analyzed by u.v. spectrophotometry[4] and gas-chromatographic analysis cannot be employed owing to their thermal instability[5]. It follows that simultaneous determination of binary mixtures of ditin compounds based on their differential rates of reaction toward silver ions, can be a useful analytical method. The method, first described by REILLEY *et al.*[6], applies second-order irreversible kinetics under conditions where the total concentration of the binary mixture is equal to the concentration of the reagent.

EXPERIMENTAL

Chemicals and reagents

Organoditin compounds were prepared and purified as previously described[1]. Ethanol (C. Erba, Milano, Italy) was dried over calcium oxide and purified by distillation. Commercial quinoline was distilled twice before use. Lithium nitrate (C. Erba) was dried in a vacuum-oven at 120° for two days and stored in a desiccator kept inside a dry-box.

Procedure

All coulometric–biamperometric analyses were carried out by means of silver ions with the coulometric apparatus described previously[1,7-9].

Ethanolic solutions of ditin compounds of suitable molarity were prepared and analyzed by means of coulometric titrations[1]; then binary mixtures at various ratios of the two components were obtained by mixing known volumes of the initial solutions. The same standard cell employed for the analysis of the single-component solutions was used to obtain the kinetic plots for the reaction between silver ions and the mixtures of ditin compounds, which were diluted to 62 ml and made 0.1 M in lithium nitrate. Suitable amounts of quinoline were added in order to reduce conveniently the oxidation rate of ditin compounds by silver ions[3] and the temperature was maintained at 20±0.2°. Photographic kinetic plots were obtained as previously described by TAGLIAVINI[1] and the quantities a_1 and a_2 of the faster and slower reagent, respectively, were obtained according to REILLEY's linear extrapolation method, by means of the following equations

$$1/(a-x) = k_{\mathrm{obs}}\, t + 1/a_2 \tag{1}$$

and

$$x = k_{\mathrm{obs}}\, a_2(a-x)t + a_1 \tag{2}$$

Figure 1 shows a typical kinetic plot (*cf.* run 18, Table III), where a is proportional to the quantity of silver ions electrolytically produced as well as to the total quantity

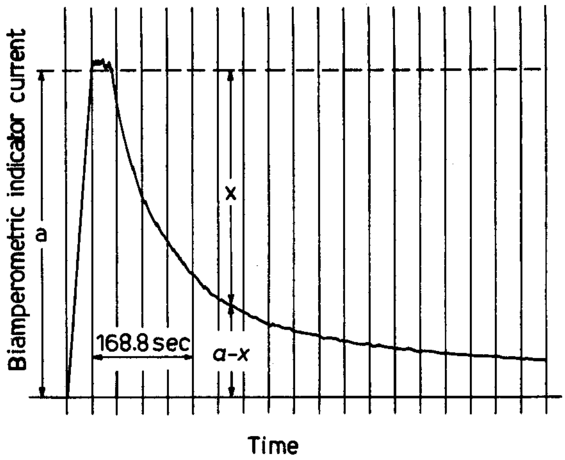

Fig. 1. Kinetic plot for a Bu_6Sn_2–Et_6Sn_2 mixture in ethanol. 0.1 M $LiNO_3$, 0.131 M quinoline at 20° (*cf.* run 18, Table III).

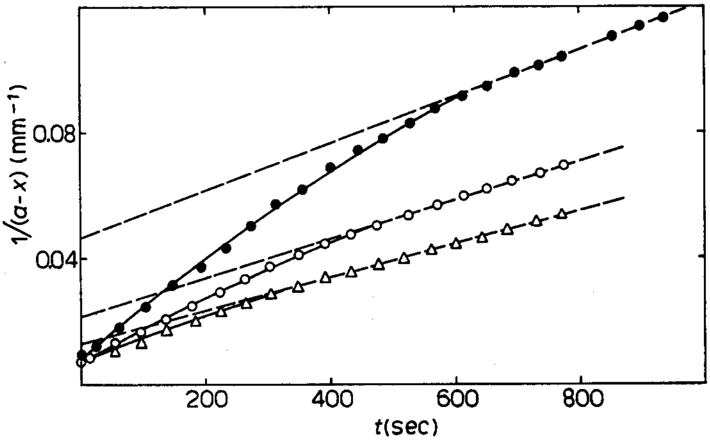

Fig. 2. Determination of the slower-reacting component (Bu_6Sn_2) in Bu_6Sn_2–Et_6Sn_2 mixtures in ethanol. 0.1 M $LiNO_3$, 0.0683 M quinoline at 20° (*cf.* Table III). (●) Run 17 (a=110 mm); (○) run 18 (a=128 mm); (△) run 19 (a=130 mm).

of the two ditin compounds introduced into the cell, and $(a-x)$ is proportional to the quantity of the unreacted silver ions or to that of the two unreacted ditin compounds at time t; k_{obs} is the observed rate constant for the reaction of the slower component with silver ions at a known quinoline concentration and at 20°. In all the calculations heights in millimeters were used since these are proportional to the quantity expressed in coulombs of the reactants. Both graphical extrapolation (*cf.* Figs. 2 and 3) and the computing of several $1/(a-x)$ *vs.* t or $(a-x)t$ *vs.* t values were employed in order to obtain the best a_1 and a_2 figures. The computing was done with an Olivetti Programma 101 desk computer.

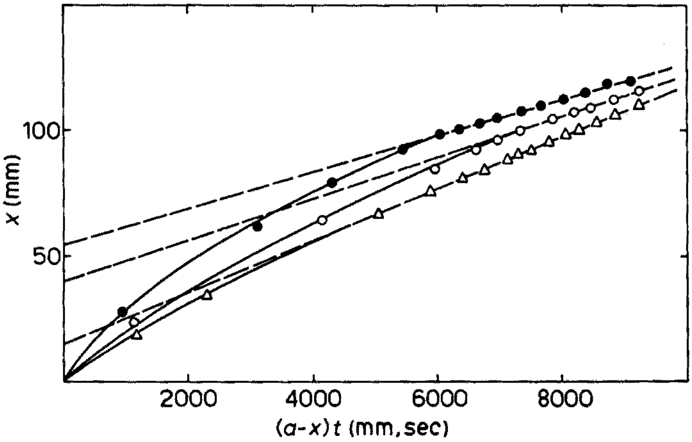

Fig. 3. Determination of the faster-reacting component (Me_6Sn_2) in Et_6Sn_2–Me_6Sn_2 mixtures in ethanol. 0.1 M $LiNO_3$, 0.131 M quinoline at 20° (*cf.* Table II). (●) Run 8 (a=124 mm); (○) run 9 (a=124 mm); (△) run 10 (a=125 mm).

RESULTS

Three binary mixtures were examined: hexabutyl- and hexamethylditin, hexaethyl- and hexamethylditin, and hexabutyl- and hexaethylditin. For each set, several solutions with different ratios of the components were analysed. Tables I–III list the results obtained in the determination of both components. Figures 2 and 3 show sets of curves for typical runs and the linear extrapolation method employed to calculate x or $1/(a-x)$ and therefore a_1 and a_2.

In all the Tables the columns give (a) the quantity in coulombs of the single components before mixing, (b) the calculated total amount of the two components in the mixture to be analyzed and then the found total amount checked by coulometric titration, (c) the calculated and found coulomb percentage for the slower and faster components. The last columns list the k_{obs} values for the slower reacting component, as obtained from the slopes of the straight-line parts of the diagrams $1/(a-x)$ *versus* time (*cf.* Fig. 2).

The reproducibility of all the measurements was checked. As an example, runs 11, 12 and 14, 15 correspond to the same mixtures.

Table III refers to the analysis of mixtures of the same system Bu_6Sn_2–Et_6Sn_2 in the presence of different concentrations of quinoline. Change in quinoline concen-

TABLE I

ANALYSIS OF Bu_6Sn_2–Me_6Sn_2 MIXTURES IN ETHANOL

(0.1 M $LiNO_3$, 0.131 M quinoline at 20°)

Run	Me_6Sn_2 *(A sec)*	Bu_6Sn_2 *(A sec)*	Bu_6Sn_2–Me_6Sn_2 *mixture (A sec)*		% Bu_6Sn_2 *slower component*		% Me_6Sn_2 *faster component*		k_{obs}[a,b] *(l mole^{-1} sec^{-1})*
			Calcd.	*Found*	*Calcd.*	*Found*	*Calcd.*	*Found*	
1	0.1538	0.1158	0.2696	0.2736	42.2	44.2	55.8	55.7	105
2	0.2562	0.3862	0.6424	0.6482	59.8	60.0	40.2	41.0	95
3	0.1878	0.4588	0.6466	0.6498	70.8	71.2	29.2	29.6	100
4	0.0942	0.4872	0.5814	0.5796	83.9	79.3	16.1	16.4	107
5	0.0404	0.5430	0.5834	0.5892	92.6	92.0	7.4	7.3	91

[a] The k_{obs} values refer to the slower reacting component and are calculated from the slope of the plot $1/(a-x)$ *vs. t*.
[b] By the normal kinetic method[3], the k_{obs} value is 96.

TABLE II

ANALYSIS OF Et_6Sn_2–Me_6Sn_2 MIXTURES IN ETHANOL

(0.1 M $LiNO_3$, 0.131 M quinoline at 20°)

Run	Et_6Sn_2 *(A sec)*	Me_6Sn_2 *(A sec)*	Et_6Sn_2–Me_6Sn_2 *mixture (A sec)*		% Et_6Sn_2 *slower component*		% Me_6Sn_2 *faster component*		k_{obs}[a,b] *(l mole^{-1} sec^{-1})*
			Calcd.	*Found*	*Calcd.*	*Found*	*Calcd.*	*Found*	
6	0.1370	0.2480	0.3850	0.3734	36.0	34.8	64.0	65.2	290
7	0.1862	0.2728	0.4590	0.4654	40.2	40.2	59.8	60.8	330
8	0.2944	0.2364	0.5308	0.5104	56.5	55.5	43.5	44.4	312
9	0.3460	0.1620	0.5080	0.5088	68.0	69.5	32.0	32.2	331
10	0.4500	0.0724	0.5224	0.5100	87.1	86.8	12.9	12.0	318

[a] See footnote (a) to Table I.
[b] By the normal kinetic method[3], the k_{obs} value is 340.

TABLE III

ANALYSIS OF Bu_6Sn_2–Et_6Sn_2 MIXTURES IN ETHANOL

(0.1 M $LiNO_3$ at 20°)

Run	Bu_6Sn_2 *(A sec)*	Et_6Sn_2 *(A sec)*	Bu_6Sn_2–Et_6Sn_2 *mixture (A sec)*		% Bu_6Sn_2 *slower component*		% Et_6Sn_2 *faster component*		k_{obs}[a,b] *(l mole^{-1} sec^{-1})*
			Calcd.	*Found*	*Calcd.*	*Found*	*Calcd.*	*Found*	
In presence of 0.131 M quinoline									
11	0.0794	0.3536	0.4330	0.4556	17.9	18.7	82.1	80.0	100
12	0.0794	0.3536	0.4330	0.4556	17.9	18.7	82.1	81.0	98
13	0.1392	0.2468	0.3860	0.3798	36.3	36.2	63.7	65.0	98
14	0.1988	0.1410	0.3398	0.3230	58.5	59.7	44.5	40	100
15	0.1988	0.1410	0.3398	0.3230	58.5	58.1	41.5	40	91
16	0.2530	0.0448	0.2978	0.3038	84.1	84.1	15.9	16	93
In presence of 0.0683 M quinoline									
17	0.0790	0.3350	0.4140	0.3988	19.5	19.2	80.5	80.0	230
18	0.1392	0.2404	0.3796	0.3442	38.5	36.5	61.5	62.5	270
19	0.1898	0.1374	0.3272	0.3344	57.3	57.5	42.7	42.3	240
20	0.2214	0.0800	0.3014	0.3038	73.1	73.9	26.9	26.0	250

[a] See footnote (a) to Table I.
[b] By the normal kinetic method[3], the k_{obs} value is 96 in 0.131 M quinoline and 230 in 0.0683 M quinoline.

tration does not affect the sensitivity of the method since the ratio of the rate constants of the two components in the mixture remains unchanged. The ratios of the rate constants (figures between brackets) for the three binary mixtures Et_6Sn_2–Bu_6Sn_2 (5), Me_6Sn_2–Et_6Sn_2 (18) and Me_6Sn_2–Bu_6Sn_2 (83), indicate that fairly good results can be obtained even when this ratio is as low as five. Moreover, the agreement of the k_{obs} values obtained by REILLEY's method and the values reported previously[3] is fairly good.

The percentage limits of the two organotin components listed in the Tables cannot be overstepped, because quantitative analysis then becomes impossible owing to uncertainties in the extrapolation.

The authors wish to thank Prof. G. TAGLIAVINI for valuable discussions. This research was supported by the Italian National Research Council, Roma (Research Grant N. 69.00540 1152508).

SUMMARY

Differential analysis of mixtures of alkylditin compounds, based on their different rates of reaction toward silver ions, is discussed. Binary mixtures of hexamethyl-, hexaethyl- and hexabutylditin can readily be determined.

RÉSUMÉ

Une étude est effectuée sur l'analyse différentielle de mélanges de composés alcoyl-di-étain, basée sur les différentes vitesses de réaction avec les ions argent. On peut ainsi doser rapidement des mélanges binaires d'hexaméthyl-, hexaéthyl- et hexabutyl-di-étain.

ZUSAMMENFASSUNG

Es wird eine Differentialanalyse von Gemischen von Alkyldizinn-Verbindungen diskutiert, die auf deren verschiedenen Reaktionsgeschwindigkeiten gegenüber Silberionen beruht. Binäre Gemische von Hexamethyl-, Hexaäthyl- und Hexabutyldizinn können leicht bestimmt werden.

REFERENCES

1 G. TAGLIAVINI, *Anal. Chim. Acta*, 34 (1966) 24.
2 G. TAGLIAVINI, S. FALESCHINI, G. PILLONI AND G. PLAZZOGNA, *J. Organometal. Chem.*, 5 (1966) 136.
3 G. TAGLIAVINI, S. FALESCHINI AND E. GENERO, *Ric. Sci.*, 36 (1966) 717.
4 D. N. HAGUE, *Ph. D. Thesis*, Cambridge, 1963.
5 R. K. INGHAM, S. D. ROSENBERG AND H. GILMAN, *Chem. Rev.*, (1960) 459.
6 H. B. MARK, JR., L. J. PAPA AND C. N. REILLEY, in C. N. REILLEY, *Advances in Analytical Chemistry and Instrumentation*, Vol. 2, Interscience, New York–London, 1963, p. 255 et seq.
7 G. TAGLIAVINI, U. BELLUCO AND L. RICCOBONI, *Ric. Sci.*, 31 (1961) 338.
8 G. TAGLIAVINI AND G. PLAZZOGNA, *Ric. Sci.*, 32 (1962) 356.
9 L. RICCOBONI, G. PILLONI, G. PLAZZOGNA AND G. TAGLIAVINI, *J. Electroanal. Chem.*, 11 (1966) 340.

Analytica Chimica Acta
Elsevier Publishing Company, Amsterdam
Printed in The Netherlands

THE CHEMICAL COMPOSITION OF ACID-OXIDIZED, WET-ASHED RESIDUES

R. E. MANSELL, R. P. TESSNER AND E. J. HUNEMORDER
Chemical Physics Research Laboratory, The Dow Chemical Company, Midland, Mich. 48640 (U.S.A.)

(Received February 12th, 1970)

The current availability of highly reproducible spectrographic instrumentation such as direct readers is having an important bearing on spectrographic analyses. These or adaptations to conventional spectrographs such as direct reader heads and recorders (*e.g.*, Baird Atomic RS-1 digital readout), have shown signal reproducibility within 0.1% when constant light tests are applied. Analytical precision obtained by arcing samples present as salts deposited on flat top electrodes, "salt caps", is rarely, if ever, as good. This indicates that the discharge employed, sample preparation and handling, standardization techniques, and other possible variables are the limiting factors in the precision that is presently obtainable. This study was initiated in an effort to achieve a better understanding of the chemical aspects of one step in sample handling, namely, acid oxidation or wet ashing, with a view to possible improvement in sample preparation.

Organic samples submitted for spectrographic analysis, whether of biological origin or otherwise, are commonly treated with oxidizing acids as part of the sample preparation procedure. Sulfuric, nitric, and perchloric acids are used separately or mixed for this purpose. In this laboratory, a mixture of 3:2 perchloric: nitric acid is preferred, particularly for biological samples, care being taken to ensure that an excess of acid is present until the digestion is completed, in order to prevent possible violent reactions. After the digestion step, the inorganic residues are commonly dissolved in a solution of sodium nitrate acidified with dilute nitric acid to provide a matrix for subsequent spectrographic analysis[1,2].

EXPERIMENTAL

Samples of particular inorganic salts or combinations of salts representative of biological materials were subjected to the usual wet-ashing treatment which terminated with evaporation of two separate small portions of nitric acid by means of a gas burner to help remove excess of perchloric acid. A comparison was also made by eliminating the extra evaporations with nitric acid. The temperature of the wet-ashing treatment was also controlled at 270° in several experiments by using a 7.5-cm high magnesium block containing drilled holes to accommodate the testtubes (15 cm long by 2.5 cm diameter) used for the sample digestion. Heating was accomplished with a standard 3-heat setting hot plate. After evaporation of all the acid present, the inorganic residues were ground and analyzed by X-ray diffraction plus infrared spectroscopy (i.r.) in certain cases to determine their chemical compositions.

RESULTS

The composition of the crystalline portion of the residues as observed by X-ray diffraction and/or i.r. when specified, are summarized in Table I; the comments are taken from DUVAL's reference work[3].

TABLE I

COMPOSITION OF CRYSTALLINE RESIDUES OBTAINED BY ACID OXIDATION

Sample	*Matrix*	*Composition of residue*	*Comments*
A	$CaCl_2$	$CaCl_2$—chief constituent. $\alpha CaCl_2 \cdot 2H_2O$—10–15%.	Calcium perchlorate decomposes at 470–478° $\rightarrow CaCl_2$.
A_1	$Ca(NO_3)_2 \cdot 4H_2O$	Same as A.	
B	$FeCl_3 \cdot 6H_2O$	Fe_2O_3—major constituent. Unidentified phase, minor constituent. IR sees no water, confirms Fe_2O_3.	
B_1	$Fe(NO_3)_3 \cdot 9H_2O$	Fe_2O_3.	
C	$MgCl_2 \cdot 6H_2O$	MgO—major constituent. Unidentified phase also a major constituent.	$MgCl_2$ converts to MgO above 615°.
C_1	$Mg(NO)_2 \cdot 6H_2O$	MgO—major constituent. Unidentified phase, same as in C, minor constituent.	
D	NaCl	$NaClO_4$.	This is a method of preparing $NaClO_4$—decomposition to chloride begins at $>471°$.
D_1	$NaNO_3$	$NaClO_4$.	$NaNO_3$ stable to 670°.
E	KCl	$KClO_4$.	$KClO_4$ is stable to 655°, then decomposes to chloride which is stable to 815°.
E_1	KNO_3	$KClO_4$.	KNO_3 dissociates between 510 and 972 to the oxide, stable up to 737–745°.
F	$Ca_3(PO_4)_2$	Mainly unidentified phase, but contains some $Ca(ClO_4)_2 \cdot 3H_2O$.	
	$Ca_3(PO_4)_2 + HClO_4$ only	Possibility of both phosphate and perchlorate ions by i.r. "Band at 620 cm^{-1} supports $(PO_4)^{3-}$ anion. Band at ~910 cm^{-1} suggests possible P–O–P linkage".	
	$Ca_3(PO_4)_2 + HNO_3$ only	By i.r. "Sample is hydrated. Sample does not contain PO_4^{3-} anion. Spectral features suggest presence of HPO_4^{2-} anion. The NO_3^- anion is detected but is not the same as our reference spectrum of $Ca(NO_3)_2$".	
	$Ca_3(PO_4)_2 + HCl$ only	By i.r. "Sample is hydrated. Sample does not compare with $CaPO_4$, $CaHPO_4$, or $Ca(H_2PO_4)_2 \cdot H_2O$; sample could be material such as $Ca(ClHPO_3)_2 \cdot (H_2O)$".	

TABLE I (Continued)

Sample	*Matrix*	*Composition of residue*	*Comments*
F_1	KH_2PO_4	KH_2PO_4. By i.r.: "No evidence for NO_3^- or ClO_4^-. Spectrum shows only evidence for KH_2PO_4".	
G	$PbCl_2$	$PbCl_2$, major constituent. Unidentified phase, minor constituent.	
G_1	$Pb(NO_3)_2$	$PbCl_2$, $Pb(NO_3)_2$—both major. By i.r.: "The sample is hydrated, a mixture of $Pb(NO_3)_2$ and presumably $Pb(ClO_4)_2$, $-ClO_4^-$ anion is present but no i.r. standard for the compound".	$Pb(NO_3)_2$ is stable to 180°, decomposes up to 500° slowly and faster to 648°.
H	Ca + Fe chlorides	Fe_2O_3. Small amount unidentified phase. Sample mainly amorphous.	
H_1	Ca + Fe nitrates	Same as H.	
I	Solution containing 3.3% NaCl, 7.8% KNO_3, 8% P_2O_5	$KClO_4$, major constituent. $NaClO_4$, minor constituent. Unidentified phase, minor constituent. By i.r.: "No evidence for NO_3^- anion. Sample contains some H_2O and also acidic OH. Compounds such as NaH_2PO_4, Na_2HPO_4 (or K analogs) are not present. Bands near 1000, 621 and 485 cm^{-1} suggest the presence of ClO_3^-. Sample does not appear to contain Na_3PO_4 or K_3PO_4. Bands near 1100 and 621 cm^{-1} could result from ClO_4^-".	
I_1	Solution containing 11% $NaNO_3$, 13% KNO_3, 24% H_3PO_3	$KClO_4$ only crystalline phase observable.	
J	NaCl, $Ca_3(PO_4)_2$, $MgCl_2$, $FeCl_3\cdot6H_2O$ combined (equal quantities)	$NaClO_4$, c.c. Unidentified phase, small amount.	
J_1	$NaNO_3$, $Ca_3(PO_4)_2$, $Mg(NO_3)_2\cdot6H_2O$, $Fe(NO_3)_3\cdot9H_2O$	Same as J above.	
	The following samples K through M_1 received no additional HNO_3 treatments at the end of the oxidation.		
K	NaCl + $NaNO_3$ (1:1)	$NaClO_4$.	
K_1	$NaNO_3$	$NaClO_4$.	
L	$Ca_3(PO_4)_2$	$Ca_{10}Cl_2(PO_4)_6$-type, major constituent. $NaClO_4$, trace. Unidentified phase, minor constituent.	
L_1	KH_2PO_4	$KClO_4$ only crystalline phase observable.	
M	NaCl, KNO_3, P_2O_5 as in I	$NaClO_4$, 10–20%. $KClO_4$, major constituent.	
M_1	$NaNO_3$, KNO_3, H_3PO_3 as in I_1	$KClO_4$.	
	The following miscellaneous samples were not given additional nitric acid treatment and heated only to 270°.		
	$Mg(NO_3)_2\cdot6H_2O$ + 3:2 acid	$Mg(ClO_4)_2$, minor. Major unidentified phase.	

TABLE I (Continued)

Sample	*Matrix*	*Composition of residue*	*Comments*
	$Mg(NO_3)_2 \cdot 6H_2O$ + HNO_3 only	$Mg(NO_3)_2$, major. $Mg(NO_3)_2 \cdot 2\frac{1}{2}H_2O$, $Mg(NO_3)_2 \cdot 6H_2O$, present.	
	$Mg(NO_3)_2 \cdot 6H_2O$ + $HClO_4$ only	$Mg(ClO_4)_2$, $Mg(ClO_4)_2 \cdot 3H_2O$ and unidentified phase.	
	$Pb(NO_3)_2$ + $HClO_4$ only	By i.r.: "Sample is hydrated. i.r. specifically detects ClO_4^-. A band at ~1190 cm^{-1} suggests NO_2^- and other bands suggest the possible presence of ClO_3^-. Sample does not contain NO_3^-".	
	Liver	$KClO_4$ as only crystalline phase. By i.r.: "Weak spectrum, no evidence for NO_3^-, but ClO_4^- appears present".	
	Kidney	$KClO_4$, c.c.; unidentified $<20\%$.	
	Spleen	$KClO_4$, c.c. plus minor unidentified phase. By IR: "Sample could be a mixture of ClO_3^- and ClO_4^-. Unidentified material is also present".	
	Muscle	$KClO_4$, c.c.	
	Bone	$Ca(NO_3)_2$, c.c. Unidentified phase, possibly $NaNO_2$, 5–15%.	
	Plasma	$NaClO_4$, major constituent ($>50\%$). Unidentified phase, $<50\%$.	

DISCUSSION

The data presented indicate the analytical difficulties in obtaining complete composition information on the wet-ashed residues with even relatively simple systems, *e.g.*, one compound reacting with one acid, or when complex mixtures may be present. Complex residues in various degrees of hydration and crystallinity are present even in the former situation.

This complexity is greatly increased with biological tissue residues in which cations may vary considerably in both number and concentration with different sample types. The lack of crystallinity of many residues seriously limits the information obtainable by X-ray diffraction, while the low concentrations of some compounds present in the residue reach the sensitivity limitations by both X-ray and infrared techniques.

Some observations can be made regarding each of the two aspects of this study: biological tissue residues, and residues obtained from known chemicals after the wet-ashing treatment.

Biological tissue residues

Tissues such as liver, kidney, and spleen are partially converted to perchlorate salts, with potassium perchlorate the only crystalline material detected by X-ray diffraction. Sodium perchlorate is the major crystalline constituent of wet-ashed plasma. Bone, which is largely modified calcium phosphate, is partially converted to calcium nitrate. The phosphate portion evidently becomes noncrystalline and is, therefore, not detected or identified by X-ray diffraction and is not completely identified by infrared.

It is significant to note that iron and magnesium compounds when wet-ashed alone are converted to the relatively insoluble oxides, Fe_2O_3 and MgO. In the case of iron(III) trioxide, solubility is poor in nitric acid but is rapid in hydrochloric acid. Solubility difficulties in dilute nitric acid would appear to present a problem which has not been recognized in past experience. In sample matrices, however, these cations evidently form complexes which are soluble in dilute nitric acid and are observed spectrographically.

Residue obtained from known chemicals after the wet-ashing treatment

Of particular interest are the following observations. Iron salts are converted to Fe_2O_3 as previously mentioned. Alkali metal salts are converted to soluble perchlorates as major crystalline components.

The lack of crystalline phosphate residues reveals uncertainty about these materials and their subsequent solubility when prepared in this manner.

The partial conversion of lead nitrate to lead chloride as seen by X-ray diffraction, but unconfirmed by i.r. analysis, is unexpected. Infrared results show that there is no nitrate left with either lead or magnesium nitrates after treatment with perchloric acid only.

Calcium phosphate is altered by both perchloric acid and nitric acid.

Even gross amounts of metals may be undetected by X-ray diffraction because of the noncrystalline products formed when mixtures of compounds (*e.g.*, sodium nitrate, potassium nitrate and phosphorous acid) are wet-ashed. In this case, potassium perchlorate was the only crystalline phase detected.

Mixtures of calcium and iron as chlorides or nitrates yield noncrystalline calcium compounds but some crystalline iron(III) trioxide.

The extensive X-ray diffraction and infrared analyses by L. R. RUHBERG and R. A. NYQUIST respectively are acknowledged.

SUMMARY

The chemical composition of inorganic residues after typical acid oxidation treatment has been investigated. X-Ray diffraction and infrared data are included for particular chemicals and biological materials which have been wet-ashed.

RÉSUMÉ

La composition chimique de résidues minéreaux, après traitement acide d'oxydation, est examinée. Des valeurs de diffraction aux rayons-X et d'infra-rouge sont données pour des substances chimiques particulières et des substances biologiques, après minéralisation par voie humide.

ZUSAMMENFASSUNG

Die chemische Zusammensetzung anorganischer Rückstände nach typischer

oxidativer Säurebehandlung ist untersucht worden. Hierzu gehören Röntgenbeugungs- und Infrarotangaben für einzelne Chemikalien und biologische Materialien, die nass verascht worden sind.

REFERENCES

1 T. M. Hess, J. S. Owens and L. G. Reinhardt, *Ind. Eng. Chem., Anal. Ed.*, 11 (1939) 646.
2 V. G. Perry, W. M. Weddell and E. R. Wright, *Anal. Chem.*, 22 (1950) 1516.
3 C. Duval, *Inorganic Thermogravimetric Analysis*, Elsevier, New York, 1963.

Analytica Chimica Acta
Elsevier Publishing Company, Amsterdam
Printed in The Netherlands

SEQUENTIAL SPECTROPOLARIMETRIC ANALYSIS OF MIXTURES OF BARIUM–CALCIUM, CADMIUM–COPPER AND CADMIUM–ZINC*

R. J. PALMA, SR.**, P. E. REINBOLD AND K. H. PEARSON***

Department of Chemistry, Texas A & M University, College Station, Texas 77843 and Cleveland State University, Cleveland, Ohio 44115 (U.S.A.)

(Received February 7th, 1970)

Spectropolarimetric titrimetry is a relatively new analytical technique first described by KIRSCHNER AND BHATNAGAR[1]. Continued interest in this technique and its potentialities was enhanced by the introduction of readily available commercial photoelectric polarimeters and later, by improvements in design and versatility. The optical rotation of the system is constantly monitored with a photoelectric polarimeter while the titration proceeds. The conditions of the analysis must be chosen so that an inflection in the optical rotation occurs at the titration end-point. This technique has been successfully applied to many different acid–base type systems[1,2], and its scope has been broadened by PEARSON *et al.* who used the two stereospecific ligands D-(−)-1,2-propylenediaminetetraacetic acid (D(−)PDTA) and D-(−)-*trans*-1,2-cyclohexanediaminetetraacetic acid (D(−)CDTA). The successful analyses of the 3*d* transition metals[3]; the heavy metals, cadmium, mercury, lead and bismuth[4]; the lanthanide metals[5]; the Group III A metals, aluminum, indium and thallium[6]; and the Group II A metals, magnesium, calcium, strontium and barium and the Group III B metal, yttrium[7,8] indicate its wide range.

An extension of the technique to the direct determination of two-component systems is described in this paper. For the three sequential spectropolarimetric titrations, the strong stereospecific chelating agent, D-(−)-1,2-propylenediaminetetraacetic acid, was selected as the titrant because of its chelating strength and its intrinsic optical activity[9]. The characteristics and advantages of this chelating agent and its metal chelates have been discussed previously[4]. This present work forms part of a systematic study of the potentialities and limitations of the spectropolarimetric titrimetric technique with D(−)PDTA. As in the sequential acid–base systems where the acid dissociation constants of the two acids titrated must have log K values that differ by greater than 2.0 units, the difference in the stability constants (log K) of the metal–chelate complexes had to be greater than *ca.* 2.5 units for the sequential titration of metal ions. Thus, two different types of aqueous sequential metal ion titrations are possible: (*a*) metals widely separated in K values, *e.g.*, barium–PDTA (log K 8.48) and calcium–PDTA (log K 11.47)[10]; and (*b*) systems with log K differences less than 2.5, but with differences in conditional constants larger than this in the presence of auxiliary complexing agents.

---

* This study was presented in part at the 157th National Meeting of the American Chemical Society on April 18th, 1969 at Minneapolis, Minn., U.S.A.

** Present address: Department of Chemistry, Midwestern University, Wichita Falls, Texas 76308.

*** Cleveland State University. Author to whom correspondence should be sent.

EXPERIMENTAL

Apparatus

The spectropolarimetric titrations were carried out at ambient temperature with a Perkin-Elmer model 141 photoelectric polarimeter and accessory equipment as previously described[4]. All pH measurements were made with an Orion model 801 digital pH meter and a Sargent combination glass electrode. All sequential spectropolarimetric titrations were performed at 365 nm.

Reagents

All solutions were prepared from analytical reagent-grade chemicals, with demineralized water, and stored in polyethylene bottles.

D-(−)-1,2-Propylenediaminetetraacetic acid monohydrate was prepared and standardized as described previously[4]. The titer and optical rotation of the standard Na_2D(−)PDTA solutions remained constant during a four-month period.

Standard solutions of EDTA were prepared from dried primary-standard $Na_2H_2EDTA \cdot 2\ H_2O$ (G. F. Smith Chemical Company).

The barium(II), cadmium(II), zinc(II) and copper(II) perchlorate solutions were prepared from the hydrated perchlorate salts (G. F. Smith Chemical Co.). The barium(II) solution was standardized with primary standard EDTA using metalphthalein as the indicator[11], the cadmium(II) and zinc(II) solutions with EDTA using eriochrome black T as the indicator[12], and the copper(II) solution against EDTA with PAN as the indicator[13]. The standard calcium(II) solution was prepared in the usual way from dried primary-standard calcium carbonate (Mallinckrodt).

The pH 10 buffer was prepared from ammonium chloride and ammonium hydroxide[4].

Sequential spectropolarimetric titrimetric procedure

The general techniques for the sequential titrations and for the establishment of the titration curves were similar to the single metal determinations described previously; volume corrections were applied as before[4]. Details of the titration conditions for the different two-component metal systems are given below.

Barium and calcium. Place aliquots of the two metal solutions to be determined in the titration vessel, add 30 ml of pH 10 buffer and dilute the sample with sufficient deionized water to bring the total volume to 100 ml. (A large amount of buffer was required to ensure that the D(−)PDTA complexes or the excess D(−)PDTA did not change coordination states or ionic species during the course of the titration.) Insert the flow-through polarimeter cell into the cell compartment and set the optical digital readout of the polarimeter to zero.

Titrate the solution with a relatively concentrated solution of Na_2D(−)PDTA, from a 5-ml microburet readable to ±0.001 ml. The ratio of the molar concentration of the Na_2D(−)PDTA titrant to that of the metal ion solution was *ca.* 50:1.

Cadmium and copper. Proceed as described for calcium and barium, but use 10 ml of pH 10 buffer.

Cadmium and zinc. Proceed as described for calcium and barium, but use 3 ml of pH 10 buffer.

After the addition of each increment of titrant, it is necessary to allow the polarimeter digital readout to stabilize. The kinetics for the two-component system titrations are slow and time must be allowed for the system to come to equilibrium. The spectropolarimetric titration of the cadmium–zinc mixture and the cadmium–copper mixture require considerably more time than the titration of the barium–calcium mixture because of slower ligand exchange kinetics involved.

RESULTS AND DISCUSSION

The protonation or deprotonation of D(–)PDTA changes its structure and charge, resulting in optical rotational dependence on pH. A spectropolarimetric titration of D(–)PDTA with standard sodium hydroxide was carried out to determine the effect of pH on the molecular rotations of D(–)PDTA. From Table I, it can be seen that in the pH region of 10, the molecular rotation can vary considerably depending upon the pH; thus, it was necessary to use sufficient buffer to ensure pH control during the titration.

TABLE I

MOLECULAR ROTATIONS OF D(–)PDTA AT VARIOUS PH VALUES

pH	$[M]_{365}$	*pH*	$[M]_{365}$
2.01	–455	7.04	–267
2.53	–393	7.50	–263
3.03	–362	8.03	–271
3.54	–362	8.59	–308
4.02	–360	9.01	–366
4.60	–360	9.52	–458
5.07	–354	10.04	–534
5.50	–341	10.56	–572
6.00	–314	11.04	–585
6.52	–284	12.01	–591

Barium–calcium mixture

The spectropolarimetric titration of the mixture of barium and calcium is an example of a direct sequential spectropolarimetric titration of a two-component system where the difference in the stability constants of the two complexes exceeds 2.5 log units. The values of log *K* for the calcium and barium ions with PDTA are 11.47 and 8.48, respectively. This difference of approximately 3.0 log units allows a direct sequential titration to be performed without the use of any auxiliary complexing agent or masking agent. At 365 nm, the molecular rotation of the calcium–D(–)PDTA complex is negative whereas the complex formed between barium and D(–)PDTA is positive. Figure 1 shows the sequential spectropolarimetric titration of calcium and barium. The first part of the curve corresponds to the formation of the calcium complex of D(–)PDTA with increasing negative rotations. After the calcium is essentially complexed, the formation of the barium–D(–)PDTA complex is initiated, and the observed rotations increased in a positive direction. After the barium has been completely complexed, the rotations decrease upon addition of excess D(–)PDTA as is expected from the molecular rotation of D(–)PDTA at pH 10 and 365 nm. From Fig. 1, it can be seen that the observed rotations are small compared to the rotations observed in the following titrations. Because of the small magnitude of the observed rotations in this sequential titration, the control of pH is very critical, necessitating the use of a large amount of the ammonia–ammonium chloride buffer. However, the reaction between the ammonia–ammonium chloride buffer and the barium and calcium ions is negligible, and the precision and accuracy of this sequential titration are excellent.

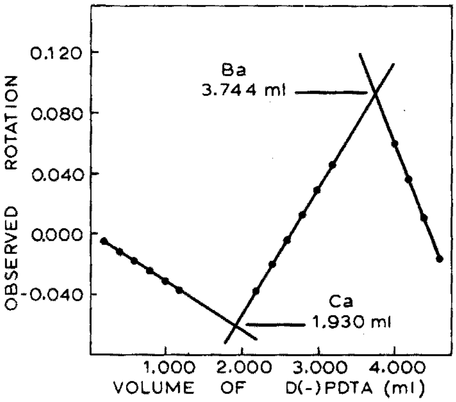

Fig. 1. Sequential spectropolarimetric titration of barium and calcium at pH 10 and 365 nm.

Cadmium–copper mixture

The sequential spectropolarimetric titration of cadmium and copper cannot be performed directly without the use of an auxiliary complexing agent. The stability constants for the cadmium and copper from aqueous solution with PDTA are 18.83 and 19.94, respectively[14], and the difference between them is insufficient for sequential titrimetry. However, through the use of the auxiliary complexing agent ammonia, which forms a stronger complex with copper than with cadmium as is evidenced by the β_4 values of 13.05 and 7.21, respectively, the difference between the conditional stability constants is approximately 3.6 log units, which is sufficient to allow a sequential titration.

However, sufficient difference in the values of the conditional stability constants is not the only criterion for a successful sequential spectropolarimetric titration; it is also necessary that the molecular rotations of the two metal complexes, as well as the molecular rotation of the titrant, be distinctly different than each other at the wavelength chosen for analysis. The molecular rotation of the cadmium–D(−)PDTA complex in ammoniacal buffer solution[4] is +1377 degree ml dm^{-1}mole^{-1}, while that of copper–D(−)PDTA complex is −722 at the same conditions[3]. Table I shows that the molecular rotation of the titrant D(−)PDTA has a negative value which is much less than the molecular rotation of the copper–D(−)PDTA complex. Figure 2 shows the sequential spectropolarimetric titration of the cadmium–copper mixture. Since the conditional stability constant of the cadmium–D(−)PDTA complex is significantly greater than that of the copper–D(∓)PDTA complex, the first branch of the sequential titration is due to the formation of the cadmium–D(−)PDTA complex. After the cadmium has been essentially complexed, there is a radical change in the observed rotation due to the complexation of the copper ion. Because of the large magnitudes of the molecular rotations and the difference in signs of the molecular rotations of the cadmium- and copper–D(−)PDTA complexes, the extrapolated first end-point is very sharp. The third straight line segment is due to the excess D(−)PDTA titrant. The second end-point is located by the extrapolation of these two straight-line segments.

Cadmium–zinc mixture

Similar to the above case with the cadmium–copper mixture, the cadmium–zinc mixture could not be titrated sequentially without the aid of an auxiliary complexing agent, since the log K values are 18.83 and 17.14, respectively, for the cadmium–D(−)PDTA[14] and the zinc–D(−)PDTA complexes[15]. In the presence of the auxiliary complexing agent ammonia ($\beta_4=7.21$ and 9.46, respectively, for the cadmium and zinc ions), the difference between the conditional stability constants is approximately 4 log units, which, in conjunction with the differences in the molecular rotations of the reacting components, is sufficient to permit the sequential spectropolarimetric titration of cadmium and zinc (Fig. 3). The first branch of the sequential titration is due to the formation of the cadmium–D(−)PDTA complex, after which there is a radical change in the observed rotation owing to the complexation of the zinc with D(−)PDTA.

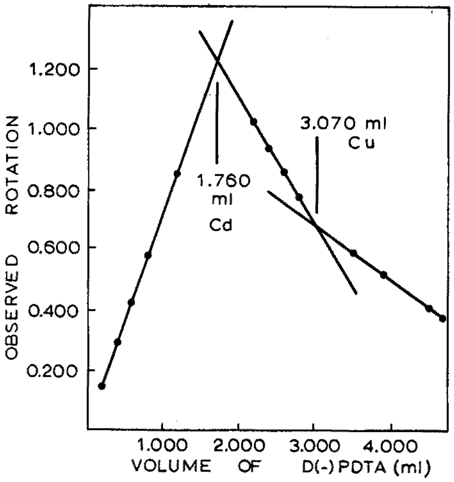

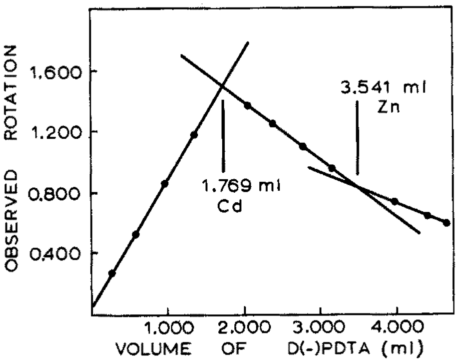

Fig. 2. Sequential spectropolarimetric titration of cadmium and copper at pH 10 and 365 nm.

Fig. 3. Sequential spectropolarimetric titration of cadmium and zinc at pH 10 and 365 nm.

Table II gives the results of the three two-metal mixtures described above. Each spectropolarimetric sequential titration value reported is the average of at least three individual sequential determinations. The deviations reported in Table II are comparisons of the amounts found by the spectropolarimetric sequential titration with the amount of metal taken as determined by conventional EDTA titrations of the individual metal ions. The range of the average deviations was 0.0 to 0.37%. Both the precision and the accuracy of the sequential spectropolarimetric titrations are excellent.

The results described in the present paper confirm the general advantages of the spectropolarimetric titration methods, which were outlined previously[4]. Additional

TABLE II

RESULTS OF THE SPECTROPOLARIMETRIC TITRATIONS

Metal	*Metal taken (mg)*	*Metal found (mg)*	*Deviation*	
			(mg)	*(%)*
$Ba^{2+} + Ca^{2+}$				
Ba^{2+}	128.8	128.8 ± 0.3	0.0	0.0
Ca^{2+}	40.08	40.14 ± 0.04	+0.06	+0.15
$Cd^{2+} + Cu^{2+}$				
Cd^{2+}	108.6	108.4 ± 0.2	−0.2	−0.18
Cu^{2+}	45.71	45.54 ± 0.21	−0.17	−0.37
$Cd^{2+} + Zn^{2+}$				
Cd^{2+}	108.6	108.7 ± 0.1	+0.1	+0.09
Zn^{2+}	63.28	63.17 ± 0.03	−0.11	−0.17

advantages are that the pH need not be altered during the titration as is usually necessary in visual titrations, and no difficulties are encountered through having to select two suitable visual indicators. The techniques of masking and demasking, as well as the difference between a metal determined at one condition and the total metal determined at a second condition (sometimes requiring two different samples), are also avoided. The sequential determination of the barium–calcium mixture particularly corroborates the advantages of this analytical technique.

This work was supported by The Robert A. Welch Foundation Fellowship Grant A-262.

SUMMARY

A direct sequential spectropolarimetric titration method based on the stereospecific ligand D-(−)-1,2-propylenediamine tetraacetic acid was developed for the following three mixtures: barium–calcium, cadmium–copper, and cadmium–zinc. In a single titration, without changing the pH or other environmental conditions, mixtures that cannot be sequentially titrated visually in aqueous solution, can be successfully titrated. Because the optically active titrant and the stereospecifically formed complexes have molecular rotations significantly different from each other, they serve as self-indicators for the two titration end-points. Both the precision and accuracy of the sequential spectropolarimetric titrations are excellent and the range of the average deviations was 0.0 to 0.37%.

RÉSUMÉ

Une méthode de titrage spectropolarimétrique direct est mise au point pour les mélanges suivants: baryum–calcium, cadmium–cuivre et cadmium–zinc. Elle est basée sur le ligand stéréospécifique acide D-(−)-1,2-propylènediaminotétracétique. Le titrant optiquement actif et les complexes stéréospécifiquement formés ayant des rotations moléculaires suffisamment différentes servent de self-indicateurs pour les deux points finals. La précision et l'exactitude sont excellentes.

ZUSAMMENFASSUNG

Es wurde eine direkte spektropolarimetrische Titrationsmethode unter Verwendung des stereospezifischen Liganden D-(−)-1,2-Propylendiamintetraessigsäure für folgende drei Gemische entwickelt: Barium–Calcium, Cadmium–Kupfer und Cadmium–Zink. Im Gegensatz zur visuellen Methode können die Gemische ohne Änderung des pH-Wertes oder anderer Bedingungen in einer einzigen Titration mit Erfolg titriert werden. Da der optisch aktive Titrant und die stereospezifisch gebildeten Komplexe deutlich voneinander verschiedene molekulare Rotationen haben, dienen sie als Selbstindikatoren für die beiden Titrationsendpunkte. Die Genauigkeit der spektropolarimetrischen Titrationen ist ausgezeichnet, die durchschnittlichen Abweichungen betrugen 0.0–0.37%.

REFERENCES

1 S. Kirschner and D. C. Bhatnagar, *Anal. Chem.*, 35 (1963) 1069.
2 K. H. Pearson and S. Kirschner, *Anal. Chim. Acta*, 48 (1969) 339.
3 R. J. Palma, P. E. Reinbold and K. H. Pearson, *Anal. Chem.*, 42 (1970) 47.
4 R. J. Palma and K. H. Pearson, *Anal. Chim. Acta*, 49 (1970) 497.
5 D. L. Caldwell, P. E. Reinbold and K. H. Pearson, *Anal. Chem.*, 42 (1970) 416.
6 D. L. Caldwell, P. E. Reinbold and K. H. Pearson, *Anal. Chim. Acta*, 49 (1970) 505.
7 R. J. Palma, P. E. Reinbold and K. H. Pearson, *Anal. Lttrs.*, 2 (1969) 553.
8 J. R. Baker and K. H. Pearson, *Anal. Chim. Acta*, in press.
9 R. J. Palma, P. E. Reinbold and K. H. Pearson, *Chem. Commun.*, 6 (1969) 254.
10 J. H. Grimes, A. J. Huggard and S. P. Wilford, *J. Inorg. & Nucl. Chem.*, 25 (1963) 1225.
11 A. Anderegg, H. Flaschka and G. Schwarzenbach, *Helv. Chim. Acta*, 37 (1954) 113.
12 W. Biedermann and G. Schwarzenbach, *Chimia (Aarau)*, 2 (1948) 56.
13 Kuang Lu Cheng and R. H. Bray, *Anal. Chem.*, 27 (1955) 782.
14 H. M. N. H. Irving and J. P. Conesa, *J. Inorg. & Nucl. Chem.*, 26 (1964) 1945.
15 H. Ogino, *Bull. Chem. Soc. Japan*, 38 (1965) 771.

Analytica Chimica Acta
Elsevier Publishing Company, Amsterdam
Printed in The Netherlands

SHORT COMUNICATIONS

A simple cheap continuous flux monitor for 14-MeV neutrons

Various techniques are available for monitoring the flux of 14-MeV neutrons. The commonest are the boron trifluoride counter, methods involving plastic scintillators, proton recoil detectors, target cooling water monitors[1] and various standard sample systems. IDDINGS[2] surveyed these techniques and concluded that the technique based on monitoring the target cooling water was the least accurate. However, because this technique has many attractive features, a brief study was made and it was shown that the technique is indeed capable of giving accurate results; because of its simplicity and freedom from interference from low energy neutrons, the method is to be preferred to others.

The advantages of this approach are quite clear. It is a continuous monitor with a neutron threshold of 10 MeV and thus is sensitive only to 14-MeV neutrons. Short time constants can be used resulting in a wide linear range, as opposed to the necessity of making time constant corrections to BF_3 counters. The equipment required need not be capable of working in a high radiation area (*viz.*, near the tritium target) and consists of only a standard scintillation detector assembly and associated electronics. The limitation in accuracy of this approach is primarily that of providing a constant flow of water.

The boron trifluoride counter, in common with other moderation counters, is sensitive to thermal neutrons and (d, d) reaction products as well as 14-MeV neutrons. Monitors based on plastic scintillators require the setting up of critical bias levels which may be difficult to reproduce. Other proton recoil detectors suffer from this same limitation. Discrete sampling systems, as advocated by IDDINGS, do not allow the continuous monitoring which is sometimes required, *e.g.*, if a fluid is continuously irradiated. If, however, the neutron dose received by a sample located close to the neutron source must be determined, undoubtedly the most accurate technique is to irradiate a standard simultaneously with the unknown sample (see IDDINGS[2]). All the neutron flux monitors then of course start with the same disadvantage, relying as they do on the precise alignment of the sample and the fact that they need to be calibrated to give absolute flux determinations.

The target cooling water method relies on the fact that in the production of 14-MeV neutrons, radioactivity is induced in the water employed for target cooling. If the flow is constant, the activity induced is proportional to the neutron flux produced at the target. The relevant reaction $^{16}O(n,p)^{16}N$ has a 10-MeV threshold; this is far higher than the energies generally associated with (d,d) reaction neutrons. The ^{16}N β-decays ($T_{\frac{1}{2}}$ 7.2 sec) to excited states of ^{16}O which in turn decay to the ground state emitting mainly 6.1- and 7.1-MeV γ-rays; counting these gives a measure of the neutron flux.

Experimental

14-MeV neutrons were produced by bombarding a tritium target with 0.8-MeV deuterons from a 3-MeV Van de Graaff accelerator. A constant-pressure valve (Valve type F36Y 0–25 p.s.i.; Bailey and Co., Ltd., Albion Works, Patricroft, Manchester, U.K.) gave a flow of target cooling water that remained constant to ±0.5% during a week's running. The water flowed through plastic tubing (5 mm i.d.) past a γ-ray detector, which was housed in a lead castle (15 cm thick walls) some 8 m from the target and shielded from it by a 1.5-m thick concrete wall. β-Rays from ^{16}N decay were absorbed in 3 cm of perspex and 1 cm of aluminium placed between the water and the detector. The detector was a 7.5 × 7.5 cm NaI(Tl) crystal and photomultiplier assembly feeding a preamplifier–amplifier–single-channel analyser–scaler–print out chain. Background counts were reduced by setting the single-channel analyser to accept only γ-rays with energies between 5.5 and 7.5 MeV. A boron trifluoride counter, 5 m from the target, was used as a monitor for comparison purposes.

Aluminium foil activation was adopted as the absolute measure of the neutron flux; the relevant reaction, $^{27}Al(n,\alpha)^{24}Na$, has a threshold of 3 MeV. A pneumatic rabbit transport system moved the samples to and from the irradiation point. The samples were irradiated for 5 min at differing neutron flux levels and allowed to cool for 300 min. The photopeak of the 2.75-MeV γ-ray was then counted for 5 min. A programmed electronic device allowed automation of the steps in the experiment.

Results

Figure 1 shows the water activity and boron trifluoride counts plotted against aluminium foil activity. The maximum neutron flux corresponds to a deuteron current of 300 μA. Similar results were obtained for fluorine samples (PTFE pellets) and also at deuteron energies of 1.0 MeV.

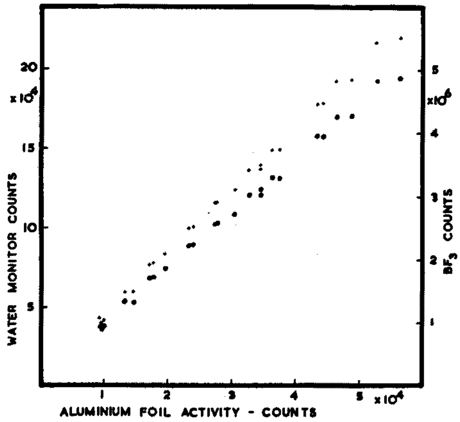

Fig. 1. Water monitor and BF_3 counts *vs.* aluminium foil activity. (+) Water *vs.* foil; (●) BF_3 *vs.* foil.

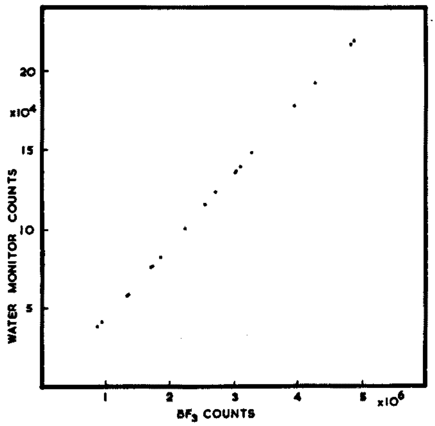

Fig. 2. Water monitor *vs.* BF_3 counts.

Although the water *vs.* foil graph shows deviations from linearity of up to 3%, the plot of water counts *vs.* boron trifluoride counts has deviations of only 1.2% (Fig. 2). (A similar correlation can be observed in IDDINGS' graphs for Pilot B and boron trifluoride.) A list of the known sources of error is as follows:

Weight of samples (830 ± 5 mg) $\approx 0.5\%$
Timing accuracy (± 20 msec) $\sim 0\%$
Water counts (~ 0.4–$2 \cdot 10^5$) 0.5–0.25%
Foil counts (~ 1–$5 \cdot 10^4$) 0.5–1%
Long counter counts ($> 10^6$) $\sim 0\%$
Constancy of water flow $\pm 0.5\%$

Thus discrepancies of about 1% should be expected in the water *vs.* boron trifluoride counts plot—the actual standard deviation is 1.2%. However, for the water *vs.* foil counts plot a 3% deviation is obtained; about 1% is contributed by the known errors, so it seems reasonable to attribute the rest to beam irregularities and variations in the mass distribution of the samples. The samples were made of aluminium foil rolled into pellets and inserted into the rabbit of the pneumatic transport system.

It is a pleasure to acknowledge many helpful discussions with Mr. G. J. McCallum in the course of this work.

Institute of Nuclear Sciences,
Department of Scientific and Industrial Research,
Lower Hutt (New Zealand)

P. J. Mathew*
K. P. Pohl

1 E. L. Steele and W. W. Meinke, *Anal. Chem.*, 34 (1962) 185.
2 F. A. Iddings, *Anal. Chim. Acta*, 31 (1964) 206.

(Received March 10th, 1970)

---

* Permanent address: P. J. Mathew, Physics Department, Victoria University of Wellington, Wellington (New Zealand)

Anal. Chim. Acta, 51 (1970) 336–338

Semi-continuous amperometric technique for ion-exchange kinetics

Amperometry with a single polarizable electrode has been applied for reaction kinetic studies[1–4]. During a kinetic study of ion-exchange reactions, some difficulties were encountered in the use of the non-continuous method[5]. The main drawback of this method is that for each measurement a new portion of ion exchanger has to be used, which causes comparison of results from inhomogeneous samples. This communication describes the application of a semi-continuous technique based on amperometric measurements for the kinetic studies of ion-exchange reactions, for a chelating resin with phosphonic acid functional groups.

Experimental

Preparation of the resin. The representative resin chosen was Bio-Rex 63 (Bio-Rad Laboratories; purified Duolite-63). The resin is of the styrene type (6% D.V.B.) and its functional group is $R{-}P({=}O)(OH)_2$.

The resin was washed with distilled water until the effluent was colorless and two column volumes of 2 *M* hydrochloric acid were added. After washing the resin free of hydrochloric acid, the exchanger was converted to the sodium form with two column volumes of 2 *M* sodium hydroxide, and washed with water. This cycle was repeated twice, the last wash in the sodium form being performed with two column volumes of 0.01 *M* sodium chloride and with only one column volume of water (to avoid hydrolysis). The resin was then air-dried, sieved (to separate the various mesh sizes) and stored in well-stoppered bottles. The mean weight capacity was found to be 5.1 meq g^{-1} resin[6].

Apparatus. A Metrohm Polarecord E 261 R with a Dropping Control Device E 354 was used for rapid polarographic measurements. A Beckman Model D-4 spectrophotometer was used for the determination of the various cations. A Beckman expanded-scale pH-meter permitting direct reading of 0.01 pH unit was employed for the various pH measurements.

The reaction vessel was a Metrohm jacketed polarographic cell in which were located the polarizable dropping mercury electrode, a reference electrode and a glass two-way stopcock and ground joint so that the nitrogen gas could flow through the solution and over it as desired. By means of a thermostat provided with a circulation pump and a thermometer, water was circulated through the double-jacketed wall of the reaction vessel to keep the solution at a constant temperature ($\pm 0.1°$). The diffusion currents at a constant applied voltage were measured with a polarograph equipped with a dropping control device for rapid polarography. The solutions were magnetically stirred.

Semi-continuous kinetic measurements. Solutions (25–50 ml) which were 0.002 to 0.01 *M* in the cation studied were introduced into the reaction vessel. Neutral salt was added to serve as the supporting electrolyte, and to increase the ionic strength of the solution to a value of 0.5 *M* or more, so as to eliminate diffusion through the liquid film surrounding the resin particle.

The required constant temperature was fixed, and the oxygen was eliminated by passing oxygen-free nitrogen for 10–15 min. After the deaeration, the nitrogen flow was passed over the solution and the initial diffusion current was recorded at a constant applied voltage using the rapid position of the polarograph and the high-speed position of the polarographic chart. A weighed amount of the resin (equivalent to the cation in the solution) was rapidly added and the stirrer started. During the exchange reaction, the changes in concentration of the cation were followed by diffusion current measurements at a constant applied potential.

However, the vigorous stirring of the solution necessary to insure particle diffusion, produced abnormal fluctuations of the diffusion current measured. A semi-continuous method was then used: after a measured time interval, the stirrer was stopped and the diffusion current was rapidly measured in the unstirred solution. The rapid halting of the stirring movement was achieved by means of two horseshoe magnets round the bottom of the reaction vessel. With rapid recording of the diffusion current, the entire operation required only 5–8 sec, so that almost continuous measurements could be obtained.

Results

To compare the feasibility of this semi-continuous method with the usual batch method for kinetic measurements of ion-exchange reactions, the semi-continuous technique was used in parallel with the non-continuous limited bath technique of KRESSMAN AND KITCHENER[5] for several cations (Fig. 1, Table I). The reactions selected had rate-determining steps governed either by particle diffusion or by a second-order chemical reaction. In the first case, the diffusion coefficient was evaluated as discussed by KRESSMAN AND KITCHENER[5], whereas the reaction rate constant was defined from the kinetic equations of FROST AND PEARSON[7]. The close similarity of the slopes of the plots in Fig. 1 shows that the various equations for the ion-exchange mechanism are unaffected by the change in measuring technique. The experimental values of D and k obtained by the two techniques (Table I) vary by 1–3% but this lies within the

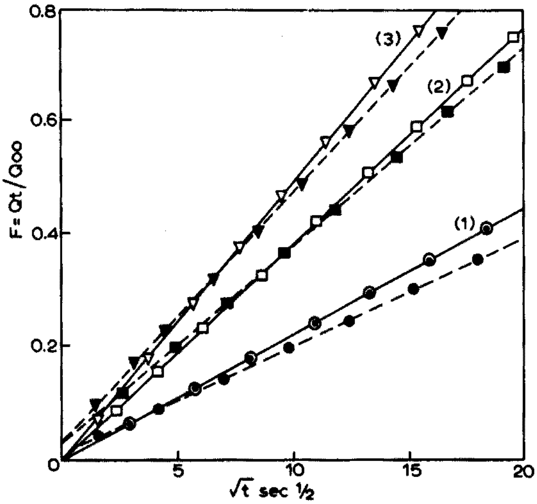

Fig. 1. Comparison between the semi-continuous (– – –) and non-continuous method (——). Solution: 2.5 mM cation in 1 M NaCl; temp. 25°. (1) Pb^{2+}/Na^+, r=0.0282 cm; (2) Cu^{2+}/Na^+, r = 0.0158 cm; (3) Ni^{2+}/Na^+, r = 0.0125 cm.

TABLE I

COMPARISON BETWEEN THE SEMI-CONTINUOUS AND THE NON-CONTINUOUS METHODS AT 25°[a]

Exchange reaction	Q_0 *(mM)*	$r \cdot 10^2$ *(cm)*	$D \cdot 10^8$ *(cm² sec⁻¹)*	
			Non-cont.	*Semi-cont.*
Ni^{2+}/Na^+	1.85	1.56	1.32	1.30
Ni^{2+}/Na^+	1.85	1.25	1.40	1.37
Cu^{2+}/Na^+	2.49	1.58	1.28	1.27
Cu^{2+}/Na^+	5.00	1.85	0.97	0.96
Pb^{2+}/Na^+	2.50	1.22	1.30	1.26
Pb^{2+}/Na^+	1.85	1.81	1.12	1.09
			$k \cdot 10^2 (l\ mol^{-1}\ sec^{-1})$	
In^{3+}/Na^+	1.67	1.58	8.10	8.10
In^{3+}/Na^+	2.50	1.47	9.40	9.34
UO_2^{2+}/Na^+	2.50	1.57	0.36	0.35
UO_2^{2+}/Na^+	1.85	1.51	0.29	0.28
UO_2^{2+}/Na^+	3.70	1.14	0.45	0.44

[a] Q_0 = Initial concentration of the cation in the solution; r = radius of the resin particle; D = diffusion coefficient; k = second-order reaction rate constant.

experimental error. The effect of the stopping procedure is to make the D and k values slightly lower.

Conclusions

Amperometry at a constant applied voltage can be used to obtain a *quasi* continuous kinetic measurement of ion-exchange reactions. Since stirring must be interrupted for 5–8 sec for each measurement, this technique is limited to reactions which are relatively slow (the half-time for completion of the reactions was about 3–4 min for divalent cations and close to 1 h for the uranyl ion exchange).

When this criterion is met, the method has various advantages. A single sample of resin and solution is used during the whole kinetic experiment, so that errors cannot arise from inhomogeneous samples for each time interval measurement. The method is simple, rapid and economic of materials and time. However, the cations used must be reducible at the polarizable cathode, and a suitable supporting electrolyte must be present. Sometimes, these provisions may represent a serious disadvantage. A single supporting electrolyte will affect (decrease) the number of reducible cations for a series of experiments whereas various supporting electrolytes for various cations may introduce undesirable anion effects. Another inconvenience is the frequent stopping of the stirring, but standardization of the procedure and routine experience reduces this to a minimum.

The kinetic results obtained are essentially the same by the proposed semicontinuous method and the batch method, and the proposed method is distinctly advantageous in the reactions to which it can be applied.

Department of Inorganic and Analytical Chemistry,
The Hebrew University of Jerusalem,
Jerusalem (Israel)

J. Kendler
C. Heitner-Wirguin

1 G. Semerano, *Ric. Sci.*, 22 (1952) 197.
2 H. Berg, *Chem. Tech. (Berlin)*, 8 (1956) 5.
3 B. Breyer, in *Polarography*, Proc. 3rd Int. Congr. Southampton, 1964, p.57.
4 J. Masek, *Allg. Prakt. Chem.*, 18 (1967) 207.
5 T. R. E. Kressman and J. A. Kitchener, *Discussions Faraday Soc.*, 4 (1949) 90.
6 C. Heitner-Wirguin and J. Kendler, to be published.
7 A. A. Frost and R. G. Pearson, *Kinetics and Mechanism*, J. Wiley, New York, 1953, p. 174.

(Received January 25th, 1970)

Analytica Chimica Acta
Elsevier Publishing Company, Amsterdam
Printed in The Netherlands

Determination of nanogram amounts of chromium by the copper-spark method

For the emission spectrographic analysis of nanogram amounts of chromium the copper-spark method[1] is the most sensitive procedure even when compared to more recent spectrographic techniques[2]. To attain maximum sensitivity with the copper-spark method, a pure solution of the trace constituent must be placed to the copper rod. For this reason, the application to trace determinations requires a separation of the trace constituent from all matrix material and from all reagents that have been used during the separation procedure. These limitations have so far confined the use of the copper-spark method to microanalysis.

It has been shown[3] that nanogram amounts of chromium can be extracted by means of oxine. The chromium oxinate can be purified from any excess reagent. The determination of the isolated chromium oxinate was done by means of a specialized X-ray fluorescence technique with which a sensitivity of about 5 ng was reached.

Biochemical studies require an even greater sensitivity. A method by which 2–20 ng of chromium can be determined with a standard deviation of about 14%, is presented in this communication.

Extraction and spectrographic technique

The extraction was done as already described[3]. After the extraction the dry chromium oxinate residue was dissolved in two 50-μl portions of dichloromethane. These solutions were added to the top of a high-purity copper rod (length 20 mm, diameter 4 mm). The technique involved warming the rod to 40° and evaporating the solution in small increments, so that none of the solution overflowed the top of the electrode. When all the chromium oxinate had been transferred (within about 5 min), 5 μl of an aqueous solution of sodium chloride (containing 10 μg NaCl per μl) were added to the electrode and evaporated. The electrodes were sparked and the spectrum registered by a photographic plate. After development, the intensity of the chromium lines was determined by photometry.

The equipment used included a Bausch & Lomb dual grating spectrograph, an RSV-Gerät (Hechendorf, Germany) for excitation, and a Zeiss Schnellphotometer.

The conditions used were as follows:

Medium voltage sparc (1000 V)
resistance 3 Ohms
capacitance 4 MF
inductance 2 mHz
burning time 0.28 sec
burning pause 0.16 sec
phase 2

electrode distance 2 mm
sparking time 15 sec
plate material Kodak SA 3

Cr lines: 3578.9 Å and
3593.5 Å

Results

The calibration curve was linear from 0 to 20 ng of chromium intersecting the origin. Data for the curve appear in Table I. The limit of detection is about 2 ng of Cr as calculated from three times the standard deviation of the blank.

TABLE I

REPRODUCIBILITY OF THE DETERMINATION OF NANOGRAM AMOUNTS OF CHROMIUM BY THE COPPER-SPARK METHOD

Amount of Cr (ng)	*No. of detns.*	*Average extinction*	*Standard deviation*	
			% rel.	*Extinction*
5	14	0.19	17	0.033
10	6	0.48	12	0.06
15	7	0.65	17	0.11

Discussion

The copper-spark method offers an independent alternative method for the determination of nanogram amounts of chromium. The sensitivity is slightly higher than that of the X-ray method and the reproducibility is about the same.

The oxine method permits a separation of chromium from all major constituents. It has an advantage over other separation procedures for chromium because separation is possible in the stable trivalent state.

Institut für anorganische Chemie und Kernchemie der Universität, D-65-Mainz
(Federal Republic of Germany)

CHARLES D. MANNING
KLAUS BEYERMANN

1 M. FRED, N. H. NACHTRIEB AND F. S. TOMKINS, *J. Opt. Soc. Am.*, 37 (1947) 279.
2 V. SVOBODA AND I. KLEINMAN, *Anal. Chem.*, 40 (1968) 1535.
3 K. BEYERMANN, H. J. ROSE AND R. P. CHRISTIAN, *Anal. Chim. Acta*, 45 (1969) 51.

(Received March 1st, 1970)

The use of an alternating electromagnetic field to modulate light in an electrodeless tube for the determination of neon and argon in helium by atomic absorption*

In a recent publication[1] it was demonstrated that neon and argon could be separately determined in helium by a new atomic absorption method. For this method, incident light that was emitted from a Geissler tube was modulated at 150 cycles with a commercial transformer. The modulated light was absorbed by atoms not in the ground state, as is the case in routine atomic absorption methods, but by atoms in excited states that were contained in a quartz absorption cell. Subsequent work with this new absorption technique used for rare gas analysis showed that comparable results were obtained by modulating incident light in an electrodeless tube with an alternating (time varying) electromagnetic field.

Electromagnetic modulation

In essence, electromagnetic modulation of incident light was accomplished with

---

* Work performed under the auspices of the U.S. Atomic Energy Commission.

relative ease. The electrodeless tube containing the rare gas was subjected to microwaves which excite the atoms and cause them to emit constant incident light having characteristic spectral lines of interest. Subsequently, the tube was subjected to an electromagnetic field by means of an electromagnet placed close to the tube. Fluctuations of the magnetic field caused the light in the tube to increase in intensity periodically. Thus, modulation was realized and the frequency of modulation was dependent on the frequency of the electromagnetic field.

The increase in light intensity for the spectral lines employed is due to "magnetic enhancement", a term first used by KLINKENBERG[2] when he investigated the effect of a magnetic field on the ionic spectra of thorium and found many lines enhanced. More recently, other workers have investigated the effect of a magnetic field on neutral atoms of other elements[3], including rare gases[4], and have found that many spectral lines are enhanced.

Magnetic enhancement is still not entirely understood[2,5]. However, the fact that spectral lines arising from ionic as well as neutral atoms are enhanced by an order of magnitude or more[3,5], suggests that this method of excitation might be useful in atomic absorption work, for example, to modulate light magnetically instead of electrically (a.c. transformer) or mechanically with a chopper. The result of modulating light in an electrodeless tube magnetically for atomic absorption of rare gases is described in this paper.

Experimental

In the previous work[1], commercial rare gas tubes were used for convenience. The inexpensive electrodeless quartz neon and argon tubes employed for this technique were made at the Argonne Laboratory. The method of making pure rare gas tubes electrodeless tubes was relatively simple. A flamed-out quartz tube, several inches long and having an internal diameter of 1/8 in, was evacuated to about $1 \cdot 10^{-5}$ mm Hg and filled with a spectroscopically pure rare gas at a pressure of 1–2 mm Hg. About one inch of the tube was sealed with a flame and used for this investigation. The lifetime of these home-made electrodeless tubes was comparable to or longer than that of the commercial tubes, and the purity of the rare gas spectrum was better.

The optical arrangement, absorption tube, vacuum line, and related readout system used for this work was essentially the same as reported previously. The emission tube was held adjacent to an antenna of a 2450 microwave generator (Raytheon Oscillator, Model No. PGM-10) which was operated at 50 W power. The light output from the tube was magnetically modulated by means of the following arrangement: the magnetic field was produced by a coil wound about a horseshoe-shaped iron bar to form an electromagnet, and positioned about an inch from the tube containing rare gas atoms that were excited by the oscillator. The plasma was in a transverse magnetic field for convenience. The frequency of modulation was 150 cycles, and the power input into the electromagnet was 5 W which produced a magnetic field near the tube of about 400 gauss. The selected modulation frequency, 150 cycles, gave a much better signal-to-noise ratio than a line frequency of 60 cycles, for example.

Results

Figure 1 shows a working curve that was obtained for neon. The neon line at 6402 Å was chosen for the reasons given previously. Standard samples were prepared on the vacuum line by mixing known amounts of neon in helium. The points on the working curve represent an average of a number of absorption readings that were obtained with a standard sample in the absorption tube.

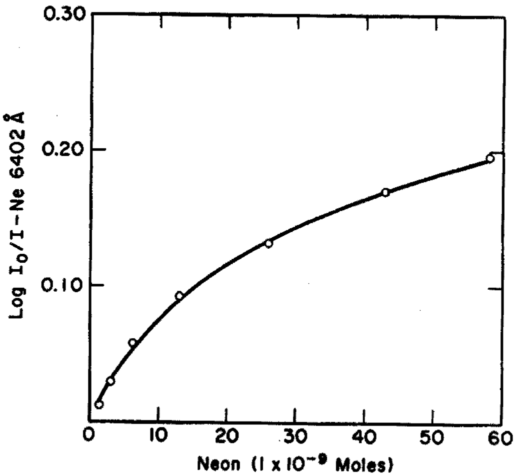

Fig. 1. Analytical curve for neon.

The procedure used to obtain absorption readings was to switch on the emission tube for several minutes to obtain a steady modulated incident light signal that passed through the absorption tube containing unexcited atoms. Next, an absorption reading was obtained by exciting the standard gas mixture in the absorption tube by switching on the power to 40 W of a Raytheon oscillator for about 1 min. More absorption readings were obtained of the same mixture by turning the oscillator power on and then off for 1-min intervals without waiting for the absorption tube to cool.

No rare gas samples were readily available to test the precision and accuracy of this atomic absorption method. As a result, to test this technique, known amounts of neon and helium were mixed on the vacuum line and introduced into the absorption tube. Corresponding absorption tracings were made for the synthetic sample, and results were obtained from the previously established analytical curve shown in Fig. 1. With $5.64 \cdot 10^{-9}$ moles of neon in the absorption tube, a mean value of $5.80 \cdot 10^{-9}$ moles was obtained from 10 determinations with a relative standard deviation of $\pm 3.6\%$; the accuracy was thus $+2.8\%$.

The technique described above for the determination of neon in helium was repeated for the determination of argon in helium. The argon line at 8115 Å was used to plot an analytical curve. The amounts of argon and helium that were used in the absorption tube to plot an argon analytical curve were nearly similar to the amounts of neon and helium employed. The argon analytical curve was similar to the neon analytical curve. The precision and accuracy that were obtained for a synthetic sample containing $6.15 \cdot 10^{-9}$ moles of argon in the absorption tube were equally as good as the precision and accuracy obtained for neon.

Discussion

A comparison of results obtained when incident light is modulated with a magnetic field and electrically (a.c. transformer) is of interest. For equal amounts of neon and argon in the absorption tube, the precision and accuracy for both methods are comparable to the precision and accuracy obtained by conventional routine atomic absorption methods. Thus, it is evident that electromagnetic modulation of incident light is useful for atomic absorption work.

The slopes of the analytical curves that were obtained with an a.c. transformer to modulate incident light are definitely steeper than the slopes of the analytical curves obtained using a magnetic field to modulate incident light. This is probably so because of the splitting of the spectral lines due to the magnetic field. At this point, it is too early to say with certainty that the slopes of analytical curves will be significantly lower when other gas pressures, spectral lines, magnetic field strengths (transverse and longitudinal) are employed. More work is required to understand magnetic modulation better.

Some of the advantages of modulating incident light magnetically instead of mechanically or electrically (a.c. transformer) are evident. For instance, the modulating frequency can readily be varied with a magnetic field to give the best signal-to-noise ratio. Mechanical modulating devices have the disadvantage that the frequency at which they operate is usually limited to a single predetermined frequency. While it is possible to vary the speed of the motor and hence the chopper, this has generally proved unsatisfactory owing to the narrow range within which the speed can be changed for a given motor. Changing motor speed also results in increasing bearing wear and shortened motor life.

Various workers have tried to modulate light in hollow-cathode tubes with alternating current, but this technique is not very satisfactory. The reason is that the life of the tube is greatly shortened because of a plating out of electrode metal on the tube window which makes it opaque and renders the tube unusable.

When the incident light is modulated magnetically, more light is available to go through the absorption tube to activate a phototube. In mechanical modulation, only a portion of incident light is allowed to pass through the chopper, the rest of the light from the emission source being lost and unavailable for absorption and detection.

Selective modulation of spectral lines arising from ionic as well as neutral atoms, can be achieved with magnetic modulation. In the past, for example, workers have obtained selective modulation of resonance lines of interest by using an a.c. resonance lamp between the plasma and the slit of the monochromator.

This new technique for the atomic absorption of rare gases uses spectral lines that have transition to metastable states instead of transition to ground states. Takeyama and Takezaki have shown that some lines having transition to metastable states are enhanced for a given set of parameters[4]. As a result, spectral lines of interest are available in the near ultraviolet–visible spectral region. This means it is possible to use numerous routine and inexpensive monochromators or band-pass filters for atomic absorption of rare gases. Earlier it was thought that expensive and sophisticated ultraviolet instrumentation would be needed for atomic absorption of rare-gas samples, because all transitions originating in absorption in the ground state for rare gases are observed in the vacuum ultraviolet.

The author is indebted to H. H. CLAASSEN of our Chemistry Division for consultations regarding the work described, and J. BOBIS and R. GEORGE of our Electronics Division for assistance with the readout system arrangement and the related electromagnet used to modulate incident light.

Chemistry Division,
Argonne National Laboratory,
Argonne, Ill. 60439 (U.S.A.)

JOSEPH A. GOLEB

1 J. A. GOLEB, *Anal. Chim. Acta*, 41 (1968) 229.
2 P. F. A. KLINKENBERG, *Physica*, 16 (1950) 185.
3 M. SOMESAN AND C. POPAVICI, *Appl. Phys. Letters*, 9 (1966) 64.
4 H. TAKEYAMA AND Y. TAKEZAKI, *J. Quant. Spectry. & Radiative Transfer*, 8 (1968) 1864.
5 E. H. PINNINGTON, *Proc. Phys. Soc. (London)*, 86 (1965) 601.

(Received October 13th, 1969)

ANNOUNCEMENT

VIth INTERNATIONAL SYMPOSIUM ON CHROMATOGRAPHY AND ELECTROPHORESIS

Brussels, 14–15 and 16 September 1970

The *Société Belge des Sciences Pharmaceutiques* are organizing an International Symposium on Chromatography and Electrophoresis which will be considered under its theoretical aspects as well as in its practical application in various fields.

Everyone interested in Chromatography and Electrophoresis is cordially invited to participate at this Symposium. The latest date at which registration forms will be accepted is 1st August 1970. The official languages are: English, French, Dutch and German.

An exhibition of scientific apparatus will take place during the three days.

The participation fee has been fixed at 1,500 BF.

Further information can be obtained from: M. L. RENOZ, Société Belge des Sciences Pharmaceutiques, Rue Archimède 11, 1040 Bruxelles, Belgium.

INTERNATIONAL UNION OF PURE AND APPLIED CHEMISTRY

ANALYTICAL CHEMISTRY DIVISION

Following the XXVth Conference of IUPAC at Cortina d'Ampezzo, Italy, the membership of the Division Committee for 1969–1971 is as follows:

President:	Prof. W. KEMULA (Poland)
Vice-President:	Prof. P. W. WEST (U.S.A.)
Members:	Prof. I. P. ALIMARIN (U.S.S.R.)
	Prof. R. BELCHER (U.K.)
	Prof. C. DUVAL (France)
	Prof. L. ERDEY (Hungary)
	Prof. W. FISCHER (Germany)
	Prof. H. FREISER (U.S.A.)
	Prof. N. TANAKA, (Japan)
Secretary:	Mr. R. W. FENNELL, Materials Department,

Royal Aircraft Establishment,
Farnborough, Hants. U.K.

The officers of the seven Commissions and the new projects undertaken are:

Commission 1 — Analytical Reactions and Reagents
Chairman: Prof. R. Belcher (U.K.)
Secretary: Prof. J. Zyka, Charles University, Department of Analytical Chemistry, Albertov 2030, Praha 2, Czechoslovakia.

Commission 2 — Microchemical Techniques and Trace Analysis
Chairman: Dr. W. Schoniger (Switzerland)
Secretary: Dr. R. Levy, Service Central de Microanalyse du CNRS, 2 rue H. Dunant, 94 Thiais, France.
New Projects: (a) The expression of errors in organic analysis.
(b) Trace analysis applicable to the determination of minor amounts of impurities in high grade chemicals.

Commission 3 — Analytical Nomenclature
Chairman: Prof. H. M. N. H. Irving (U.K.)
Secretary: Prof. T. S. West, Department of Chemistry, Imperial College, South Kensington, London, S.W.7.
New Project: Nomenclature in kinetic methods of analysis.

Commission 4 — Spectrochemical and Other Optical Procedures for Analysis
Chairman: Prof. H. Kaiser (Germany)
Secretary: Prof. V. A. Fassel, Institute for Atomic Research, Iowa State University, Ames, Iowa 50010, U.S.A.

Commission 5 — Electroanalytical Chemistry
Chairman: Prof. I. M. Kolthoff (U.S.A.)
Secretary: Prof. P. Zuman, Department of Chemistry, Clarkson College of Technology, Potsdam, N.Y. 13676, U.S.A.
New Projects: (a) Use of the coulomb as a secondary standard.
(b) pK values of organic bases.
(c) Activity in electroanalytical chemistry in India.

Commission 6 — Equilibrium Data
Chairman: Prof. D. N. Hume (U.S.A.)
Secretary: Dr. F. J. C. Rossotti, Inorganic Chemistry Laboratory, South Parks Road, Oxford OXl 3QR, U.K.
New Projects: (a) Compilation of selected stability constants.
(b) Selection of standard media.
(c) Application of information retrieval to equilibrium data.

Commission 7 — Analytical Radiochemistry and Nuclear Materials
Chairman: Dr. G. B. Cook (Austria)
Secretary: Dr. W. W. Meinke, National Bureau of Standards, Analytical Chemistry Division, Washington, D.C. 20234, U.S.A.
New Project: Conventions for flux monitoring and definition of sensitivity in radiochemical methods.

Working Group

The IUPAC Bureau appointed an ad-hoc Working Group to study the establishment of an International Centre for Analytical Chemistry. The Division is represented on this Group by Prof. H. Malissa (Austria) as Chairman and seven Members. Representatives of IAEA, ILO and UNIDO are also Members. The Group Secretary is

Dr. D. Merten,
International Atomic Energy Agency,
Kärntner Ring 11,
A-1010 Vienna,
Austria.

CONTENTS

(continued on page 4 of cover)

Continued from inside page of cover

Short Communications

PRINTED IN THE NETHERLANDS